UNIVERSITA' DEGLI STUDI DI CATANIA

FACOLTÀ DI SCIENZE MATEMATICHE FISICHE E NATURALI

DIPARTIMENTO DI SCIENZE CHIMICHE

DOTTORATO DI RICERCA INTERNAZIONALE
IN SCIENZE CHIMICHE
XXIV CICLO

Dott. La Paglia Fragola Valentina

SYNTHESIS OF CHROMO FLUOROGENIC SENSORS FOR MOLECULAR RECOGNITION

Final report

Tutor:

Chiar. mo Prof. Francesco P. Ballistreri

I. INTRODUCTION

According to the IUPAC definition a chemical sensor is a device that transforms a chemical information, ranging from the concentration of a specific sample component to total composition analysis, into an analytically useful signal. The chemical information, mentioned above, may originate from a chemical reaction of the analyte or from a physical property of the system investigated.[1]

Chemical sensors contain two basic functional units, a receptor part and a transducer part. In the receptor part of the sensor the chemical information is transformed into a form of energy which may be measured by a transducer. In the transducer part there is a device capable of transforming the energy carrying the chemical information about the sample into a useful analytical signal.

The receptor part of a chemical sensor can be based on various principles:

1) Physical, where no chemical reaction take place. Typical examples are those based upon measurement of absorbance or conductivity.

2) Chemical, in which a chemical reaction between the sensor and the analyte to detect gives an analytical signal (chemosensors).

3) Biochemical, in which a biochemical process is the source of the analytical signal (biosensors).

In some cases it is not possible to define unequivocally how a sensor operates, as in the case of a signal due to an absorption process.

Optical devices, based on optical phenomena, represent a family of sensors characterized by an absorption event which involves an interaction of the analyte with the receptor part. Based on the type of optical properties we can classified:

- **Absorbance** measured in a transparent medium, caused by absorpitivity of the analyte itself .
- **Reflectance** that is measured in a non-transparent media, usually using an immobilized indicator.
- **Luminescence**, based on the measurement of the intensity of light emitted by a chemical reaction
- **Fluorescence**, measured as the positive emission effect caused by irradiation; also could be detected by quenching of fluorescence.
- **Refractive index**, measured as the result of a change in solution composition.

- **Opto-thermal effect**, based on the measurement of the thermal effect caused by light absorption.
- **Light scattering**, based on effects caused by particles of definite size present in the sample.

The development of chemosensors is already revolutionizing the protocol of chemical analysis. The classical methods require collection, transportation and treatment of the sample and, often, complex instrumentations. Modern chemical sensors are designed considering a generic sensor as a species that responds to external stimuli (*Stimuli Responsive Materials*). Therefore, following a chemical or a physical perturbance (due to an interaction with the analyte) the sensor must respond with a variation of any of its measurable properties.[2-3]

Moreover, chemosensors are of particular interest not only because they are cheap and easy to use but also because, if properly designed, can allow the monitoring of concentrations of an analyte in time and sometimes in real space.

Currently, sensor devices are present everywhere with the intention of improving the quality of life in every application. They are now widely applied in various fields such as environmental monitoring, food analysis, medicine, industrial automation, telecommunications, agriculture and, more recently, also in the detection of toxic gases and explosive materials.[4-5]

I.2 SUPRAMOLECULAR CHEMISTRY

A general requisite of all chemical sensors is that the interaction with the target molecule must be selective, reversible and must occur in a very short time. An approach used by chemists to design new chemosensors is based on the principles of supramolecular chemistry.[6-7-8]

A supramolecular system is an organized architecture of molecular units, where each unit retains most of the intrinsic properties and the various components are linked together by weak forces like hydrogen bonds, Van Der Waals forces, electrostatic interactions and so on. The interesting feature of supramolecular systems is that the interactions that exist between different subunits may lead to the disappearance of the properties of individual components and the appearance of new relevant properties of the supramolecular aggregate.

These new systems have stimulated chemists to undertake the construction of new devices and machines at molecular level.[9-10]

In the last years a large number of systems with properties related to phenomena of molecular recognition, signalling, transport and transformation of chemical species has been designed.[11]The general properties of these entities are correlated both with the type of components and to the level of organization, for example dendrimers, amphiphilic aggregates such as surfactants or mono and multi layers etc. This kind of architectures is giving a strong contribution to the development of nanotechnologies, especially the opportunity to control and to intervene on the composition and on the structure of these molecular assemblies has opened the way for the construction of molecular devices, systems capable to transfer energy, electrons and so on; properties that can be used to obtain useful functions, as the storage of information or signal transduction.

I.3 SCHEME OF A CHEMOSENSOR

The field of optical chemical sensors has been a growing research area over the last three decades. A wide range of review articles has been published by experts in the field who have highlighted the advantages of optical sensing over other transduction methods. An appropriate definition of a chemical sensor is the so-called "Cambridge definition": *Chemical sensors are miniaturised devices that can deliver real time and on-line information on the presence of specific compounds or ions in even complex samples.*[12]

Optical chemosensors employ optical transduction techniques to yield analyte information. The most widely used techniques employed in optical chemical sensors are optical absorption and luminescence, but sensors based on other spectroscopies as well as on optical parameters, such as refractive index and reflectivity, have also been developed.

Recent developments in the field have been driven by such factors as the availability of low-cost, miniature optoelectronic light sources and detectors, the need for multianalyte array-based sensors particularly in the area of biosensing and imaging technology.

While the optical principles used in chemical sensing have not changed substantially over the years, in many cases the transduction platforms have changed considerably, yielding sensors with vastly improved performance, the most relevant performance parameters being sensitivity, stability, selectivity, and robustness.

In general, optical chemical sensors may be categorized under the headings of direct sensors and reagent-mediated sensors. In a direct optical sensor, the analyte is detected directly via some intrinsic optical property such as, for example, absorption or luminescence. In reagent-mediated sensing systems, a change in the optical response of an intermediate agent, usually an analyte-sensitive dye molecule, is used to monitor analyte concentration. This latter technique is useful particularly in the case where the analyte has no convenient intrinsic optical property, which is the case for many analytes.

A chemosensor is constituted of three different components as shown in **Fig. 1**:

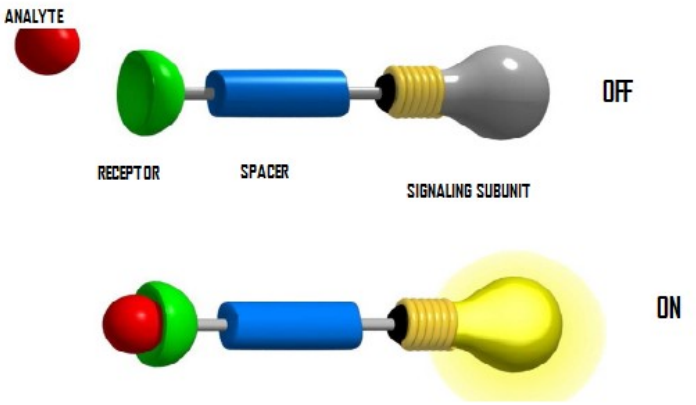

Fig. 1 Scheme of a chemosensor

A *receptor* portion (responsible for selective interaction with the analyte) and a *signalling* portion (whose properties vary as a result of the state of the receptor) linked together by a *spacer* that regulates geometry and electronic interaction. Signalling subunit must possess a certain property detectable and quantifiable, optical or potential for example, that changes with the state of the system, depending on whether the receptor is free or involved in the interaction with the analyte.[13]

Moreover, the following requisites must be present:

1. receptor must have a selectivity for the target molecule much higher than that of potentially interfering substances;
2. the recognition process must be fast and reversible;
3. the system must have a good global chemical stability.

Optical chemical sensors employ optical transduction techniques to yield analyte information. The most widely used techniques employed in optical chemical sensors are optical absorption and luminescence, but sensors based on other spectroscopies as well as on optical parameters, such as refractive index and reflectivity, have also been developed.

Recent developments in the field have been driven by such factors as the availability of low-cost, miniature optoelectronic light sources and detectors, the need for multianalyte array-based sensors particularly in the area of biosensing and imaging technology.

In recent years, While the optical principles used in chemical sensing have not changed substantially over the years, in many cases the transduction platforms have changed considerably, yielding sensors with vastly improved performance, the most relevant performance parameters being sensitivity, stability, selectivity, and robustness.

In general, optical chemical sensors may be categorized under the headings of direct sensors and reagent-mediated sensors. In a direct optical sensor, the analyte is detected directly via some intrinsic optical property such as, for example, absorption or luminescence. In reagent-mediated sensing systems, a change in the optical response of an intermediate agent, usually an analyte-sensitive dye molecule, is used to monitor analyte concentration. This latter technique is useful particularly in the case where the analyte has no convenient intrinsic optical property, which is the case for many analytes.

I.4 HOW TO DESIGN A CHEMOSENSOR

A fluorescent or colorimetric chemosensor is defined as a compound of abiotic origin that complexes an analyte with a concomitant fluorescent or colorimetric signal transduction. Generally there are three different approaches to designing a chemosensor:

a. Binding Site- Signalling Subunit Approach

This approach, that is the most popular, involves covalently introducing binding site and signalling subunits to the chemosensor. As can be seen in the **Fig. 2**, the coordination site binds the analyte in such a way that the properties of the signalling subunit are changed giving rise to variation either in the colour (chromogenic chemosensor) or in its fluorescence behaviour (fluorogenic chemosensor)

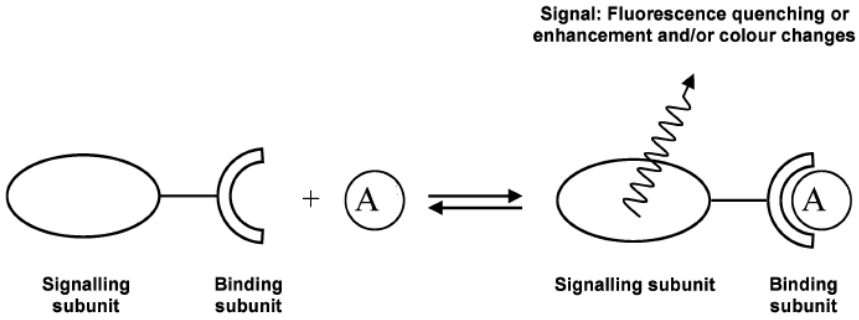

Fig. 2. Signalling subunit approach

b. Displacement approach

This approach also involves, as in the above case, the use of a binding site and signalling subunits; in this case both subunits are not covalently attached but form a coordination complex. When a target is added to the solution containing the binding site, there is a displacement reaction, the binding site coordinates the target whereas the signalling subunits returns to the solution retrieving its noncoordinated spectroscopic behaviour (**Fig. 3**). If the spectroscopic characteristics of the signalling subunit in the molecular complex are different of

those in its noncoordinate state, then the binding process is coupled to a signalling event.

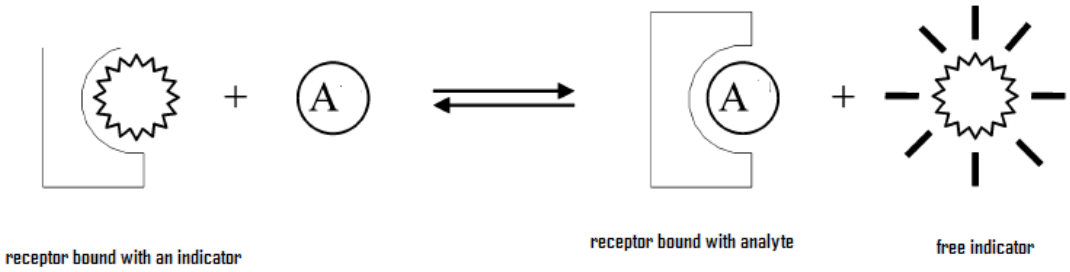

Fig. 3. Displacement approach

c. Chemodosimeter approach

This kind of approach involves the use of a specific chemical reaction (usually irreversible) induced by the presence of a target molecule that is coupled to a colour or emission variation. If the chemical reaction is irreversible the term chemosensor can't be strictly used and we will refer to these systems as chemodosimeters or chemoreactants.

The underlying idea of these irreversible systems is to take advantage of the selective reactivity that certain target molecules may display.[14- 15]

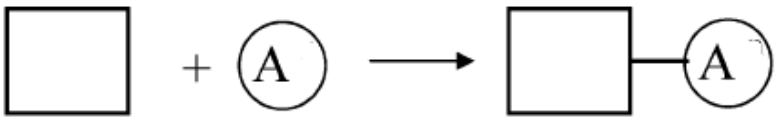

Fig. 4. Chemodosimeter approach

I.5 COVALENTLY ASSEMBLED MONOLAYER

Once developed a system that gets all the characteristics identified, it is necessary to make it actually usable as a sensor. So far the use of sensors in solution is rather limited in domains such as biochemistry, where the use of sensors free in solution is used for real-time monitoring of concentration of a given analyte.[16]

For many applications in biology and in environmental field, the use of sensors it's easier if these are previously anchored on an inert surface.

An anchored sensor has many advantages. If the receptor-analyte binding is reversible, it's possible to make multiple measurements with the same surface, reducing in this way time and costs. Furthermore a system on solid support has the advantage that it can be stored and transported easily and used also by inexpert staff. Under this respect engineering of inorganic surfaces by covalent bonding of organic molecules represents an interesting approach to the synthesis of hybrid inorganic/organic nanomaterials. Synthesis based on covalent assembly of appropriate molecules on inorganic substrates represents one of the most powerful approaches to obtain materials with single- molecule properties and to study functional molecular architectures. A typical approach involves the covalent bonding of an appropriate coupling layer (CL) with the starting substrate and a subsequent anchoring of functional molecules.[17-18]

Many different interesting molecular properties can be investigated by optical measurements e.g molecular switch, luminescence quenching, variation in optical absorbance, non linear optical properties, molecular recognition properties and many others. In these cases, transparent silica substrates are useful for the covalent assembly of functional molecule.

II. STATE OF THE ART

II.1 ORGANOPHOSPHATE DETECTION

The current rise in international concern over criminal terrorist attacks via chemical warfare agents (CWAs) as brought about the need for reliable detection of these toxic agents. According to the organization for the prohibition of Chemical Weapons and the Chemical Weapons Conventions, some substances are considered chemical weapons if they, through a "chemical effect on living processes, may cause death, temporary loss of performance or permanent injury to people or animals".

CWAs are classified into several groups according to their lethality, e.g. nerve agents, asphyxiant agents, vesicant agents, pulmonary agents, lachrymatory agents and incapacitating agents; among all the most dangerous are certainly nerve agents.[18]

Nerve agents are a family of highly toxic phosphoric acid esters, structurally related to the larger family of organophosphate compounds; in fact development of nerve agents was a by-product of insecticide research and development of the early 1930s when German chemists observed that organo-phosphorous compounds could be poisonous. Deadly nerve agents have rapid and severe effects on human and animals health, either as a gas, aerosol or liquid form.

OP pesticides are synthetic esters, amides, or thiol derivatives of phosphoric, phosphonic, phosphorothioic, or phosphonothioic acids. There are over 100 OP compounds currently in the market, representing a variety of chemical, physical, and biological properties. As the name indicates, all OP pesticides have a central phosphorus atom, with either double bonded oxygen (P=O), or a double bonded sulfur atom (P=S). A P=O pesticide is called an oxon pesticide, and the P=S is termed as a thion pesticide as shown in Figure below[19-20]:

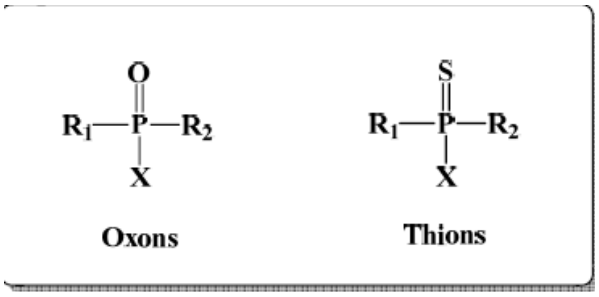

Fig. 5. general chemical structure of OP compounds

Structurally, both oxons and thions show variety in the single-bonded R1, R2 and X groups attached to the central pentavalent phosphorus atom. However, R1 and R2

generally tend to be alkoxy, aryloxy and thioalkoxy groups, while X is a labile leaving group.

Their effect are mainly due to their ability to inhibit the action of acetylcholine esterase, a critical central nervous system enzyme. The sequence of symptoms varies with the route of the exposure.

While respiratory symptoms are generally the first to appear after inhalation of the nerve vapour, gastrointestinal symptoms are usually the first after ingestion. Inhibition of acethylcholinesterase is a progressive process and depends not only on the concentration but also on the time of exposure.

The ease of production and extreme toxicity of organophosphorous nerve agents underscores the need to detect these odourless and colourless chemicals. As a consequence intense research efforts have been directed to develop sensitive and selective systems for the detection of these compounds. A variety of detection methods for CWAs has been developed include enzymatic assays[21], GC-MS spectrometry[22-23-24-25], electrochemical[26] and so on. However, all the method presented at least one of the following limitations: low sensitivity, limited selectivity, non portability , difficulties in real time monitoring and false positive readings.

An alternative to those classical methods is the design of colorimetric[27-28] or fluorimetric chemosensors[29-30-31]. In fact one of the most convenient and simplest means of chemical detection is the generation of an optical event, e.g. change in absorption or emission bands in the presence of a target analyte. Especially, optical detection often require a low- cost and widely used instrumentation and offers the possibility of so-called “naked eye detection”.

The first example of colorimetric probe for detection of nerve agents were described in 1944 by Schonemann, and was based in the oxidation of certain amines, such as o-toluidine, benzidine and so on, to give coloured products in the presence of several organophosphorous compounds. The mechanism was based in the formation of a peracid derived from the organophosphorous compound that induced the oxidation of the amine.

Moreover, these are rare studies and the development of chromo-fluorogenic sensors for nerve agents detection have been very scarce. The development of chromo-fluorogenic sensors has been abandoned for many years and only recently these studies were taken into account, giving rise to the development of chemosensor more sophisticated than the earliest published works, we can cite sensors based on Photoinduced-electron-transfer (PET) process used in the development of highly sensitive fluorescent chemosensor just used for the recognition of cations and anions, and by the same principle, recently applied to the detection of organophosphorous agents. The ease which one can modulate the emission intensity due to the possibility of functionalization with an appropriate fluorophore, which have certain binding sites has created a myriad of receptors in recent years.

Fluorescence in a molecule is observed when an excited electron placed in the LUMO orbital goes to the HOMO releasing the excess of energy in form of light. If the energy of another “external” orbital lies between the energy gap of the HOMO and LUMO of the fluorophore a PET process from the external orbital to the photo-

excited fluorophore take place inducing a quenching process through a non radiative path. When coordination of a target guest induces the removal of the energy level between the HOMO and the LUMO of the fluorophore, the emission intensity increases resulting in the corresponding detection of the guest.

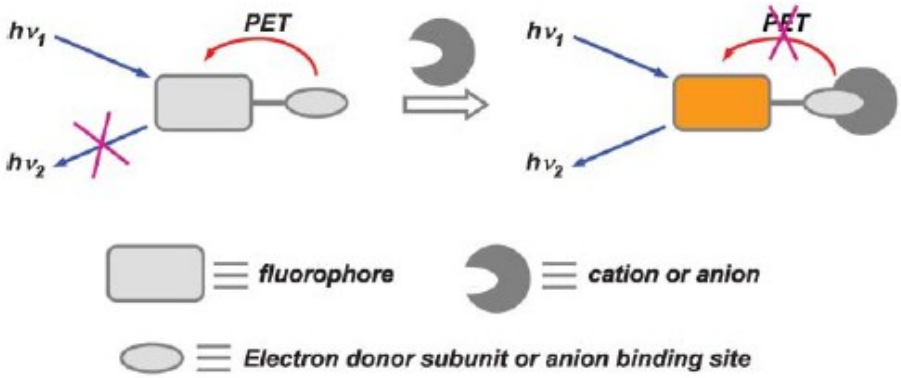

Fig. 6. Scheme of PET in a generic sensor

The chemical structures of these chemosensors were characterized by the presence of a rigid scaffold functionalized with two subunits. One of this subunits possesses a nucleophile which is highly reactive towards phosphorous substrates (a hydroxyl unit for example) and the other is a tertiary amine with an appended fluorophore through a methylene spacer. As a consequence of this design, the emission of the fluorophore is quenched via PET process from the lone pair of the tertiary amine to the photo-excited fluorophore. Upon addiction of the target an acylation reaction with the primary alcohol takes place. This reaction induces a rapid intramolecular N-alkylation that leads to the formation of a quaternary ammonium salts (**Fig. 7**).

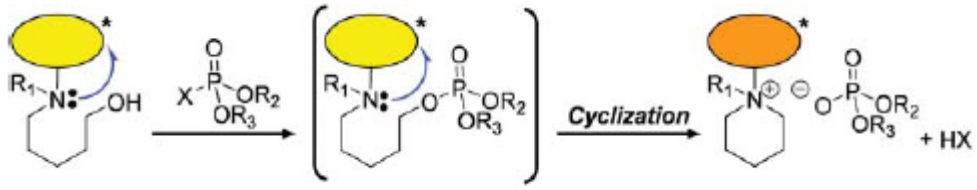

Fig. 7. General scheme of PET indicator molecules for the fluorogenic detection of nerve agent

This quaternization induced the inhibition of the PET and the restoration of the full emission of the appended fluorophore. One important limitation of PET-based sensors is related with the usually slow rates of phosphorylation reactions. In order to avoid this problem it's possible to use highly nucleofilic moieties in combination with a colorimetric system as an alternative strategies for the detection of CWAs simulants.

Oximates and Hydrazones are the higher nucleophilic moieties employed in the development of these colorimetric indicators; these moieties are well known as "super-nucleophiles" in which an atom containing a lone pair is adjacent to a

nuclophilic centre[32]. If these "supernuclophiles" are implemented into an organic scaffold with absorption bands centred in the visible region, the reaction with the phosphorous centres from the nerve agents might induce changes in these bands leading to consequent colorimetric recognition of these deadly gases[33-34].

Significant progress has been achieved toward the development of fluorescent chemosensors for toxic organophosphorus pesticides and chemical warfare agent mimics. These chemosensors have been demonstrated to be time-effective and more robust that biosensors. It is clear that future improvements in this area will require the design of new fluorescent chemosensors with additional modes for signal transduction. Such sensors will play an important role in minimization or elimination of false-positives. Due to the structural similarity of OP compounds, it is also paramount that the designed sensors must be fabricated such that they are highly selective toward specific OP compounds.

A second generation of azastilbene-based OP sensors will seek to:

(*a*) increase sensor multimodality,

(*b*) enhance sensor selectivity between oxons and thions, and (*c*) develop robust sensors with real world capability in complex matrices, including aqueous systems[35-36].

II.2 METAL SENSING

The development of chemosensors that are capable of sensing different target species is currently a topic of major interest in supramolecular chemistry.

Then, considerable efforts have been made to design new molecular probes able to recognize and sense environmentally and biologically important ionic species for example highly noxious, heavy and transition metal ions are currently a task of prime importance for medical, environmental, and biological applications. Consequently, the construction of chemosensor molecules with high selectivity and sensitivity for the detection of transition- and heavy-metal cations has received substantial attention, as these ions play important roles in living systems and have an extremely toxic impact on the environment.

Presently, one of the most attractive approaches focuses on the research of novel colorimetric and fluorescent metal ion sensors, which allow naked-eye detection of color and fluorescent emission change upon metal ion binding without the use of a spectroscopic instrument.

Fluorescent sensors for the detection and measurement of transition-metal ions are widely investigated because of their simplicity and high sensitivity of response. In particular, the development of a fluorescent probe for copper ions in the presence of a variety of other metal ions has received great attention.

In chemosensors, a selective binding motif is attached to a fluorophore for signal transduction. However, one disadvantage is that the recognition event is sometimes difficult to detect because the fluorophore does not directly contact the bound metal ion. In this aspect, an ideal fluorescent probe would be one whose fluorescent unit is directly involved in the interaction with the metal ions.

Cation-specific fluorescence sensors are powerful tools for the measurement of metal ion concentrations in environmental and biological samples. They typically combine high optical sensitivity with excellent cation selectivity, and are therefore particularly well suited for the non-invasive visualization of labile metal pools in a biological environment. Perhaps the largest class of fluorescence sensors function as simple cation-responsive switches. The linear relationship between intensity and cation concentration allows for quantitative measurements; however, the emission intensity depends also on the sensor concentration, which is often not known with sufficient accuracy in biological samples. Fluorescence sensors which undergo a spectral shift upon binding of the cation inherently provide concentration information of the metal-free sensor and are principally suitable for accurate quantitative measurements via ratiometric fluorescence imaging. Despite their usefulness, only a handful of ratiometric sensors have been developed, indicating the considerable challenges in the probe design[37].

II.3 METALS IN NEUROBIOLOGY

The brain is a singular organ of unique biological complexity that serves as the command center for cognitive and motor function. As such, this specialized system also possesses a unique chemical composition and reactivity at the molecular level. In this regard, two vital distinguishing features of the brain are its requirements for the highest concentrations of metal ions in the body[38-39] and the highest per-weight consumption of body oxygen. In humans, the brain accounts for only 2% of total body mass but consumes 20% of the oxygen that is taken in through respiration[40]. As a consequence of high oxygen demand and cell complexity, distinctly high metal levels pervade all regions of the brain and central nervous system.

Structural roles for metal ions in the brain and the body include the stabilization of biomolecules in static (e.g., Mg^{2+} for nucleic acid folds, Zn^{2+} in zinc-finger transcription factors) or dynamic (e.g., Na^{+} and K^{+} in ion channels, Ca^{2+} in neuronal cell signaling) modes, and catalytic roles for brain metal ions are also numerous and often of special demand. Because of the intimate connection between its unique composition and function, the inorganic chemistry of the brain is inherently rich and remains an open frontier for study. Traditional studies of metals in neurobiology have focused on the chemistry and structural biology of redoxactive s-block metal ions, including Na^{+}, K^{+}, Mg^{2+}, and Ca^{2+}.

Na^{+} and K^{+} are present in high concentrations in the body (~0.1 M) and possess distinct compartmentalizations, with resting Na^{+} levels higher in the extracellular space and K^{+} levels higher inside cells. The dynamic partitioning of these metal ions is controlled by ion-specific channels that selectively allow passage of either Na^{+} or K^{+} in and out of cells[41].

Less thoroughly studied are the roles of d-block metals in the brain. Zinc, iron, copper, and related d-block metals are emerging as significant players in both neurophysiology and neuropathology, particularly with regard to aging and neurodegenerative diseases. Because the concentrations of these d-block metals in brain tissue are up to 10000-fold higher than common neurotransmitters and neuropeptides, referring to these essential brain nutrients as trace elements is a clear misnomer, in fact not only do these metals serve as components of various proteins and enzymes essential for normal brain function, but their labile forms, particularly those of Zn^{2+} and $Cu^{+/2+}$, are also connected to specialized brain activities.

In this context, labile metal ion pools can possess protein or small molecule ligands or both that can be readily exchanged between different ligand sets. The far-reaching connections of inorganic chemistry to unexplored aspects of brain function, aging, and disease have prompted demand for new methods to study metal ion function, misregulation, or both within intact, living samples.

In this regard, molecular imaging with metal-responsive small-molecule probes coupled to optical fluorescence imaging (OI) and magnetic resonance imaging (MRI) modalities is emerging as a powerful approach to interrogating metal ion chemistry from the subcellular to the organism level[42].

II. 4 COPPER SENSING

Copper plays an important role in various biological processes. It is a vital trace element, the third most abundant in humans, and is present at low level in a variety of cells and tissues, with the highest concentration in the liver. The average concentration of blood copper in the normal group is 100-150 mg/dL (15.7 and 23.6 mM). As is well-known, Cu^{2+} plays an important role in living systems such as those occurring in the human nervous system, gene expression, and the functional and structural enhancement of proteins.2 However, under overloading conditions, copper can be toxic and can cause oxidative stress and disorders associated with neurodegenerative diseases, including Menkes and Wilson diseases, familial amyotropic lateral sclerosis, Alzheimer's disease, and prion diseases.

The U.S. Environmental Protection Agency (EPA) has set the limit of copper in drinking water to be 1.3 ppm (20 mM). As a pollutant due to its extensive industrial use and an essential trace element in biological systems, chemosensors for copper(II) based on chromogenic or fluorogenic probes that are expected to quickly, non - destructively, and sensitively detect copper ions have drawn a lot of attention.

However, only few of them exhibit good performance in aqueous media, which is a very important factor for potential biological applications.

For these reasons the design and the development of fluorescent and colorimetric sensors for Cu^{2+} has received considerable attention in particular because they combine the sensitivity of fluorescence with the convenience and

aesthetic appeal of a colorimetric assay[43].

In particular, ratiometric fluorescent sensors are preferred because the ratio between the two emission intensities can be used to evaluate the analyte concentration and provide a built-in correction for environmental effects, such as photobleaching, sensor molecule concentration, the environment around the sensor molecule (pH, polarity, temperature, and so forth), and stability under illumination. Nevertheless, only a few ratiometric fluorescent sensors for Cu^{2+} have been reported due to the fluorescence quenching nature of paramagnetic Cu^{2+} [44-45-46-47]. However, these reported sensors were mostly only utilized in pure organic solvents or organic-aqueous solutions, and often showed poor selectivity with other metal ions such as Co^{2+}, Ni^{2+}, Ag^{+}, Hg^{2+} and Pb^{2+}. To date, there have been no reports of ratiometric fluorescent and colorimetric sensors that are completely selective for Cu^{2+} that can be used in 100% aqueous solution.

Even though some examples of selective recognition sensors for Cu^{2+} have been reported,4 most of these sensors show "turn-off" manner in emission spectra upon Cu^{2+} binding due to the fluorescence-quenching nature of paramagnetic Cu^{2+} .5 Furthermore, only a few examples can display "turn-on" or ratiometric fluorescent changes in emission spectra, which are desirable for analytical purposes by the enhancement of fluorescence or changes in the ratio of the intensities of the emission at two wavelengths.

There are two basic requirements to construct a ratiometric fluorescent sensor for Cu^{2+}:

1. a signaling mechanism is required, which can turn the Cu^{2+} recognition event into a ratiometric fluorescence signal, for instance the internal charge transfer (ICT) mechanism has been widely exploited for cation sensing. The interaction between receptor and cation would blue shift the fluorescence spectra.
2. there is the requirement to protect fluorescence from being quenched by Cu^{2+}.

Another issue is related to the recognition is that of serious interference by other metal ions such as Ni(II),5 Ag(I),6 and Hg(II).6,7 To achieve Cu(II)-only sensing, fluorescent chemosensors require deliberate design.

II.5 COPPER IN NEUROBIOLOGY

Basic Aspects of Copper in the Brain. As just said copper is the third-most abundant transition metal in the body and in the brain, with average neural copper concentrations on the order of 0.1 mM[48].

This redox-active nutrient is distributed unevenly within brain tissue, as copper levels in the gray matter are 2- to 3-fold higher than those in the white matter[49]. Copper is particularly abundant in the locus ceruleus (1.3 mM), the neural region responsible for physiological responses to stress and panic, as well as the substantia nigra (0.4 mM), the center for dopamine production in the brain. The major oxidation states for copper ions in biological systems are cuprous Cu^{+} and cupric Cu^{2+}; Cu^{+} is more common in the reducing intracellular environment, and Cu^{2+} is dominant in the more oxidizing extracellular environment. Levels of extracellular Cu^{2+} vary, with Cu^{2+} concentrations of 10-25 μM in blood serum, 0.5-2.5 μM in cerebrospinal fluid (CSF),331 and 30 μM in the synaptic cleft.1 Intracellular copper levels within neurons can reach 2 to 3 orders of magnitude higher concentrations.

Like zinc and iron, brain copper is partitioned into tightly bound and labile pools. Owing to its redox activity, copper is an essential cofactor in numerous enzymes, including cytochrome c oxidase (CcO), Cu/Zn superoxide dismutase (SOD1), ceruloplasmin (Cp), and dopamine _ monooxygenase (D_M), that handle the chemistry of oxygen or its metabolites.

Labile brain copper stores have been identified in the soma of cortical pyramidal and cerebellar granular neurons, as well as in neuropil within the cerebral cortex, hippocampus, red nucleus, cerebellum, and spinal cord[50].

The widespread distribution and mobility of copper required for normal brain function, along with the numerous connections between copper misregulation and a variety of neurodegenerative diseases, have prompted interest in studying its roles in neurophysiology and neuropathology.

Brain Copper Homeostasis. Because of its central importance to neurological health and its propensity to trigger aberrant redox chemistry and oxidative stress when unregulated, the brain maintains strict control over its copper levels and distributions[51-52]. An overview of homeostatic copper pathways in the brain is summarized in the Figure below.

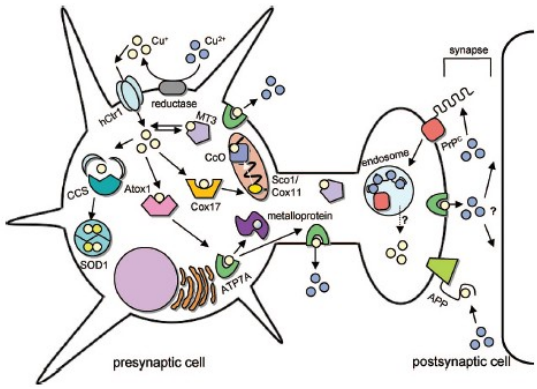

Fig. 8. A schematic model of neuronal copper homeostasis

Many of the fundamental concepts for neuronal copper homeostasis are derived from rigorous studies of simple model bacterial or yeast microbes, but the brain provides a more complex system with its own unique and largely unexplored inorganic physiology. For example, work by O'Halloran and co-workers indicates that there is little "free" copper in the cytoplasm of bacteria and yeast, which is due to the tight regulation of metallochaperones. However, many open questions remain concerning the homeostasis of organelle copper stores, particularly in higher organisms with specialized tissues. In this context, Winge and co-workers have presented data that suggests that even yeast possess stores of labile copper in their mitochondria[53].

Uptake of copper by the blood-brain barrier (BBB) is not well understood but is proposed to occur through the P-type ATPase ATP7A, which can pump copper into the brain. Mutations in this specific gene lead to *Menkes disease*, an inherited neurodegenerative disorder that is characterized by global brain copper deficiency. This phenotype is mirrored by *Wilson disease*, which involves mutations in the related ATP7B gene responsible for excretion of excess copper from the liver into the bile[54]. Loss of ATP7B function leads to abnormal build up of copper in the liver. The extracellular trafficking of brain copper is also different from that in the rest of the body. Cerebrospinal fluid (CSF), the extracellular medium of the brain and central nervous system, possesses a distinct copper homeostasis from blood plasma, which carries copper to organs throughout the rest of the body.

The primary protein or small-molecule ligands for copper in CSF remain unidentified. Uptake of copper into brain cells requires reduction of Cu^{2+} to Cu^{+}.

Following reduction, Cu^{+} ions can be transported into cells through a variety of protein-based pathways. For example, a major class of proteins involved in cellular

copper uptake is the copper transport protein (Ctr) family. Human copper transporter-1(hCtr1) is a representative member that is expressed ubiquitously in all tissues.

II.6 PATHOLOGICAL FUNCTIONS OF BRAIN COPPER

Copper Neuropathology. Disruption of copper homeostasis is implicated in a number of neuro degenerative diseases, including *Alzheimer's disease* (AD), *Prion diseases*, *Parkinson's disease* (PD), familial *amyotrophic lateral sclerosis* (fALS), *Menkes disease*, and *Wilson disease*.[55-56-57]

In all these disorders, the deleterious effects of copper stem from its dual abilities to bind ligands and trigger uncontrolled oxidation reduction chemistry.

The connection between copper and AD pathology is due mainly to its molecular reactions with APP and it's A_amyloid cleavage product (A_) that result in imbalance of extracellular and intracellular brain copper pools. The function of APP in the brain has not been fully elucidated but is plausibly linked to copper homeostasis[58-59-60]. However, aberrant binding of Cu^{2+} to APP triggers its reduction to Cu^{+} with concomitant disulfide bond formation; this misregulated metalloprotein intermediate can then participate in harmful Fenton-type chemistry. For example, the reaction between the APP-Cu^{+} complex and H_2O_2 causes oxidation to Cu^{2+} and APP fragmentation, leading to a cycle of oxidative stress and aggregation of A_ peptides that results in the ultimate formation of amyloid plaques in the extracellular cerebrospinal fluid. Extracellular amyloid deposits from the brains of AD patients are rich in Cu in addition to Zn and Fe, and Raman studies of senile plaques reveal Cu^{2+} centers bound by histidine donors that can result from direct cascade reactions between Cu^{2+} and A_peptides.

Moreover, administration of Zn/Cu chelators such as clioquinol can redistribute brain metal pools and reverse amyloid aggregation[61]. Finally, addition of Cu^{2+} to cell cultures alters APP processing, resulting in increased levels of intracellular and secreted forms of APP and decreased levels of A_.

Prion diseases also have links to brain copper misregulation[62], where opposing Cu^{2+} and Mn^{2+} levels and availabilities may influence the conversion of the protease sensitive PrPC into the toxic, protease-resistant form, PrPSc.

PrPC can bind between four and seven Cu^{2+} ions at various binding sites, including the octapeptide repeat regions that have micromolar affinity for Cu^{2+}.

In one proposal for prion toxicity, PrPC is involved in copper homeostasis and binding of Mn^{2+} to the protein facilitates its conversion to toxic PrPSc; the resulting excess free copper further exacerbates the disease by promoting oxidative stress.

Onset of Parkinson's disease is accompanied by death of dopaminergic neurons and intracellular accumulation of Lewy bodies, which are protein aggregates of the brain protein R-synuclein. In its unmodified form, R-synuclein exists as an unfolded protein, but factors including oxidative stress and presence of various metal cations promote its fibrillation[63].

In particular, Cu^{2+} effectively promotes the self-oligomerization of R-synuclein through the acidic C-terminal region of the protein and its oxidation and aggregation in the presence of H_2O_2[64].

Structural details of the Cu^{2+}-R-synuclein interaction have been reported recently and identify two main copper binding sites in the protein.

One site is comprised of the carboxylate-rich C-terminus of the protein and has a micromolar affinity for copper. The other site binds copper with nanomolar affinity; initial reports suggested that both the N-terminus and His50 were necessary in Cu^{2+} binding, but more recent work refutes the involvement of His50 as a ligand.

Familial amyotrophic lateral sclerosis (fALS) is an inherited neurodegenerative disorder stemming from mutations in the copper-dependent metalloprotein Cu/Zn SOD1.[65]

Three main hypotheses exist regarding the molecular mechanism(s) of deterioration in this disease: (i) the loss-of function mechanism, which results in toxic accumulation of superoxide by lack of SOD1 protection, (ii) the gain-of function mechanism, in which SOD1 exhibits enhanced peroxidase activity by aberrant redox chemistry, and (iii) the aggregation mechanism, where SOD1 aggregates are formed by increased or decreased availability of copper for binding.

The roles of copper homeostasis in this disease remain ambiguous because modifications of the metal-binding domains in the enzyme active site can lead to activity associated with the loss- or gain-of-function mechanisms and mice expressing SOD1 mutants unable to bind copper ions still exhibit symptoms of ALS[66].

II.7 COPPER DETECTION METHODS

The broad participation of copper in both neurophysiological and neuropathological events has prompted demand for ways to trace this metal in biological systems. In this regard, both major oxidation states of copper, the $4s^2 3d^{10}$ cuprous oxidation state (Cu^+) and the $4s^2 3d^9$ cupric oxidation state (Cu^{2+}), are important for rigorous considerations of its chemistry in natural settings. Radioactive copper isotopes such as ^{67}Cu[336] and atomic absorption spectroscopy have proven to be useful for studying many aspects of copper biology but lack spatial resolution and cannot differentiate between Cu^+ and Cu^{2+} .

The existence of two high abundance naturally occurring isotopes of copper, ^{63}Cu (69.17%) and ^{65}Cu (30.83%), has also been exploited to study copper in specific organs by analyzing the $^{63}Cu/^{65}Cu$ ratio using inductively coupled plasma mass spectrometry (ICP/MS) or thermal-ionization mass spectrometry (TIMS).444–447 These methods are quite useful for studying complex organisms but again lack subcellular resolution and cannot distinguish between different oxidation states of copper. Finally, a myriad of histochemical indicators have been developed to stain for copper, including hemotoxylin, rubeanic acid (dithiooxamide), rhodanine and diphenylcarbazide, diethyldithiocarbamate, dithizone, Timm's staining, orcein, and bathocuproine disulfonate (BCS). A modified Timm's method using trichloroacetic acid can isolate Cu^{2+} pools with some fidelity,460 whereas BCS is a dual colorimetric and fluorescence quenching indicator for Cu^+ and Cu^{2+}. The main disadvantages of these histochemical stains are that they cannot image copper in living samples and are limited in terms of metal and redox specificity.

Many different solutions have been proposed but, among them, sensing systems based on nanoparticles are certainly one of the most interesting and promising. In particular, the use of *dye-doped silica nanoparticles*[67] can offer intriguing advantages in this field, such as a great sensitivity enhancement through the occurrence of amplification processes, the possibility to have an internal reference signal, thus avoiding further calibrations, and good water solubility. An additional interesting feature is the possibility to monitor chemical species *in vivo*, since silica is a biocompatible material. This feature could be of crucial importance: metallostasis alteration, namely, zinc and copper homeostatic levels, has already been observed both in the biological fluids and tissues of patients affected by breast, prostate, lung and gastrointestinal tumours and in some neurodegenerative disorders like Parkinson's (PD) and Alzheimer's diseases (AD).

In particular, copper has been implicated in Amyloid β peptide (Aβ) aggregation and neurotoxicity and it is generally accepted that in AD brains there is an excess of Cu in the extracellular space and in amyloid plaques. On the other hand, a decrease of the intracellular copper in AD as compared to healthy control brain is also reported. All these findings explain the need for new efficient chemosensors for copper ions.[68]

II.8 ENANTIOSELECTIVE OXYGEN TRANSFER

Enantioselective catalytic reactions in which the chirality of an asymmetric catalyst induces the preferred formation of a given product enantiomer have been one of the most important achievements in chemistry during the 20th century. Initially the successful enantioselective reactions using homogeneous chiral catalysts were limited to stereospecific alkene hydrogenations using chiral binaphthylphosphine ligands[69] and to the Sharpless epoxidation of allylic alcohols using tartaric acid derivatives as ligands[70-71].

After proof of the principle of enantioselective catalysis, there was an evident interest in expanding these results to virtually any substrate as well as for any reaction type.

In this context, a limitation of the Sharpless enantioselective epoxidation was the failure to induce enantioselectivity in simple alkenes lacking allylic hydroxy groups. For this reason, the report by Jacobsen and Katsuki that chiral (salen)-Mn(III) complexes act as highly enantioselective catalysts for the asymmetric epoxidation of simple alkenes constituted a breakthrough in the field of asymmetric catalysis[72a-e].

Following the lead of alkene epoxidation, Jacobsen, Katsuki, and other groups expanded the scope of enantioselective catalysis to other reactions[73a-f]. The outcome of this body of research is that metal complexes derived from chiral salen ligands are among the most powerful enantioselective catalysts. The importance of chiral salen ligands in enantioselective catalysis is due to the high enantiomeric excesses that can be achieved and their general applicability to many different reaction types. Apparently, chiral salen ligands with bulky substituents create a strongly stereogenic environment at the active metal center, producing a remarkable discrimination between the two transitions states leading to each enantiomer. The result is a very effective transmission of chirality to the reaction product for a broad range of substrates and reaction types.

One general trend in catalysis is to develop systems that allow the recovery and reuse of the catalyst[74].

Environmental concerns together with economic considerations make necessary and convenient this recovery. The high catalyst cost, usually considerably much higher than that of the products, can be affordable in commercial applications only when the productivity of the catalyst, measured as total kilograms of product produced per kilogram of catalyst, is sufficiently high to make the process economically viable.

On the other hand, the principles of green chemistry require industry to make all necessary efforts to minimize wastes, particularly those of substances that contain noxious transition metals such as those typically present in metallic catalysts.

There have been published numerous reviews and account describing the use of salen-metal complexes as catalysts, including enantioselective reactions, focusing mainly on the outcome of the reaction[75-76].

The various kind of metal complexes, the reaction's type and the enantiomeric excesses (e.e) obtained catalyzed can be summarized on the table below :

Metal Salen Complexes	*Reactions*	*e.e (%)*
Mn	**Alkene epoxidation**	**89-99**
Cu	Alkene aziridination	30-98
Cr	• Epoxide ring opening	81-95
	• Hetero Diels-Alder	70-93
Co	Epoxide cinetic resolution	84-98
Al	• Conjugate addition of cyanide to α,β unsaturated imides	87-98
	• Addition of cyanhydric acid to imines (Streker-reaction)	37-95
Ru	• Sulfimidation	8-99
	• cyclopropanation	78-99
Ti	Sulfoxidation	92-96
Zn	Addition of diethylzinc to aldehyde	69-91
V	• Cyanosilylation of aldehyde	
	• Cyanidrine synthesis	68-96

An important aim to achieve for these catalysts is the reusability and the strategies that has been developed to recover chiral salen complexes are of general applicability for other types of metal complexes or ligands. Thus, it can be assumed that most of the methodologies described for chiral salen complexes have been already used or can be used for other complexes as well. However, there are notable differences in the synthetic routes depending on the actual structure of the ligand. Some of the peculiarities of salen ligands arise from the ease and mild conditions required for their synthesis, which, in the most frequent case when the two phenolic moieties are identical, is a single-step process.

In the simplest approach, the salen-metal complex can be exactly the same as that used in conventional organic solvents, without the need of functionalization that may require dedicated organic synthesis. In the case of *homogeneous catalysis*, separation of the reaction mixture from the catalyst after the reaction finishes has to be done on the basis of selective filtration, extraction, crystallization, etc., of the products while the catalyst is retained in the phase where the reaction has occurred. Homogeneous phase recoverable systems enjoy several advantages with respect to heterogeneous catalysts including:

(i). the maximum synthetic economy because no special salen functionalization is needed
(ii). higher reaction rates
(iii). simpler kinetics because no interfacial mass transport is occurring.

Most of the disadvantages of the homogeneous phase arise from the difficulty in designing continuous flow processes for this type of catalysis and catalyst recovery. Furthermore when the salen metal complex is in a solid phase, being inorganic, carbonaceous, and polymeric or hybrid organic-inorganic.

Catalysis is *heterogeneous media*, and the solid can be immobilized in a fixed bed reactor or can be suspended in the reaction medium using stirred tank reactors and recovered by filtration. Prototypical industrial catalysts are solids, because this allows the design of continuous flow processes. However, preparation of supported salen complexes requires indefinitely stable complexes, and a suitable funtionalization to bind the complex to a solid; otherwise, long-term leaching of the metal from the solid to the fluid phase and/or complex decomposition can occur. Also, kinetics in heterogeneous catalysis can be controlled by diffusion and mass transport through the interfacial surface. These aspects determine that, normally, heterogenization used to be considered as the last step in the evolution toward a reusable and recoverable catalyst[77].

However, recent developments in homogeneous catalysis based on the use of novel "green" liquid media may lead to changes in the preference for heterogeneous versus homogeneous catalysis.

II.9 CHIRAL SALEN COMPLEXES

The word "***salen***" is an acronym widely used to denote a family of bis-imine compounds having a structure derived from the *N*,*N*'-bis(salicylidine)ethylenediamine. The first salen-metal complex was probably reported by Pfeiffer et al. in 1933[78]. Salen ligands are generally obtained by the uncatalyzed condensation of a salicylaldehyde with a 1,2-diamine. The numbering corresponding to the carbon of the phenolic moieties has been shown in Scheme 1. The imine functional group is generally known as a Schiff base.48 Schiff bases are among the most general N ligands, because the basicity of the sp^2-hybridized N lone pair, although lower than that of amines (sp^3 hybridization), is well suited to form complexes with metal ions. The salicylidene imine group is prone to undergo an acid-catalyzed hydrolysis, reverting to the corresponding salicylaldehyde and diamine in the presence of water.

However, the stability of the Schiff base group increases considerably upon coordination with a metal ion and formation of the salen-metal complex. For this reason, in contrast to the salen ligand, the salen-metal complex can be used in

wet solvents or even in aqueous media without undergoing hydrolysis.

Chiral salen ligands are easily synthesized starting from enantiomerically pure diamines. 1,2-Cyclohexadiamine and 1,2-diphenylethylene-1,2-diamine are the two chiral diamines most frequently used. Chiral salens together with 1,1'-binaphthyls and bisoxazolidines are the chiral ligands that have been used to develop the most powerful metallic complexes in asymmetric catalysis.

For most of the transition metals, the corresponding metallic complex using salen as ligand has been reported for instance includes among other metals Mn, Cr, Co, V, Cu, Ti, Ru, Pd, Au, Zn, and Al. Depending on the tetradentate N_2O_2 or pentadentate N_2O_2X coordination around the metal center, the complexes exhibit a distorted square planar or square pyramidal geometry[79-80]. Distorted octahedral $N_2O_2X_2$ coordination has been very frequently postulated for many intermediates involving salen-metal complex catalysts.

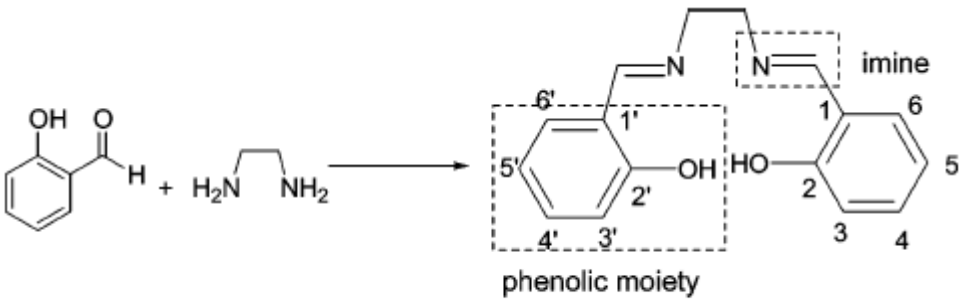

Scheme 1. Preparation of Salen Ligand and Numbering of Their Phenolic Moieties

Chiral salen complexes have been found to act as catalysts of many different reaction types including alkene epoxidation, epoxide ring opening, cyclopropanations, aziridination, selective hydrogenations, carbonyl cyanosilylation, imine additions, and others. The table mentioned above provides a list of the reaction types reported using non recoverable chiral salen complexes, together with the enantiomeric excess (*e.e*) achieved in each reaction and leading references.

II.10 METHODOLOGIES TO TRANSFORM HOMOGENEOUS SALEN-METAL COMPLEXES INTO REUSABLE CATALYSTS.

The trend toward the commercial production of optically pure compounds in the pharmaceutical and fine chemical industries has undoubtedly increased in recent years[81].

Among the various methods to selectively produce a single enantiomer, asymmetric catalysis is the most attractive method due to its synthetic economy and amplification of chirality. However, the contribution of asymmetric catalysis to the overall production of chiral chemicals is growing at a much slower rate than originally expected. The main reason for this slow industrial implementation is the need to have reusable chiral catalysts.

One of the major drawbacks of homogeneous enantioselective catalysis is the need for separation of the extremely expensive catalysts from the reaction mixture at the end of the process. Given the high value of the chiral catalysts, their recovery is a necessary condition to the development of a viable industrial process. Recoverable enantioselective catalysts with a high productivity are, therefore, necessary from the industrial point of view.

For these reasons, a general evolution in catalysis is the transformation of successful homogeneous catalysts into recoverable catalytic systems that can be easily separated from the reaction mixture and reused multiple times without the loss of the high activity and selectivity characteristic of the original catalyst. In addition, to minimize the impact of the high cost of ligands and metals on the products, process design and waste minimization often require catalyst immobilization and catalyst recovery. On the one hand, the conversion from a batchwise operation to a continuous flow process is facilitated by having the catalyst in a separate phase. On the other hand, complexes may have some noxious metal that have to be completely removed (even in trace quantities) from the reaction products and the disposal of which may be harmful for the environment and would require special handling.

Among the different strategies that have been used for the purpose of converting highly efficient homogeneous catalysts into recoverable and reusable catalytic systems, the simplest one consists of using the same complex, but changing the medium from conventional volatile organic solvents to novel “green” liquids. The necessary condition is that the catalyst has to remain in the novel liquid, whereas the products have to be separated by extraction, distillation, precipitation, membrane filtration, or other physical means. Given the relatively large molecular weight and structure of most catalysts, and specifically here those metal complexes based on salen ligands, the selective solubility requirement is often easily met when the liquid-liquid extraction is performed with an immiscible solvent with low solubility power such as an alkane or an ether. Organic products are commonly more soluble in such solvents than salen-metal complexes.

In this regard, the usual trend has been to combine the recovery of the catalyst with the use of an environmentally friendly novel medium. On the basis of the principles of green chemistry aimed at avoiding or reducing the use of volatile organic solvents, for liquid substrates one option is to perform catalytic reactions under solvent-free conditions.

However, in many cases solvents are still needed. Solventless conditions have as a general limitation the fact that the reaction products may act as quenchers or inhibitors of the catalyst. An important role of solvents in catalytic reactions is to assist desorbing products from the catalytic sites. Also, even though solventless conditions may be considered as ideal from the environmental point of view, this is true only when substrate conversion reaches very high percentages.

Otherwise, product separation and catalyst recovery from unreacted starting material may be even more difficult, hazardous, or environmentally unfriendly than using conventional organic solvents.

Among the novel solvents that have been considered "green" as opposed to conventional volatile organic liquids, the most frequently used are water, perfluorinated liquids, supercritical fluids, and ionic liquids. Given the importance of salen-metal complexes, examples of the use of salen metal complexes as catalysts in any of these green solvents have been reported and reusability accomplished with a variable degree of catalyst activity decay.

In addition to the previous approach based on homogeneous catalysis in special liquid media, the next evolution for developing a recoverable and reusable catalytic system is transforming a homogeneous into a heterogeneous catalyst.

Heterogeneous catalysts are easily separated from the reaction mixture and can be recovered and reused provided that they do not become deactivated during recycling. Also, if deactivation occurs, a suitable reactivation protocol can be devised to regain most of the initial activity, as, for instance, replenishing the depleted metal ions.

The simplest methodology to accomplish is to support the active salen-metal complex onto or into an insoluble solid. The interaction between the complex and the support can range from physisorption to Coulombic forces and covalent anchoring. It is generally assumed that the latter approach, even though synthetically more demanding, gives the strongest complex-support binding, but, as we will show, this assumption should not be taken for granted and must be critically evaluated in each case. Concerning the support, it can be either organic polymers or inorganic oxides, each of them having advantages and limitations with respect to the other. The complex supported on a solid can be simply separated from the reaction mixture by filtration or placed in a continuous flow reactor[82].

II.11 STABILITY OF METAL SALEN COMPLEXES

Ideally for reusability, the complex has to be perfectly stable under the reaction conditions, a prerequisite that is difficult to meet. Although most of the salen-metal complexes have very high binding constants in the range of log K >20,70-72 demetalation of the complex can occur due to competitive complexation with reagents and products that can be favoured by changes in the metal oxidation state during the catalytic cycle. Metal oxide formation is also common depending on the pH at which the reaction is performed and the presence of bases.

Besides demetalation, ligand degradation is also an important cause of complex instability, particularly when the catalytic reaction requires the presence of strong acids or oxidizing or reducing reagents. Acids can cause demetalation by protonation of the phenolate groups. This demetalation leads to the metal-free salen ligand that, as was stated earlier, is very prone to undergoing hydrolysis to salicylaldehyde and diamine.

Oxidation reactions require the presence of an oxidant in addition to certain acidic or basic conditions. Oxidizing reagents can attack the salen ligand at various sites including the imine and the phenolic ring. In general, Schiff bases can be easily oxidized. Reduction can also lead to complex degradation that is usually initiated by a reduction in the metal coordination number from penta- to tetracoordinate.

In addition to advantages in terms of reaction mixture and engineering of the process, heterogenization can be also advantageous from the point of view of catalyst stability, as immobilization frequently improves catalyst stability compared to the homogeneous analogues. This stabilization can be attributed to steric constraints and site isolation that minimize complex degradation.

In general, it can be said that there is a paucity of studies dealing with salen-metal complex degradation even though these studies are necessary to assess the maximum theoretical productivity of the catalytic system. These stability studies should be performed prior to the determination of the most suitable immobilization procedure, because it may be useless to anchor a complex that will become degraded in a few catalytic cycles. Nevertheless, from the literature reports about reusability, it can be deduced that salen complex stability is significantly reduced in the presence of oxidizing reagents, as for instance in alkene epoxidation, and less problematic for epoxide ring opening and other nucleophilic additions.

Kim and co-workers have recently developed a novel concept of heterometallic chiral salen catalysts formed by the addition to chiral salen Co(II) of an alkali earth halide (BF3, AlX3, or GaX3) in a molar ratio of 2:1[83a-c]. Apparently the Lewis acid acts as bridge of two salen complexes forming a dimer that is more active and selective than the monomer for the asymmetric ring opening of terminal epoxides or hydrolytic kinetic resolution of terminal epoxides. Although the idea of obtaining dimeric and oligomeric salen units with enhanced catalytic activity by simple interaction with Lewis acid halides is certainly interesting and represents high synthetic economy, the stability of these entities is low and they are not sufficiently

stable to be reused, due probably to hydrolysis of these entities under reaction conditions.

On the negative side of supporting a chiral catalyst is the fact that the enantioselectivity of the heterogenized catalyst is commonly lower than that of the analogous salen-metal complex in solution. Although the origin of this lower asymmetric induction must be determined and addressed in each specific case, a general cause of negative influence on the asymmetric induction ability of supported chiral catalysts is the disturbance that the support imposes on the approach of the substrates to the metal centre. For this reason, although not frequently the subject of detailed study, the tether or linker connecting the complex and the support has to be of sufficient length to allow the complex to move into the liquid phase far from the solid surface. In this way, there is a continuous effort to develop more efficient and practical immobilization methods for homogeneous chiral catalysts.

II. 12 REUSABLE CHIRAL SALEN COMPLEXES SUPPORTED ON INORGANIC SOLIDS AS HETEROGENEOUS CATALYSTS

Inorganic solids have been widely used as supports of chiral salen complexes. In the past decades there has been an enormous evolution in the strategies to immobilize salen complexes in inorganic supports, going from the encapsulation within the cavities of tridirectional large-pore zeolites of homogeneous salen complexes without any specific functionalization for this purpose to synthetically more demanding methodologies whereby specific salen complexes with appropriate structures have been synthesized to effect covalent immobilization on the support.

The use of inorganic solids has some advantages over other types of supports. The chemical and thermal stability of the inorganic supports makes them compatible with the widest range of reagents and experimental conditions. Also, mechanical resistance of the solids makes these inorganic particles less prone to attrition due to stirring and solvent attack during their use in a chemical reactor under continuous operation. One of the major problems in the design of an Industrial process is the possible decrease of catalyst particle size due to mechanical abrasion, this issue being particularly important when polymer beads are used as supports.

It's possible to divide the immobilized salen-metal complexes into/onto inorganic supports in three main groups on the basis of the support-catalyst interaction:

a. encapsulation within the cages of tri-directional large-pore zeolites using a methodology generally known as "*ship in a bottle*" (SIB) synthesis, the resulting salen complex becoming mechanically immobilized

b. immobilization by weak dipolar or strong Coulombic interactions, where in the latter case the salen complex is adsorbed onto the support by ion-pairing with an anionic or cationic solid

c. connection by covalent bond of the salen ligand and the support, which requires the necessary functionalization of the complex to allow the immobilization.[84]

III. AIM OF THE WORK

This work aims to explore the possibility of design, synthesize and test capabilities, firstly in solution and then into the solid state later on in the form of monolayer new molecules, that present the ability to recognize a substrate and to transform this recognition event into a detectable signal or into a real reaction. What we expect is a change of the optical properties of these compounds, for instance expressed by a colour switching or a fluorescence alteration both in solution and on the solid state.

During the first two year we synthesized a series of molecule in order to recognize nerve agent simulant like DMMP (dimethylmethyphosphonate) by using firstly simple molecules as oximes (4-hydroxy benzaldoxime, 4-amino-3-nitro benzaldoxime) that is well known are used in the detoxification therapy after nerve agents exposure. Unfortunately the change of the behaviour of these molecule was not as we expected into the solid state because the detectable signal (that was expected to be a weak interaction) was too low in order to think to transform this monolayer into a device, so we decided to move our research into another class of compounds at last to achieve a higher detectable signal by using aza-compounds (4-hydroxy-2'-nitro-4'-oxime-azo-benzene and 4-hydroxy- 4'-oxime-azo-benzene) with the same oxime moiety, but in this case we used as recognition event a reaction by using another nerve agent simulant DCP (diethylchlorophosphate). The solution measurements are promising and we are going to perform the same test on solid state.[29-36]

Another aim of our research was to selectively recognize biological important metal transition ions as Cu^{+} and Cu^{2+} both in solution and into solid state by colorimetric or fluorescent essay; for this purpose we employed organic scaffolds that show a change of one of the properties mentioned above, for instance aromatic rings that bear chromophoric groups or napthyl amide derivates, covalently bonded with functional groups, such as di-picolyl amine, that as it is well known have not only a great change in their photochemical behaviour but also they present great selectivity.[32-42]

We synthesized a novel N-tyramine-di[2(dipicolyl)amino]1,8 naphtalimide that showed the ability to selectively recognise Cu^{2+} as we expected[85], and then we try to synthesized another derivate of this compound that bear in order three and four picolyl groups but we stopped our synthesis at the three armed derivate (that showed a good sensibility but not a great sensitivity); the four armed was too difficult to obtain (very low yields and difficulties in purification).

During the third year we focused our attention into the recognition of transition metal ions, specifically Cu^{+} and Cu^{2+}, in biological environment that is very important for in vivo and in vitro studies for many associated diseases related to the change of their homeostasis.[43-68]

Firstly we focused our attention on a bodipy derivate presented in literature, we embody this molecule into silica-doped-nanoparticles in collaboration with other research groups obtaining very promising results in the recognition of Cu^{+}.[86]
Secondly we synthesized a derivate of di[2(dipicolyl)amino]1,8 naphtalimide linked with a disaccharide (threalose, that shown to be very effective in inhibiting aggregation of the Alzheimer's related β-amyloid peptide Aβ and in reducing its cytotoxicity) in order to obtain a water soluble chemosensor; also this work is in partnership with another research group and the first results are promising.
We also studied the possibilities of selectively transfer oxygen onto a specific substrate for instance unfunctionalized alkenes[69-84] by using salen-Mn(III) complexes as catalysts, both in solution and on solid support, in order to obtain a reusable device.

IV. RESULTS AND DISCUSSION

IV.1 Synthesis of 4-hydroxy benzaldoxime

Commercially available 4-hydroxy benzaldehyde was reacted with hydroxylamine hydrochloride in ethanol like solvent under stirring for 6 hours, giving 87% of yields (**Scheme 1**).[87]

This compound was fully characterized using IR, m.p, ^{1}H-NMR, ^{13}C-NMR.

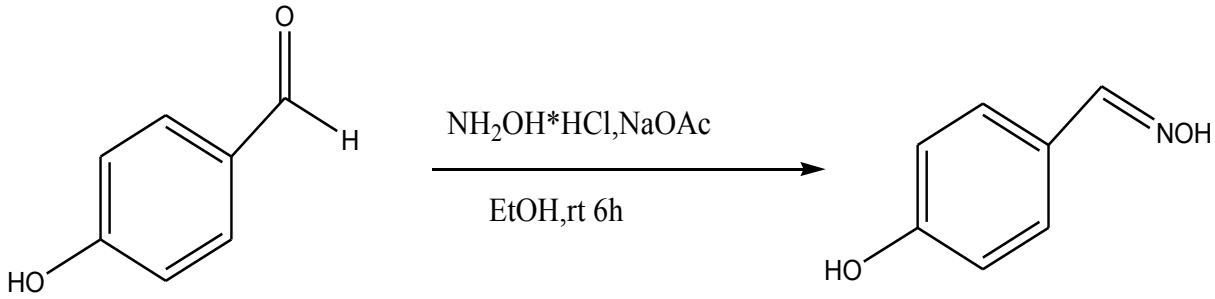

Scheme 2. Synthesis of 4-hydroxy benzaldoxime

IV.2 Synthesis of 4-amino-3-nitro benzaldoxime

Commercially available 4-acetamidobenzaldehyde was reacted with fuming nitric acid (> 90%). The nitro group is introduced into *meta* position in relation to the aldehyde functionality and the *ortho* position in relation to the amide group of the aromatic ring, forming 4-acetamido-3-nitrobenzaldehyde in moderate yield, typically around 50% , because of the concomitant formation of the corresponding di-nitro. Addition of hydrochloric acid to 4-acetamido-3-nitrobenzaldehyde subsequently produces 4-amino-3-nitro benzaldheyde in 80% yield.

This compound is converted into the oxime by reacting the aldehyde with hydroxylamine hydrochloride and sodium hydroxide in 70 % of yield. All these compounds were characterized by IR, m.p., ^{1}H-NMR e ^{13}C-NMR.[88]

STEP 1

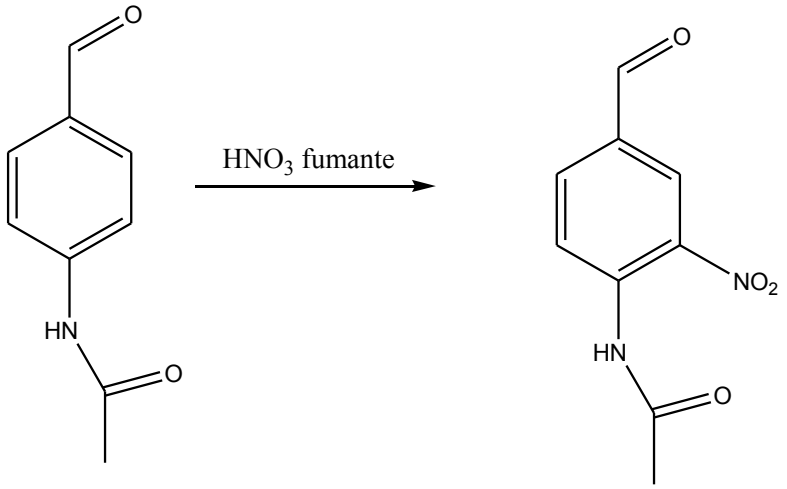

STEP 2

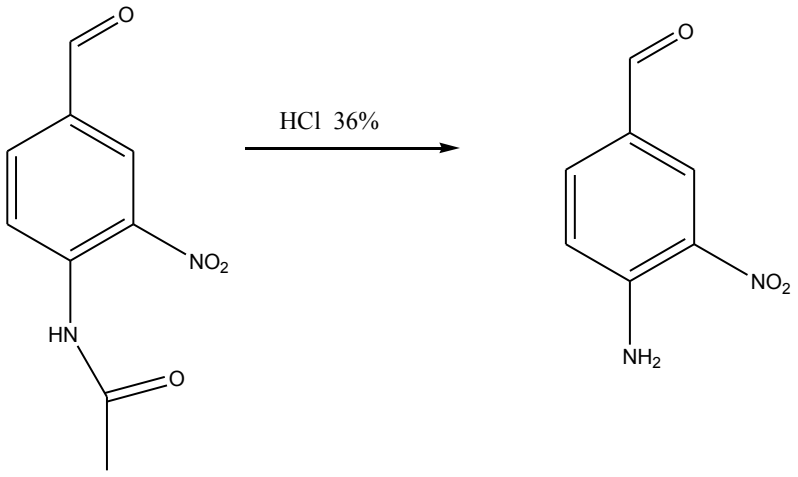

STEP 3

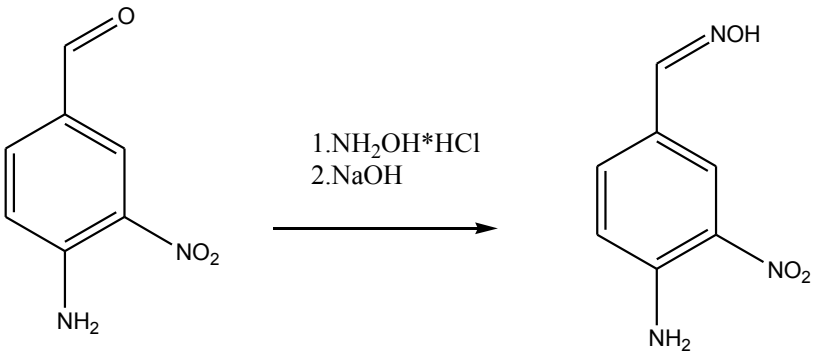

Scheme 3. Synthesis of 4-amino-3-nitro benzaldoxime

IV.3 Synthesis of 4-hydroxy-2'-nitro-4'-oxime-azo-benzene

This reaction consist of two steps; in the first one we have the formation of the diazo-compound that goes by adding to a suspension of 4-amino-3-nitro benzaldehyde an acid solution (hydrochloridric acid 24%) of sodium nitrite at 0° C for 40 minutes; when the diazotation reaction is completed we adjusted the pH of the solution to neutrality by adding a 6% solution of sodium hydroxide.[89]

Still stirring and cooling we added a basic solution of phenol (in order to obtain the fenolate intermediate). When the diazo copulation is completed the reaction product was precipitated by addiction of sodium chloride and filtered off.[90]

The crude product was recrystallized from acetic acid to give a bright orange product 80% yield.

The second step of this reaction consist of the formation of the oxime moiety by the reaction of the aldehyde sinthesized with hydroxylamine hydrochloride and sodium hydroxide to give a magenta powder with 60 % of yield. These compounds were characterized by IR , m.p., ^{1}H-NMR e ^{13}C-NMR and ESI-MS.

STEP 1

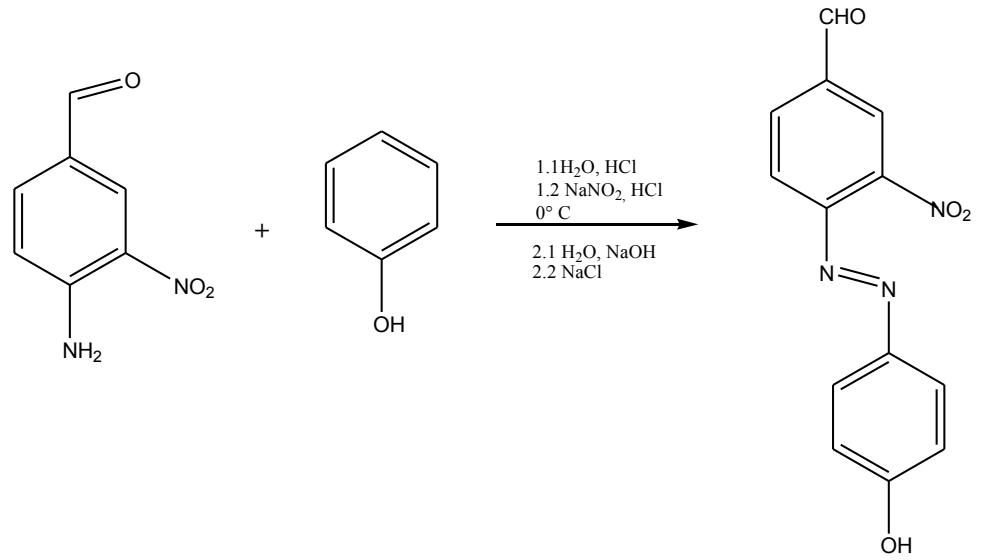

STEP 2

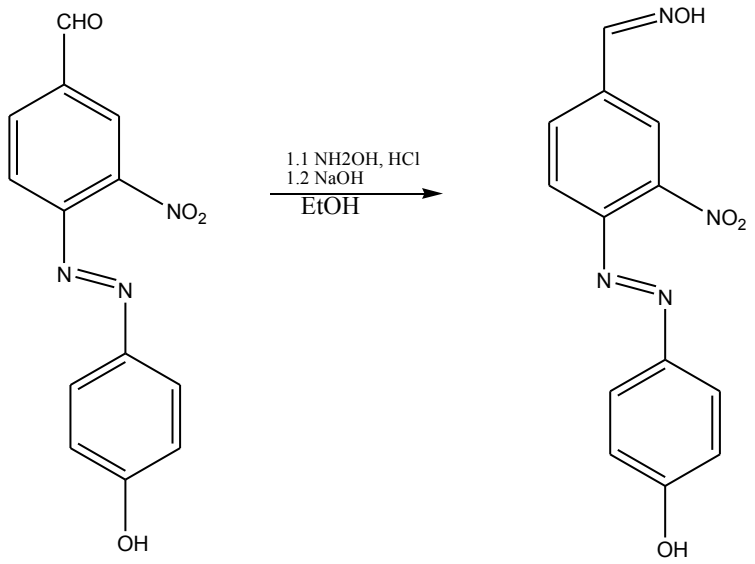

Scheme 4. Synthesis of 4-hydroxy-2'-nitro-4'-oxime-azo-benzene

IV.4 Synthesis of 4-bromoacenaphtene

To realize sensors able to give fluorescence variation, for instance emission enhancement or quenching of emission, in presence of a target analyte, there must be a fluorescent group. To this purpose naphtyl-derivaties are particular interesting because they present high quantum yield and also they are easy to functionalize.

4-bromoacenaphtene was obtained in 80 % yield by bromination of acenaphtene with N-bromosuccinimide in DMF.[91]

The compound was characterized by m.p., ^{1}H-NMR.

STEP 1

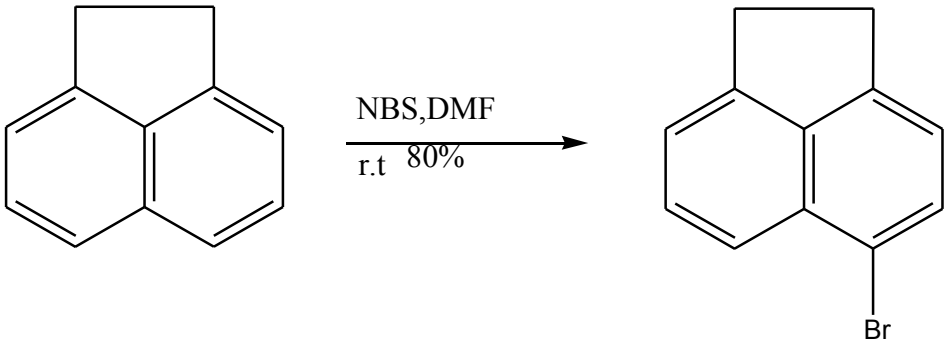

Scheme 5. Synthesis of 4-bromoacenaphtene

IV.5 Synthesis of 4-bromo-5-nitro acenaphtene

4-bromoacenaphtene was stirred into a solution of glacial acetic acid and a mixture of fuming nitric acid in glacial acetic acid.[92]

The compound was characterized by m.p., ^{1}H-NMR.

STEP 2

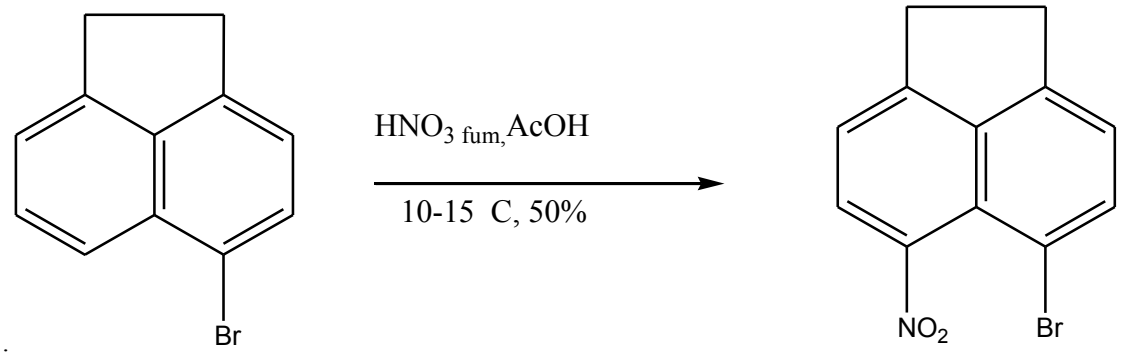

Scheme 6. Synthesis of 4-bromo-5-nitro acenaphtene

IV.6 Synthesis of 4-bromo-5-nitro 1,8 naphtalic anhydride

4-bromo-5-nitroacenaphtene was stirred into a mixture of glacial acetic acid and sodium dichromate and the resulting liquor whilst heating slowly to reflux.

The resulting solution was diluted with cold water, cooled and filtered. After filtration, the yellow-orange residue was washed with a little amount of glacial acetic acid and the crude collected stirred into a 3 % aqueous sodium hydroxide at 50 ° C.

After filtering the filtrate was neutralized with a 5% aqueous solution of hydrochloric acid, to give a cream-.orange needles of 4-bromo-5-nitro-1,8 napthalic anhydride.[92]

The compound was characterized by m.p., ^{1}H-NMR.

STEP 3

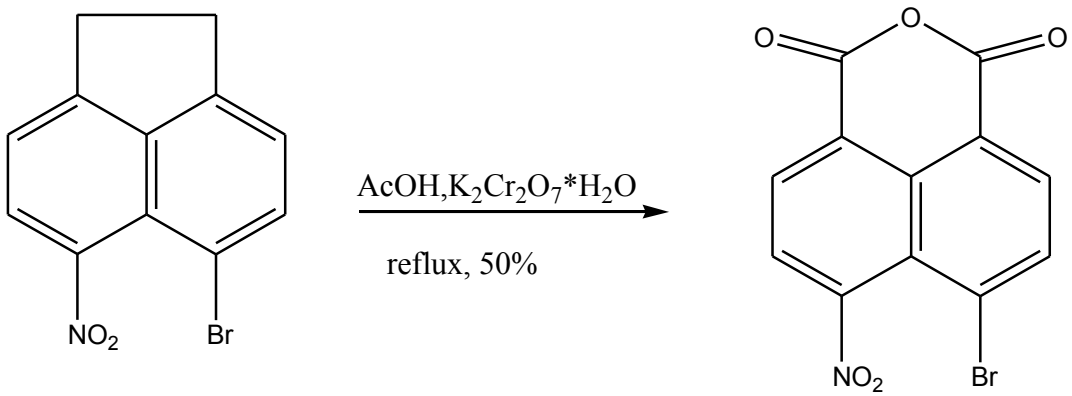

Scheme 7. Synthesis of 4-bromo-5-nitro 1,8 naphtalic anhydride

IV.7 Synthesis of 4-bromo-5-nitro naphtalimide

To a solution of 4-bromo-5-nitro-1,8 napthalic anhydride in ethanol was added dropwise tyramine in ethanol. The solution was heated to reflux and monitored by TLC. The crude product was then purified by column chromatography.[93]

The compound was characterized by ^{1}H-NMR and ESI-MS.

STEP 4

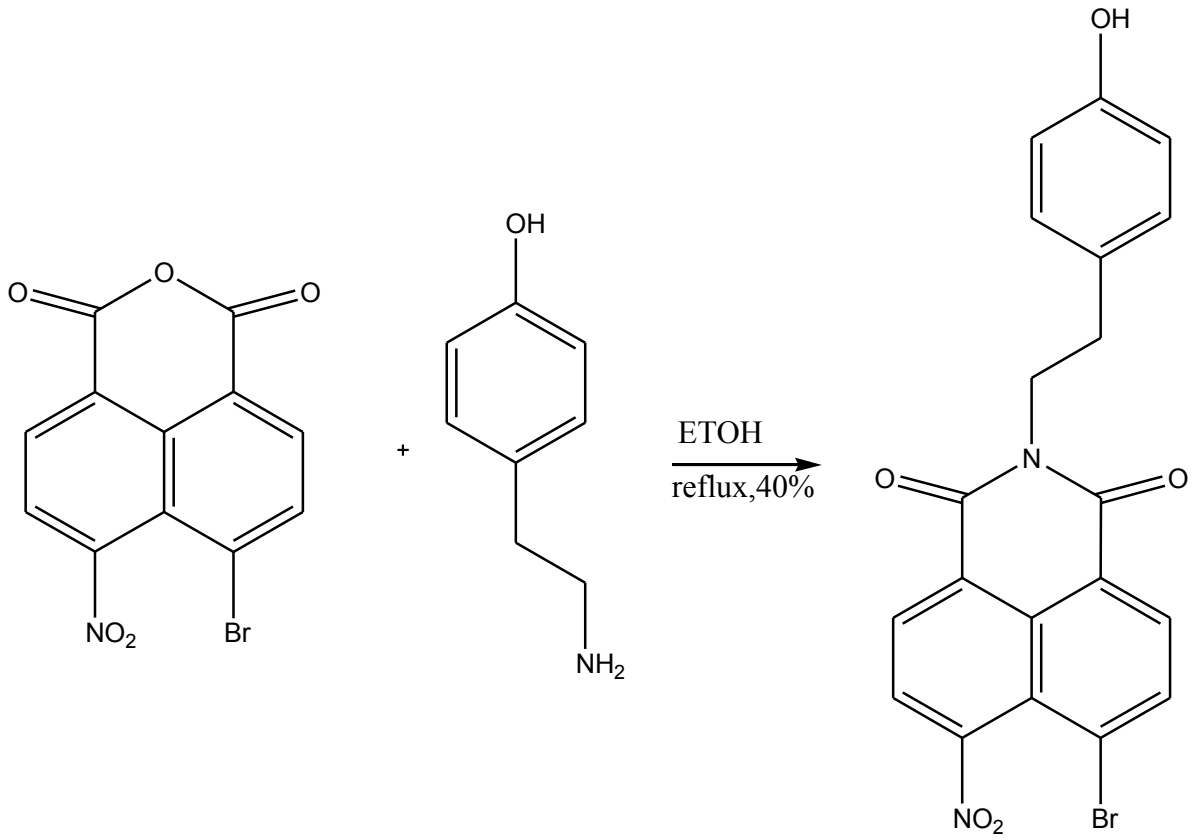

Scheme 8. Synthesis of 4-bromo-5-nitro naphtalimide

IV.8 Synthesis of N-tyramine-di[2(dipicolyl)amino]1,8 naphtalimide

A solution of picolyl-2-amine was added dropwise to a solution of N-tyramin-4-bromo-5nitro-1,8 napthalimide in 2-methoxyethanol and the mixture was quickly heated to reflux and the reaction monitored by TLC. After the reaction was completed, the solution was cooled. The crude product was then purified by column chromatography to give 80% yield.[94]

The compound was fully characterized by ^{1}H-NMR, ^{13}C-NMR, g-COSY, ESI-MS.

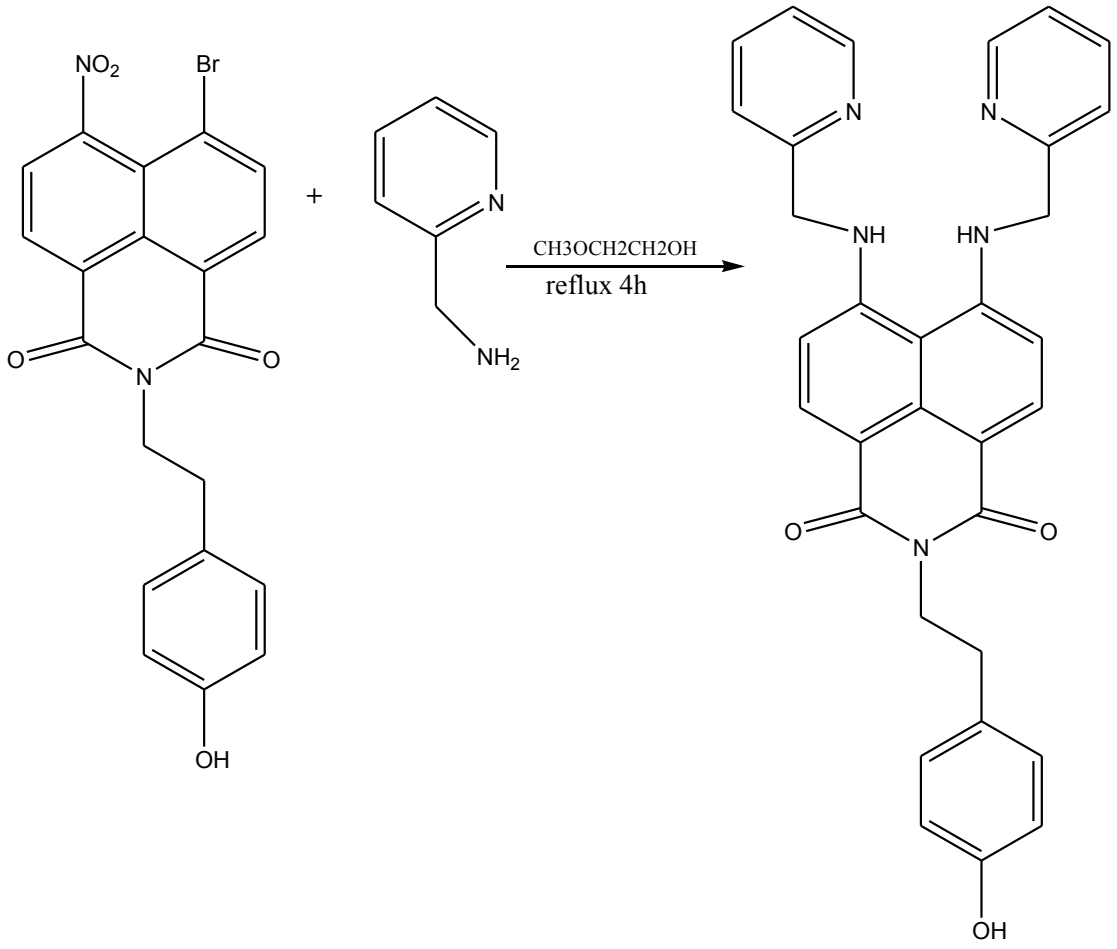

Scheme 9. Synthesis of N-tyramine-di[2(dipicolyl)amino]1,8 naphtalimide

IV.9 Synthesis of N-tyramine-tri[2-(dipicolyl)amino]1,8 naphtalimide

To a solution of N-tyramine-di[2-(dipicolyl)amino]1,8 naphtalimide in aceto nitrile dry were added picolyl chloride and potassium carbonate. The mixture were heated to reflux for 3h under nitrogen atmosphere and the proceed of the reaction was monitored by TLC.[94] The crude product was purified by alumina chromatography (CH_2Cl_2:MeOH 100:5) to give two products as shown in the **Scheme 9**. The predominant compound was fully characterized by ^{1}H-NMR, ^{13}C-NMR, g-COSY, ESI-MS.

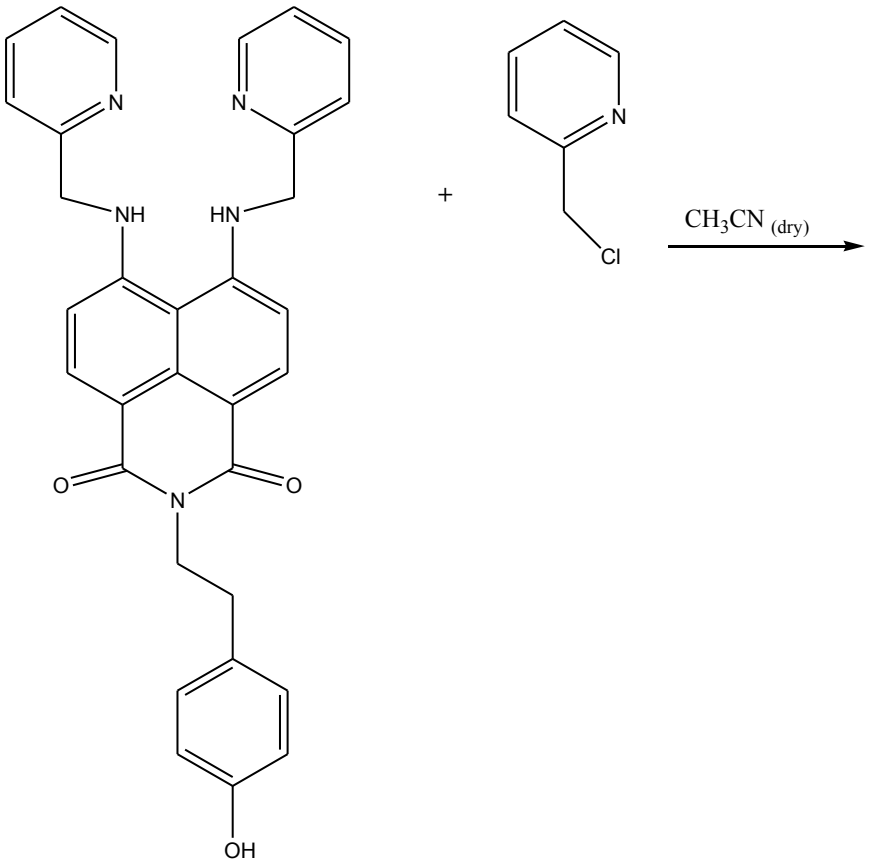

1

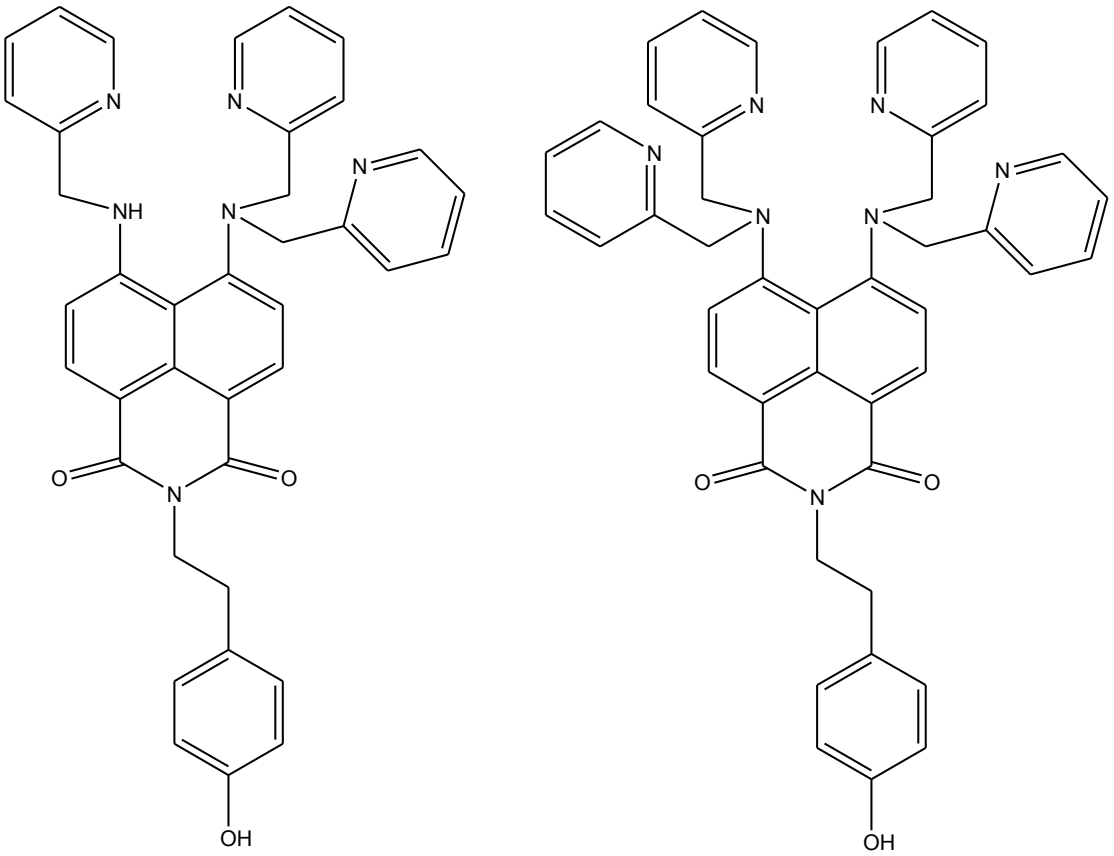

PREDOMINANT PRODUCT

2 **3**

Scheme 10. Synthesis of N-tyramine-tri[2-(dipicolyl)amino]1,8 naphtalimide

We also expected the formation of the product **3** but only a very few amount was formed, and we couldn't characterize it.

The reason why the predominant product is **2** could be attributable to the strong hydrogen bond between the pycolil amino arms which makes it difficult to remove from a base such as carbonate.

This hypothesis is reasonable if we compare the ^{1}H-NMR spectra carried out in different solvents as we can see in the **Fig. 7**.

In the next future what we are going to do is to start from the isolated product **2** and use a harder base such as NaH to extract this proton and to achieve the desired product in a good quantity.

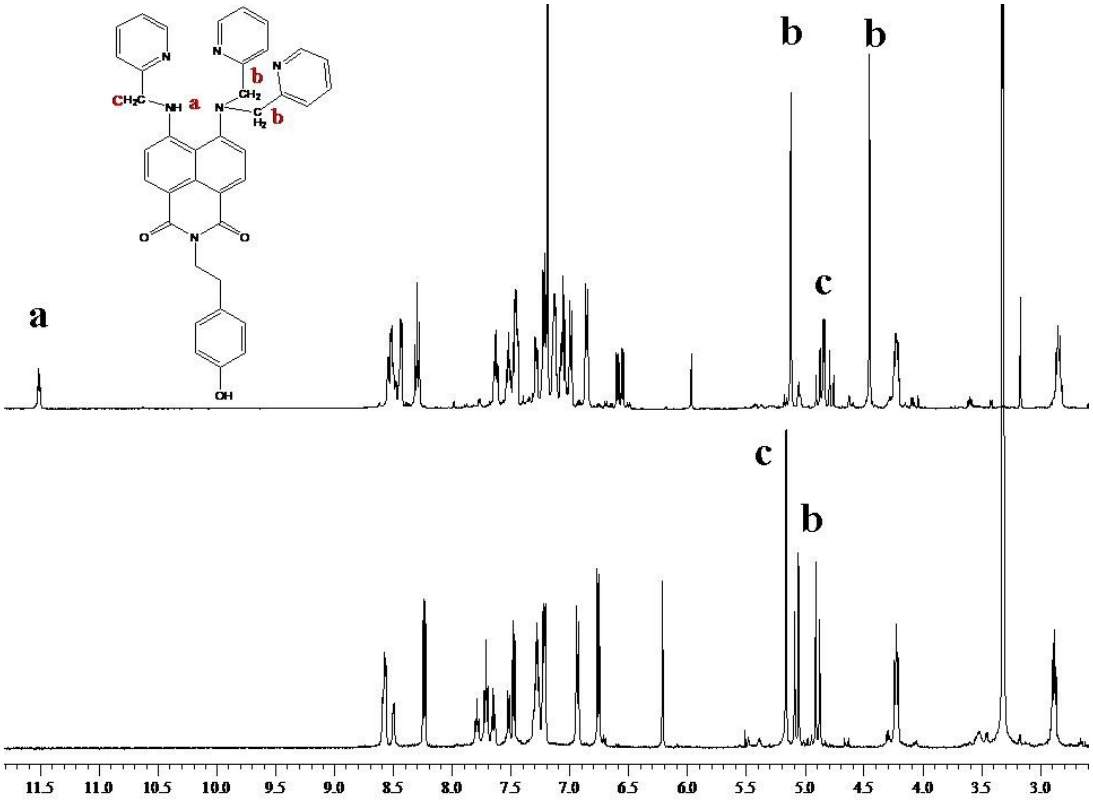

Fig. 10. ^{1}H-NMR spectra of 2 in $CDCl_3$ (up) and in acetone-d_6 (down)

In **Fig. 7** are reported the ^{1}H-NMR spectra of **2** in different solvent: the first spectrum has been recorded in $CDCl_3$; we can clearly see the signal of NH at 11.5 ppm as a triplet (we named this signal **a**); if we see the portion between 4.5 and 5.2 ppm we can distinguish three sets of signals: two singlets (4.46 and 5.12 ppm) named **b** due to two 2-pycolil-amino groups bonded to the same nitrogen and a multiplet centred at 4.84 ppm named **c**, that appears as a multiplet for the scalar coupling with the **NH**; each of them integate for 2Hs. This could indicates the presence of an hydrogen bond between two different nitrogens of the 2-pycolil-amino groups.

The second spectrum has been recorded in acetone-d_6; in this case we don't have the signal due to NH, and the portion between 4.5 and 5.2 ppm appears quite different from the previous: in fact we can observe that protons **b** splitting in two diastereotopic signals and **c** is now a singlet.

This evidence suggest that in polar solvents such as acetone we broke this hydrogen bond.

IV. 10 UV-VIS measurements

To verify the interaction between synthesized molecules and the simulant, DMMP (dimethymethylphosphonate), a molecule that is used widely in literature as a chemical agent that mimics chemical aggressive, UV-VIS studies have been performed to compare the behaviour in solution and on the monolayer.

All spectra were recorded at increasing amount of DMMP.

- **DMMP (dimethylmethylphosphonate) spectrum**

5,52 * 10^{-3} M

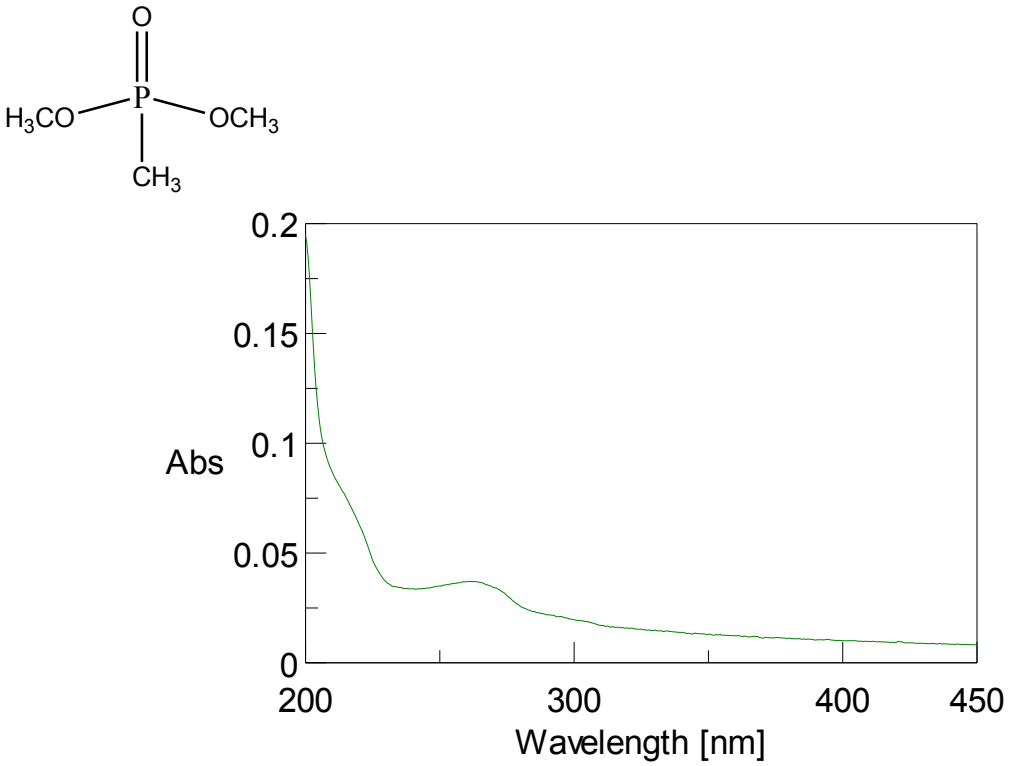

Fig. 9. UV- Visible spectrum of the stimulant

- **4-Hydroxybenzaldoxime**

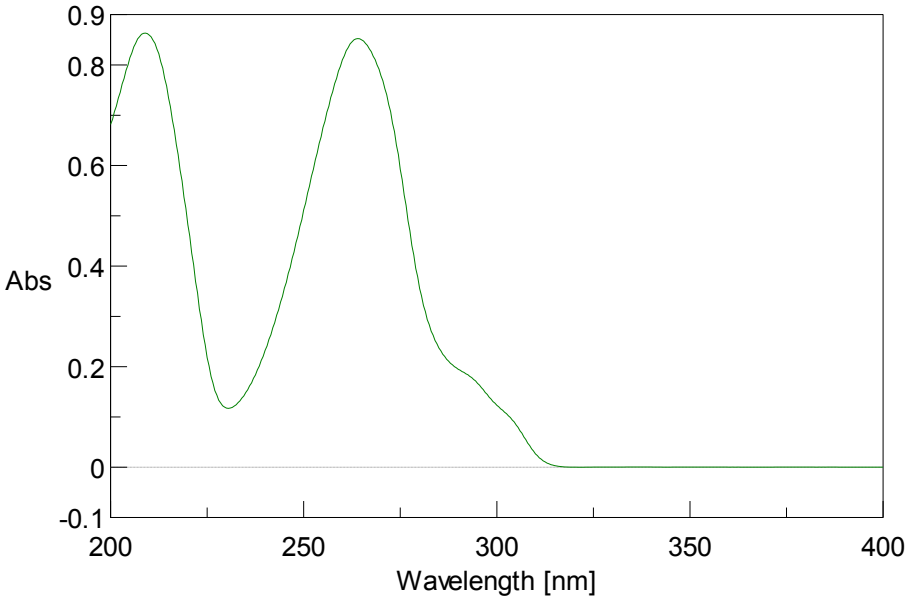

Fig. 10. UV- VIS spectrum of 4-OH-benzaldoxime

ε=4595; λ_{max}= 264 nm

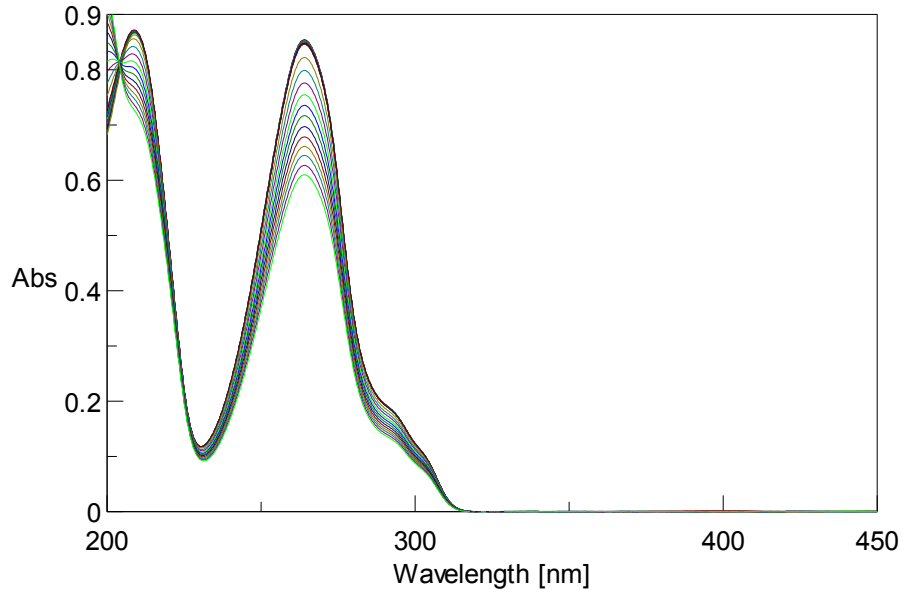

Fig. 10. UV- VIS spectra at differemt amount of DMMP added

- **4-amino-3-nitro-benzaldoxime**

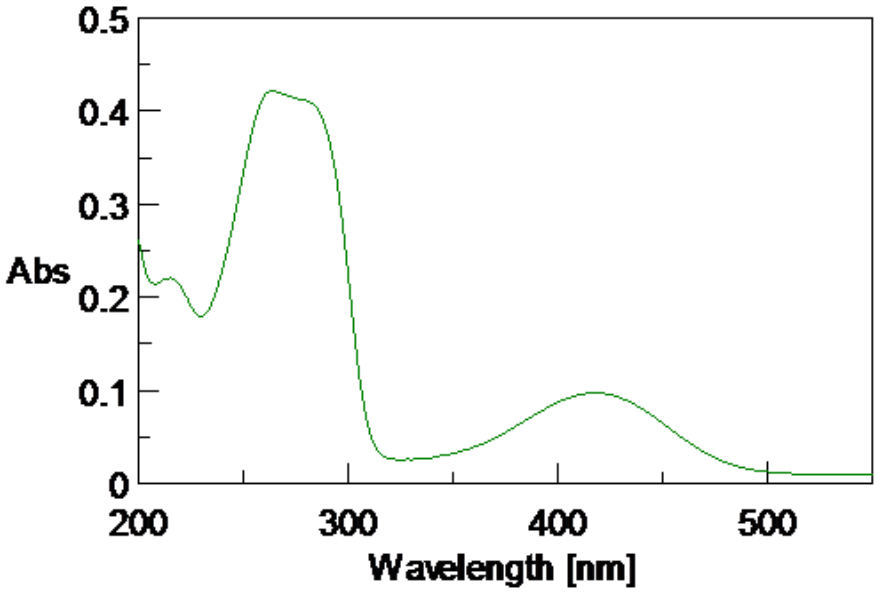

Fig. 11.UV-VIS spectrum of 4-amino-3-nitro benzaldoxime

ε=5000 **λmax= 264 nm**

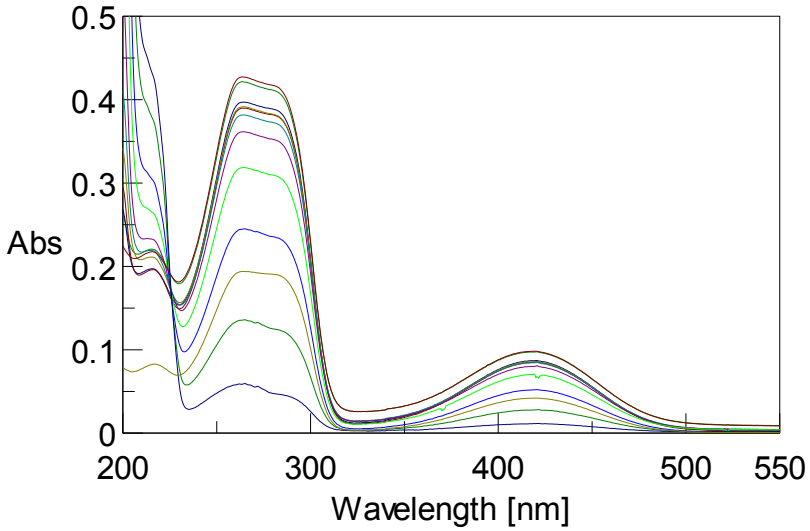

Fig. 12. UV- VIS spectra at differemt amount of DMMP added

As it's possible to see we had obtained very encouraging results in solution, the addition of simulant rates later observed a lowering of the band of the oxime portion, based on the calculation of the constants we obtained a value close to an hydrogen bond, so we decided to investigate by ^{31}P-NMR and T- ROESY experiments to verify what was the interaction that causes this phenomenon.

In order to achieve further information in support of this hypothesis, we performed the spectra in solution of ^{31}P-NMR at various ratios oxime / DMMP, and a study of two-dimensional 2D NMR T-ROESY related to 4-amino-3-nitro-benzaldossima. By ^{31}P-NMR spectra performed at different stoichiometric ratios of DMMP (**Fig. 13**) we observe a downfield shift of the signal, indicating an interaction between DMMP and the oxime used.

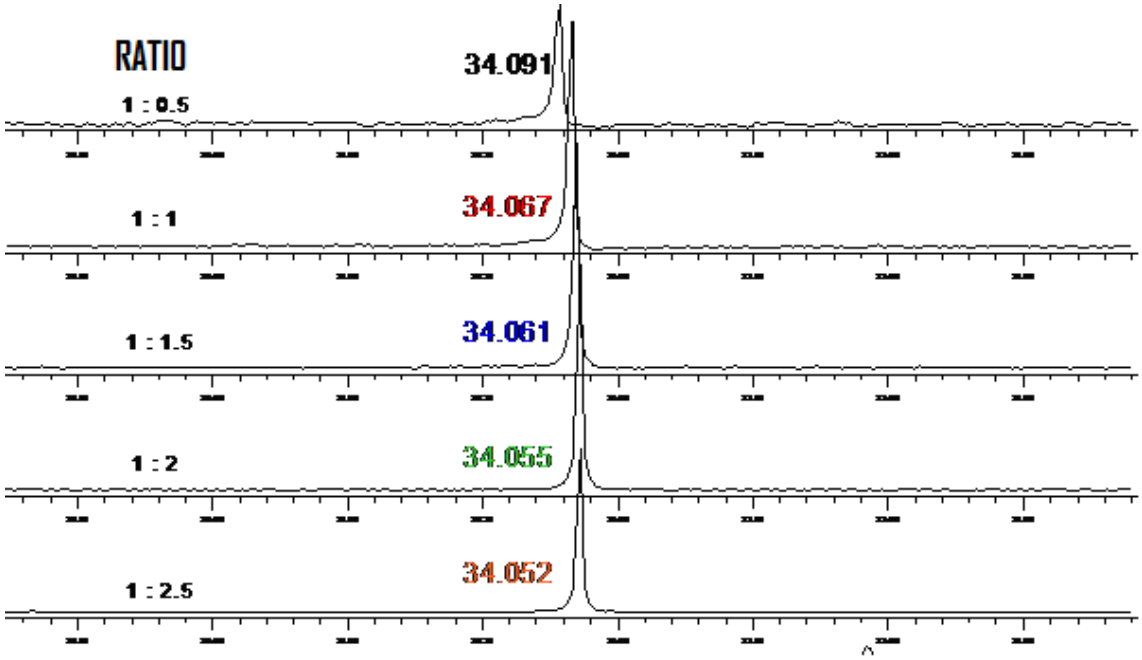

Fig. 13. ^{31}P-NMR titration

On the T-ROESY spectrum it's possible to see the interaction between C**H**=NOH portion and the methyl group of DMMP **CH_3**$PO(OCH_3)_2$ as is shown in **Fig. 14 - 15**.

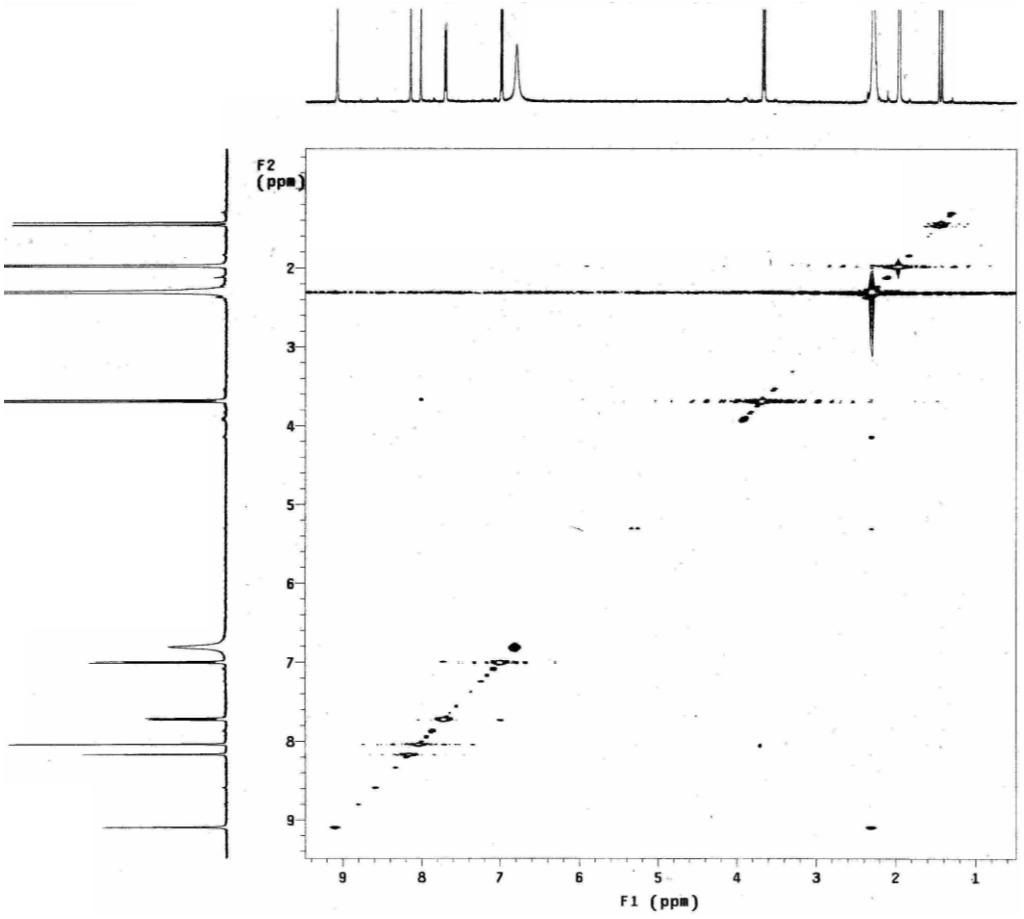

Fig. 14. T-ROESY spectrum

These results represent the first example of an interaction probably via hydrogen bonding between the oxime and the standard used as a nerve agent simulant DMMP that can have interesting implications for the manufacture of reversible sensors capable of detecting ppb of nerve gases present environment.

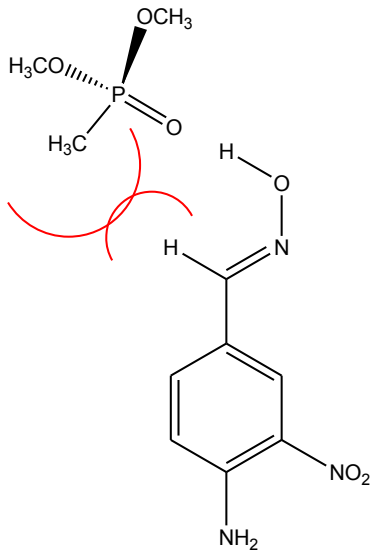

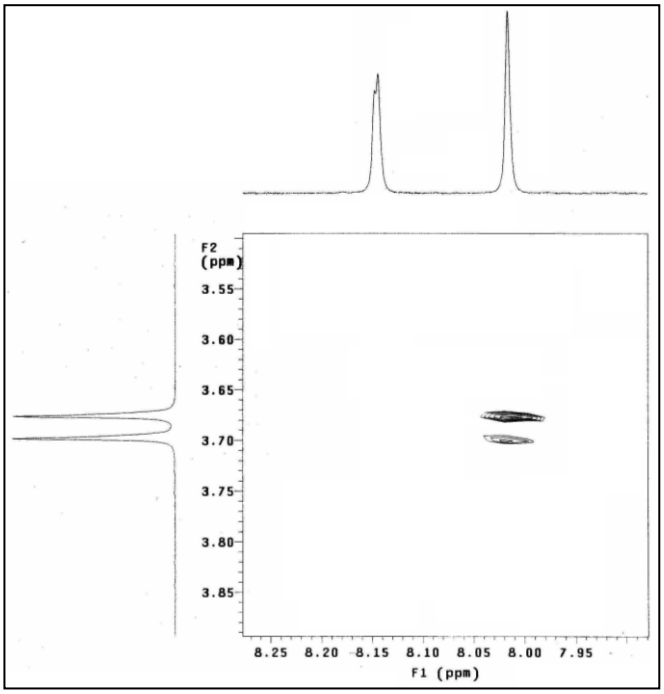

Fig. 15. T-ROESY spectrum expansion

IV. 11 Covalent assembly monolayer

Designing device monolayer-based sensors requires not only selectivity and sensitivity towards a specific analyte, but also a high degree of stability and a fast, non-destructive read-out process.[95-96-97] In addition, sensor regeneration is another key requirement which needs to be taken into account. In the light of these potential advantages, we have developed a monolayer with these oximes covalently bound to quartz substrates. The advantages of oxime-monolayer-based should include:

a. the need of only a small amount of oxime to generate a large active surface
b. no consumption of sensing material

c. no diffusion limitations because the surface-confined sensing molecules will be in direct contact with the target analyte.

This overall activity focuses on the development of a platform that will pave the way for direct switching in the solid state, potentially useful for molecularly based information storage materials.

Fused silica (quartz) substrates were cleaned by immersion into a ‘‘piranha’’ solution (98% H2SO4 : 30% H2O2, 70 : 30, v/v) at 90 °C for 60 min and then left to cool to room temperature. Substrates were then rinsed several times with double distilled water and kept in a H2O : 30% H2O2 : NH3 5 : 1 : 1 v/v/v mixture at room temperature for 1 h.20–22 A final 10 times wash with double distilled water followed by drying under vacuum was carried out just prior to coupling agent (CA) deposition. All the successive substrate treatments were performed in a glove box under nitrogen atmosphere.

Routinely, freshly cleaned substrates were immersed, at room temperature for 25 min, in a 0.4 : 100 v/v n-pentane solution of the chemisorptive reagent,trichloro[4(chloromethyl)phenyl]silane (siloxane), to afford a CAmonolayer.[17-22-24] The siloxane-coated substrates were washed several times with n-pentane in the glove box, sonicated in the same solvent for 10 min in order to remove any physisorbed CA, immersed into a stirred 10^{-3} M CH_3CN/toluene (50:50, v/v) solution oxime and kept at 90 °C for 75 h. The SAM thus formed was left to cool to room temperature and sonicated with a solution of CH_3CN, toluene and THF to remove any residual unreacted materials.

Step 1:

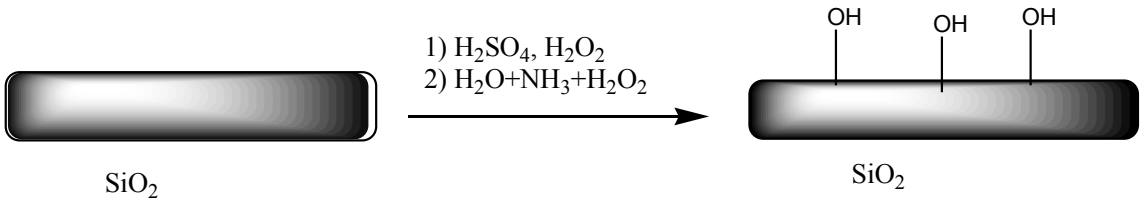

Step 2:

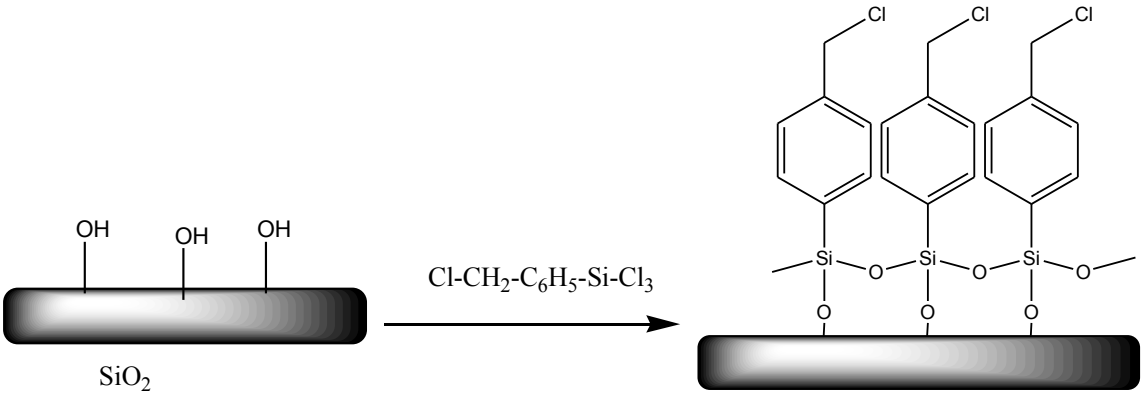

Step 3 :

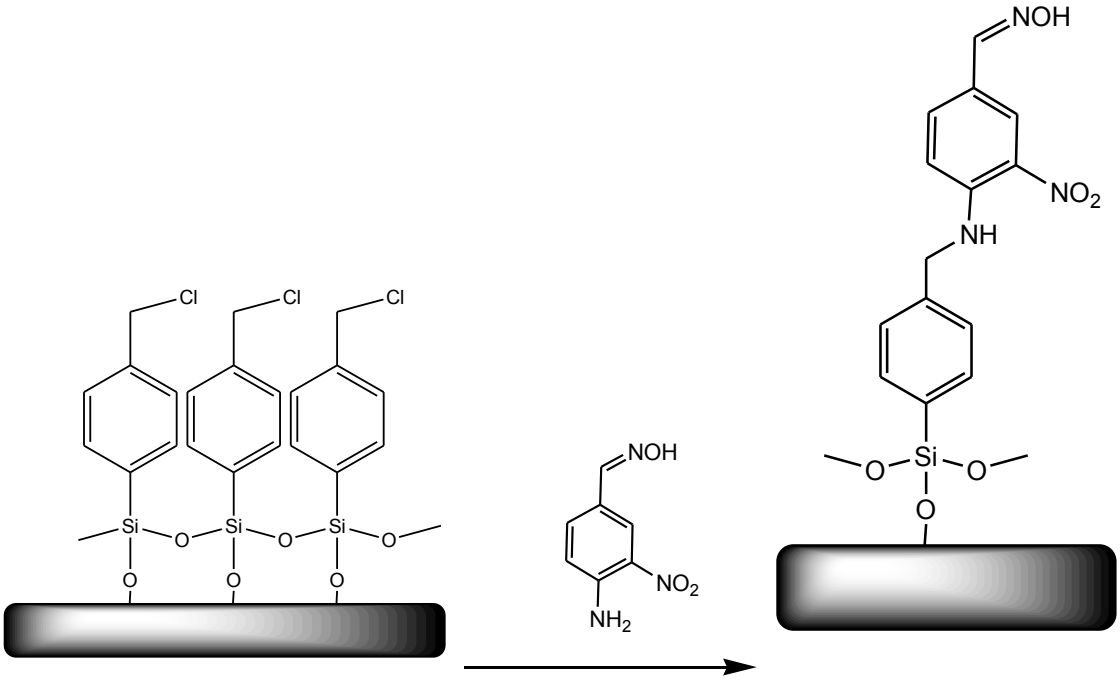

Scheme 11. Covalent assembly monolayer

Once the monolayer was prepared, we carried out UV-VIS measuraments to test the effectiveness properties of the monolayer, namely the interaction with the nerve agent simulant DMMP (dimethylmethyphosphonate).[98]

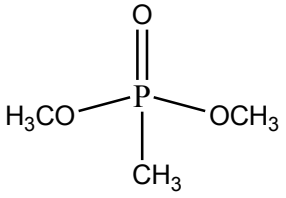

DMMP

This simulant is largely use because is no toxic and it hasn't a leaving group so is quite stable and not easily hydrolysable.

The functionalized monolayer gave the following results as shown below: (**Fig. 16**):

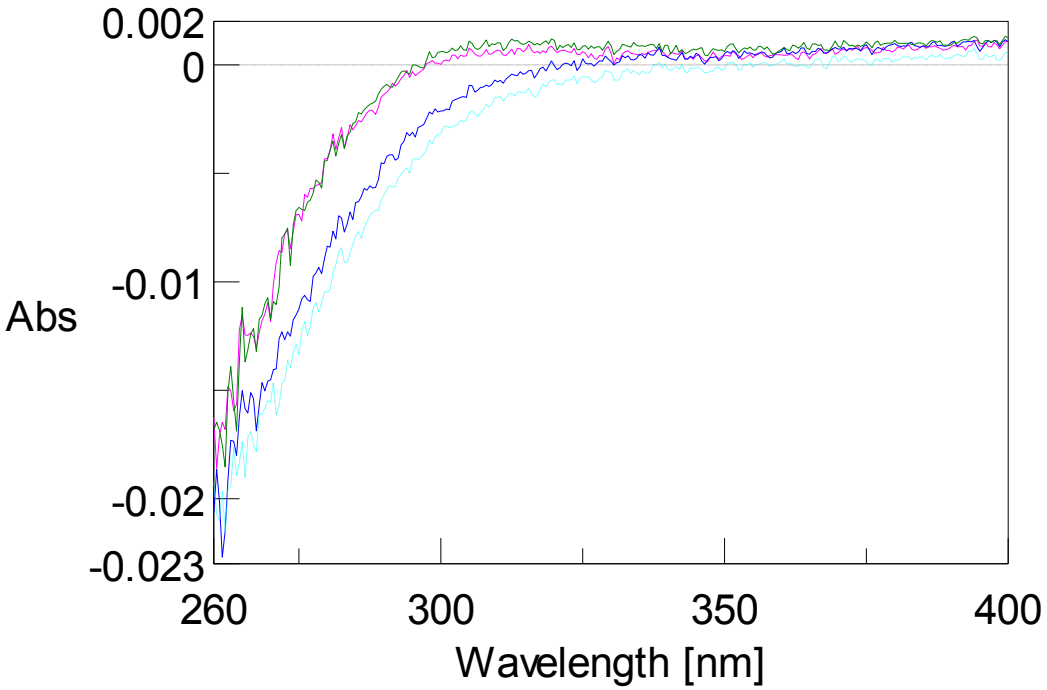

Fig. 16. UV-VIS spectra of the monolayer; maroon: UV-VIS spectrum of the Monolayer; light blue: UV-VIS spectrum of the Monolayer recorded after immersion in a solution of DMMP for a minute; blue: Monolayer after immersion in a solution of DMMP for 20 minutes; green: UV-VIS spectrum recorded after heating for a minute at 130 °C

As it is shown we obtained an encouraging result, the monolayer seems to recognize the simulant we used and moreover seems to be a reversible recognition event, because after heating the monolayer the spectrum comes back to its original appearence.

Unfortunately this is not sufficient, because the signal produced is very low due to the very small molar extinction coefficient coupled with the very little amount of molecules on the surface. Starting from this evidence we started to think how to increase the ε by designing another molecule that has the same functional groups of the molecules synthesized previously. In this case we want to test the oxime group not with a weak kind of interaction like an hydrogen bond could be, but with a real reaction by creating an oximate system that react with a nerve agent simulant via nucleofilic attack; in this case our choice is DCP (diethylchloroposhate) which has a leaving group (Cl).

What we aspected now is the formation of a new species as shown in the proposed mechanism below in **Scheme 17**:

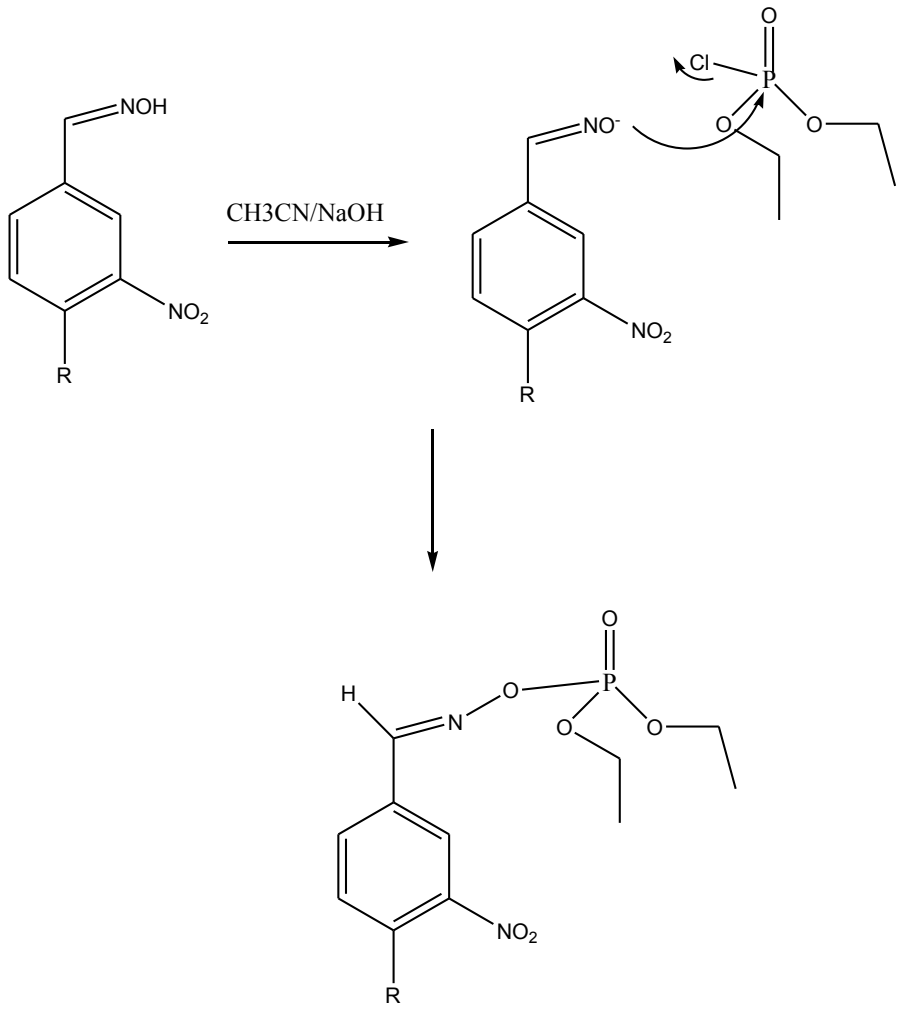

Scheme 17. Proposed mechanism of the nucleofilic attack

We chose a diazo-derivate that is well known that they are dyes with high ε and show different colours depending on the level of conjugation; in fact increasing attention has been devoted to materials containing photochromic azobenzene moiety because of interest in their application fields such as optical switching,[99] optoelectronics[100-101] and also to chromogenic recognition of organophosphate.

IV. 12 UV-VIS Measurements II

In order to obtain a molecule with a higher **ε** we synthesized this azo compound, 4-hydroxy-2'-nitro-4'-oxime-azo-benzene and the UV-VIS spectrum show that this compound is in a trans [E] configuration λ_{max} 370 nm.

ε= 25000

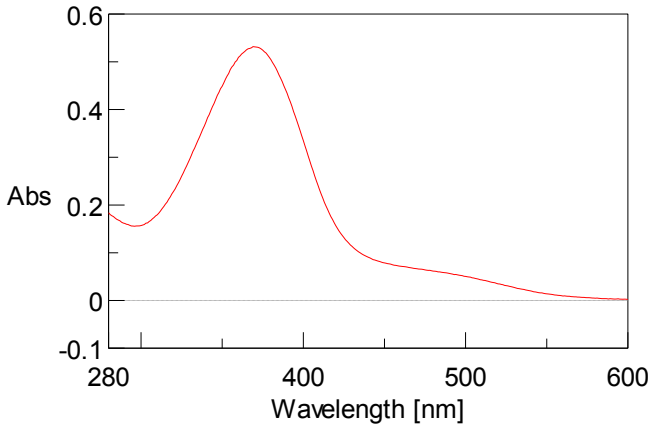

Fig. 17. UV-VIS spectrum of 4-hydroxy-2'-nitro-4'-oxime-azo-benzene

The spectrum below exhibit a large red shift of the azo-compound when the molecule is dissolved in a 1 : 1 solution CH_3CN/ NaOH (aq)

λ 524 nm **ε** = 32550

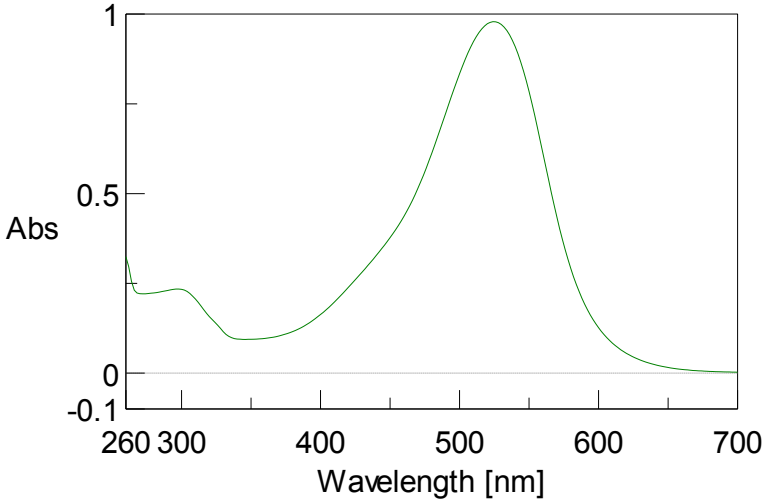

Fig. 18. UV-VIS spectrum of 4-hydroxy-2'-nitro-4'-oxime-azo-benzene in a solution CH_3CN/NaOH 1:1

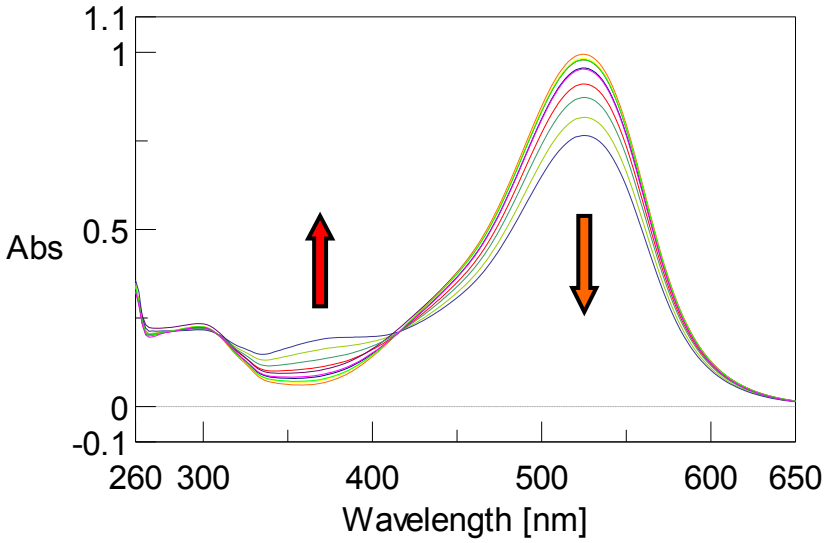

Fig. 19. UV-VIS titration

Experiments were carried out by titrating aliquots of DCP into a 1:1 (CH_3CN-NaOH) solution at room temperature of oximate-azo-dye (3.0 exp -7 M). The initial UV-VIS spectrum showed a band at λ_{max} 524 nm.

Upon the gradual addition of DCP the absorbance intensity at 461 nm decreased with the concomitant appearance of a band hypsocromically shifted to 374 nm through an isosbestic point centred at 414 nm (**Fig. 19**).

(In solution, it's well documented that DCP in unstable to basic medium over a prolonged period of time so all samples were prepared as a fresh solutions before each studies).[59]

We also perform a set of ^{1}H-NMR experiments to determine if our product is susceptible to nucleophilic attack by the phosphorous center. A sample of the azo-compound were prepared by dissolving it in a mixture of acetone-d_6 and NaOH (D_2O) solution and the ^{1}H-NMR was recorded.

The DCP signals are: δ 1.3, q, 6 H and δ 3.5, t, 4 H.

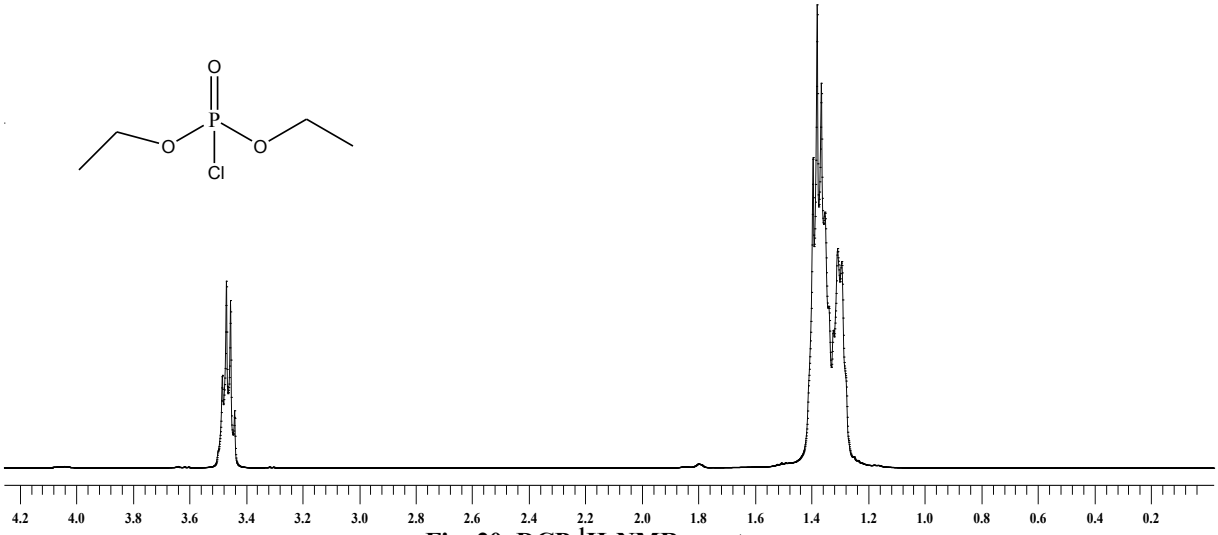

Fig. 20. DCP ^{1}H-NMR spectrum

If we compare the initial spectrum of the azo-compound with the one recorded in presence of the basic solution we clearly see an upfields shift of all signals, indicating that the deprotonation is occurred, we also noticed a loss of resolution due to the negative charge delocalized all over the molecule (**Fig. 21**). This event is accompanied by a drastic change of colour from orange to purple red.

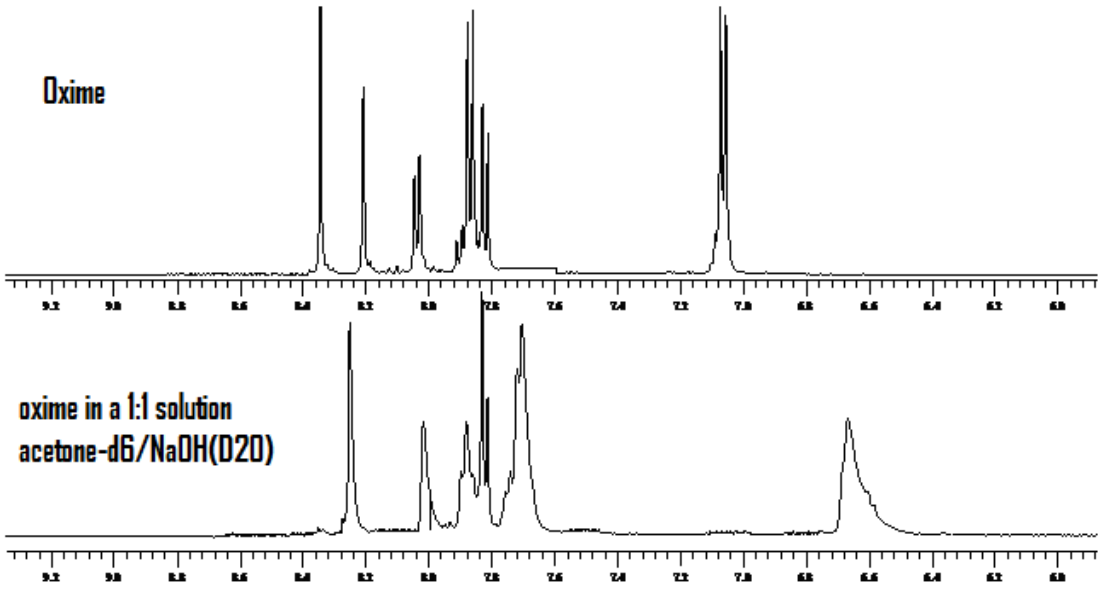

Fig. 21. Compared spectra of azo-oxime with azo-oximate compounds

During the titration performed by adding increasing amounts of DCP was also observed again a downfields shift (**Fig. 22-23**); this could indicates that the deprotonated species is reacting and the signals return to their original chemical shift. The sum of these events is accompanied by a colorimetric change, infact the solution returns orange coloured.

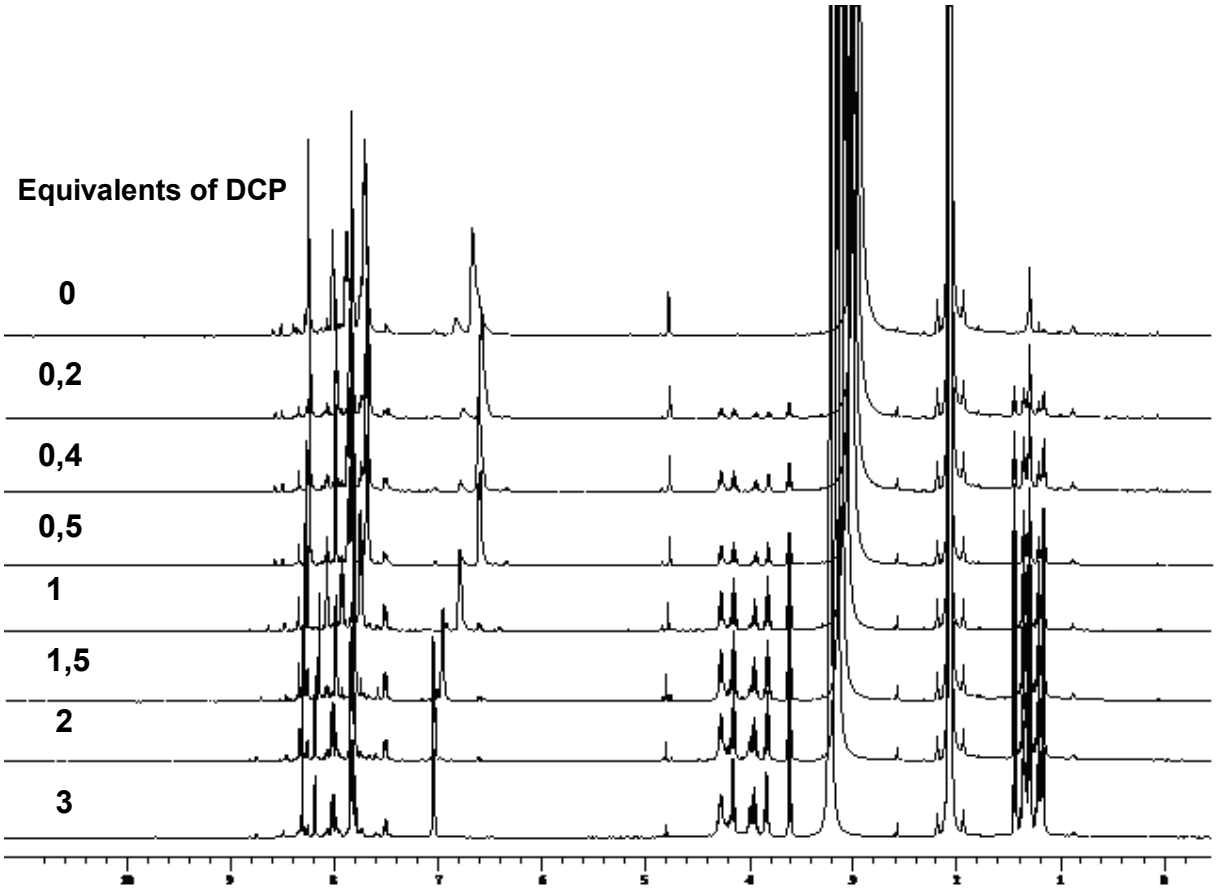

Fig. 22. ^{1}H-NMR titration at increasing amount of DCP

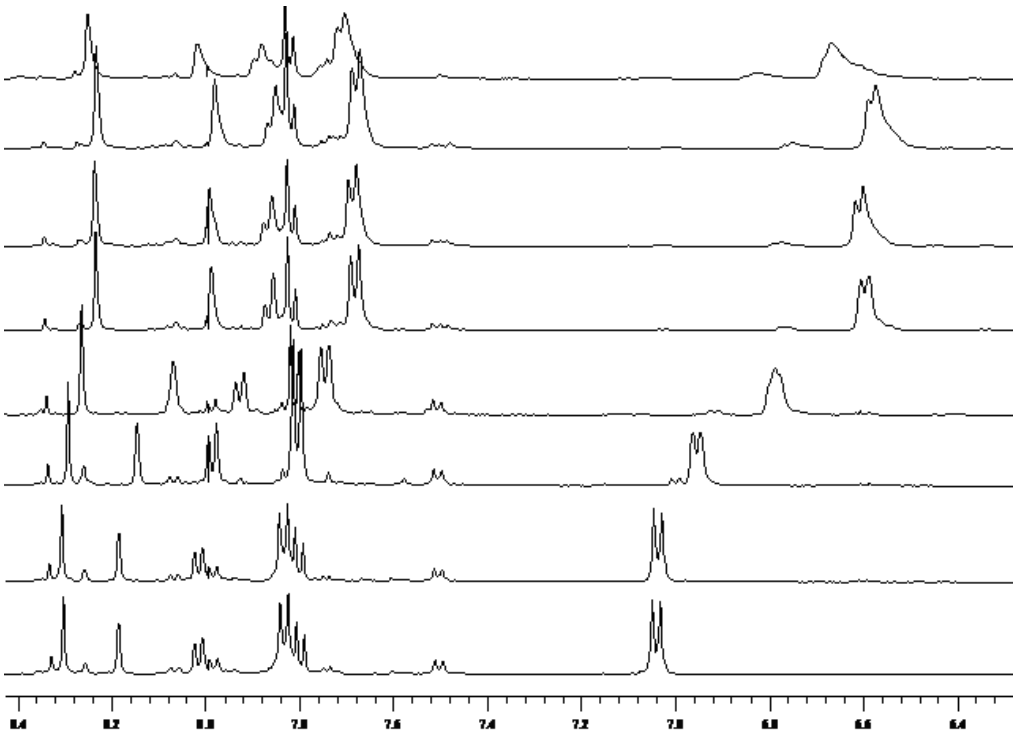

Fig. 23. Zoom of the aromatic zone

IV. 13 UV-VIS Measurements III

In order to verify the ability of recognition of N-tyramine-tri[(2-picolyl)-amino]-1,8-naphthalimide we tested our molecule with different cations (Ba^{2+}, Ca^{2+}, Fe^{2+}, Mg^{2+}, Hg^{2+},Ni^{2+}, Pb^{2+}, Cu^{2+}, Zn^{2+}, Zr^{2+}) (**Fig. 24-33**).

The concentration of the solution of N-tyramine-tri[(2-picolyl)-amino]-1,8-naphthalimide and the various salts is 6.0 exp -5 M. The salts were dissolved in water and then diluted in acetonitrile. The ratio between host and guest is 1:1 for all solutions prepared.

As a qualitative aspect we show the spectra collected below:

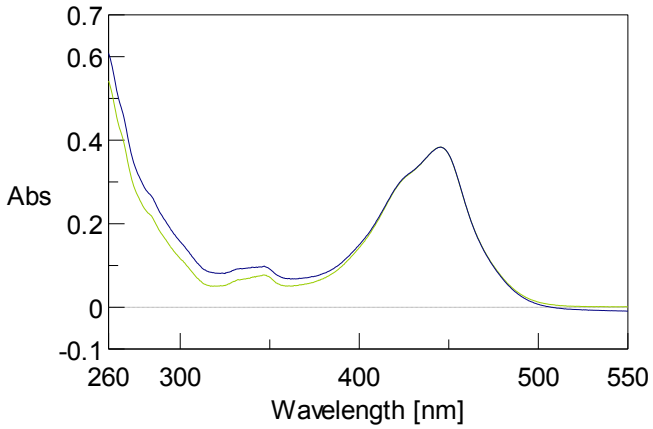

Fig. 24. Barium ($BaCl_2$*$2H_2O$)

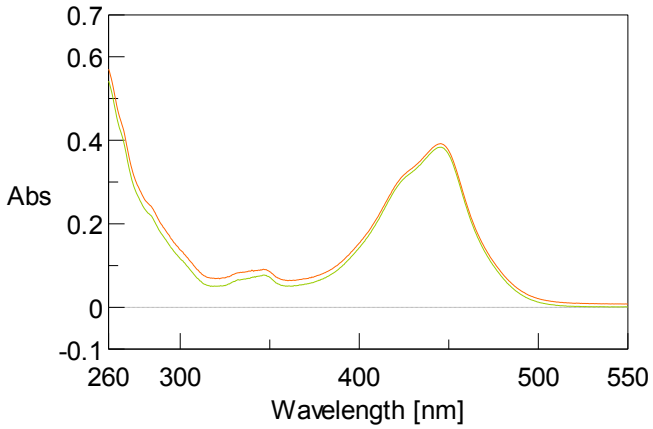

Fig. 25. Calcium ($CaCl_2$)

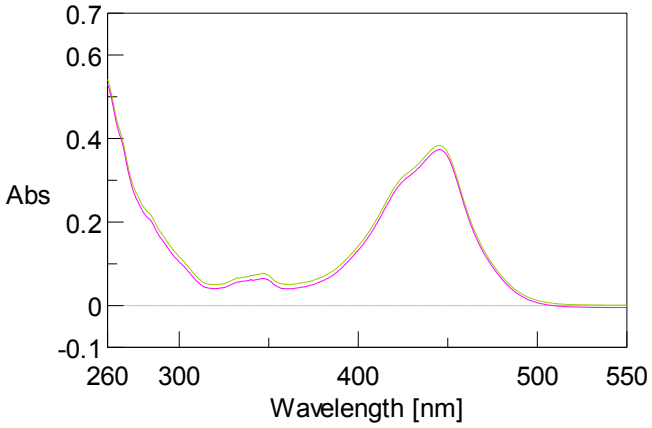

Fig. 26. Mercury ($HgCl_2$)

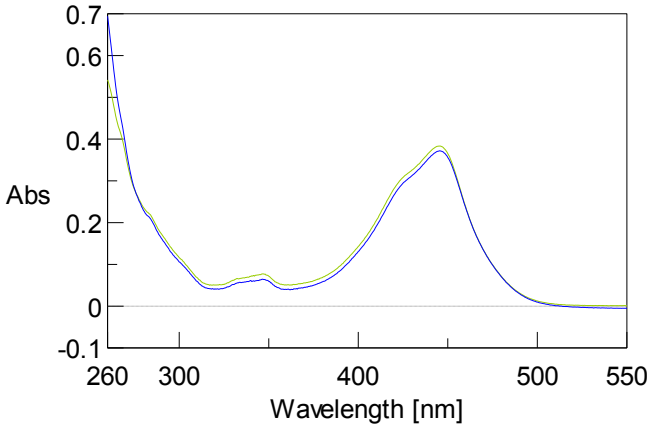

Fig. 27. Magnesium ($MgClO_4$)

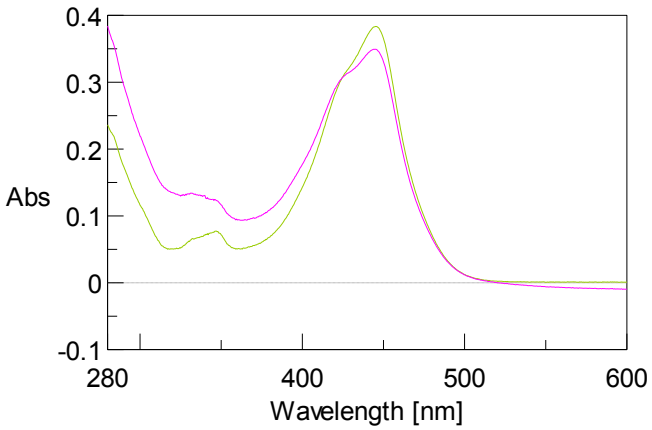

Fig. 28. Lead ($Pb(NO_3)_2$)

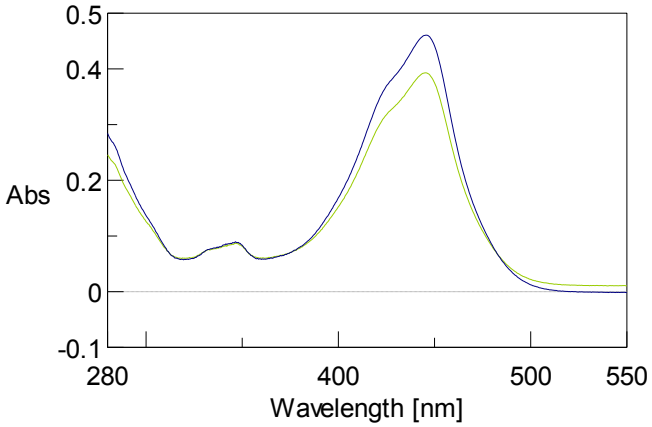

Fig. 29. Zirconium ($ZrOCl_2$)

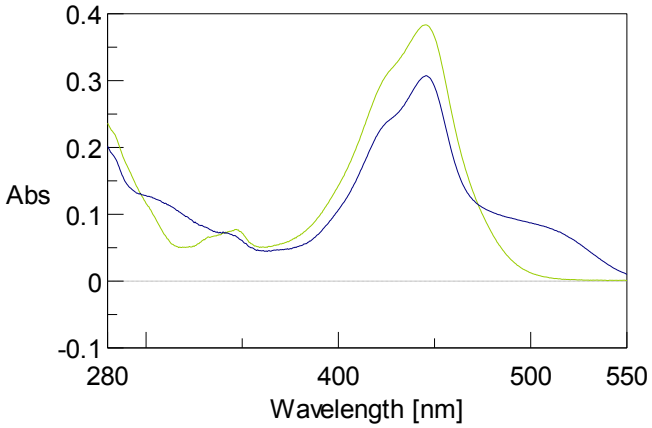

Fig. 30. Zinc ($ZnCl_2$)

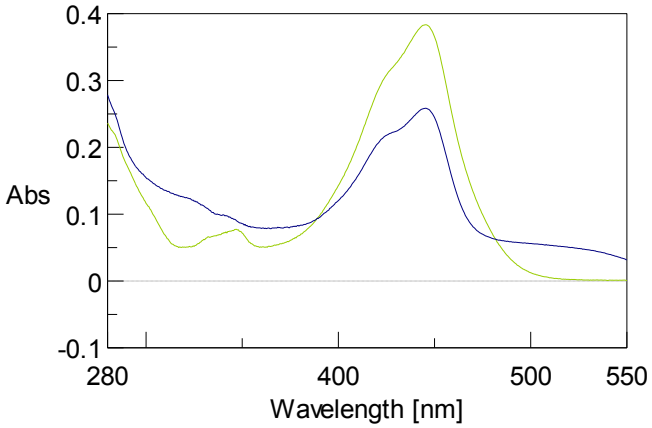

Fig. 31. Copper ($CuCl_2*2H_2O$)

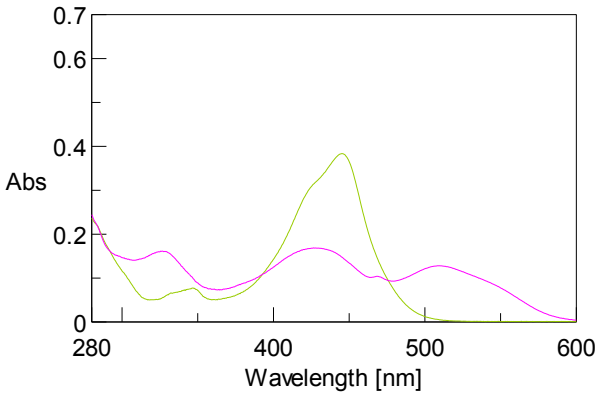

Fig. 32. Nickel ($NiCl_2*6H_2O$)

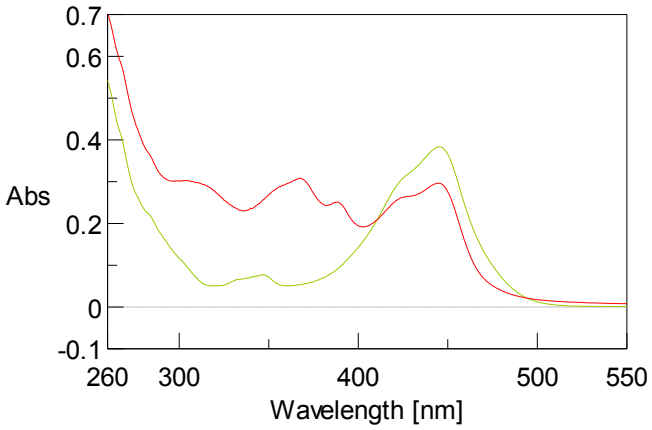

Fig. 33. Iron ($FeCl_2*4H_2O$)

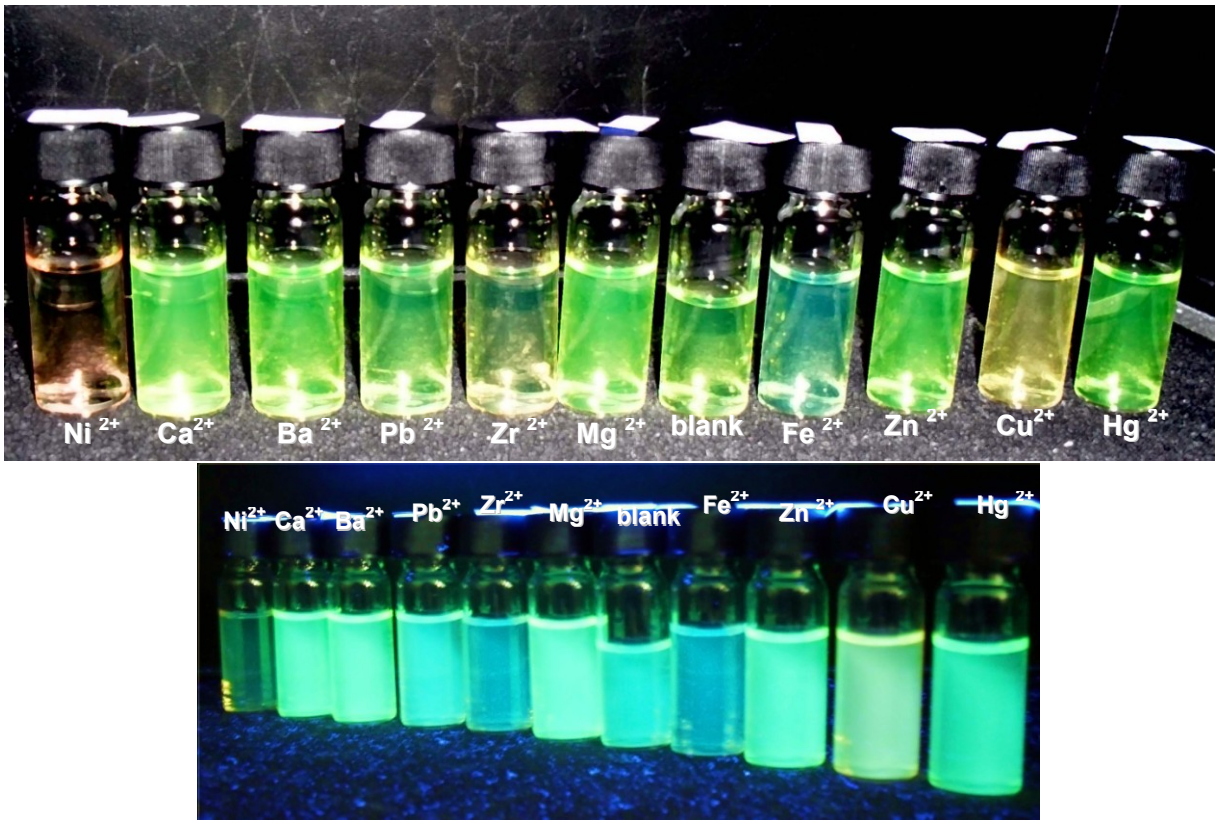

Fig. 34. Snapshots under UV-VIS lamp respectively at 356 nm and 254 nm

The stoichiometry of the complex was monitored by Job plot.[64] The process consists of mixing different rates of equimolar solutions of GUEST and HOST and so as to the total concentration (formal concentration) is constant. We measured the absorbance of each solution at a set wavelength that correspond to the λ_{max}. The graph shows the absorbance corrected as a function of the molar fraction of the complex. The maximum of the graph corresponds to the stoichiometry of the predominant complex in solution. As an exemplum we prepared a job-plot with N-tyramine-tri[(2-picolyl)-amino]-1,8-naphthalimide and $ZnCl_2$ that exhibits a 1:1 ratio as we expected for a tri-arms. The measurements were performed in acetonitrile, λ_{max} 430nm.

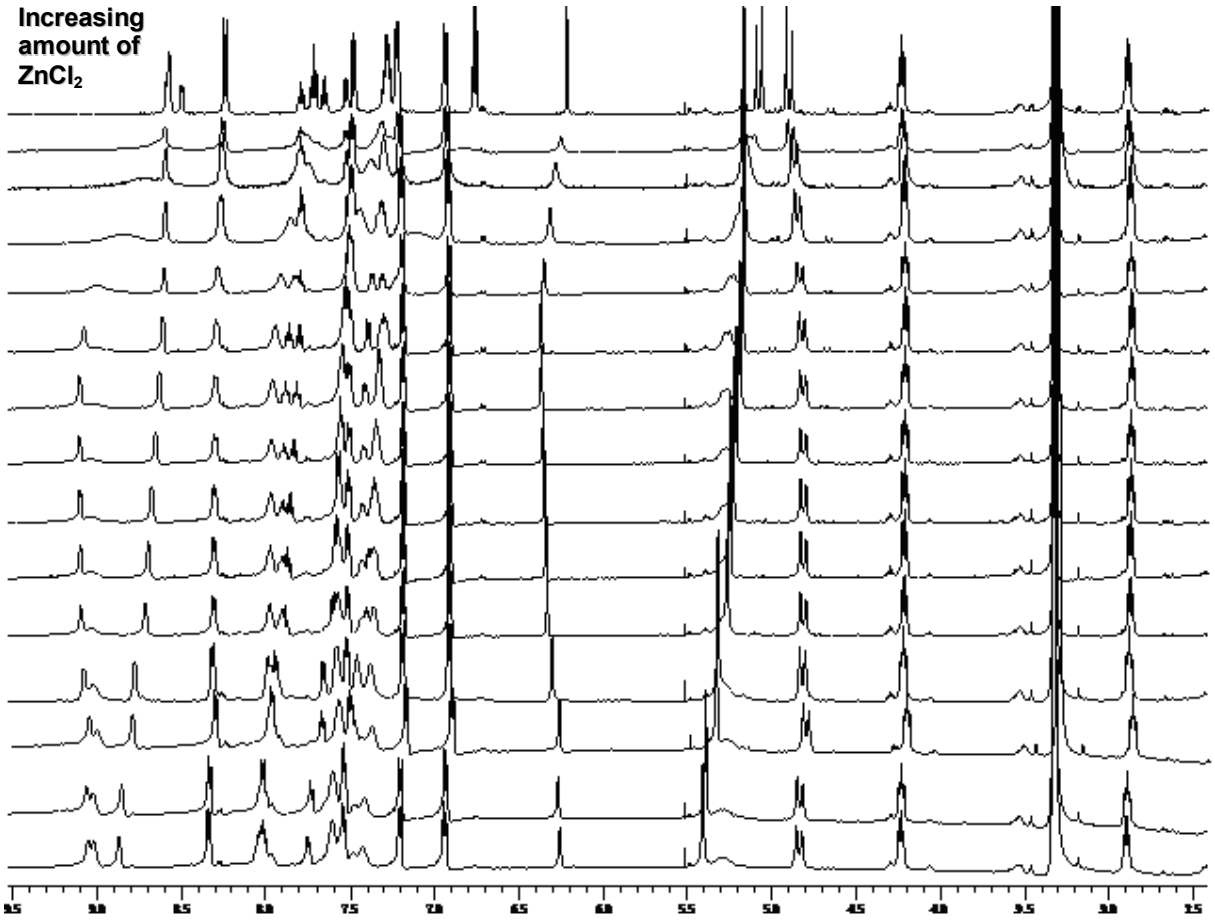

Fig. 35. ^{1}H-NMR titration of N-tyramine-tri[(2-picolyl)-amino]-1,8-naphthalimide Vs $ZnCl_2$

The collected data about the titration show that we have a situation of "no-hydrogen-bond" so if we take a look in the region of methylen groups we can observe a downsfield shift of only one of the two diastereotopic signals, moreover at the same time a downsfield shift of the singlet relative to methylen of the single arm (**Fig. 35**).

For what concern the aromatic region we see that at increasing amount of $ZnCl_2$ added, we have a large shift of the pycolil signals (**Fig. 36**).

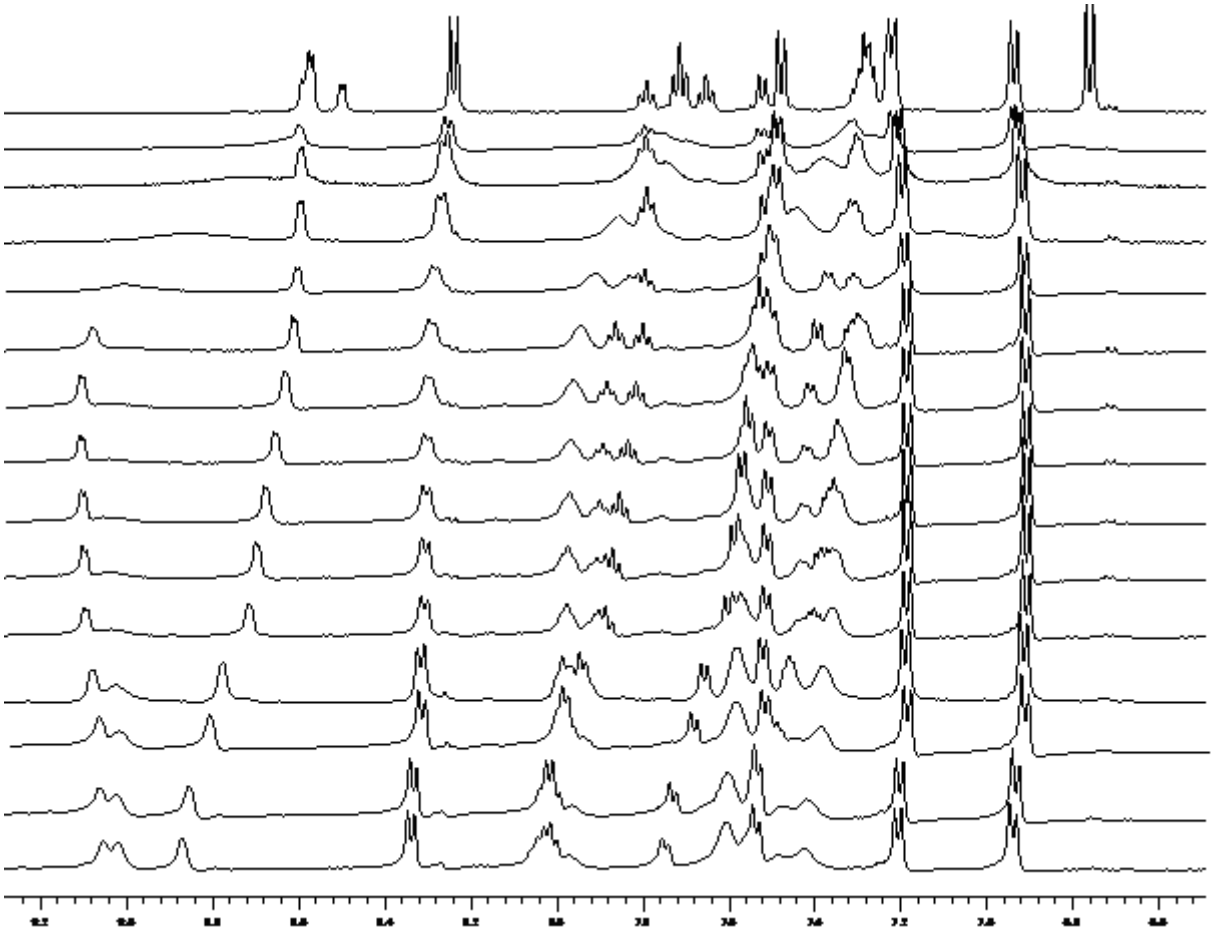

Fig. 36. Zoom of the aromatic zone

IV. 14 Synthesis of 8-chloromethyl-2,6-diethyl-4,4-difluoro 1,3,5,7-tetramethyl-4-bora-3α,4α-diaza-s-indacene

The BODIPY was synthesized by using a literature procedure. Chloroacetyl choride and 2,4-dimethyl-3-ethyl-pirrole were poured into a flask by using dichloromethane as solvent previously degassed under nitrogen atmosphere.

The mixture was stirred for two hours at 50° under inert atmosphere; after this time the solvent was removed under reduced pressure and to the crude was added toluene, dichloromethane and triethylamine, the resulting mixture was stirred at room temperature for half a hour. After this time was added boron trifluoride diethyl etherate and newly the mixture was stirred for two hours at 50 °.

The solvent was removed under reduced pressure and the residue replaced by dichloromethane. The organic phase was washed with water, dried with magnesium sulphate and the solvent removed under reduced pressure.

The crude was purified by column chromatography (mix: toluene/exhane 9/3) and the product crystallized from hexane to give a purple solid. The compound has been characterized by NMR spectroscopy.

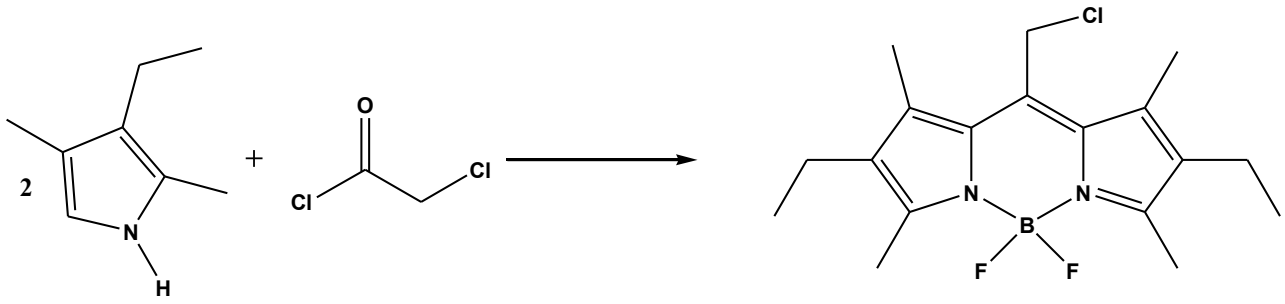

Scheme 12. Synthesis of 8-chloromethyl-2,6-diethyl-4,4-difluoro 1,3,5,7-tetramethyl-4-bora-3α,4α-diaza-s-indacene

IV.15 Synthesis of 3-thiapentan-1-thiol

3-thiapentan-1-thiol was also prepared by using a literature procedure. A mixture of ethyl 2-hydroxy ethyl sulphide and thiourea were mixed in a 48% of hydrobromic acid and refluxed for a night under inert atmosphere.

Then the reaction was cooled to room temperature, and to the solution was slowly added a NaOH solution and the resulting solution was refluxed and stirred for 10 hours under nitrogen atmosphere.

The resulting mixture was than cooled to room temperature, neutralized with HCl and extracted with dichloromethane.

The organic layers were dried over magnesium sulphate, filtered and the solvent removed under reduced pressure, to give a pale yellow, pungent oil used without any further purification.

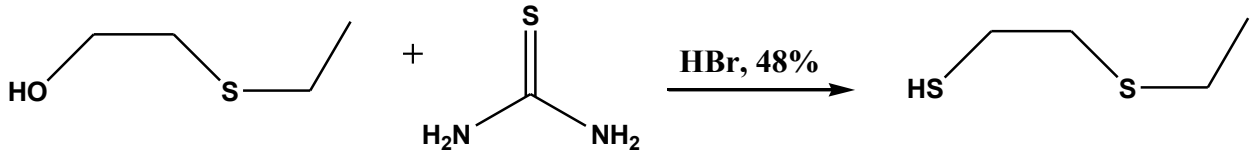

Scheme 13. Synthesis of 3-thiapentan-1-thiol

The product was characterized by NMR.

IV.16 Synthesis of 3,6,12,15,Tetrathia-9-monoazaheptadecane

This compound was synthesized according to a modified literature procedure.

3-thiapentan-1-thiol were diluted in absolute ethanol, to this solution was added sodium and the resulting solution were heated to reflux.

At the same time a solution of bis-(chloroethyl)-amine hydrochloride previously diluted in absolute ethanol was added dropwise and the resulting mixture stirred for 4 hours. At the end of the reaction the solvent was removed under reduced pressure and the crude product was replaced with chloroform.

The organic phase was washed with water dried over magnesium sulphate, filtered and the solvent removed under vacuum. The crude was purified by column chromatography (dichloromethane as eluent) to give a red solid.

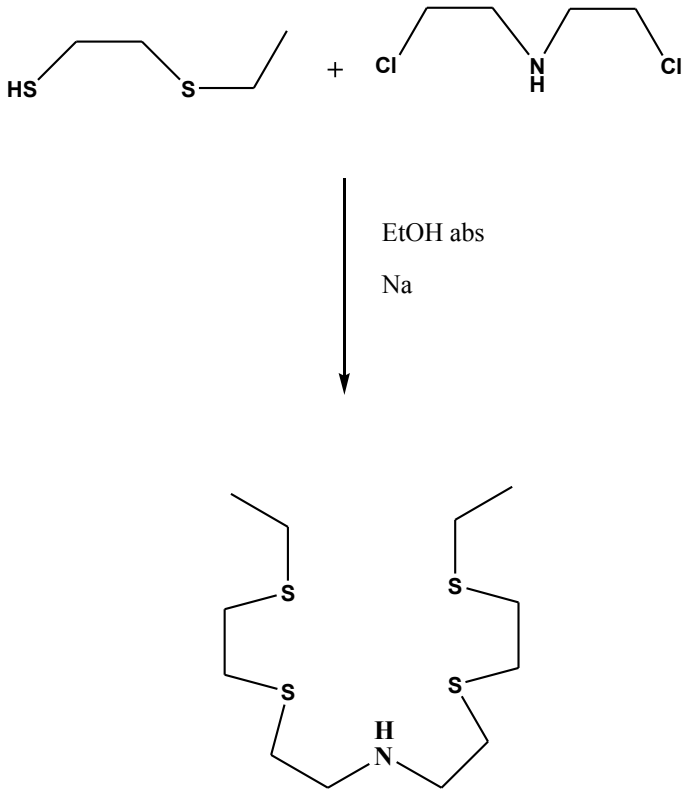

Scheme 14. Synthesis of 3,6,12,15,Tetrathia-9-monoazaheptadecane

The product was characterized by ^{1}H-NMR.

IV.17 Synthesis of 8-[N,N-bis(3',6'-dithiaoctyl)-aminomethyl]-2,6-diethyl-4,4-difluoro-1,3,5,7-tetramethyl-4-bora-3α,4α-diaza-s-indacene CS1(Copper sensor-1)

A suspension of 8-chloromethyl-2,6-diethyl-4,4-difluoro1,3,5,7.tetramethyl-4-bora-3α,4α-diaza-s-indacene and 3,6,12,15,tetrathia-9-monoazaheptadecane were mixed with KI and K_2CO_3 in dry acetonitrile and refluxed overnight under inert atmosphere. At the end of the reaction the solvent was removed under vacuum and the residue replaced with dichloromethane; the organic phase was washed with water, dried with sodium sulphate, filtered and the solvent removed by reduced pressure. The crude product was purified by column chromatography (dichloromethane as solvent) to give a bright red powder.[86]

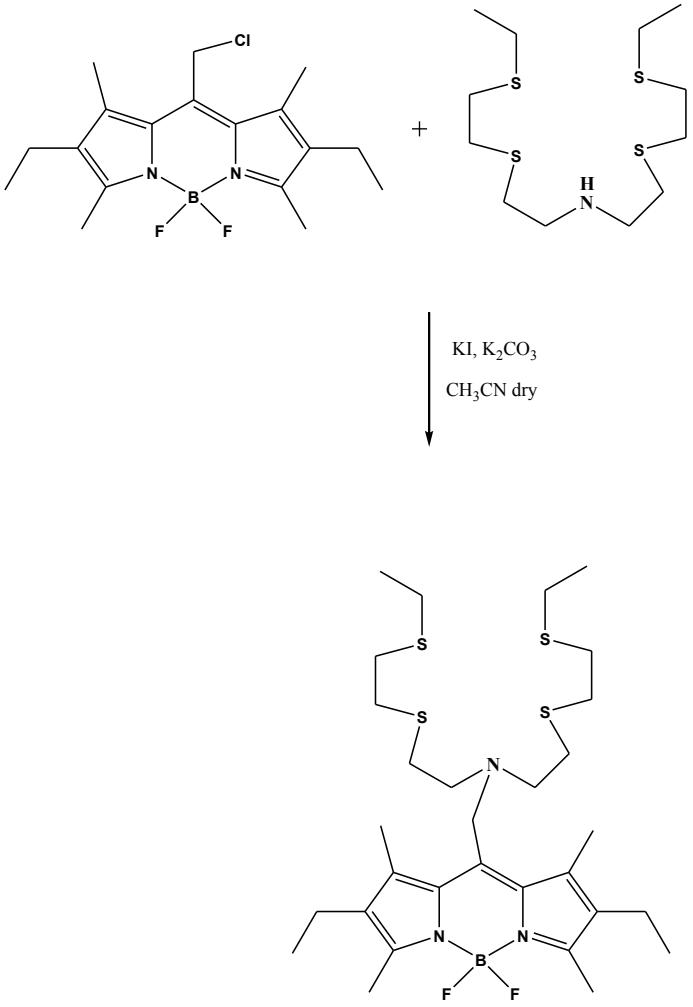

Scheme 15. Synthesis of CS1

IV.18 Synthesis of 4-Br-5-NO_2-1,8-naphtalic anhydride

In order to design a selective, water soluble Copper II chemosensor we started with a rigid organic scaffold that is 4-bromo-5-nitro 1,8 naphtalic anhydride as reported in the scheme below:

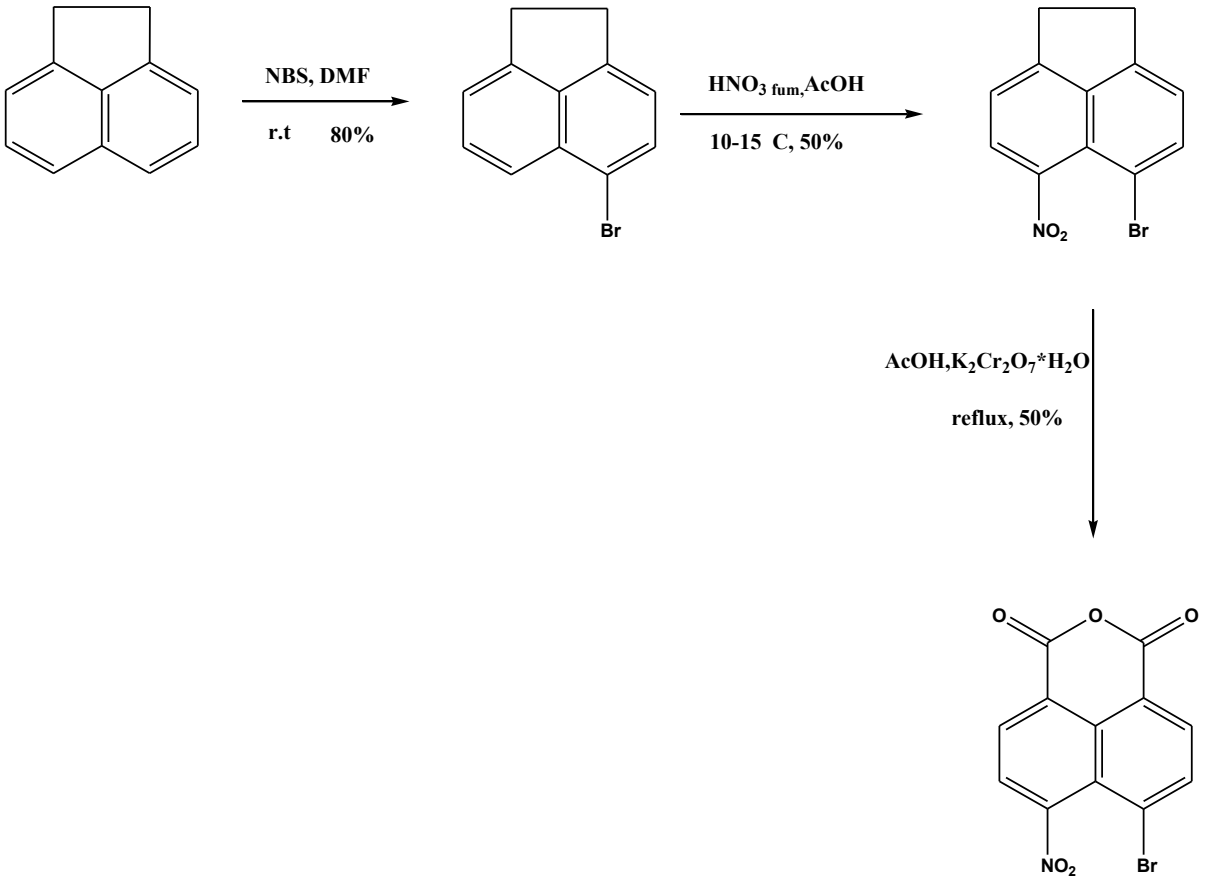

Scheme 16. Synthesis of 4-Br-5-NO_2-1,8-naphtalic anhydride synthetic pathway

Water solubility is guarantee by attaching a trehalose (α,α-trehalose) functionality, that is a disaccharide resulting from a 1,1 linkage of two D-glucose molecules[102]; this molecule is a non-reducing sugar that is not easily hydrolyzed by acid, and whose glycosidic bond is not cleaved by α-glucosidase, (optical rotation $[\alpha]_D^2$ +178°).

This sugar[103] is present in a wide variety of organisms, including bacteria, yeast, fungi, insects, invertebrates, lower and higher plants, where it may serve as a source of energy and carbon. It can protect proteins and cellular membranes from inactivation or denaturation caused by a variety of stress conditions, including desiccation, dehydration, heat, cold, and oxidation.

Trehalose has also been shown to be very effective in inhibiting aggregation of the Alzheimer's related β-amyloid peptide Aβ and in reducing its cytotoxicity.[104]

The insertion of this sugar gave N-trehalose-4,5-4-bromo-5-nitro 1,8-naphthalimide.

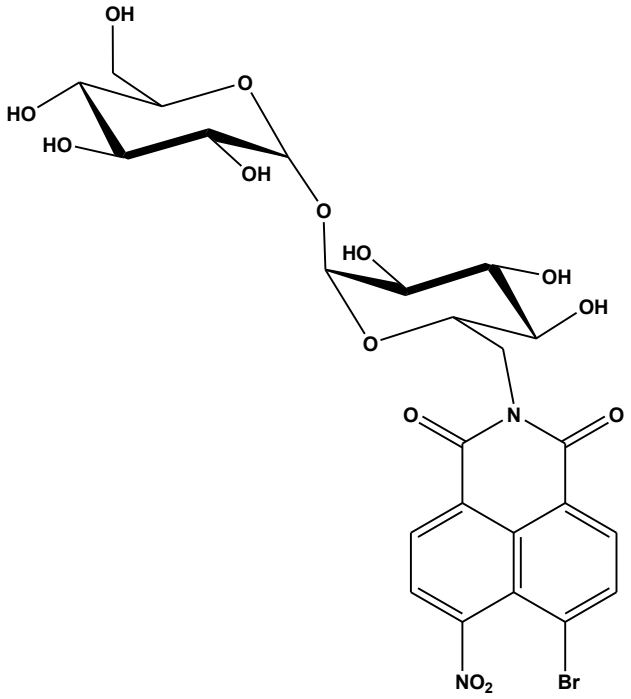

Then the insertion of two units of picolyl amine in 4,5 position permit the formation of the new chemosensor N-trehalose-4,5-di[2(picolyl)amino]1,8 naphtalimide.

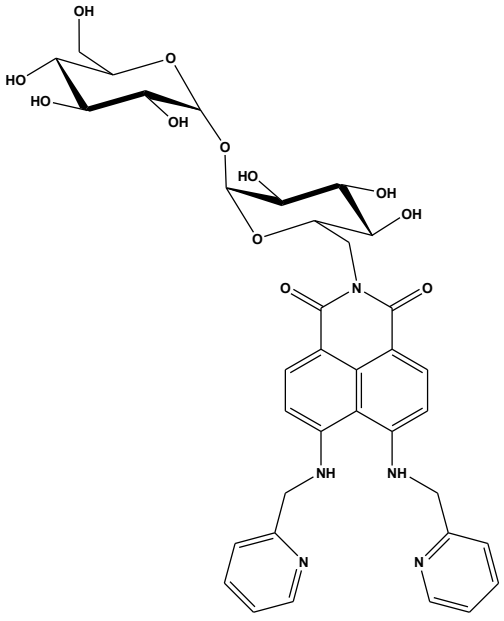

Scheme 17. N-trehalose-4,5-di[2(picolyl)amino]1,8 naphtalimide

IV.19 Synthesis of 6-bromo-6-deoxy-α,α'-trehalose (TH-Br)

The synthesis of the copper (II) chemosensor involves different steps. Starting from TH-Br in order to synthesize TH-NH_2. The bromination was performed according to the methods reported in literature[105]. These methods are efficient and selective for the replacement of the primary hydroxyl group in carbohydrates and consist in treatment of the alcohol with NBS and PPh_3. The reaction with NBS-PPh_3 most probably proceeds by the initial formation of an alkoxyphosphonium ion, which reacts with bromide ions give the product obtained.

Triphenylphosphine was added to a solution of anhydrous trehalose in dry DMF in a molar ratio of 2:1. The reaction was cooled under stirring to 0°C. Then N-bromosuccinimide in an equimolar ratio with Ph_3P was added dropwise under stirring, after the addition the reaction was left to room temperature for a time of 48 h until the end of the reaction that is the maximum formation of the product. At the reaction mixture were added methanol were added in order to decompose the excess of the starting reagent. The organic solvent was removed under vacuum at 35 °C. The crude product was washed with ethanol; the white crystals formed were filtered off using a Millipore apparatus. The filtered solution was evaporated under vacuum at 35 °C. The solid was purified by chromatography on an RP_8 column, using a linear gradient H_2O-EtOH (0-25%) as eluent.

TH-Br yield: 40%.

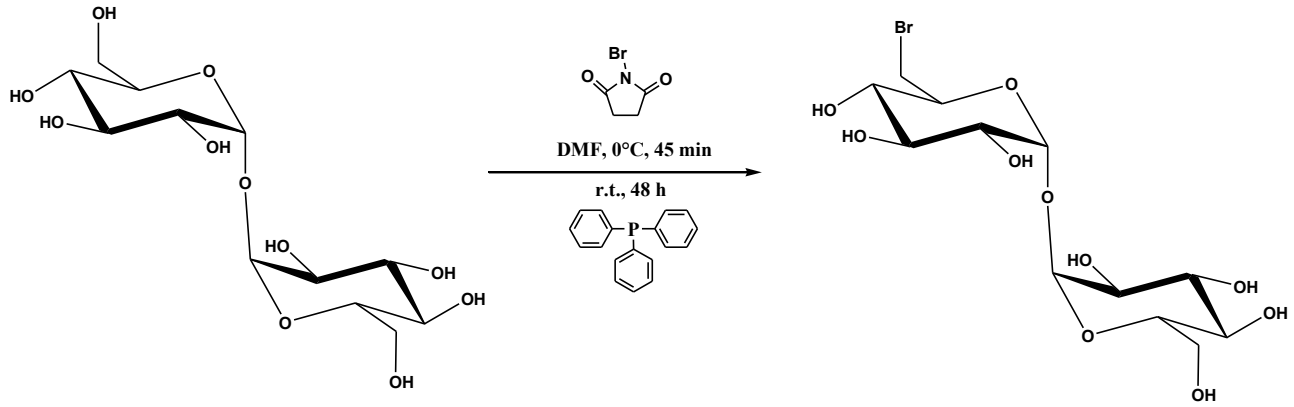

Scheme 18. 6-bromo-6-deoxy-α,α'-trehalose synthesis.

The product has been characterized by ^{1}H-NMR

IV.20 Synthesis of 6-azido-6-deoxy-α,α'-trehalose (TH-N_3)

Trehalose was aminated according the methods reported in literature[106]. The reaction proceeded via two steps, i.e. the synthesis of TH-N_3 by TH-Br and the reduction of azide group to amino group. The reaction of TH-Br with NaN_3 in aqueous solution gave the azido derivative which was isolated by chromatography. The reduction of TH-N_3 with triphenylphosphine in DMF followed by the hydrolysis of the iminophosphorane intermediate with NH_4OH yielded the amino derivative.

TH-Br was diluted in H_2O, then NaN_3 was added to the solution in a molar ratio of 1:10. The reaction was carried out at 100 °C under stirring for 4 h. The solvent was removed at 35 °C under reduced pressure. The crude was purified by chromatography on an RP_8 column, using a linear gradient of H_2O-EtOH (0-30%) as eluent.

TH-N_3 yield: 52%.

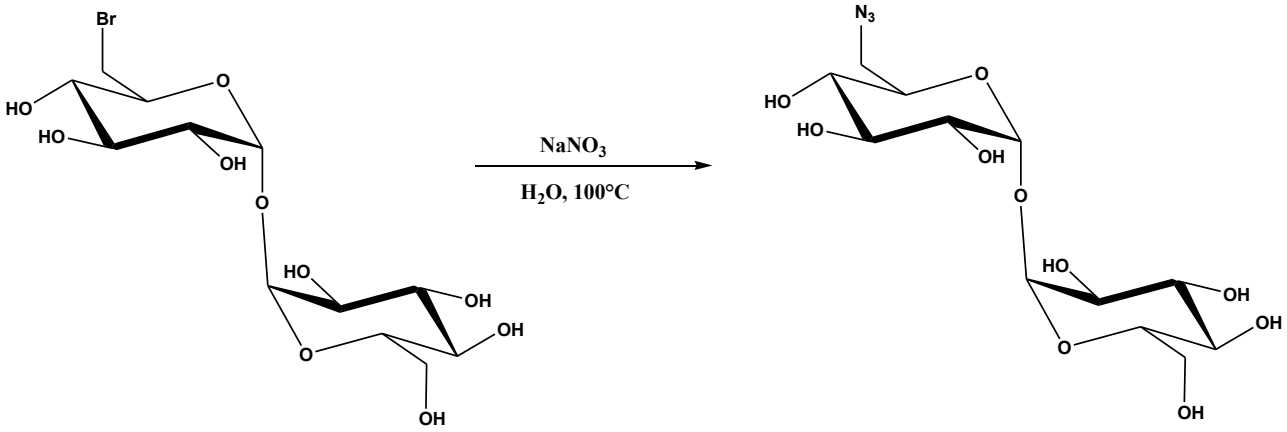

Scheme 19. synthesis of the 6-azido-6-deoxy-α,α'-trehalose

The pure product has been characterized by ^{1}H-NMR

IV.21 Synthesis of 6-amino-6-deoxy-α,α'-trehalose (TH-NH_2)

TH-N_3 was solubilised in DMF to this PPh_3 was added to the solution. The reaction was carried out at 40 °C under stirring for 1 h. The product was then treated with 30% of NH_4OH at room temperature. After 23 h, white crystals were formed and filtered off using a Millipore apparatus. The filtered solution was evaporated under reduced pressure. The crude was purified by column chromatography of CM-Sephadex C-25 (20x600 mm, NH_4^+ form), using a linear gradient of H_2O-NH_4HCO_3 (0-0,3 M) as eluent.

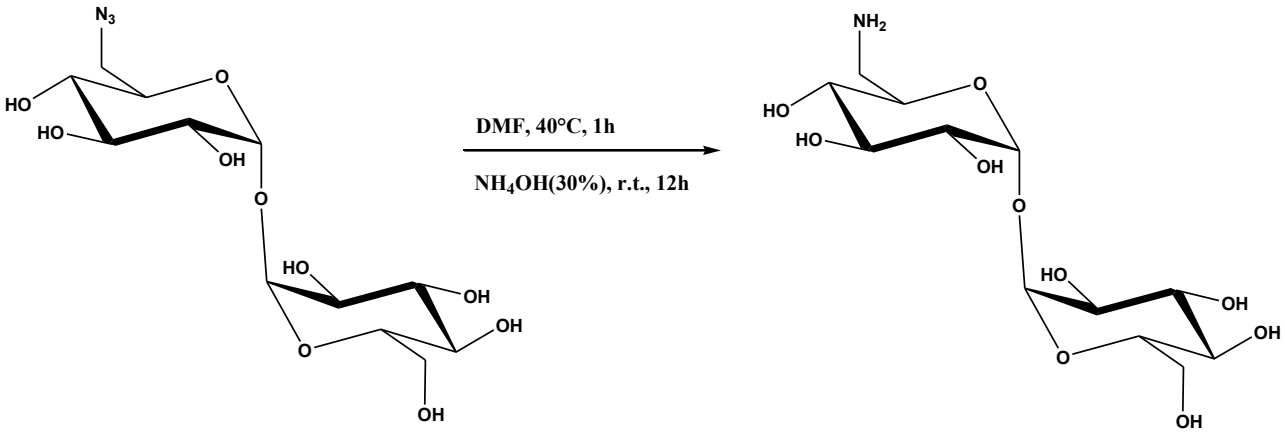

Scheme 20. synthesis of 6-amino-6-deoxy-α,α'-trehalose

IV.22 Synthesis of 4-bromoacenaphtene

IV.23 Synthesis of 4-bromo-5-nitro acenaphtene

IV. 24 Synthesis of 4-bromo-5-nitro 1,8 naphtalic anhydride

See scheme 16.

IV. 25 Synthesis of N-trehalose-4-bromo-5-nitro-1,8 naphthalimide

TH-NH_2 was diluted in DMF, to this solution was added a equimolar solution of 4-bromo-5-nitro-1,8-naphthalic anhydride. The reaction was carried out at 60 °C under stirring for 5 hrs[94], at end of the reaction the solvent was removed under reduced pressure. The crude of reaction was purified by column chromatography on an RP_8 resyn, using a linear gradient of H_2O-EtOH (0-30% and 30-60%) as eluent.
N-trehalose-4-bromo-5-nitro-1,8 naphthalimide yield: 69%.

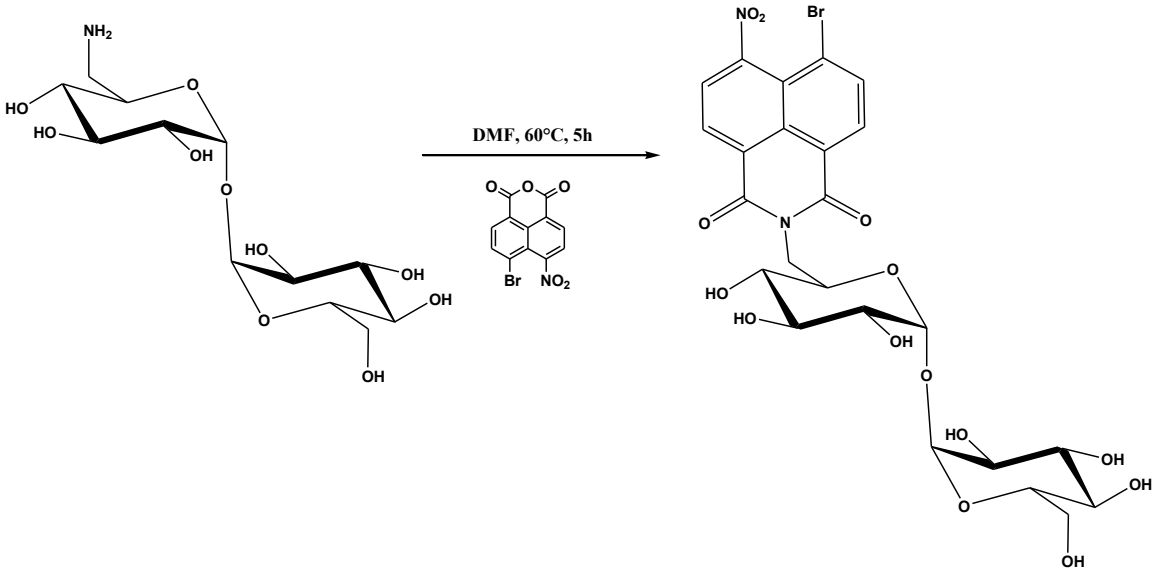

Scheme 21. Synthesis of N-trehalose-4-bromo-5-nitro-1,8 naphthalimide

The product was characterized by ^{1}H-NMR.

IV.26 Synthesis of N-trehalose-4,5-di[(2 picolyl amino]-1,8 naphthalimide (CSTH)

N-trehalose-4-bromo-5-nitro-1,8 naphthalimide was diluted in 15 ml of 2-methoxyethanol and left stirring, at the same time was prepared a solution of 2-picolylamine by using 2-methoxyethanol as solvent and was added dropwise to the solution containing the naptalimide in a molar ratio of 1:21[107]. The reaction was carried out at 130 °C under stirring for 4 hrs, when TLC indicated the formation of the maximal amount of the product; at the end of the reaction the solvent was removed under reduced pressure. The crude product was then purified by column chromatography on an RP_8 resyn using a linear gradient of H_2O-EtOH (0-30% and 30-70%) as eluent.
CST yield: 20%.

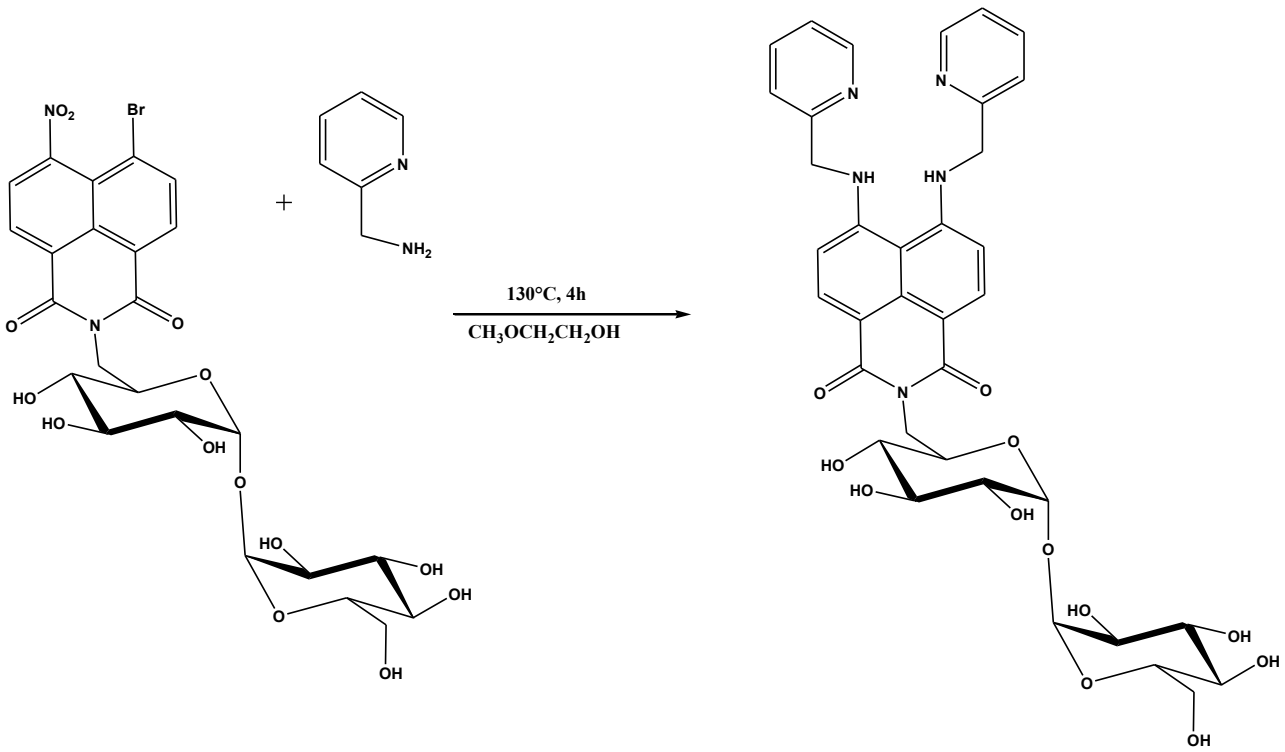

Scheme 22. Synthesis of N-trehalose-4,5-di[(2 picolyl amino]-1,8-naphthalimide

IV.27 ENANTIOSELECTIVE OXYGEN TRANSFER

In order to obtain reusable catalysts able to transfer enantioselectively oxygen to a substrate (like alkenes),we have designed and synthesized three new salen ligands that bear respectively:

- **CAT_1** that contains two C_{12} chain arms in 3-3' position
- **CAT_2** that contains two C_6 arms in 5-5' position and
- **CAT_3** that contains only one C_6 arm on one two in 5' position and a tert-butyl group in position 5.

The structural characterization of all new compounds was carried on by ESI-MS measuraments and by NMR spectroscopy.

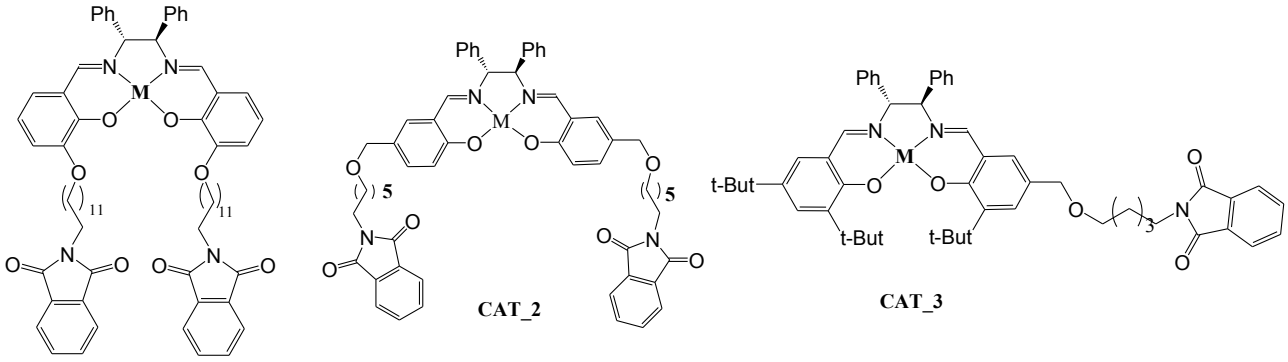

Scheme 23. Schematic representation of CAT_1, CAT_2, CAT_3

IV.28 Synthesis of N-(12-bromododecyl)pthalimide

To create a spacer between the anchoring groups and the active functionality we synthesized the N-(12-bromododecyl) pthalimide[108];
the synthesis is describe in the scheme below:

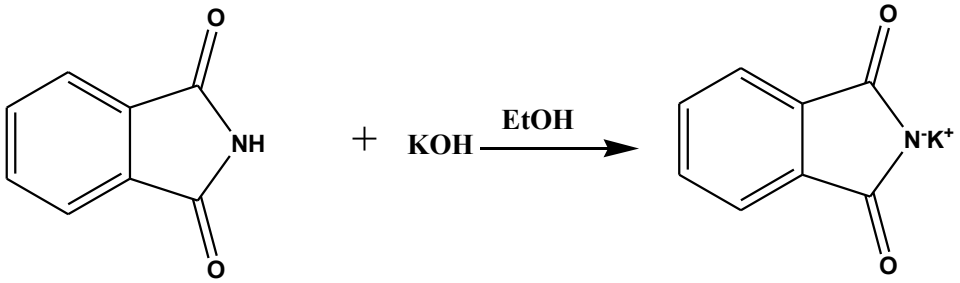

Scheme 24. Synthesis of potassium phtalimide

Firstly we prepared potassium pthalimide starting from pthalimide and by using KOH and EtOH as solvent. This intermediate reacted with 1-12-dibromododecane to give N-(12 bromododecyl) pthalimide

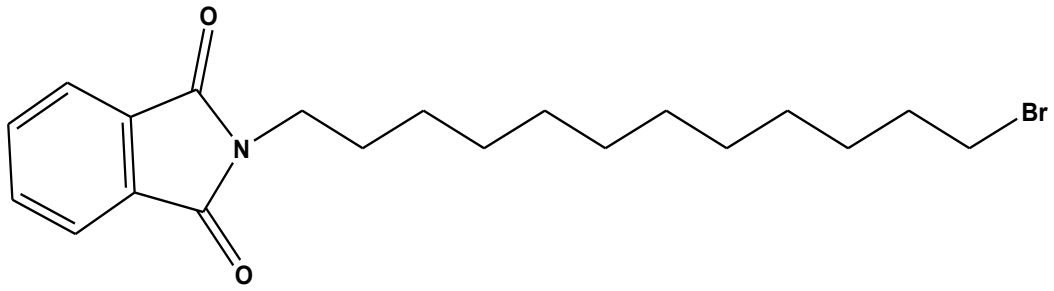

Scheme 25. Synthesis of N-(12-bromododecyl)pthalimide

The synthesized compound has been charachterized by m.p. ^{1}H-NMR e ^{13}C-NMR.

IV.29 Synthesis of 2-hydroxy-3-oxy-dodecylpthalimido benzaldehyde

This is an O-alchilation reaction of the oxygen in position 3, without protection of the hydroxyl group in position 2 by using a coordinative solvent as DMSO. To 2,3-di-hydroxy-benzaldehyde was added a suspension of NaH (68%) as base in DMSO as solvent previously washed in pentane. The reaction proceeded for a hour, then N-12-bromododecyl-pthalimide was added dropwise and left reacting for 7 hours. The reaction was monitored by TLC, we noticed the formation of two spots, one attributable to the formation of a mono-alkylated compound and one attributable to a dialkylated one. The compound was purified by chromatographic column to give a pale yellow solid and characterized by ^{1}H-NMR e ^{13}C-NMR.

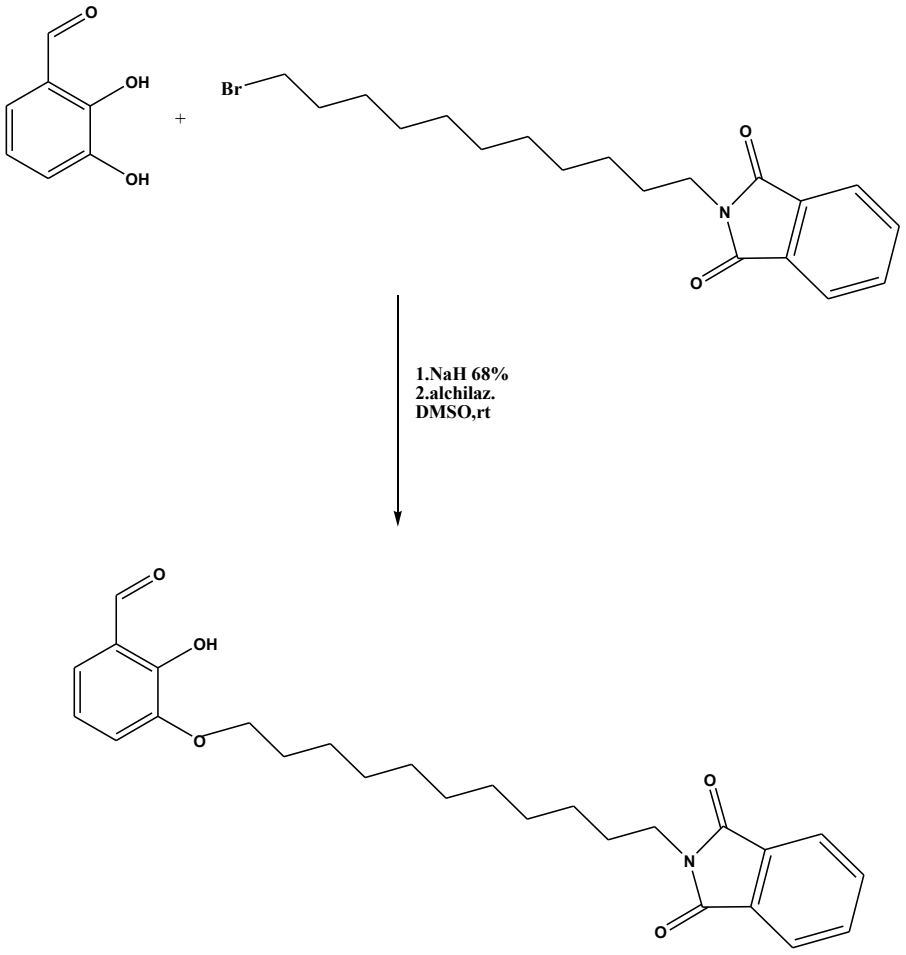

Scheme 26. Synthesis of 2-hydroxy-3-oxy-dodecylpthalimido benzaldehyde

IV.30 Synthesis and deprotection of the ligand salen-PHT

The ligand precursor of **CAT_1** was obtained as follow: to a solution of 1R-2R diphenylethylendiamine was added 2-hydroxy-3-ossi-dodecylpthalimido benzaldehyde in ethanol absolute as solvent, the reaction was monitored by TLC until disappearance of the reagent (approximately 24 h); the salen is formed with a quantitative yield .

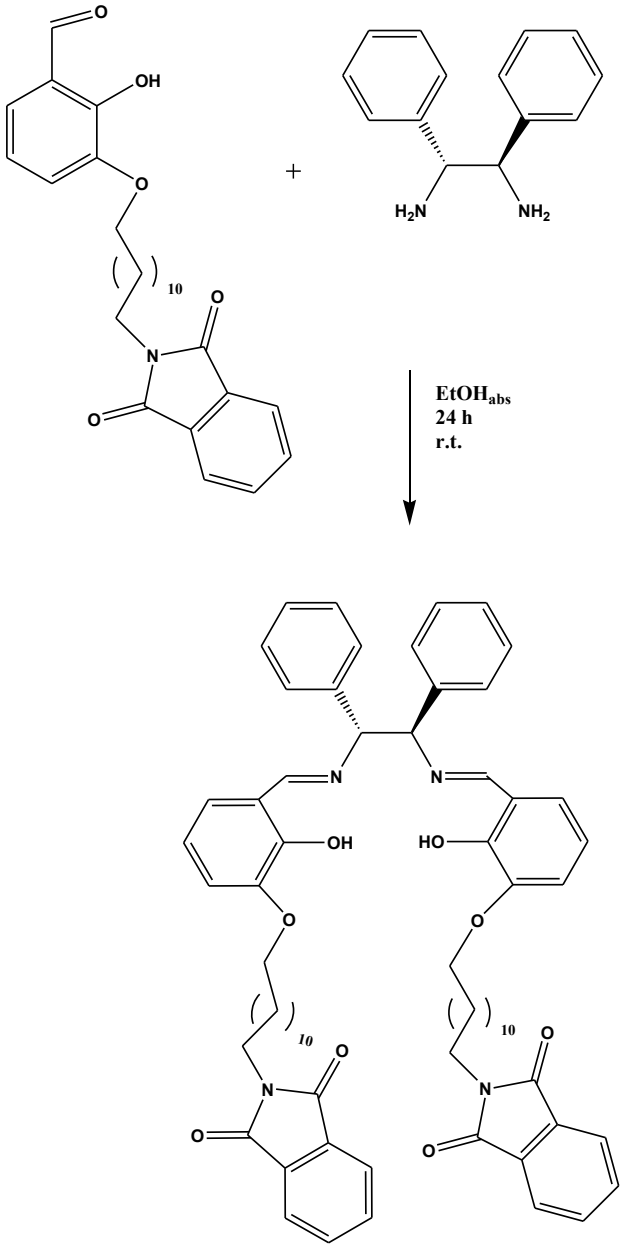

Scheme 27. Synthesis of the ligand salen-PHT

The compound was completely characterized by ESI-MS, ^{1}H-NMR, ^{13}C-NMR.
To anchor the compound on the silica surface was necessary to deprotect the two amino groups from phtalimidic functionalities.
For this purpose to a ethanol absolute solution of the ligand precursor was added a solution of hydrazine monohydrate and the reaction proceeded under reflux for 5 hours by monitoring the reaction by TLC.
Pthalates residue were removed by precipitation with chloroform and filtrated under vacuum, to give the deprotected salen ligand with quantitative yield.

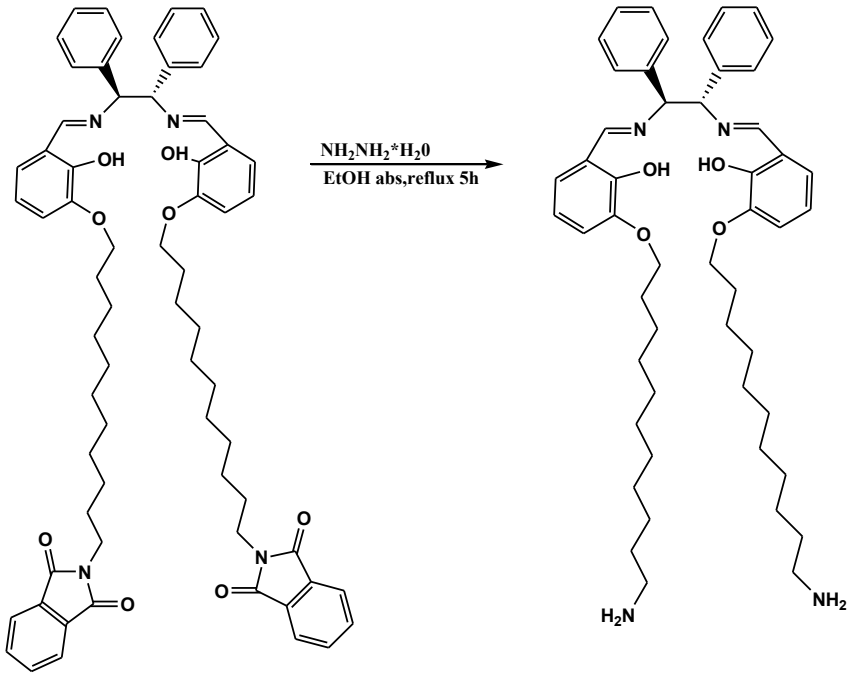

Scheme 28. Deprotection of the salen PHT

The compound was characterized by ESI-MS and ^{1}H-NMR.

IV.31 Synthesis of the Mn(III)-salen complex (CAT_1)

To prepare the catalyst was necessary the complexation reaction between the previously synthesized ligand and Mn(III) acetate. The ligand was diluted in dichloromethane and to this solution was added Mn(III)acetate in ethanol absolute as solvent overnight at room temperature. The reaction was monitored by TLC until the disappearing of the starting reagent. At the end of the reaction the solvent was removed under reduced pressure and the residue diluted in dichloromethane, filtered off and the solvent removed under reduced pressure. Quantitative yield.
The compound has been charachterized by ESI-MS.

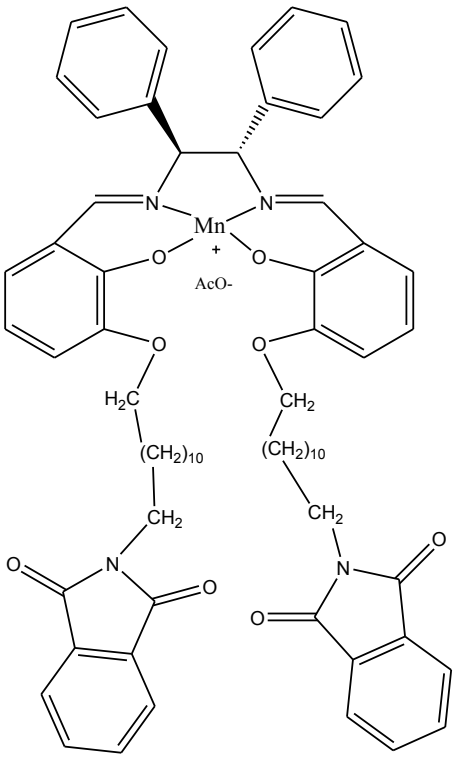

Scheme 29. Synthesis of CAT_1

IV.32 Synthesis of 3-tert-butyl-2-hydroxybenzaldehyde

To synthesized 3-tert-butyl-2-hydroxybenzaldehyde was used as precursor 2-tert-butylphenol through a Gross phormylation. These reaction proceeded in an ice bath for 1 hour with di- chloro-methyl methyl ether as coordinating agent and tin tetrachloride as catalyst and chloroform as solvent to give the product of our interest.[109]

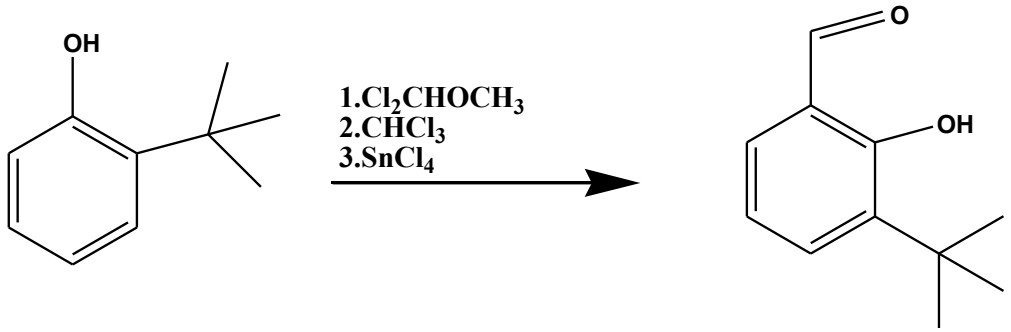

Scheme 30. Synthesis of 3-tert-butyl-2-hydroxybenzaldehyde

The aldehyde obtained was purified by column chromatography (exane / ethyl acetate as eluent), and characterized by ^{1}H-NMR spectroscopy.

IV. 33 Synthesis of 3-tert-butyl-5-chloromethyl-salicilic aldehyde.

3-tert-butyl-2-hydroxybenzaldehyde was chloromethylated in metha position by using p-formaldehyde and chloridric acid as solvent.[110]

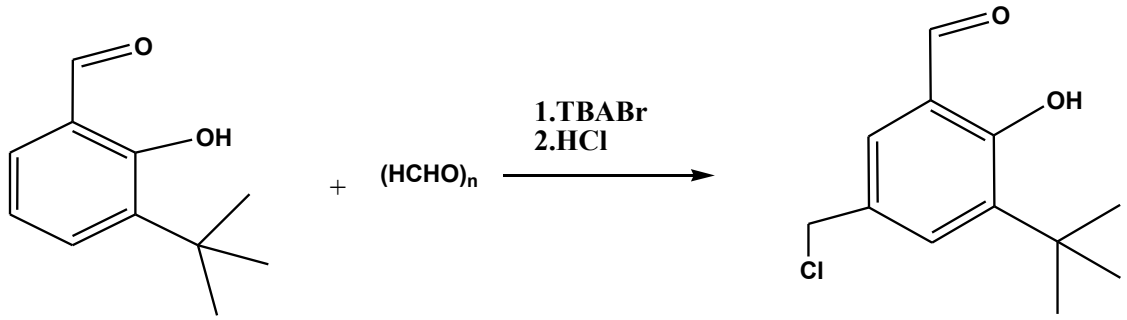

Scheme 31. Synthesis of 3-tert-butyl-5-chloromethyl-salicilic aldehyde.

The product obtained was characterized by ^{1}H-NMR spectroscopy. Quantitative yield.

IV.34 Synthesis of hexanol-phtalimide

Hexanol-pthalimide was synthesized starting from 6-amino-1-hexanol and phtalic anhydride under microwave condition by optimizing a literature procedure[111].
No solvent was needed for this reaction, the mw parameters chosen were the following:

- Temperature: 160°C
- Time: 5 minutes
- Power: 300W

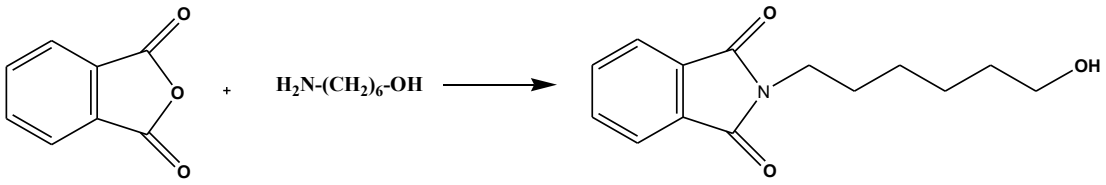

Scheme 32. Synthesis of hexanol-phtalimide

The product was fully characterized by ^{1}H-NMR spectroscopy.

IV.35 Synthesis of 3-tert-butyl-5-methoxy-exhyl-pthalimido-salicyl aldehyde

This compound was obtained from the condensation of 1-exhanol-pthalimide and the 3-tert-butyl-5-chloromethyl-salicyl-aldehyde under microwaves conditions by adapting a literature procedure.
The parameters utilized were:

- Temperature: 127°C
- Power: 30 W
- Time: 45 minutes

In the presence of potassium carbonate and potassium hydroxide as bases[112].

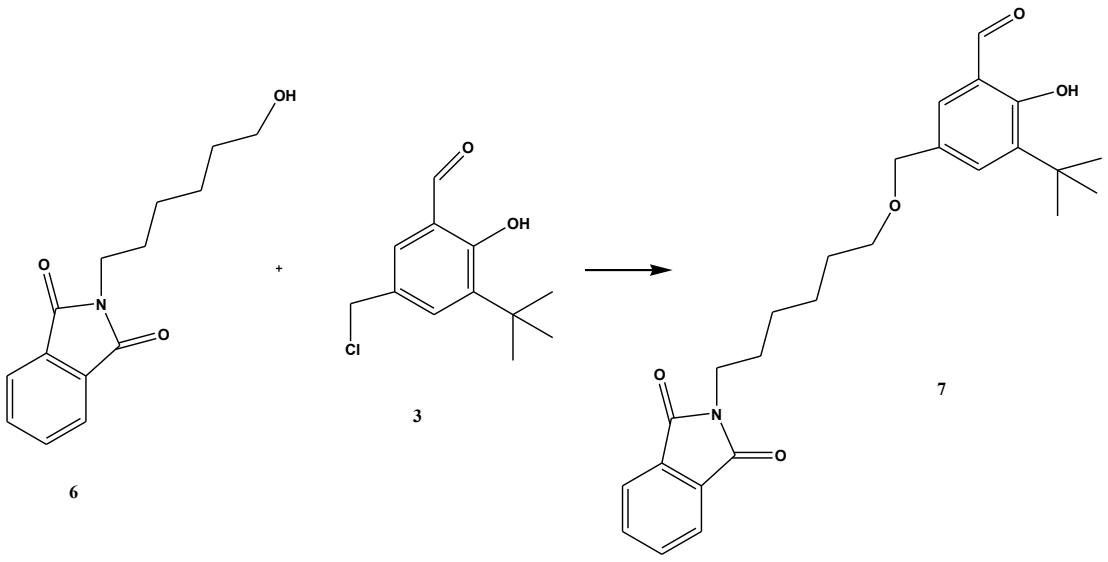

Scheme 33. Synthesis of 3-tert-butyl-5-methoxy-exhyl-pthalimido-salicyl aldehyde

The synthesized compound was fully characterized by NMR.

IV. 36 Synthesis of 1R,2R diphenylethylendiamine chloridrate

In order to prepare the asymmetric ligand that link two different groups it was necessary to protect one of the two amino groups of the 1R,2R diphenyl-ethylen amine selected as chiral bridge, by a reaction of salification with a 2 N solution of hydrochloridric acid in anhydrous ether (30%) to abtain the hydrochloride salt, the procedure allow to use only one equivalent of the acid and the product was obtained by precipitation; the white solid collected after filtration (yield 94%) and characterized by ^{1}H-NMR .

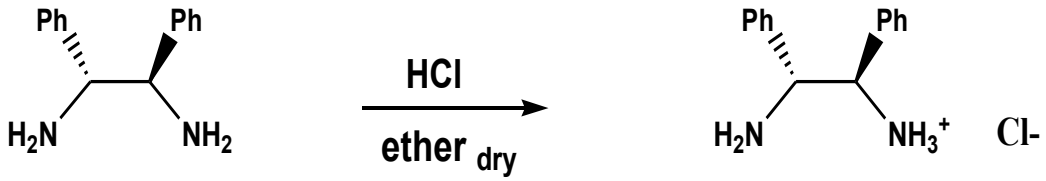

Scheme 34. Synthesis of 1R,2R diphenylethylendiamine chloridrate

Once the mono-imino-amino was obtained it was performed the reaction between the diamine salified with the 3,5-di-tert-butyl-salicyl-aldehyde, to abtain the mono-imino-amine. To isolate the reaction product from the unreacted reagent it was necessary to wash with water to remove the unreacted amine and with diethyl ether to remove the unreacted aldehyde. In both solvents infact the product of the reaction is not soluble[113].

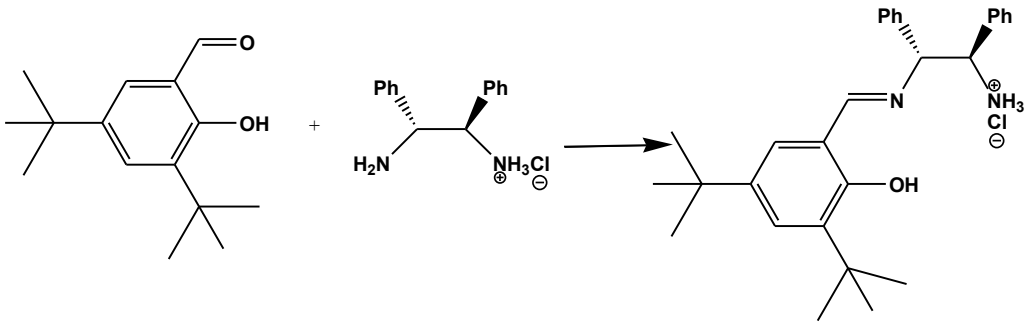

Scheme 35. Synthesis the mono-imino-amine chloridrate

IV.37 Synthesis of the asymmetric salen ligand

The next synthetic step consist to prepare the ligand by the condensation reaction between 3-tert-butyl-5-methoxy-exyl-phtalimido-salycil-aldehyde and the chiral mono-imino amine by using triethylamine as base[101].

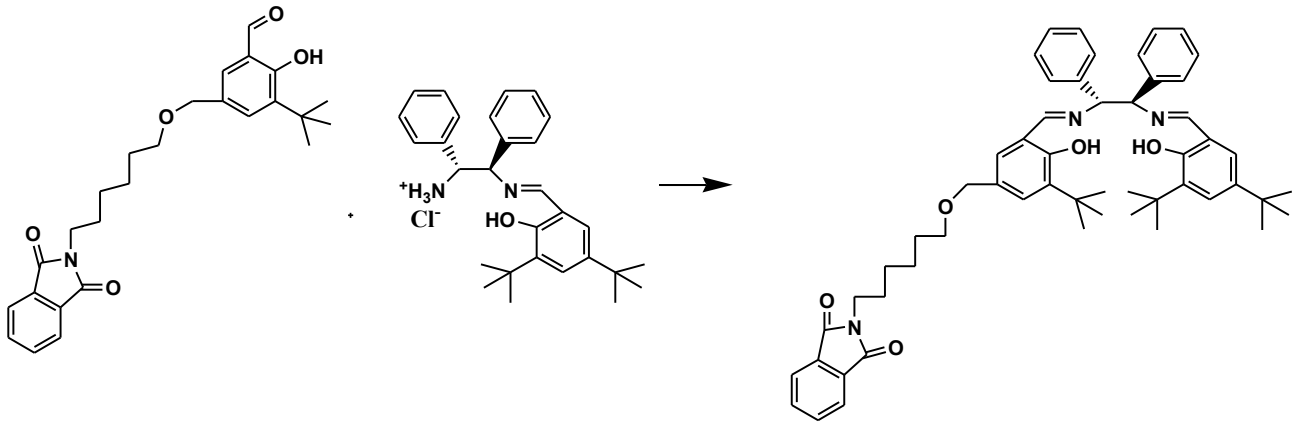

Scheme 36. Synthesis of the asymmetric salen ligand

The ligand obtained it was fully characterized by ^{1}H-NMR,^{13}C-NMR,^{1}H-^{1}H COSY

IV.38 Synthesis Salen-Mn(III) complex (CAT_3)

The salen-Mn (III) complex was obtained by the reaction between the ligand previously synthesized and manganese acetate (III), stirring for 36 h, at room with EtOH as solvent in order to form the coordination complex.

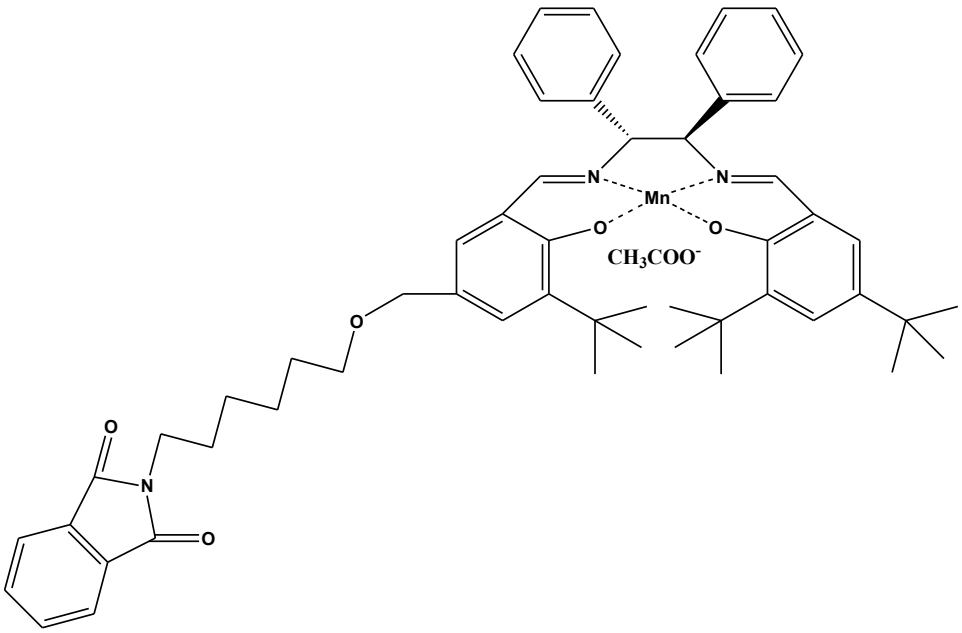

Scheme 37. Synthesis Salen-Mn(III) complex (CAT_3)

The product was fully characterized by ESI/MS,

IV.39 Synthesis of salen ligand precursor of CAT_2

In this case it was performed the condensation reaction between two units of 3-tert-butyl-5-methoxy-exyl-phtalimido-salycil-aldehyde and the 1R,2R diphenylethylendiamine.
The reaction was carried out in absolute ethanol at room temperature overnight, after this time the solvent was removed under reduced pressure and the product used without any further purification to prepare the metal salen complex.
Quantitative yield.

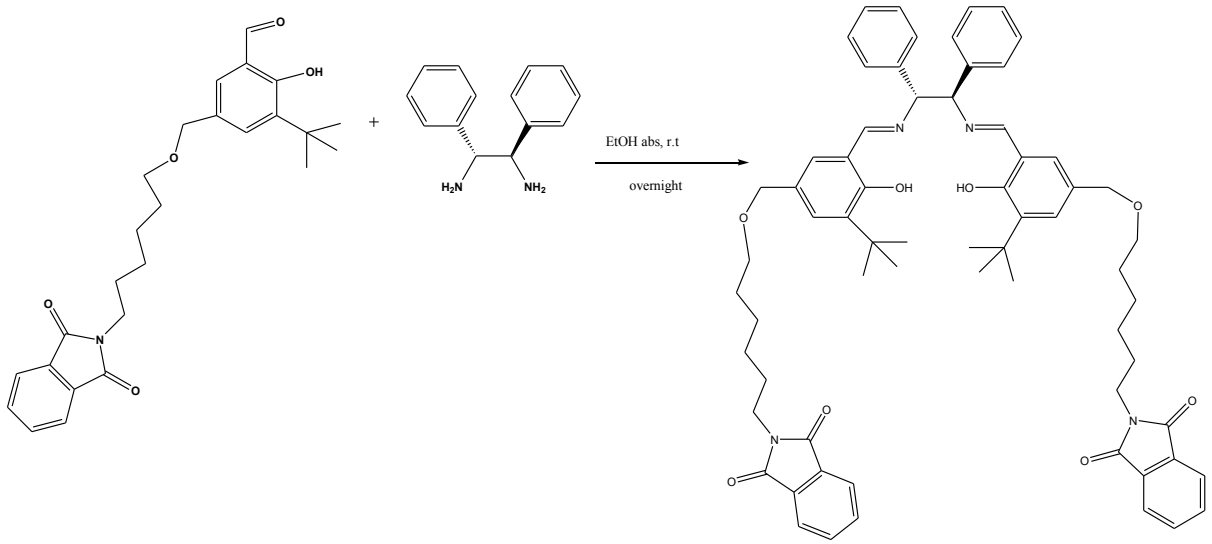

Scheme 38. Synthesis of salen ligand precursor of CAT_2

IV.40 Synthesis of Mn(III) salen complex CAT_2

The next step of the synthesis consist to prepare the manganese (III) salen complex.
The reaction was performed by diluting the ligand in the minimum amount of dichloromethane and then by adding absolute ethanol as solvent, then was added to mixture Mn(III) acetate and the reaction was carried out under stirring, at room temperature overnight, and the proceeding of the reaction was monitored by TLC.
At the end of the reaction the solvent was removed by reduced pressure, and the crude was replaced with dichloromethane in order to eliminate the excess of Mn(III)acetate, the residue was filtered off with a Millipore apparatus and the filtered was rotovaporated to give CAT_2.

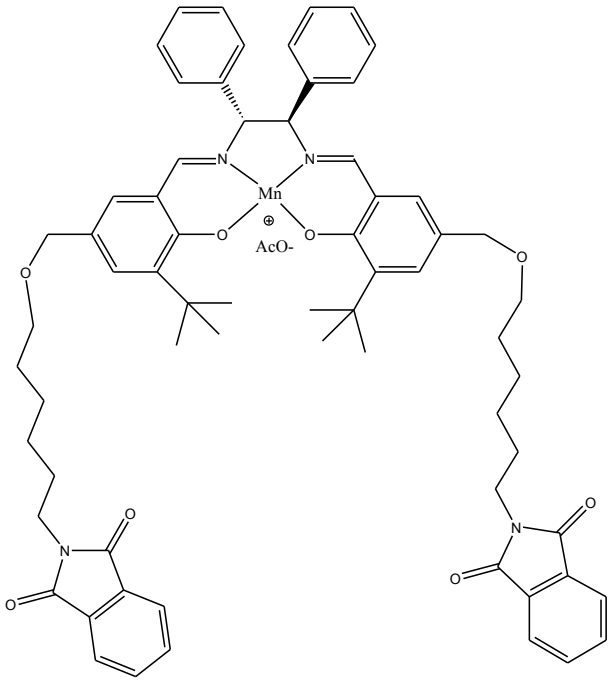

Scheme 39. Synthesis of Mn(III) salen complex CAT_2

V. CONCLUSIONS

In this PhD work were synthesized and characterized a series of new organic molecules with different aims, in order:

1. To detect CWAs simulant by synthesizing a series of oximes with an active functional group in order anchor these molecules on silica surface. A preliminary study in solution shows that the molecules synthesized interact with the nerve agent simulant used (DMMP, dimethyl-methyl phosphonate), but they do not give a high detectable signal. With the second generation of oxymes synthesized we tried to perfom a reaction with the simulant used (in this case the DCP, diethylchlorophosphate), and we obtain a very promising device to detect CWAs because of the dramatic change of colour after the interaction, followed by a significant change in the UV-Vis and ^{1}H NMR titrations.
2. To recognize metal transition ions by synthesizing a series of naphtilamide derivates that has been tested both in solution and anchored on silica surphace; firstly we synthesized the N-tyramine-di[2(dipicolyl)amino]1,8 naphtalimide that selectively recognize copper both in solution and also anchored on silica surface, then we synthesized napthilamide derivate linked with a trealose derivate to recognize copper in biological environment, studies are underway to determine the selectivity of the sensor.
3. To selectively transfer oxygen by synthesizing three different catalysts that bear salen units; these catalysts has been designed with three different anchoring groups to obtain a reusable and environmental friendly devices. The results are very promising in the regard of the reusability, and the enantiomeric excess obtained are similar with whose presented in literature.

VI. EXPERIMENTAL

VI.1 General

All starting materials and solvents were purchased from Sigma-Aldrich and used as received. Melting points were determined on a Kofler hot stage apparatus and are uncorrected. The NMR experiments were carried out at 27 °C on a Varian UNITY Inova 500 MHz spectrometer (^{1}H-NMR at 499.88 MHz, ^{13}C NMR at 125.7 MHz in $CDCl_3$) equipped with pulse field gradient module (Z axis) and a tunable 5 mm Varian inverse detection probe (ID-PFG). The chemical shifts (ppm) were referenced to TMS. Mass spectral data were obtained by employing an ES-MS Thermo-Finnigan LCQ-DECA spectrometer equipped with an ion trap analyzer. UV-VIS measurements: UV-Vis spectra were recorded with a Jasco V-650 spectrophotometer. Epoxidation reaction: Gas chromatographic analysis of the reaction mixture were carried out on a PERKIN- ELMER 8420 gas chromatograph equipped with a flame ionization detector and program capability. The *ee were* determined employing the chiral column DMePeBETACDX (25m x 0.25 mm ID x 0.25 μm film) to detect 1,2 dihydronaphtalene; DMeTButiSililBETA PS086 (25m x 0.25 mm ID x 0.25 μm film) to detect cis β methylstirene and DIMEPEBETA-086 (25m x 0.25 mm ID x 0.25 μm film) to detect 6-ciano-2,2-dimethyl chromene. XPS measurements: PHI ESCA/SAM 5600 Multy technique spectrometer equipped with a monochromatized Al Ka X-ray source. The analyses were carried out either at 45° or at 20° photoelectron take off angle relative to the sample surface with an acceptance angle of ±7°. Binding Energy (BE) scale was calibrated by centering the adventitious/hydrocarbon carbon C1s at 285.0 eV.

VI.2 Synthesis of 4-hydroxy benzaldoxime

To a solution of 4-hydroxybenzaldehyde 1,25 g (10,24 mmol) in ethanol 20 mL was added a solution composed of 1,29 g (18,6 mmol) of hydroxylamine hydrochloride and sodium acetate 1,67 g (20,4 mmol) in ethanol. The reaction was stirred for 6 h at room temperature and monitored by TLC (n-hexan/EtOAc 6:4); after the reaction was competed the solvent was removed under reduced pressure; the resulting was replaced with water and then extracted with diethyl ether (3 times). The organic phase was dried with magnesium sulphate, filtered and the solvent removed under reduced pressure. The solid was recrystallized from dichloromethane, washed with cold dichloromethane and dried in the air to give pure oxime as pale yellow needle, with a 87% yield.
m.p 136-138°C. ^{1}H-NMR (500 MHz, DMSO-d_6): δ 10,79 (s, 1H, CHO), 9,71 (s, 1H, OH), 9,71 (s, 1H, CH), 6,7 (d, 2H, CH), 7,4 (d, 2H, CH). ESI-MS *m/z* 138 $[M+H]^{+}$

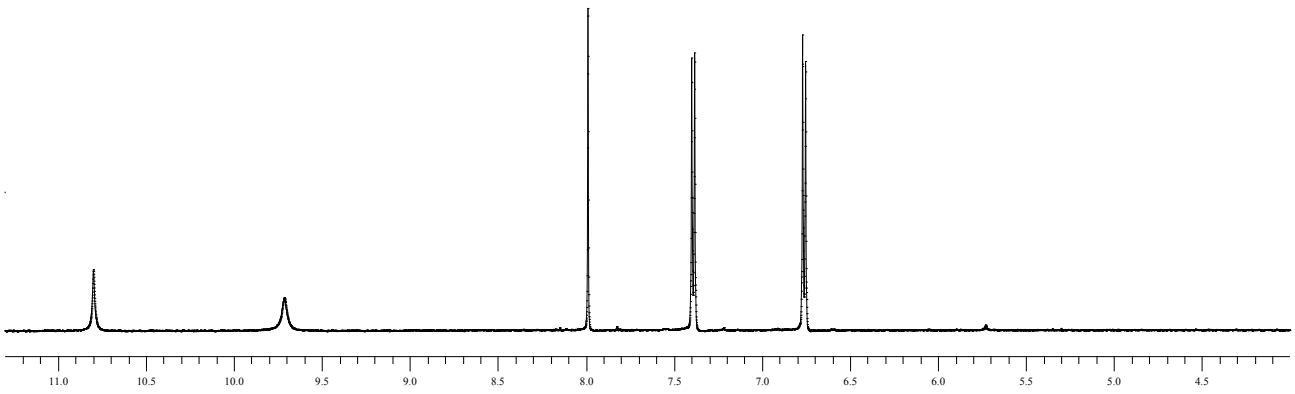

Fig. 37. ^{1}H-NMR spectrum of 4-hydroxy benzaldoxime

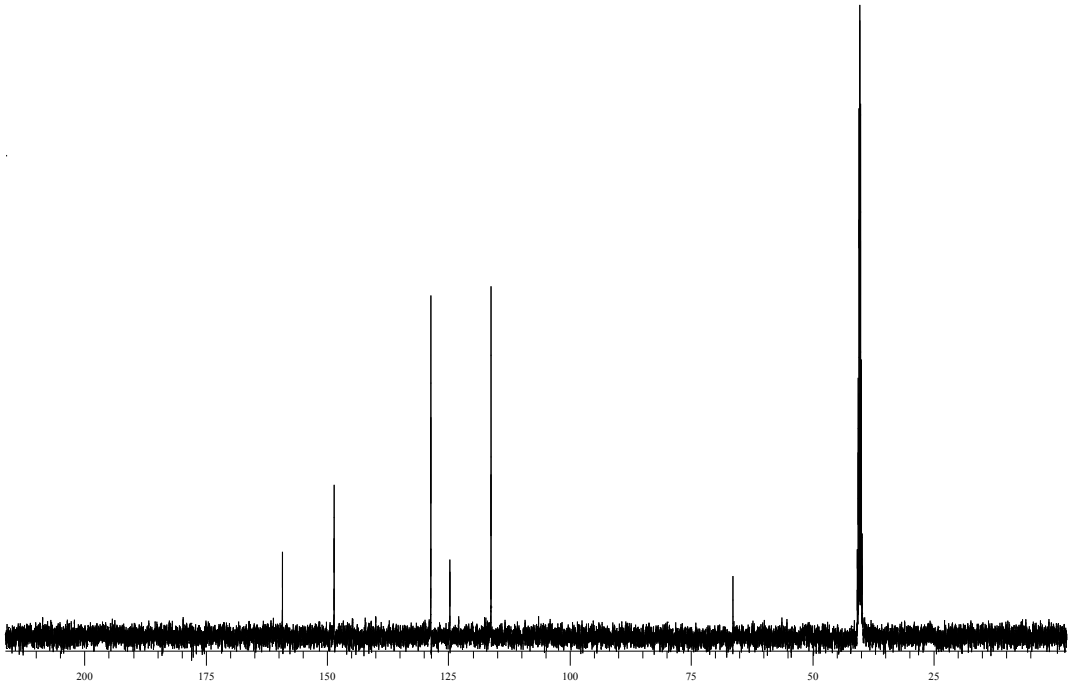

Fig. 38. ^{13}C-NMR spectrum of 4-hydroxy benzaldoxime

VI.3 Synthesis of 4-acetamido-3-nitro benzaldehyde

4-acetamidobenzaldehyde (17g ,104 mmol) was added slowly to a cold solution (0-5°C) of fuming nitric acid (44 ml; 940 mmol) and stirred for 2 h. The solution turns soon from yellow to dark brown. The solution was then poured into cold water (500 mL) and the resulting deep yellow solid was filtered and triturated with cold water (300 mL) for just an hour. The solid was filtered and then recrystallized from 2-propanol (175 mL), filtered and washed with cold 2-propanol twice; the resulting solid was dried in the air for 24 hours. The resulting yield is in agreement with literature, 52%.
IR: NO_2 stretching symmetric and asymmetric respectively at 1458 e 1377 cm^{-1}.
m.p. 155° C. ^{1}H-NMR (500 MHz, $CHCl_3$): δ 2.37 (s, 3H, CH_3), 8.16 (dd, 1H, ArH), 8.73 (d, 1H, ArH), 9.03 (d, 1H, ArH), 9.9 (s, 1H, CHO), 10.62 (s, 1H, NH)
^{13}C-NMR(125.7 MHz, $CHCl_3$) δ 25.71, 122.71, 127.90, 135.44, 135.79, 139.35, 169.17,188.74. ESI-MS *m/z* 208 $[M+H]^+$

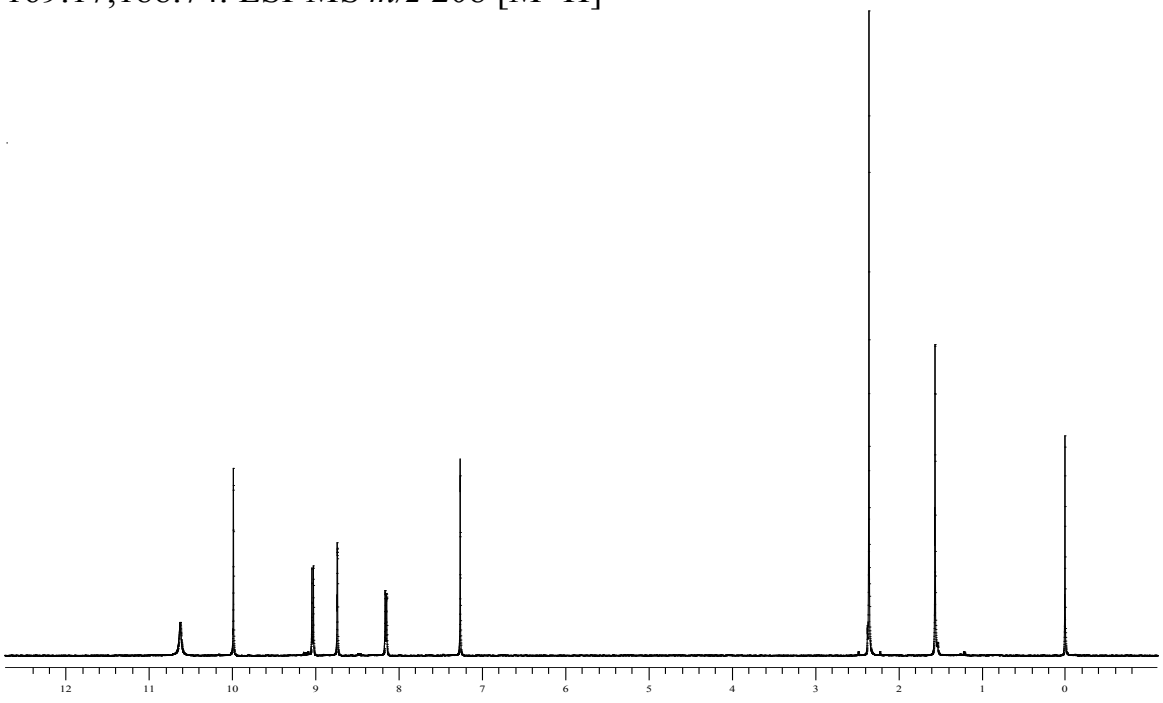

Fig. 39. ^{1}H-NMR spectrum of 4-acetamido-3-nitrobenzaldehyde

VI.4 Synthesis of 4-amino-3-nitro benzaldehyde

4-acetamido-3-nitrobenzaldehyde (5g, 24 mmol) were added to concentrated HCl 36% (25 mL). The suspension was stirred for 2 hours at 75°C. At the end of the reaction cold water (150 mL) was added to the suspension and stirred for further 1 hour. The resulting solid was filtered and triturated with cold water (150 mL) containing $NaHCO_3$ (2,75 g, 33,5 mmol) for 1 hour. The solid was filtered, washed two times with cold water (50 mL) and crystallized from 2-propanol (200 mL), then filtered and washed with cold 2-propanol to give 75% yield.

m.p 191-192 °C ^{1}H-NMR (500 MHz, DMSO-d_6) δ 7.12 (d, 1H, ArH), 7.81 (dd, 1H, ArH), 8.18 (s, 2H, NH), 8.56 (d, 1H, ArH), 9.76 (s, 1H, CHO).
^{13}C-NMR (125.7 MHz, DMSO-d_6) δ 119.89, 124.56, 129.70, 132.45, 132.74, 149.81, 189.73. ESI-MS *m/z* 166 $[M+H]^+$.

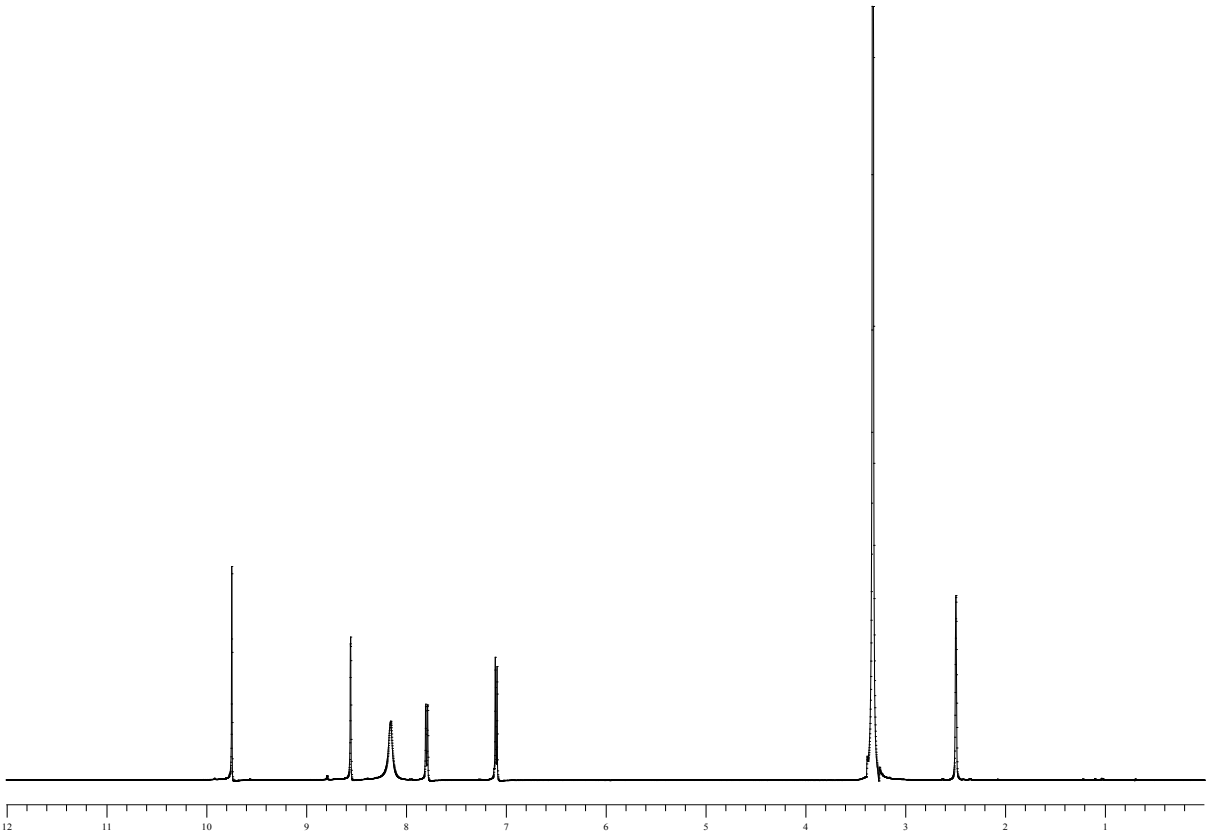

Fig.40. ^{1}H-NMR spectrum of 4-amino-3-nitrobenzaldehyde

VI.5 Synthesis of 4-amino-3-nitro benzaldoxime

A suspension of 4-amino-3-nitro benzaldehyde (800 mg, 4,8 mmol) in ethanol (15 mL) was added to a solution of hydroxylamine hydrochloride (670 mg, 9,6 mmol) and sodium hydroxide (386 mg, 9,6 mmol) in 10 mL of water and stirred at room temperature for 7 hours. At the end of the reaction the ph was adjusted to ph 6 by addiction of glacial acetic acid and placed into an ice bath for 1 hour. The resulting yellow solid was filtered, washed one time with a mixture of glacial acetic acid and water (50 mL 5:1) and recrystallized from ethanol- water to give bright yellow solid in 68 % yield.
m.p 207° ^{1}H-NMR (500 MHz, DMSO-d_6) δ 7.05 (d, 1H, ArH), 7.70 (s, 3H, NH_2,OH), 8.15 (d, 1H, ArH), 11.03 (s, 1H, oxime).
^{13}C-NMR (125.7 MHz, DMSO-d_6) δ 119.8, 120.8, 124.43, 129.69, 132.20, 146.20, 146.74. ESI-MS *m/z* 182 $[M+H]^+$.

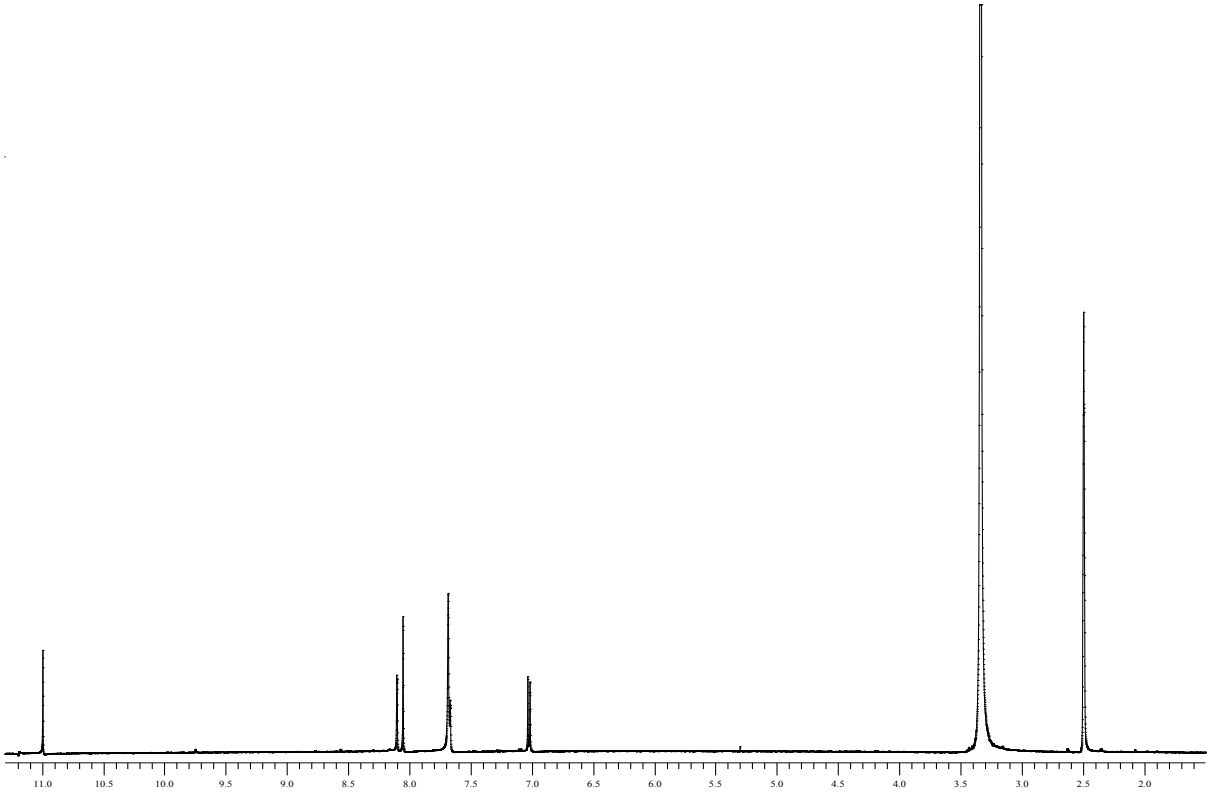

Fig. 41. ^{1}H-NMR spectrum of 4-amino-3-nitrobenzaldoxime

VI.6 Synthesis of 4-hydroxy-2'-nitro-4'-phormyl -azo-benzene

A suspension 0,460 mg (3,85 mmol) of 4-amino-3-nitro benzaldehyde was prepared at 0° C in 15 ml of water. At the same temperature was separately dissolved 247 mg (3,6 mmol) of sodium nitrite in 10 ml of water. The suspension of the 4-amino-3-nitro benzaldehyde was simultaneously added at vigorous stirring the solution of sodium nitrite and 5 ml (33 mmol) of 24% hydrochloridric acid solution. The completion of diazotation reaction was monitored with a starch-iodide paper strip test. The solution of diazo compound was then adjusted to pH 7 by adding a 6% solution of sodium hydroxide. To the neutral solution of diazo compound at cooling and stirring was added a cool solution of 0,300 g (3,2 mmol) of phenol dissolved in 5 ml of water at pH 6 by sodium hydroxide. The of the reaction was monitored by TLC (esane: ethyl acetate 8:2). The reaction product was precipitated by adding to the reaction mixture 1g of sodium chloride, the precipitate was filtered off and the precipitate recrystallized from acetic acid. Yield of the orange product 80% (530 mg).
^{1}H-NMR (500 MHz, acetone-d_6): δ 7 (d, 2H, ArH), 7.9 (d, 2H, ArH), 8.3 (d, 1H, ArH), 8.5 (d, 1H, ArH), 7.9 (s, 1H, ArH), 10.2 (s, 1H, CHO).
^{13}C-NMR (125.7 MHz, acetone-d_6) δ 116.3, 119.5, 125.1, 126.6, 133.4, 137.4, 146.4,162.6,190.2 ESI-MS *m/z* 272 $[M+H]^+$

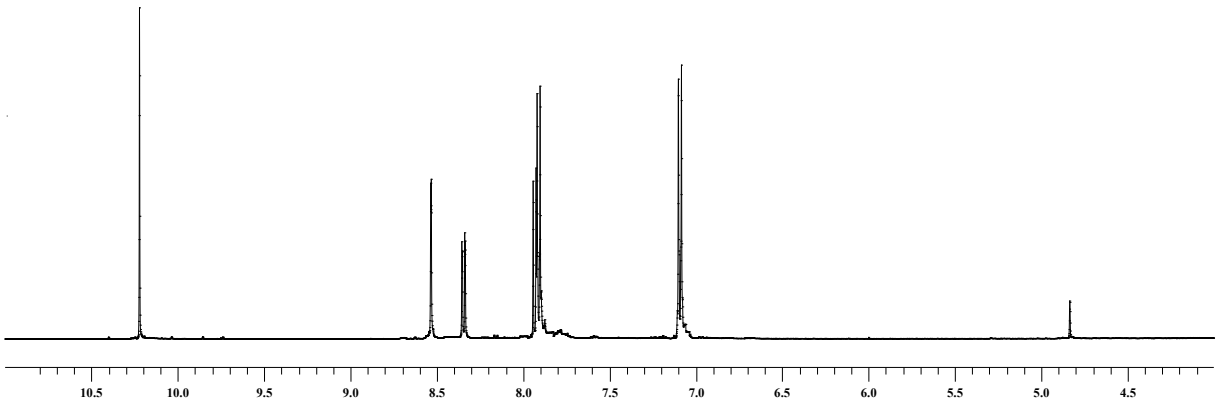

Fig. 42. ^{1}H-NMR spectrum 4-hydroxy-2'-nitro-4'-phormyl -azo-benzene

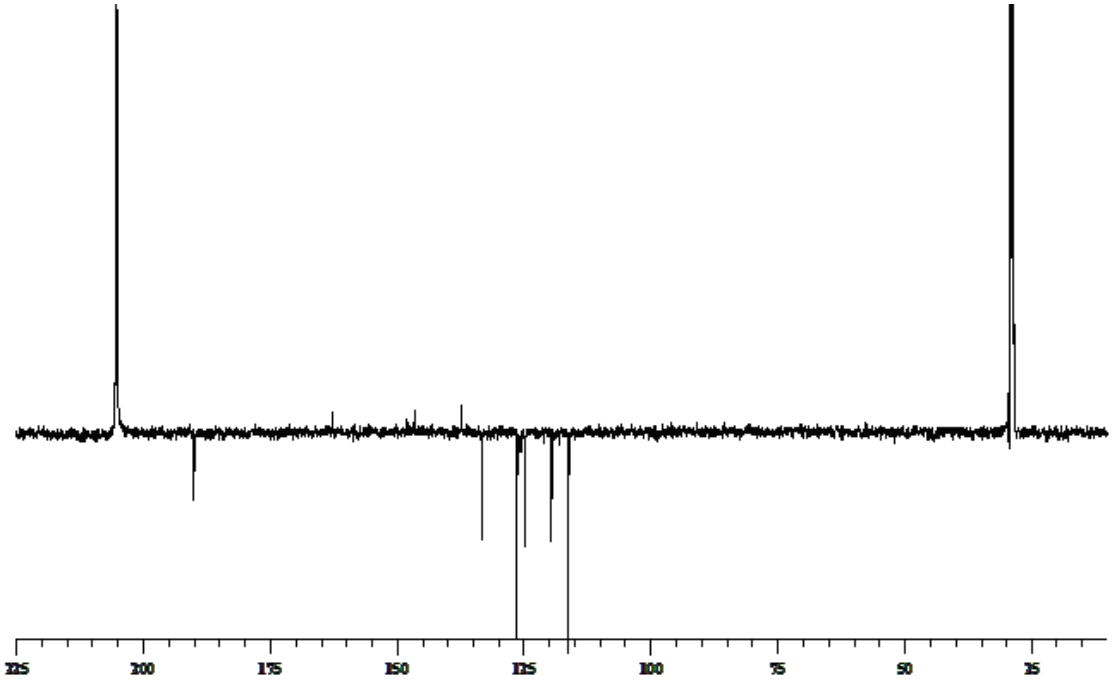

Fig. 43.^{13}C-NMR 4-hydroxy-2'-nitro-4'-phormyl -azo-benzene

VI.7 Synthesis of 4-hydroxy-2'-nitro-4'-oxime -azo-benzene

A suspension of 4-hydroxy-2'-nitro-4'-phormyl -azo-benzene (200 mg, 0,74 mmol) in ethanol absolute (10 ml) was added to a solution of hydroxylamine hydrochloride (103 mg, 1,5 mmol) and sodium hydroxide (96 mg, 2,4 mmol) in 3 mL of water and stirred at room temperature for 7 hours. At the end of the reaction the pH was adjusted to pH 6 by addiction of glacial acetic acid and placed into an ice bath for 1 hour. The resulting red brown solid was filtered, washed one time with a mixture of glacial acetic acid and water (50 mL 5:1) and recrystallized from ethanol- water to give bright magenta powder 197 mg 68 % yield.

^{1}H-NMR (500 MHz, acetone-d_6) δ 11 (s, 1H, oxime), 7.70 (s, 1H, ArH), 8.2 (d, 1H, ArH), 8 (d, 1H, ArH), 7.9 (d, 2H, ArH),7.8 (d, 1H, ArH), 7 (d, 2H, ArH)

^{13}C-NMR (125.7 MHz, acetone-d_6) δ 116, 116.1, 118.9, 120.8, 125.8, 130.4, 135.20, 156. ESI-MS *m/z* 287 $[M+H]^+$.

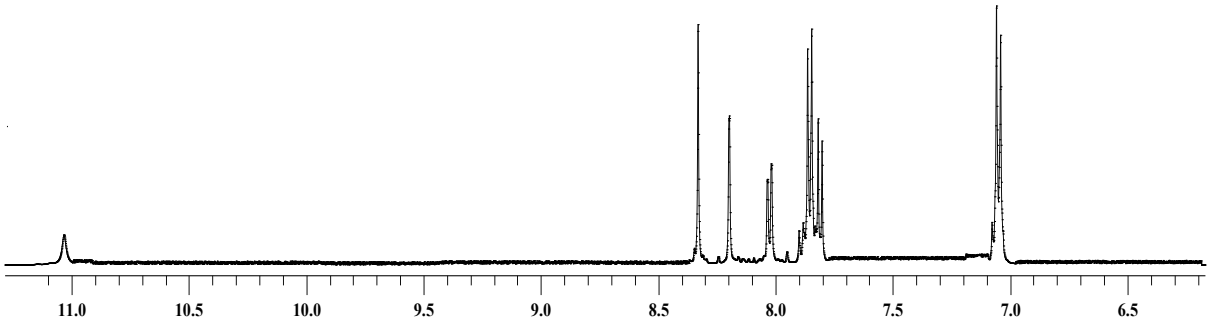

Fig. 44. ^{1}H-NMR spectrum of 4-hydroxy-2'-nitro-4'-oxime -azo-benzene

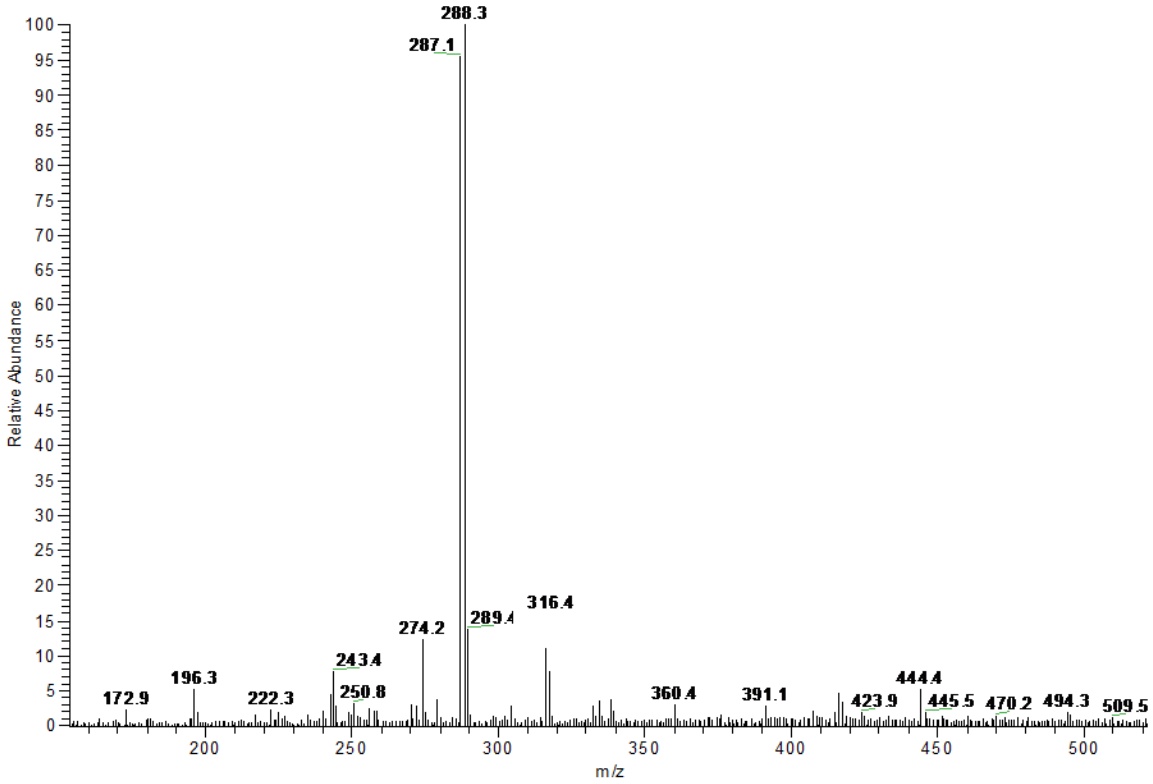

Fig. 45. ESI-MS spectrum of 4-hydroxy-2'-nitro-4'-oxime -azo-benzene

VI.8 Synthesis of 4-bromoacenaphtene

A solution of N-bromosuccinimide, (18 g, 0,1 mol) in 50 mL of DMF was added to a suspension of acenaphtene (15,4 g, 0,1 mol) in 50 mL of DMF at room temperature. Heated was evolved and after 2 hours, the solution was

poured into a litre of cold water. Filtration gave 23 g of crude product. After crystallization from ethanol gave 18,5 g (79%) of 4-Bromoacenapthene.[48]
^{1}H-NMR (500 MHz, $CDCl_3$) δ 7,7 (d, *J* = 8 Hz, 1H, ArH), 7.65 (d, *J* = 7 Hz, 1H, ArH), 7,54 (t, *J* = 6,5 Hz, 1H, ArH), 7,32 (d, *J* = 6,5 Hz, 1H, ArH), 7,13 (d, *J* = 7 Hz, 1H, ArH), 3,37 (m, 4H, CH_2). ESI-MS *m/z* 231,9 $[M+H]^+$.

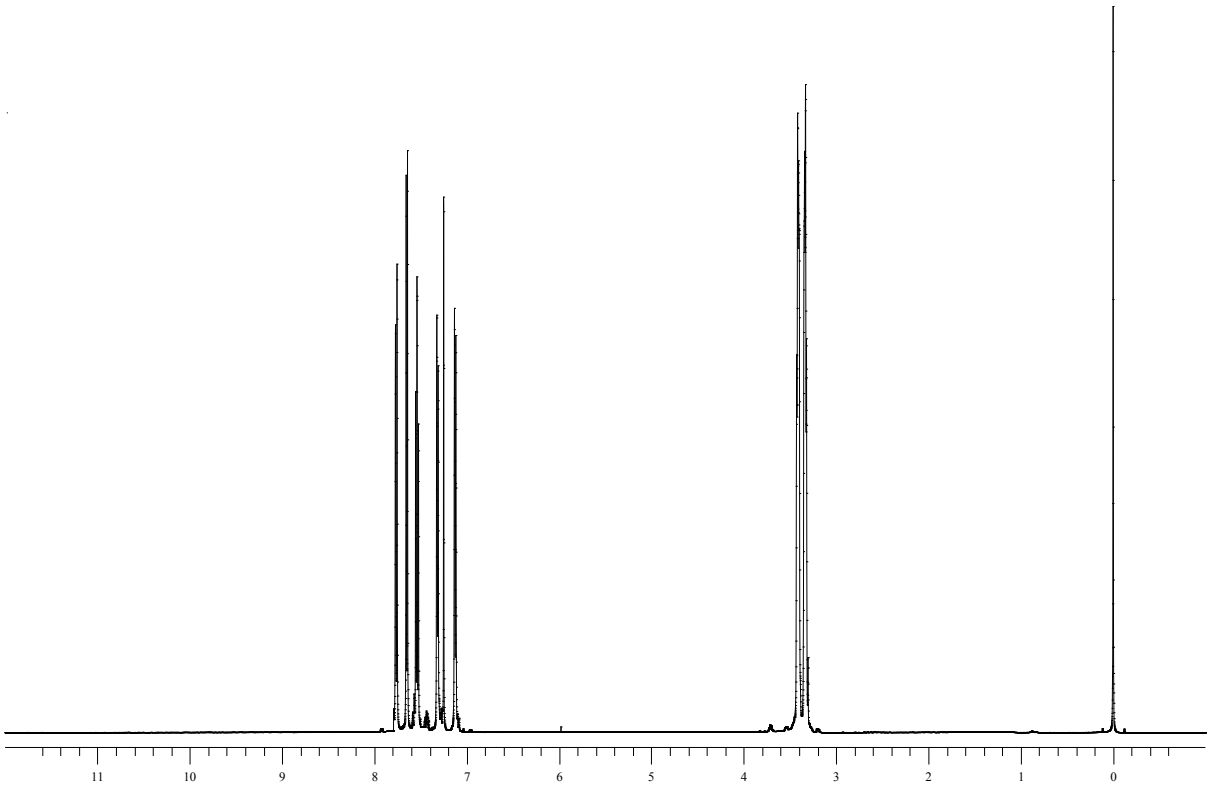

Fig. 46. ^{1}H-NMR spectrum of 4-bromoacenaphtene

VI.9 Synthesis of 4-bromo-5-nitro acenaphtene

4g of 4-bromoacenapthene was stirred into glacial acetic acid (33 mL) at 15°C and a mixture of fuming nitric acid (2,5 mL) and glacial acetic acid (7,5 mL) run in over 30 minutes, maintaining at maximum of temperature of 15° C. The suspension was stirred for 10 hours at 10-15°C, filtered and the yellow residue (3,0 g) was crystallized from glacial acetic acid in yellow needles of 4-bromo-5-nitroacenaphtene.
m.p. 158°C. ^{1}H-NMR (500 MHz, $CDCl_3$) δ 7,85 (d, J = 7,5 Hz, 1H, ArH), 7.74 (d, J = 7,5 Hz, 1H, ArH), 7,31 (d, J = 7,5 Hz, 1H, ArH), 7,27 (d, J = 7,5 Hz, 1H, ArH), 3,43 (m, 4H, $2CH_2$).

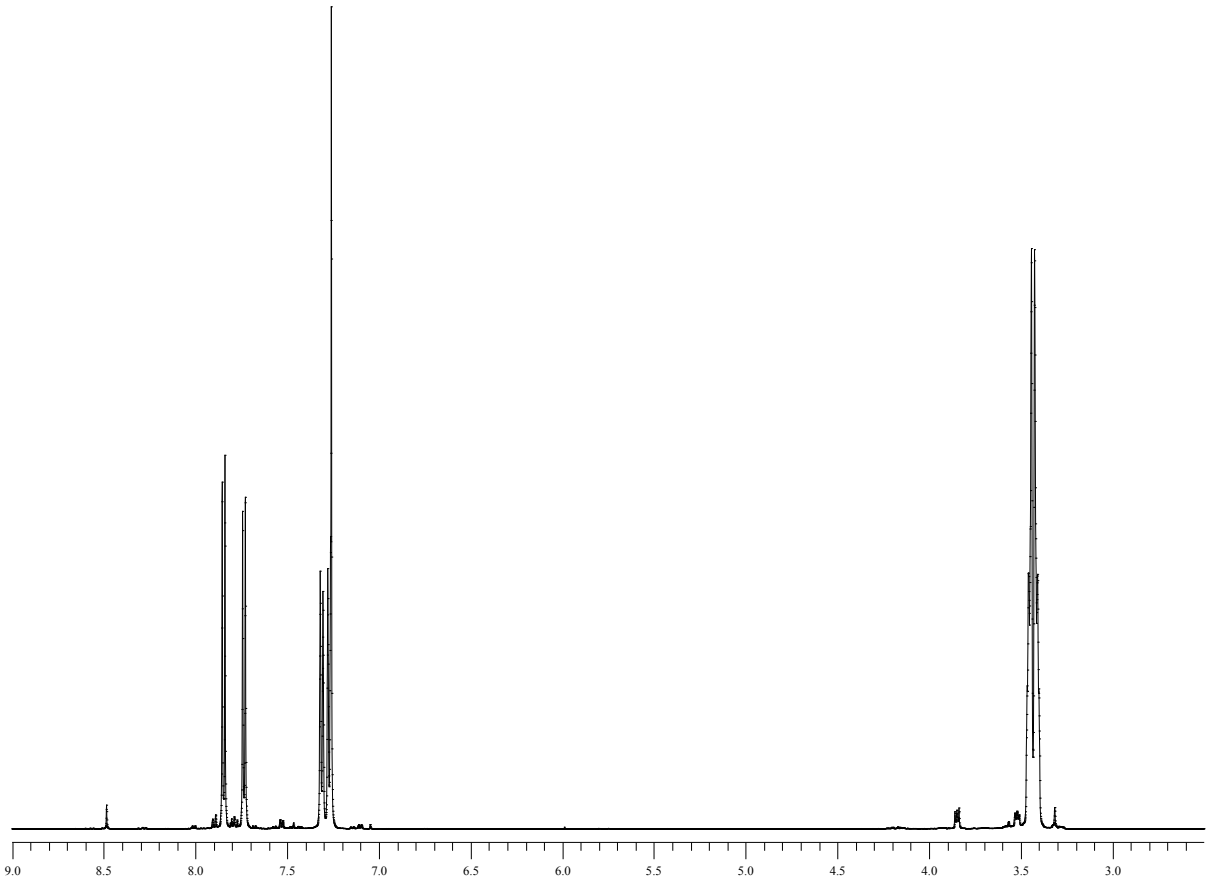

Fig. 47. ^{1}H-NMR spectrum of 4-bromo-5-nitro acenaphtene

VI.9 Synthesis of 4-bromo-5-nitro 1,8 naphtalic anhydride

4-bromo-6-nitro acenapthene (2,3 g 9,35 mmol) was stirred into a mixture of glacial acetic acid (25 mL) and sodium dichromate * 2 H_20 (6 g) and the solution slowly heated to reflux. The solution change color from bright orange to dark green (because of this reaction $Cr^2O^{7--} \rightarrow Cr^{3+}$); after refluxing for 3 hours the dark green liquor was diluted with 10 mL of cold water, cooled, filtered and the yellow-orange residue washed with a little amount of glacial acetic acid and then stirred into a 4% aqueous solution of sodium hydroxide. After filtering, the filtrate were neutralized with 5% solution aqueous solution of hydrochloric acid to give cream-orange precipitate of 4-bromo-5-nitro-1,8naphtalic anhydride. 42% yield.
^{1}H-NMR (500 MHz, $CDCl_3$) δ 7,84 (d, *J* = 7 Hz, 1H, ArH), 7.72 (d, *J* = 8 Hz, 1H, ArH), 7,31 (d, *J* = 7 Hz, 1H, ArH), 7,25 (d, *J* = 8 Hz, 1H, ArH). ESI-MS *m/z* 322,93 $[M+H]^+$.

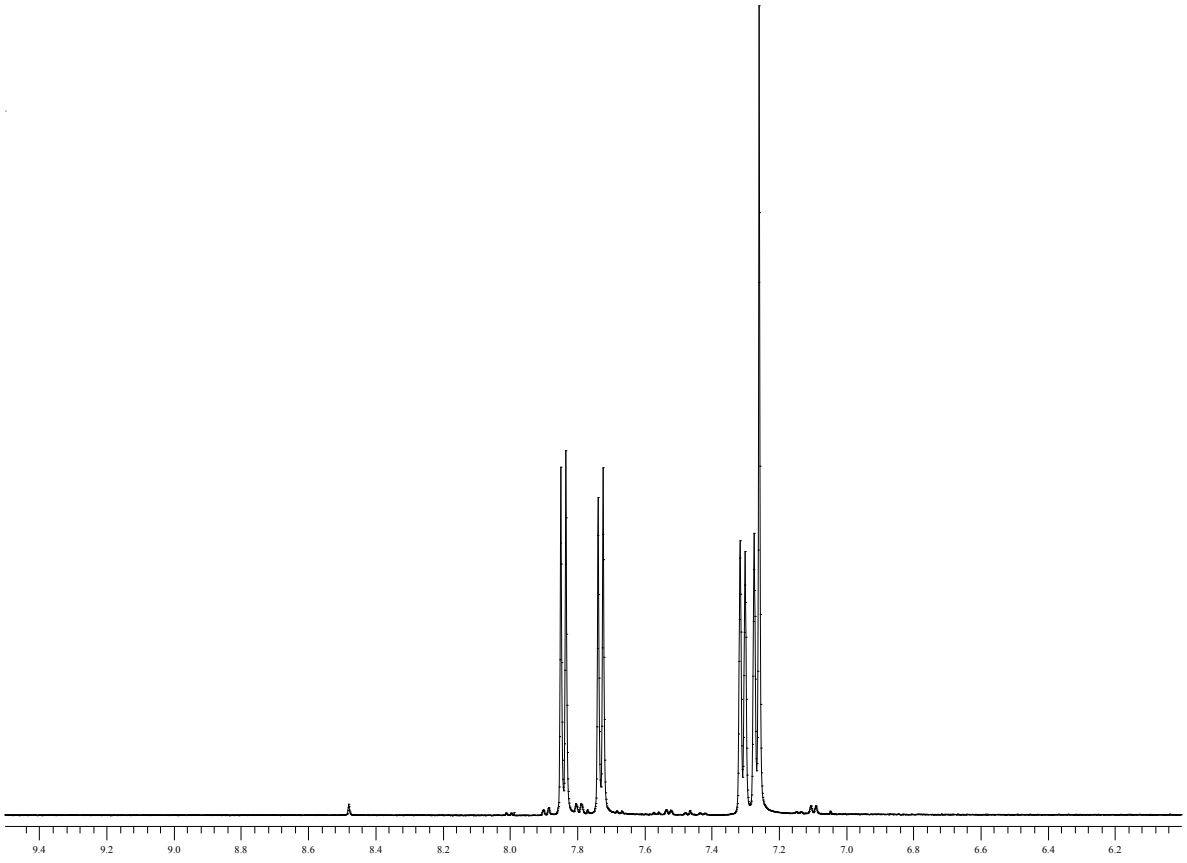

Fig. 48. ^{1}H-NMR spectrum of 4-bromo-5-nitro naphtalic anhydride

VI.10 Synthesis of 4-bromo-5-nitro naphtalimide

To a solution of 1,3 g (4,0 mmol) of 4-bromo-5-nitro-1,8 naphtalic anhydride in 30 mL of ethanol was added dropwise 0,4 g of tiramine in 15 mL of ethanol. The mixture was then heated to reflux and monitored by TLC (CH_2Cl_2-EtOAc 8:2). After the reaction was completed, the solvent was removed under reduced pressure and the crude product was purified by column chromatography (SiO2, CH_2Cl_2-EtOAc 9:1) to give N-tiramine-di[2-(dipicolyl)amino]1,8 naphtalimide as a deep yellow solid in 40,5% yield (670 mg).
^{1}H-NMR (500 MHz, $CDCl_3$) δ 8,70 (d, *J* = 8 Hz, 1H,ArH), 8.50 (d, *J* = 8 Hz, 1H, ArH), 8,21 (d, *J* = 8 Hz, 1H, ArH), 7,93 (d, *J* = 8 Hz, 1H, ArH) 7,19 (d, *J* = 8 Hz, 2H, ArH), 6,77 (d, *J* = 8 Hz, 2H,ArH), 4,62 (s, 1H, OH), 4,4 (t, *J* = 8 Hz, 2H, CH_2), 2,9 (t, *J* = 8 Hz, 2H, CH_2). ESI-MS *m/z* 440 $[M+H]^+$.

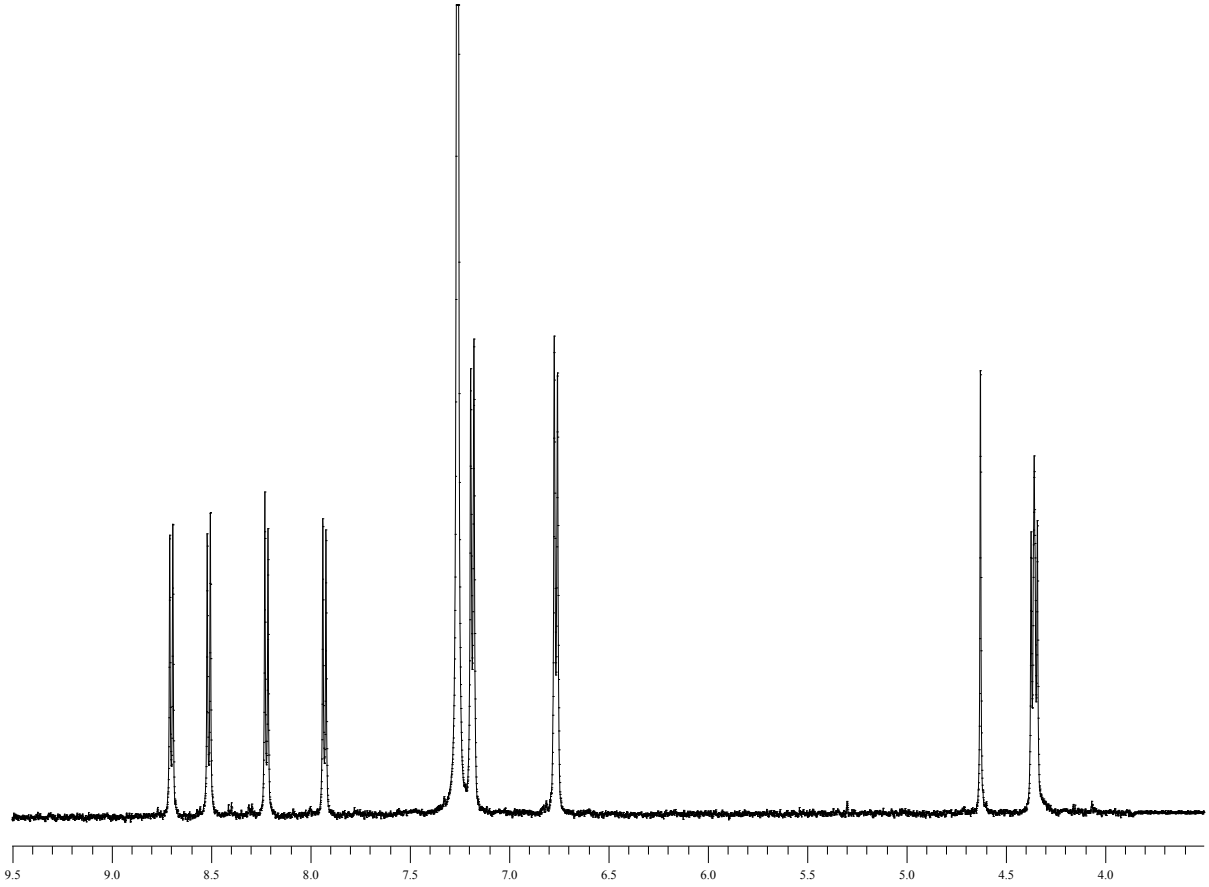

Fig.49. ^{1}H-NMR spectrum of4-bromo-5-nitro naphtalimide

VI.11 Synthesis of N-tiramine-di[2-(dipicolyl)amino]1,8 naphtalimide

0,8 mL (7.5 mmol) of picolyl-2-amine were added dropwise to a solution of 0,2 g (0,4 mmol) of N-tyramine-1,8 naphtalimide in 3mL of 2-methoxyethanol; the solution were quickly heated to reflux for 4 hours and monitored by TLC (CH_2Cl_2/MeOH 95:5). After the reaction was completed the solution was quenched with 10 mL of cold water and still stirring cooled at room temperature. A solid that is formed were filtered with a millipore filtering system and the crude product were purified by chromatography (SiO_2 , start CH_2Cl_2 to a eluent mix of CH_2Cl_2:MeOH 90:10) to give the pure product as a yellow powder with 80% (0,190 g) of yield. ESI-MS m/z 530 $[M+H]^+$.
^{1}H-NMR (500 MHz, $CDCl_3$) δ 8,5 (d, *J* = 8 Hz, 1H, ArH), 8.3 (d, *J* = 8 Hz, 1H, ArH), 7.7 (t, *J* = 8 Hz, 1H, ArH), 7,4 (d, *J* = 8 Hz, 1H, ArH), 7,2 (t, *J* = 8 Hz, 2H, ArH), 6,8 (d, *J* = 8 Hz, 2H, ArH), 6.8 (d, 1H, ArH) 4,7 (s, 4H, CH_2), 4,4 (t, *J* = 8 Hz, 2H, CH_2), 2,9 (t, *J* = 8 Hz, 2H, CH_2).
^{13}C-NMR (**$CDCl_3$**, 125 MHz) δ 33.5, 41.8, 47.5, 104.4, 108.2, 115.4, 122.9, 124.8, 125.8, 128.9, 130, 131.2, 134.5, 137, 149.7, 150.9, 154.7, 155.9, 164.1. ESI-MS *m/z* 530 $[M+H]^+$.

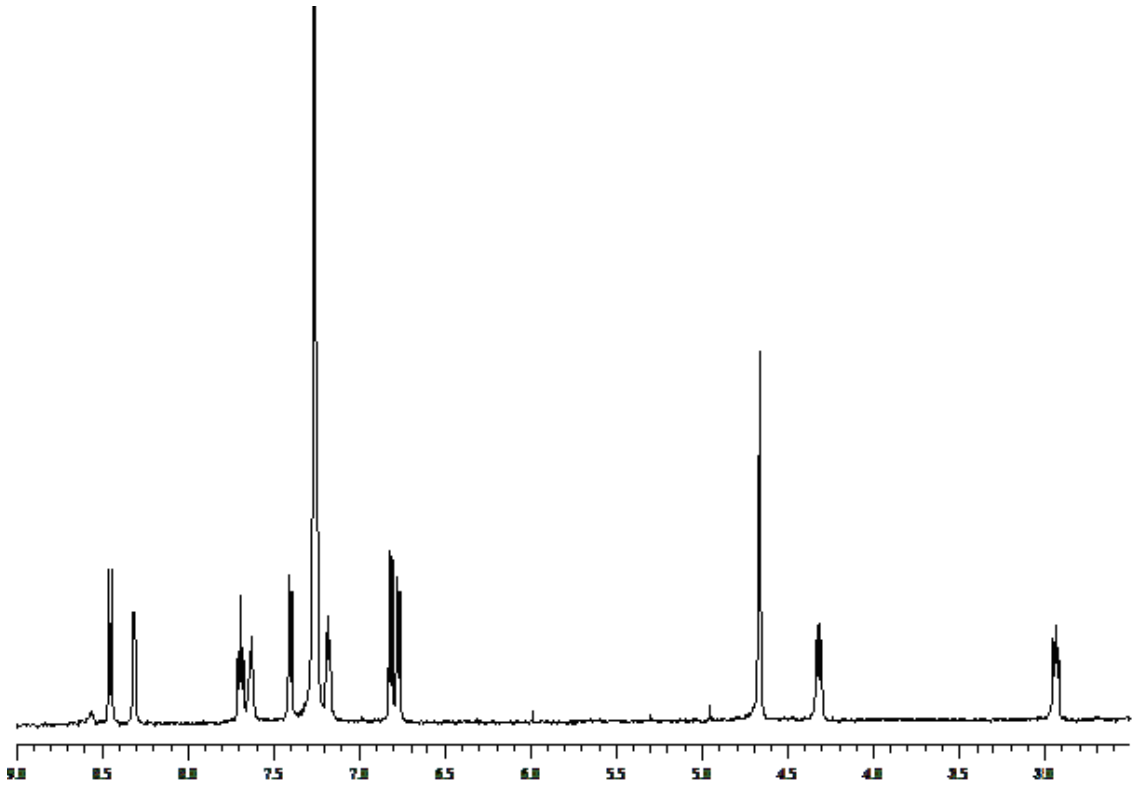

Fig.50. ^{1}H-NMR spectrum of N-tiramine-di[2-(dipicolyl)amino]1,8 naphtalimide

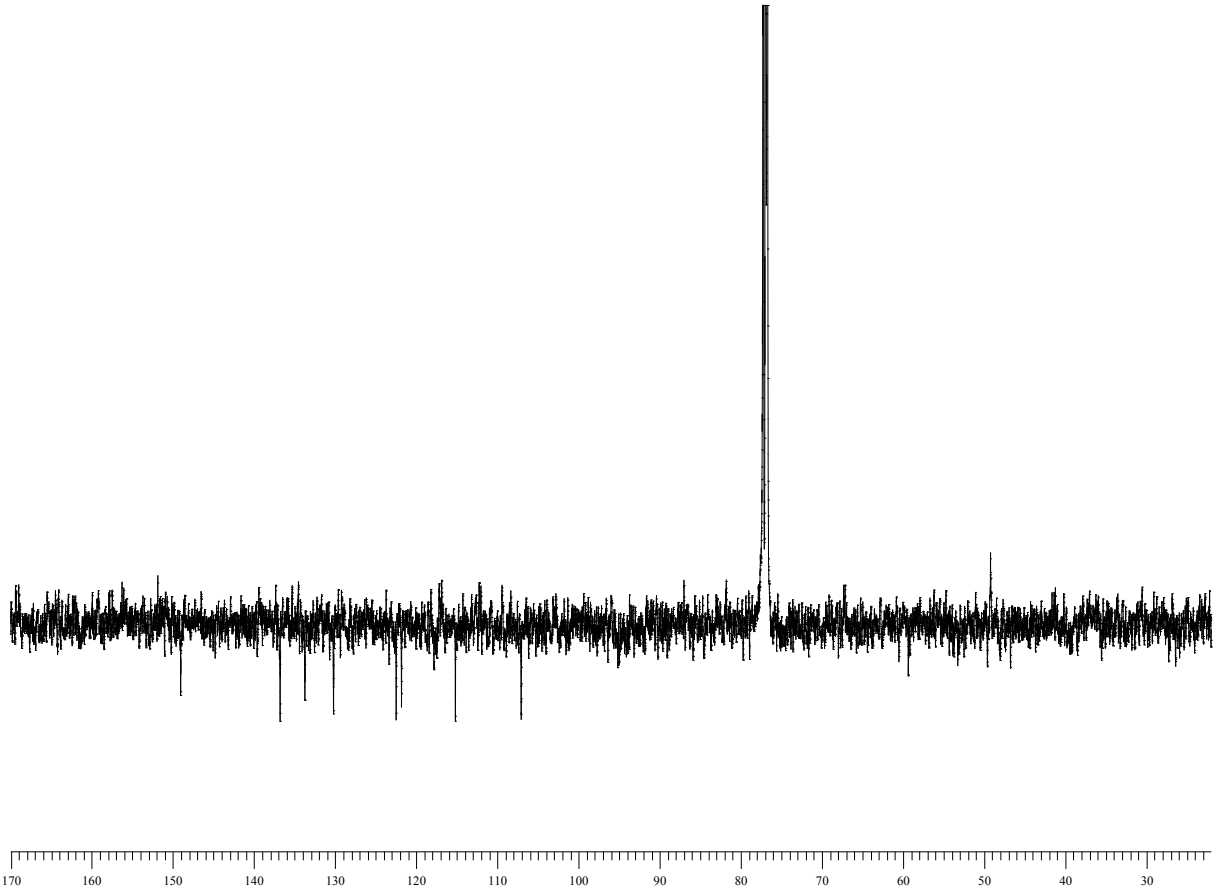

Fig.51. ^{13}C-NMR spectrum of N-tiramine-di[2-(dipicolyl)amino]1,8 naphtalimide

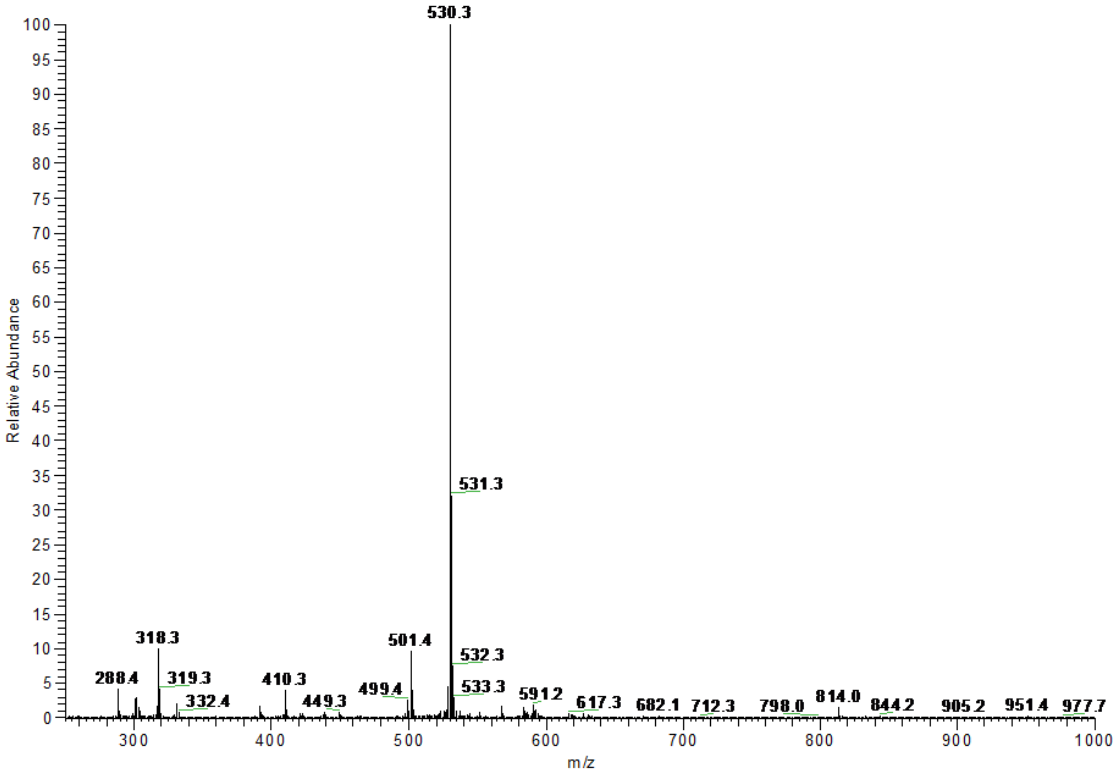

Fig . 52. ESI-MS spectrum of N-tiramine-di[2-(dipicolyl)amino]1,8 naphtalimide

VI.12 Synthesis of N-tyramine-tri[2-(dipicolyl)amino]1,8 naphtalimide

To a solution of 0,1 g (0,2 mmol) of N-tyramine-di[(picolyl)amino]1,8 naphtalimide in aceto nitrile dry as solvent were added picolyl chloride 0,05 g (0,4 mmol) and 0,3 g (2,2 mmol) of potassium carbonate. The mixture were heated to reflux for 3h under nitrogen atmosphere and the proceed of the reaction were monitored by TLC. The crude product were purified by alumina chromatography (CH_2Cl_2:MeOH 100:5) to give two yellow products one of these is the predominant product, that shows the insertion of three picolyl arms and the other one is four armed. The compounds were fully characterized by ^{1}H-NMR, ^{13}C-NMR, g-COSY, ESI-MS.

^{1}H-NMR (500 MHz, acetone-d_6) δ 8,6 (d, J = 8 Hz, 1H, ArH), 8.5 (d, J = 8 Hz, 1H, ArH), 8.2 (d, J = 8 Hz, 1H, ArH), 7,8 (t, J = 8 Hz, 1H, ArH) 7,7 (t, J = 8 Hz, 2H, ArH), 7.6 (t, J = 8 Hz, 2H, ArH), 7.5 (d, 1H, ArH), 7.3 (m, 1H, ArH), 7.2 (d, 2H, ArH), 6.9 (d, 2H, ArH), 5.9 (s, 2H, CH_2), 5.0 (d, 2H, CH_2), 4.9 (d, 2H, CH_2), 4.2 (t, 2H, CH_2), 2.9(t, 2H, CH_2).

^{13}C-NMR (CDCl3, 125 MHz) δ 33.7, 41.5, 55.1, 70.7, 72.7, 104.3, 107,108.8, 111.4, 112.1, 114.7, 120.2, 121.1, 121.2, 122.7, 123.7, 124.9, 130.4, 132.1, 133.9, 134.5, 136.8, 137.1, 137.3, 145.4, 146.1, 149.1, 149.8, 150.2, 155.9, 156.8, 158.3, 164.1, 164.2. ESI-MS *m/z* 642.7 $[M+Na]^+$.

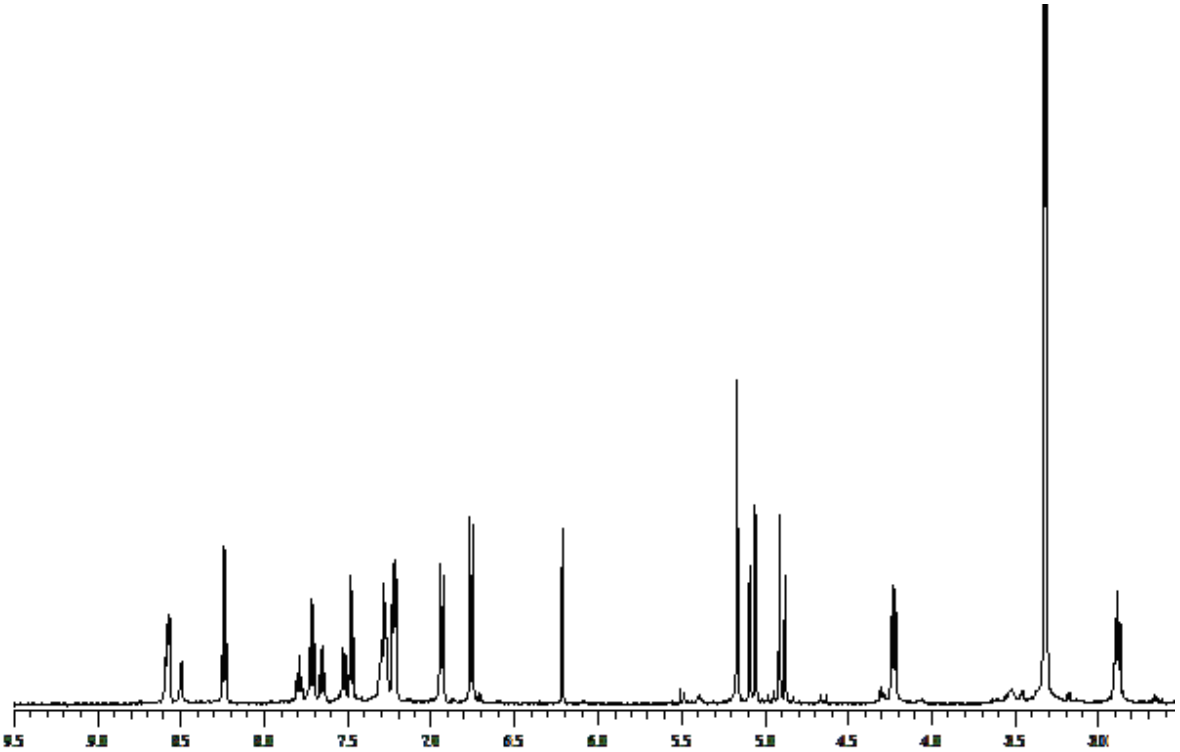

Fig. 53. ^{1}H-NMR spectrum of N-tiramine-tri[2-(dipicolyl)amino]1,8 naphtalimide

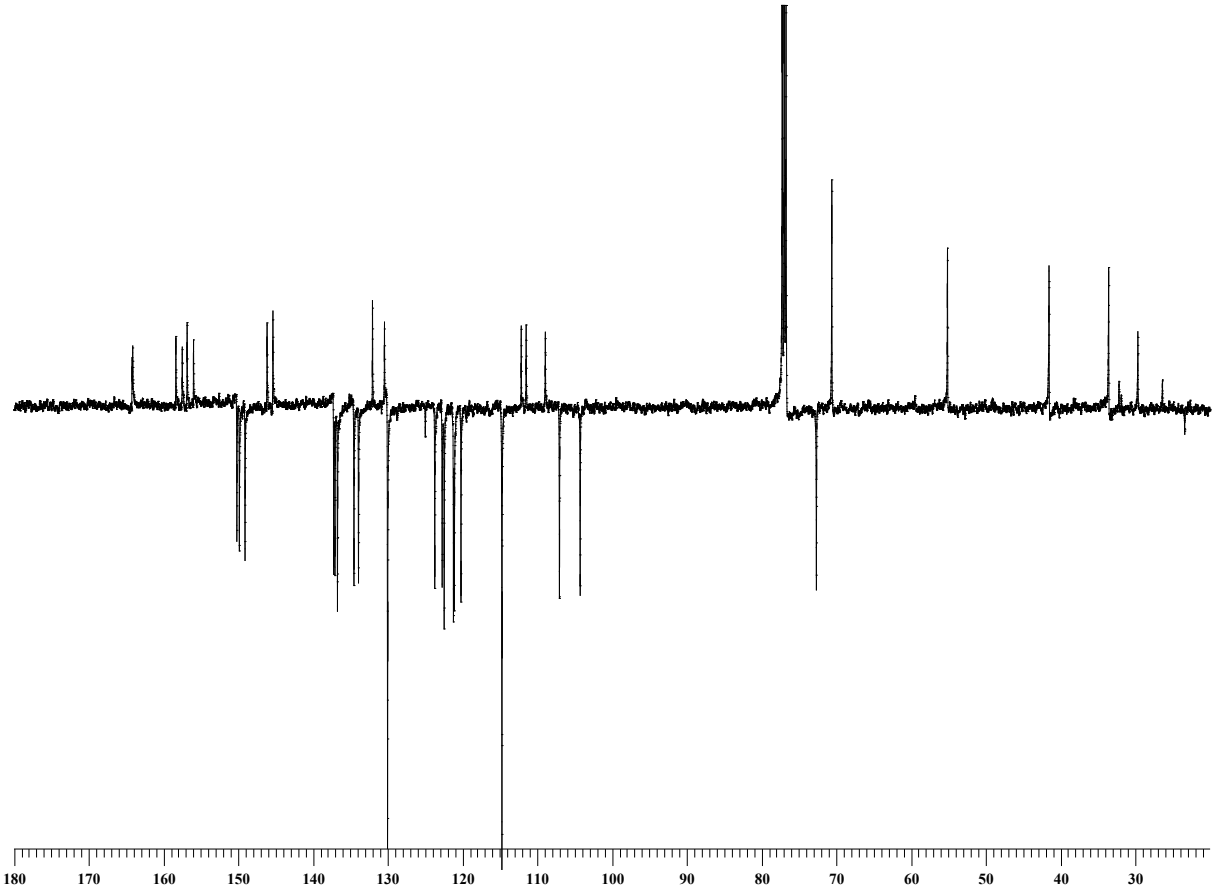

Fig. 54. ^{13}C-NMR spectrum of N-tiramine-tri[2-(dipicolyl)amino]1,8 naphtalimide

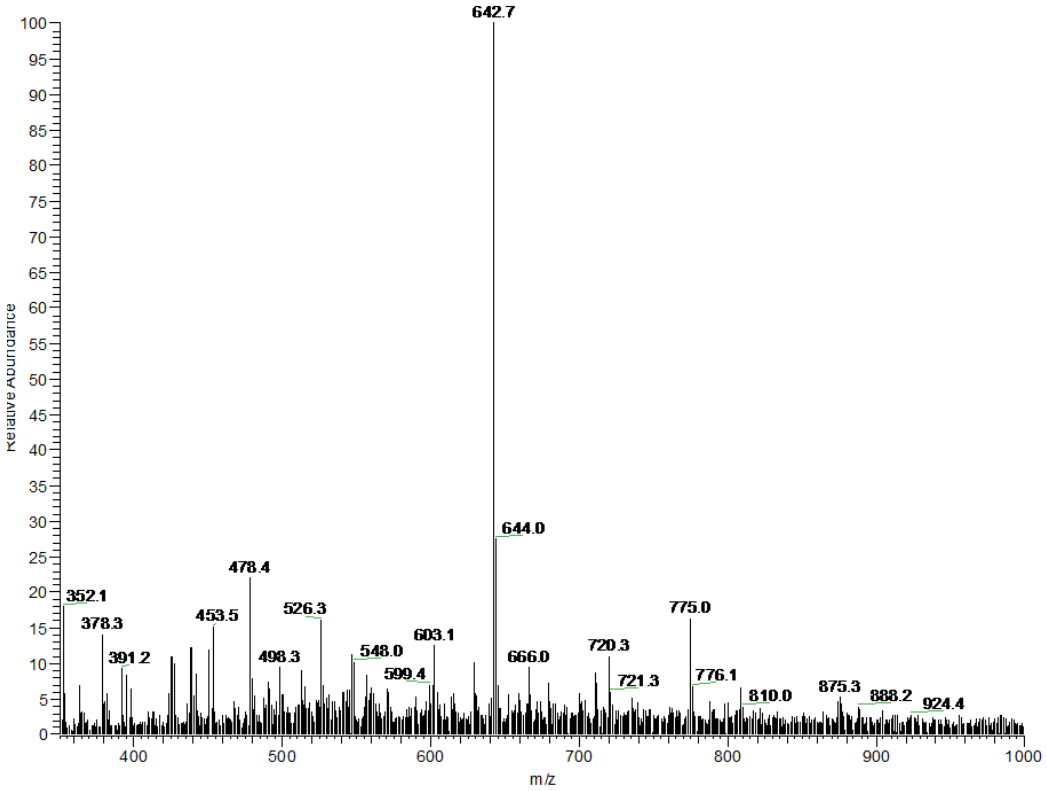

Fig. 55. ESI-MS spectrum of N-tiramine-tri[2-(dipicolyl)amino]1,8 naphtalimide

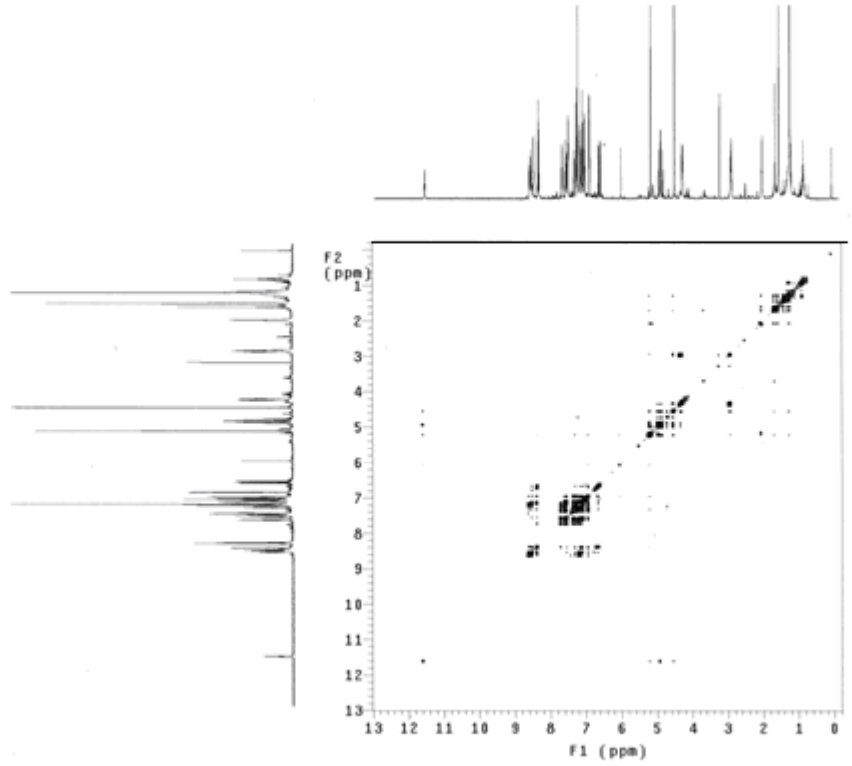

Fig. 56. g-COSY of N-tyramine-tri[2-(dipicolyl)amino]1,8 naphtalimide

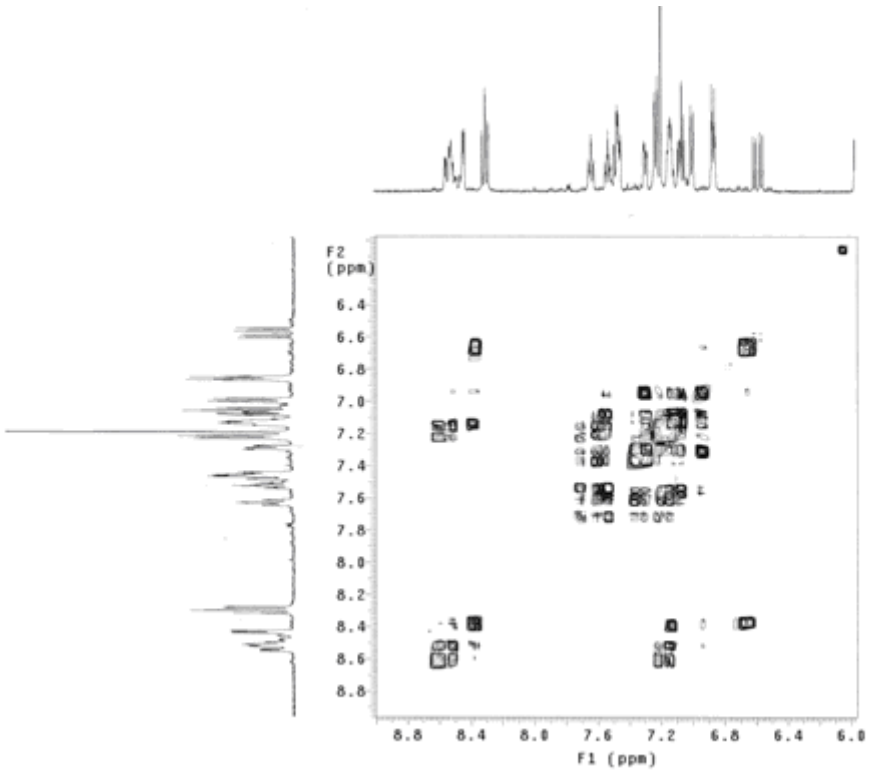

Fig. 57. g-COSY aromatic zone

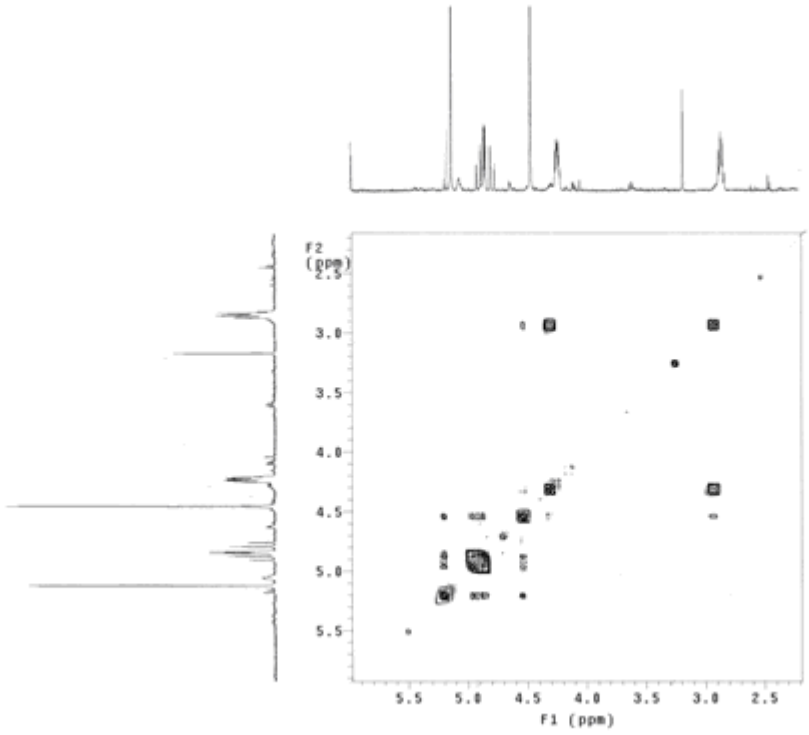

Fig. 58. g-COSY zoom aliphatic zone

VI. 13 UV-VIS and NMR Measurements I

For each sample was prepared a stock solution, which is then diluted to a concentration most appropriate to fit within the range of Lambert-Beer low. Spectra are carried out keeping constant the concentration of the host and adding progressively increasing amounts of guest (DMMP). The solution of DMMP was prepared by diluting 16.5 mg (d = 1,032 g / ml) in 25 ml of acetonitrile. All spectra were recorded in acetonitrile.

- **4- OH- Benzaldoxime**

  ✓ Stock solution [oxime]= $3,7*10^{-3}$
  ✓ [DMMP] = $1,7*10^{-3}$
  ✓ sample solution = $3,7*10^{-5}$

Solution	4-OH benzaldoxime	[DMMP]	$A_{264\ nm}$
1	5,84E-05	0	0,85236
2	5,81E-05	1,48E-05	0,85348
3	5,79E-05	2,94E-05	0,85404
4	5,77E-05	4,40E-05	0,85323
5	5,74E-05	5,84E-05	0,85218
6	5,72E-05	7,27E-05	0,85033
7	5,70E-05	8,70E-05	0,84890
8	5,68E-05	1,01E-04	0,84738
9	5,66E-05	1,15E-04	0,84610
10	5,64E-05	1,29E-04	0,84671
11	5,61E-05	1,43E-04	0,84637
12	5,41E-05	2,75E-04	0,82206
13	5,21E-05	3,98E-04	0,79873
14	5,00E-05	5,12E-04	0,77603
15	4,86E-05	6,18E-04	0,75470
16	4,70E-05	7,18E-04	0,73543
17	4,56E-05	8,12E-04	0,71686
18	4,42E-05	1,06E-03	0,69688
19	4,29E-05	1,15E-03	0,67833
20	4,17E-05	1,24E-03	0,66102
21	4,00E-05	1,32E-03	0,64492
22	3,94E-05	1,39E-03	0,62677
23	3,84E-05	1,72E-03	0,60972

- **4- amino- 3 – nitro Benzaldoxime**

  ✓ Stock solution [oxime]= $3,7*10^{-3}$
  ✓ [DMMP] = $1,7*10^{-3}$
  ✓ sample solution $3,7 *10^{-5}$

Solution	4-amino-3-nitro benzaldoxime	[DMMP]	$A_{264\ nm}$
1	2,01E-05	0	0,42713
2	1,98E-05	6,08E-05	0,42139
3	1,95E-05	1,20E-04	0,39697
4	1,91E-05	1,77E-04	0,38982
5	1,88E-05	2,32E-04	0,39146
6	1,83E-05	3,37E-04	0,38149
7	1,72E-05	5,30E-04	0,36153
8	1,44E-05	1,06E-03	0,31849
9	1,09E-05	1,91E-03	0,24471
10	4,57E-06	3,60E-03	0,13557
11	1,43E-06	6,15E-03	0,05889

VI. 14 UV-VIS and NMR measurements II

The molar estinction coefficient for the azo-compound was determined preparing stock solution at different concentration of azo-compound:

- 5.0 exp -6
- 1.5 exp -5
- 3.0 exp -5

ε = 25000

The UV-VIS titration was prepared by dissolving 8,6 mg (0,03 mmol) in 0,01 L of acetonitrile, from this solution was kept a rate of 20 μL and diluted to 2 μL to have a concentration of 3exp-5 M.
The spectrum registered shows an ε 32550 at λ_{max} 524 nm.
The UV-VIS titration was conducted by preparing 11 solutions of azo-oximate in a 1:1 CH3CN/NaOH (aq) solution at different ratio oximate-DCP as it is shown in the grid below:

Solution	[G]/[H]	V_{host}	V_{guest}	V_{CH3CN}	[guest]	A_{524nm}
1	0	20	0	1980	0	0
2	0.25	20	5	1980	$7.5x10^{-6}$	0,9944
3	0.50	20	5	1980	$1.5x10^{-5}$	0,9984
4	0.75	20	5	1980	$2.25x10^{-5}$	0,9828
5	1.00	20	5	1980	$3x10^{-5}$	0,9789
6	2.25	20	25	1980	$4.5x10^{-5}$	0,9554
7	3.5	20	25	1980	$6x10^{-5}$	0,9526
8	6	20	50	1980	$9x10^{-5}$	0,9103
9	8.5	20	50	1980	$1.2x10^{-4}$	0,8721
10	12.25	20	75	1980	$1.2x10^{-4}$	0, 8159
11	16	20	75	1980	$1.2x10^{-4}$	0,7669

Volumes are expressed in μL.

^{1}H-NMR titration

Two equimolar (10^{-3} M) stock solutions of the azo-oxime and of DCP were prepared in acetone-d_6/$NaOH_{(D2O)}$ (in order to form the oximate moiety). Progressive additions of DCP are made to obtain the following ratios: 0, 0.2, 0.4, 0.5, 0.75, 1, 1.25, 1.5, 2.00, 3.00, 5. The spectrum was recorded after each addiction.

VI. 15 UV-VIS and NMR measurements III

A stock solution 6.0exp-5 of $BaCl_2x2H_2O$, $MgCl_2$, $CaCl_2$, $FeCl_2x4H_2O$, $NiCl_2x6H_2O$, $ZnCl_2$, $CuCl_2x2H_2O$, $HgCl_2$, $Pb(NO_3)_2$, $ZrOCl_2$ were prepared in CH_3CN.
At the same time we prepared a solution at the same solvent and concentraiotn of N-tyramine-tri[(2-picolyl)-amino]-1,8-naphthalimide; every salts were mixed with a solution of 3-arms to get a 1:1 ratio.

Job plot N-tyramine-tri[(2-picolyl)-amino]-1,8-naphthalimide Vs $ZnCl_2$

A stock solution of the host 2.5x10-5M, and a stock solution of CH3CN equimolar of the guest were prepared. We prepared 11 solutions at different host / guest ratios, see table below, and then the absorbance was measured at 445 nm for each sample:

Punto	χ	V_{host}	V_{guest}	V_{CH3CN}	ΔA_{445nm}
1	0	1000	0	1000	0,05706
2	0.1	900	100	1000	0,05070
3	0.2	800	200	1000	0,04525
4	0.3	700	300	1000	0,03895
5	0.4	600	400	1000	0,03137
6	0.5	500	500	1000	0,02663
7	0.6	400	600	1000	0,02093
8	0.7	300	700	1000	0,01569
9	0.8	200	800	1000	0.009278
10	0.9	100	900	1000	0,002986
11	1	0	1000	1000	0

Volumes are espressed in μL.

The graph report ΔA/χ Vs χ:

Fig. 59. Job plot N-tyramine-tri[(2-picolyl)-amino]-1,8-naphthalimide Vs $ZnCl_2$

^{1}H-NMR titration

Two equimolar (M = 2.9exp-3) stock solutions were prepared in acetone-d6 of N-tyramine-tri[(2-picolyl)-amino]-1,8-naphthalimide and $ZnCl_2$. Progressive additions of ZnCl2 are made to obtain the following ratios: 0, 0.2, 0.4, 0.6, 0.8, 1, 1.2, 1.4, 1.6, 1.8, 2, 2.2, 3, 4, 5. Each spectrum was recorded after every addiction.

VI.16 Synthesis of 8-chloromethyl-2,6-diethyl-4,4-difluoro1,3,5,7-tetramethyl-4-bora-3α,4α-diaza-s-indacene

In a 250 mL flask were poured 0.46 g (4.05 mmol) of chloroacetyl chloride and 0,995 g (8.1 mmol) were added to 50 mL of dichloromethane previously degassed under nitrogen atmosphere. The reaction mixture was stirred at 50°C for a time of two hours in dry condition. After this time the solvent was removed under reduced pressure and to the mixture were added dichloromethane 5 mL, toluene 95 mL and 2.7 mL (1.96 g) of triethylamine, the resulting mixture was stirred for two hours at 50° C.
At the end of the reaction the solvent was removed under reduced pressure and the crude products were replaced with dichloromethane (100 mL).
This organic phase was washed with 50 mL of water, dried over magnesium sulphate, filtered and the solvent removed under reduced pressure.
The product was purified by column chromatography (SiO_2 , toluene/hexane) and then crystallized from hexane, to give a purple solid. (200 mg, 14% yield)
^{1}H-NMR ($CDCl_3$, 500 MHz, δ ppm) 4.82 ppm (s, 2H), 2.50 ppm (s, 6H), 2.45 ppm (s,6H), 2.40 (4H,q, J=7.5), 1.05 (6H, t, J=7.5)

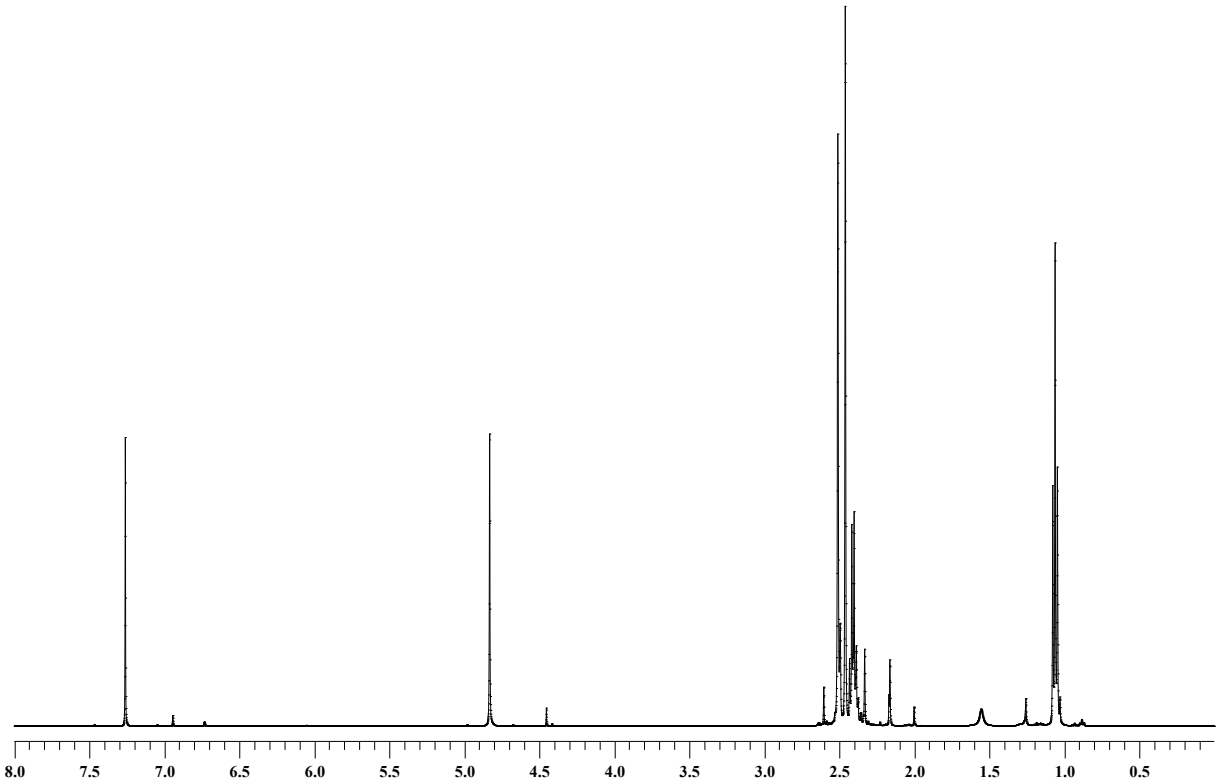

Fig. 60. ^{1}H-NMR spectrum of the Bodipy

VI. 17 Synthesis of 3-pentan-1-thiol

In a 100 mL two naked flask were poured 3.4 g (44.73 mmol) of thiourea and 4.16 mL (44.73 mmol) of mercaptoethanol with 48% bromidric acid 10 mL; the mixture were stirred and refluxed overnight under inert atmosphere for a time of 8 hours.
After this time the reaction was cooled to room temperature and a solution prepared with 4 g of NaOH and the resulting mixture was refluxed overnight under inert atmosphere.
The reaction was then cooled to room temperature, neutralized with HCl, and extracted with dichloromethane (40 mL x 3) and the organic phase washed with water, dried with sodium sulphate, filtered and the solvent removed under reduced pressure to dryness to give the pure product as a very pungent, pale yiellow oil, that was used without any further purification (3 g)
^{1}H-NMR ($CDCl_3$, 500 MHz δ ppm) 2.66-2.78 (4H, m), 2.56 (2H, q, J=7), 1.73 (1H, t, J=7), 1.25 (3H, t, J=7)

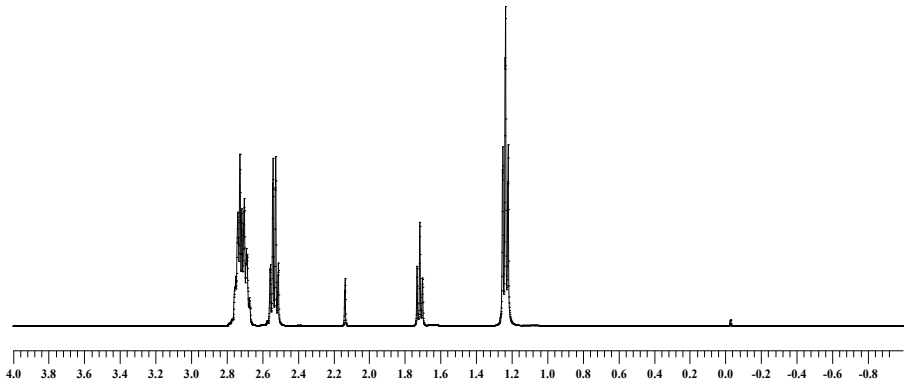

Fig. 61. ^{1}H-NMR spectrum of 3-pentan-1-thiol

VI. 18 Synthesis of 3,6,12,15,Tetrathia-9-monoazaheptadecane

In a two nacked flask under nitrogen atmosphere were poured 2.76 g (120 mmol) of sodium, 2.5 g (33.6 mmol) of 3-thiapenthan-1-thiol in 75 mL of ethanol absolute and the resulting mixture were slowly heated to reflux; at the same time a previously prepared solution of ethanol 40 mL and bis-(2-chloroethyl) amine hydrochloride 1.5 g (16.8 mmol) for 4 hours. Then the solvent was removed under vacuum.
The product was purified by column chromatography (SiO_2, eluent mix 5% Methanol/ dichloromethane) to give the desired product as a brown oil.
^{1}H-NMR ($CDCl_3$, 500 MHz δ ppm) 2.81 (4H, t, J=6.5 Hz), 2.64-2.75 (12H, m), 2.52 (4H, q, J=7 Hz), 1.79 (1H, br), 1.22 (6H, t, J=7 Hz).

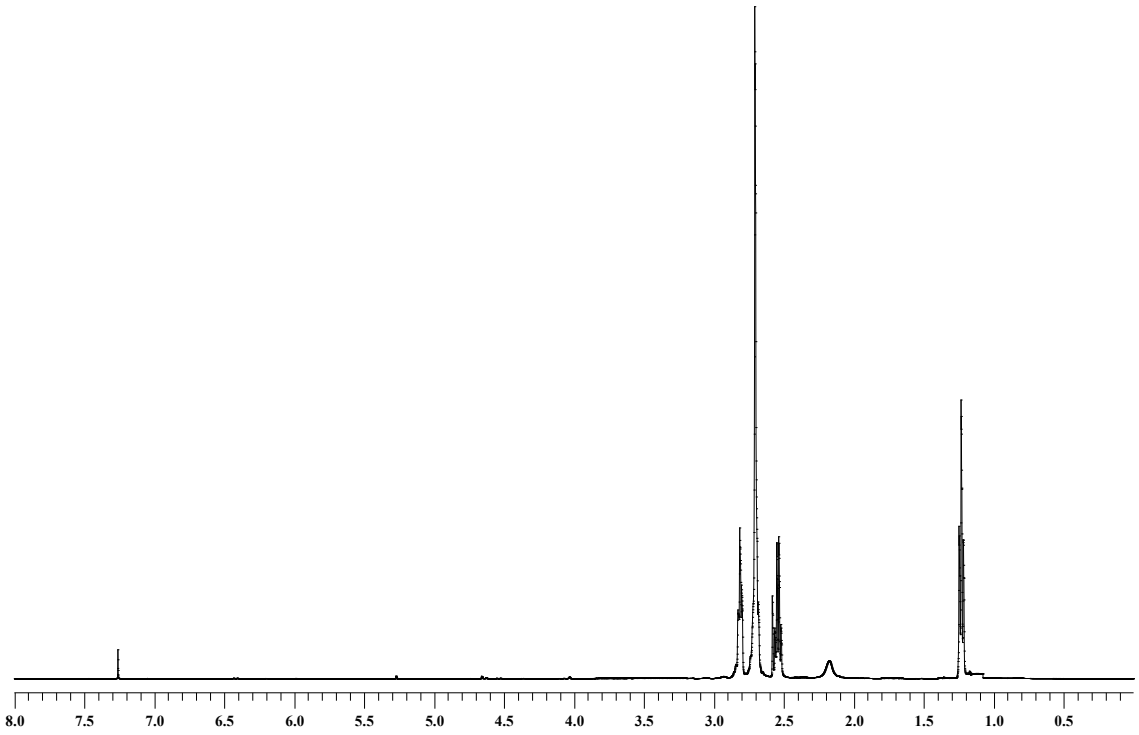

Fig. 62. ^{1}H-NMR spectrum of 3,6,12,15,Tetrathia-9-monoazaheptadecane

VI.19 Synthesis of 8-[N,N-bis(3',6'-dithiaoctyl)-aminomethyl]-2,6-diethyl-4,4-difluoro-1,3,5,7-tetramethyl-4-bora-3α,4α-diaza-s-indacene CS1(Copper sensor-1)

A suspension of 150 mg of BODIPY (0.25 mmol) and 260 mg (0.82 mmol) of 3,6,12,15,Tetrathia-9-monoazaheptadecane with 150 mg (0,9 mmol) of KI and 125 mg (0.9 mmol) of K_2CO_3 in 50 mL of dry acetonitrile was refluxed under nitrogen atmosphere overnight.
Then the solvent was removed under vacuum and the residue replaced with dichloromethane (100 mL).
The organic phase was washed with water, dried with magnesium sulphate,filtered and the solvent removed under reduced pressure.
The crude was purified by column chromatography and the product re-purified by flash chromatography (SiO2, eluent mixing: dichloromethane/exhane 1:1) to give 19.2 mg (12% yield) of pure product as a bright red solid.
^{1}H-NMR ($CDCl_3$, 500 MHz, δ ppm) 4.02 ppm(2H, s), 2.87 ppm (4H,t, J=7.5 Hz), 2.52-2.65 ppm (16 H, m), 2.5 ppm (6H, s), 2.4 ppm (6H, s), 2.38 ppm (4H, q, J=7.5 Hz), 1.24 (6H, t, J= 7.5 Hz), 1.05 (6 H, t, J=7 Hz).
^{13}C-NMR ($CDCl_3$, 125 MHz, δ ppm) 134.43, 131.15, 129.96, 128.83, 124.98, 124.74, 122.88, 115.5, 104.7, 68.07, 65.49, 59.13, 47.46, 41.82, 38.64, 33.47, 32.21, 31.68, 29.63, 24.11, 19.72.

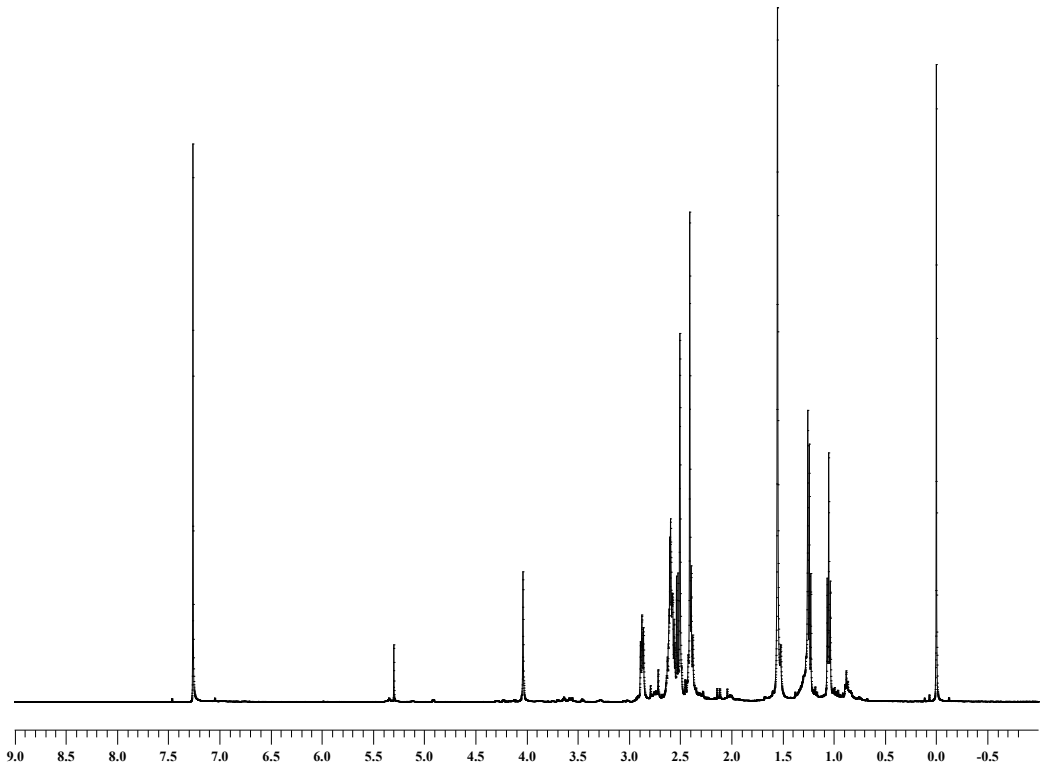

Fig. 63. ^{1}H-NMR spectrum CS1

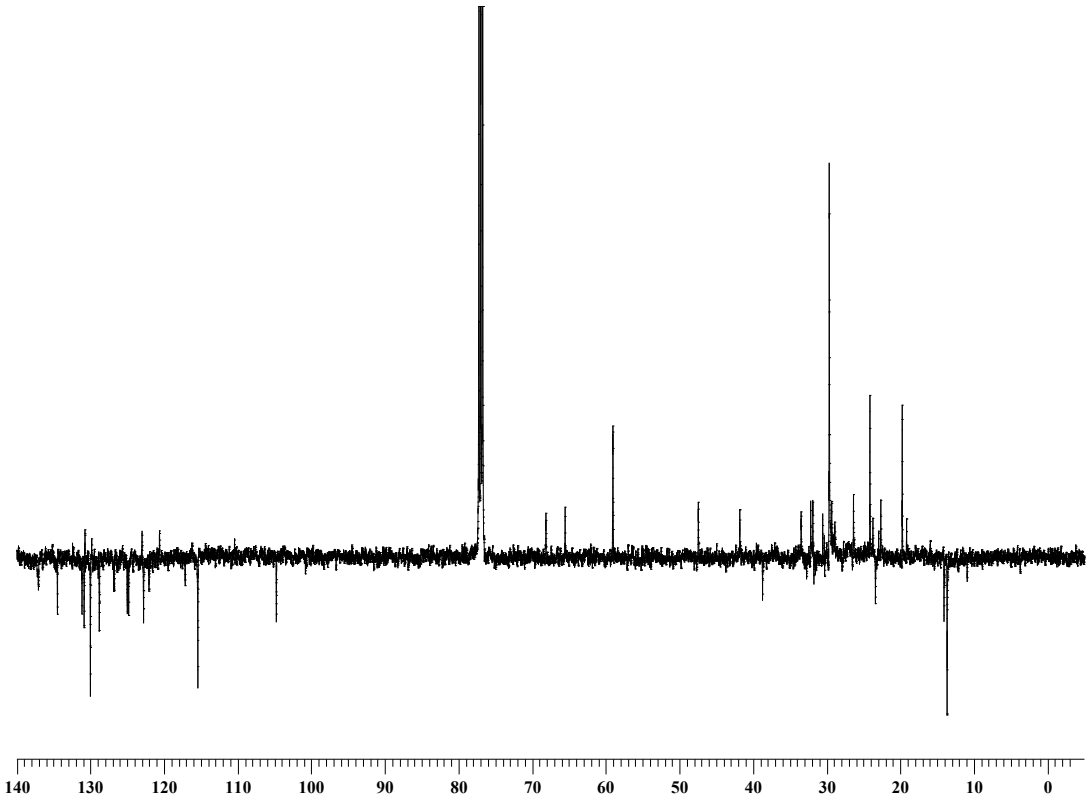

Fig. 64. ^{13}C-NMR of CS1

VI. 20 Synthesis of 6-bromo-6-deoxy-α,α'-trehalose (TH-Br)

16.6 g (63.34 mmol) of triphenylphosphine was added to a solution of 10.8 g (31.6 mmol) anhydrous trehalose in DMF in a molar ratio of 2:1. The reaction was cooled under stirring. 11.4 g (64 mmol) of N-bromosuccinimide in an equimolar ratio of triphenylphosphine was slowly added under stirring, the reaction mixture was then left stirring at room temperature for 48 h.
Then were added 100 mL of methanol to the mixture just to decompose the excess of the starting reagent. Solvents were then removed under reduced pressure. The crude product was washed with ethanol; the white crystals formed were filtered off using a Millipore apparatus. The filtered solution was evaporated under vacuum and the solid purified by column chromatography on an RP_8 by using a linear gradient H_2O-EtOH (0-25%) as eluent.
TH-Br yield: 40%.
^{1}H NMR(D_2O, 500 MHz, δ ppm) 5.12 (d, 1H), 5.10 (d, 1H), 3.90 (m, 1H), 3.66-3.78 (m, 6H), 3.54-3.62 (m, 3H, H-2), 3.40 (t, 1H), 3.35 (t, 1H).

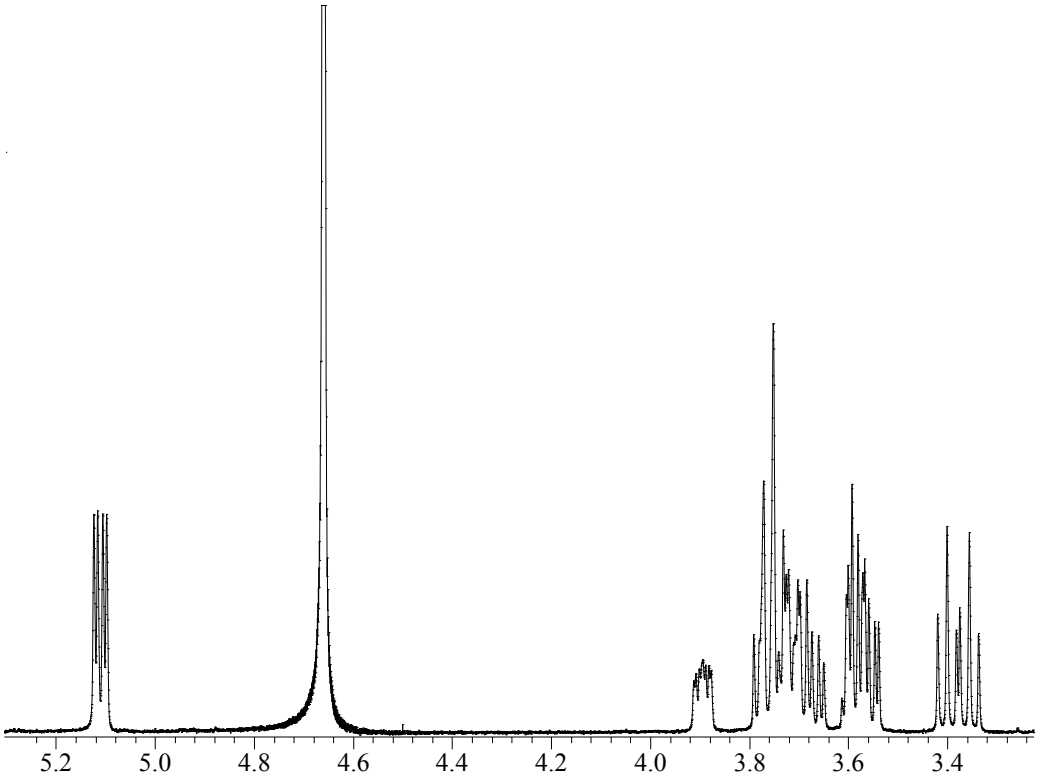

Fig. 65. ^{1}H-NMR 6-bromo-6-deoxy-α,α'-trehalose

VI. 21 Synthesis of 6-azido-6-deoxy-α,α'-trehalose (TH-N_3)

g (5.94 mmol) of TH-Br was diluted in 30 ml of H_2O; to this solution were added 3.86 g (59.4 mmol) of NaN_3 was added to the solution in a molar ratio of 1:10. The reaction was carried out at 100 °C under stirring for a time of 4 h. The solvent was removed under reduced pressure and the crude was purified by column chromatography on an RP_8 resyn by using a linear gradient of H_2O-EtOH (0-30%) as eluent. TH-N_3 yield: 52%
^{1}H-NMR(D_2O, 500 MHz, δ ppm) 5.03 (t, 1H, J= 4 Hz), 3.90 (m broad,1H), 3.63-3.71 (m, 6H), 3.59 (dd, 1H, J=4), 3.46-3.54 (m, 3H), 3.40 (dd, 1H, J= 5.5), 3.25-3.32 (m, 1H).

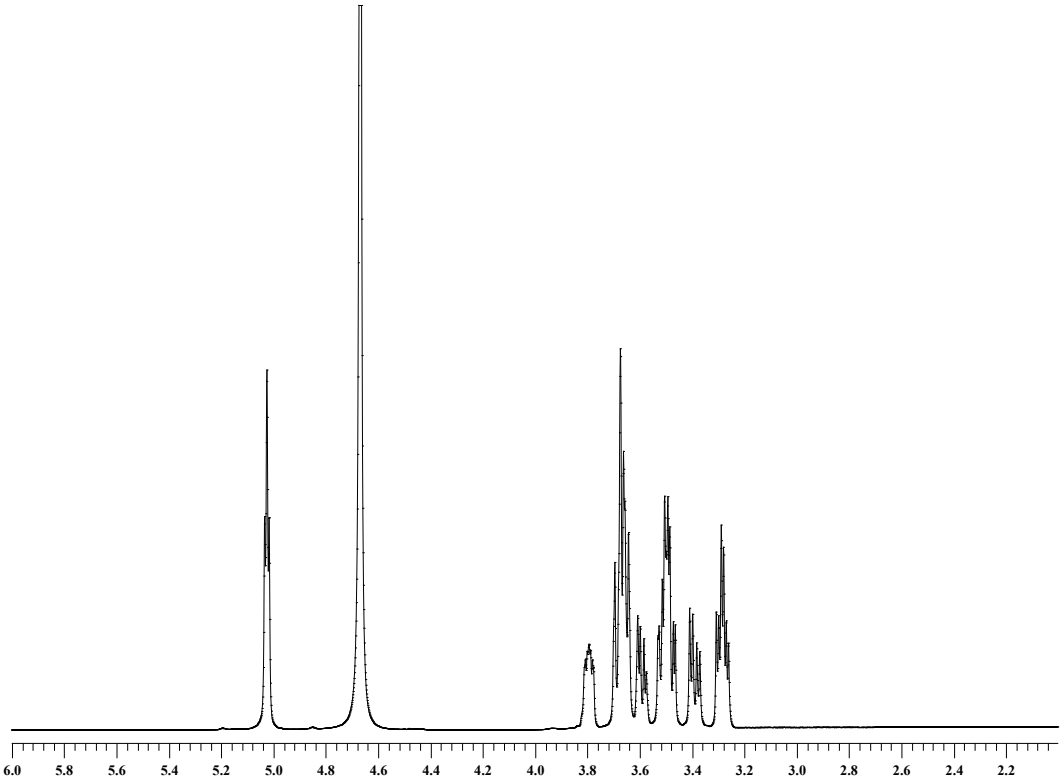

Fig, 66. ^{1}H-NMR 6-azido-6-deoxy-α,α'-trehalose

VI. 22 Synthesis of 6-amino-6-deoxy-α,α'-trehalose (TH-NH_2)

1.05 g (2.86 mmol) of TH-N_3 was diluted in DMF, to this solution was added 5.25 g (20.04 mmol) of PPh_3. The reaction was carried out at 40 °C under stirring for 1 h. The product was treated with 30% of NH_4OH at room temperature. After 23 h, white crystals were formed that has been filtered off using a Millipore apparatus. The filtered solution was evaporated under reduced pressure and the product was purified by column chromatography of CM-Sephadex C-25 (20x600 mm, NH_4^+ form), using a linear gradient of H_2O-NH_4HCO_3 (0-0,3 M) as eluent.
TH-NH_2 yield: 61%.
^{1}H-NMR(D_2O, 500 MHz, δ ppm) 5.1 (m, 2H), 3.78-3.64 (m, 6H), 3.57-3.53 (m, 2H), 3.34 (t, 1H, J=9 Hz), 3.24 (t, 1H, J=9 Hz), 3.03 (dd, 1H, J=3Hz), 2.77 (dd, 1H,J=3Hz).

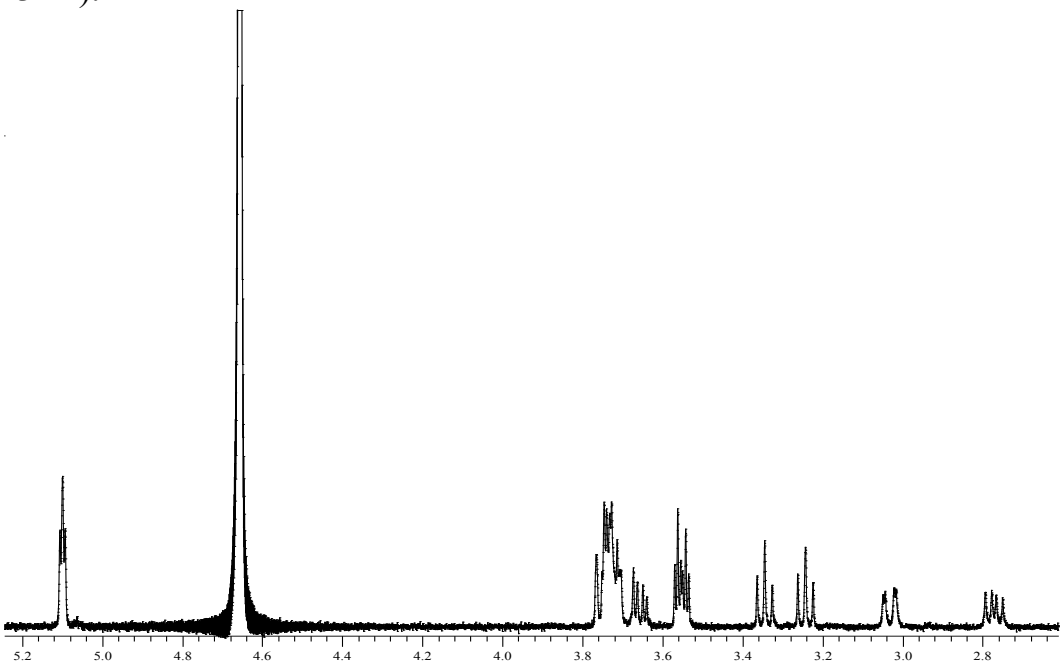

Fig. 67. ^{1}H-NMR 6-amino-6-deoxy-α,α'-trehalose

VI. 23 Synthesis of N-trehalose-4-bromo-5-nitro-1,8 naphthalimide

0.130 g (0.38 mmol) of TH-NH_2 was diluted in dry DMF, to this solution was added 0.120 g (0.38 mmol) of 4-bromo-5-nitro-1,8-naphthalic anhydride. The reaction was carried out at 60 °C under stirring for 5 hrs. The solvent removed under reduced pressure and the resulting solid was purified by column chromatography on an RP_8 resyn, using linear gradients of H_2O-EtOH (0-30% and 30-60%) as eluent.
N-trehalose-4-bromo-5-nitro-1,8 naphthalimide yield: 69%.
^{1}H-NMR(500 MHz, $CDCl_3$ δ ppm) δ 8.70 (d, *J* = 8 Hz, 1H, ArH), 8.50 (d, *J* = 8 Hz, 1H, ArH), 8.21 (d, *J* = 8 Hz, 1H, ArH), 7.93 (d, *J* = 8 Hz, 1H, ArH) 7.19 (d, *J* = 8 Hz, 2H, ArH), 6.77 (d, *J* = 8 Hz, 2H, ArH), 4.62 (s, 1H, OH), 4.4 (t, *J* = 8 Hz, 2H, CH_2), 2.9 (t, *J* = 8 Hz, 2H, CH_2).

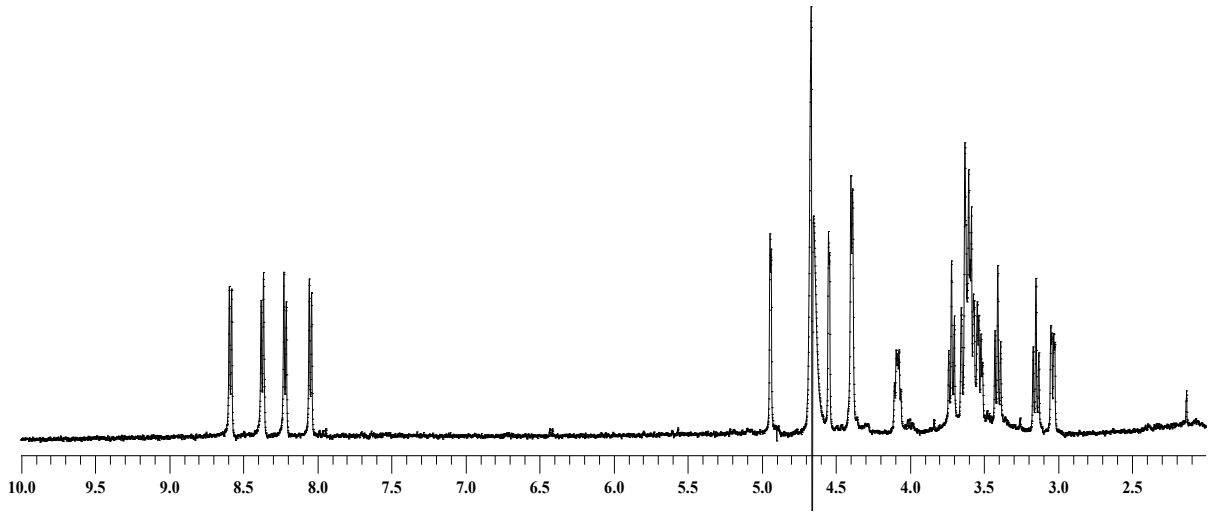

Fig. 68. ^{1}H-NMR N-trehalose-4-bromo-5-nitro-1,8 naphthalimide

VI. 24 Synthesis of N-trehalose-4,5-di[(2-picolylamino)]-1,8-naphthalimide

0.170 g (0.26 mmol) of N-trehalose-4-bromo-5-nitro-1,8 naphthalimide was dissolved in 15 ml of 2-methoxyethanol under stirring at the same time a was prepared a solution of 570 µl (5.54 mmol) of 2-picolylamine previously diluted in 5 mL of the same solvent. The reaction was refluxed under stirring for 4 hrs, when TLC indicated the formation of the maximal amount of the product. At the end of the reaction the solvent was removed under reduced pressure and the resulting was purified by column chromatography on an RP_8 resyn by using a linear gradients of H_2O-EtOH (0-30% and 30-70%) as eluent.
CST yield: 20%.
^{1}H-NMR (500 MHz, CD_3OD δ ppm) δ 8.45 (d, J =4.5 Hz, 2H), δ 8.29 (d, J=8.5 Hz, 2H), δ 7.82 (t, J = 7.5 Hz, 2H), δ 7.60 (d, J = 8 Hz, 2H), δ 7.32 (t, J= 7 Hz, 2H), δ 6.81 (d, J =9 Hz, 2H), δ 4.97 (d, J =4 Hz), δ 4.75 (s), δ 4.5-4.43 m, δ 4.40(d, J =4 Hz), δ 4.38(d, J =4.5 Hz), δ 4.29-4.23 (m, broad), δ 3.79-3.72 (m), δ 3.71-3.66 (m), δ 3.56 (dd, J =6 Hz), δ 3.46 (dd, J =4 Hz), δ 3.29-3.16 (m).

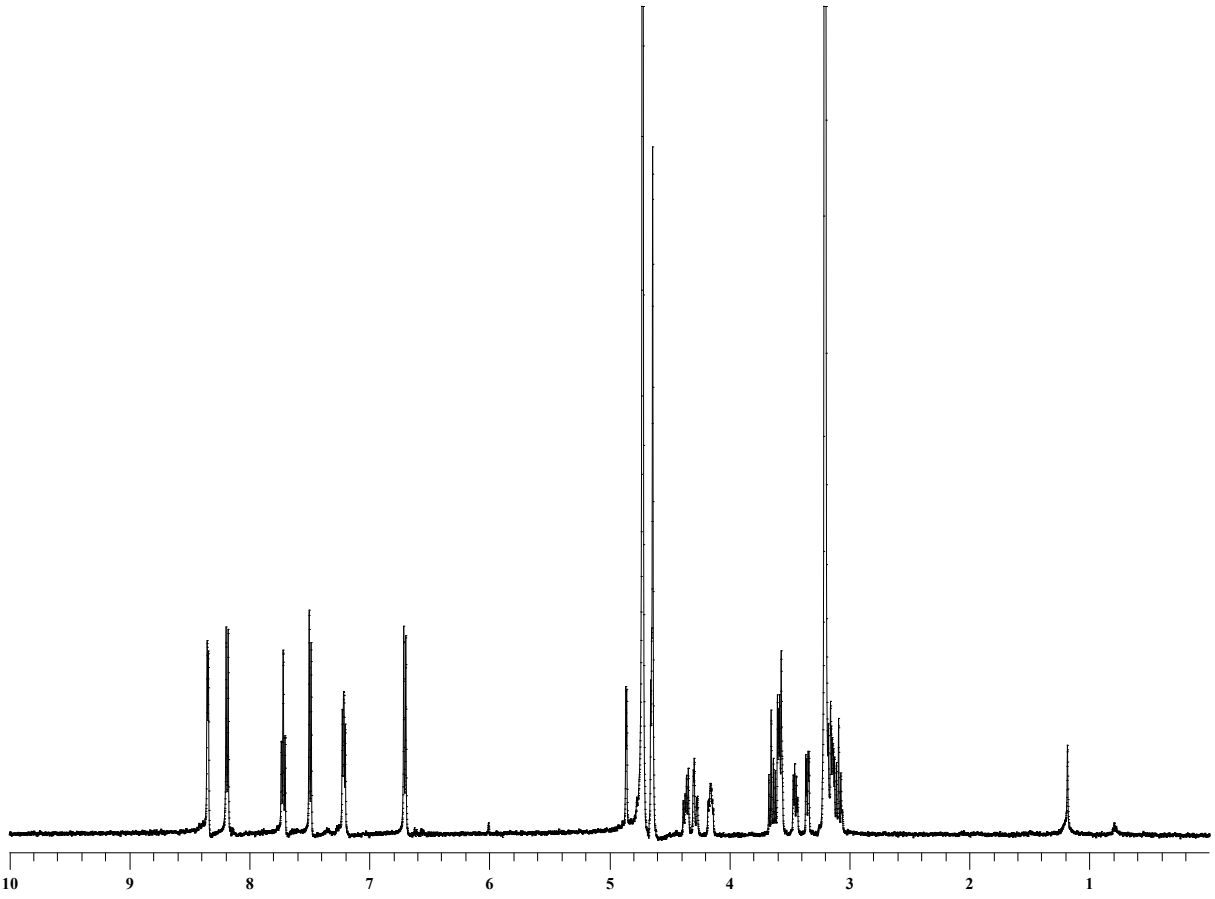

Fig. 69. ^{1}H-NMR N-trehalose-4,5-di[(2-picolylamino)]-1,8-naphthalimide

VI.25 Synthesis of N-(12-bromododecyl)pthalimide

10,285 g (70 mmol) of pthalimide were diluted in a 250 mL flask with 205 mL of ethanol (96%).
The solution were stirred and refluxed for 30 minutes; after this period, the hot solution were filtered and poured onto an hydroalcoholic solution prepared with 3.92 g (70 mmol) of KOH in 3,75 mL of water and 11,25 mL of absolute ethanol and the mixture was left stirring until the formation of a white precipitate.
Potassium pthalimide obtained 1,8 g (10 mmol) were mixed with 1-12 dibromododecane 9,8 g (30 mmol) in a solvent free reaction and left stirring at 180° C for a time of 16 hours..
The reaction mixture is warmed to room temperature washed with chloroform and filtered, the filtrate is then brought to dryness under reduced pressure and the mixture replaced with petroleum ether (fraction 60-80°) then sonicated to remove the potassium phtalimide unreacted. The resulting crude of the reaction were filtered and taken to dryness under reduced pressure, and then purified by column chromatography (petroleum ether / ethyl acetate 95:5), followed by crystallization from petroleum ether to give of 50 %..
m.p 62-63°C.
^{1}H-NMR (500 MHz,$CDCl_3$, δ ppm) 7.83(dd, 2H, J= 8.4, Ar-**H**), 7.70 (dd, 2H, J= 8.4, Ar-**H**), 3.67 (t, 3H, J= 7.5, Pht***CH*****$_2$**$(CH_2)_{11}$Br), 3.42 (t, 2H, J=7, Pht$(CH_2)_{11}$***CH*****$_2$**-Br), 1.3 ÷ 1.26 (m, 20 H, Pht-CH_2(***CH*****$_2$***$)_{10}CH_2$Br). ESI-MS 380 $[M+H]^+$

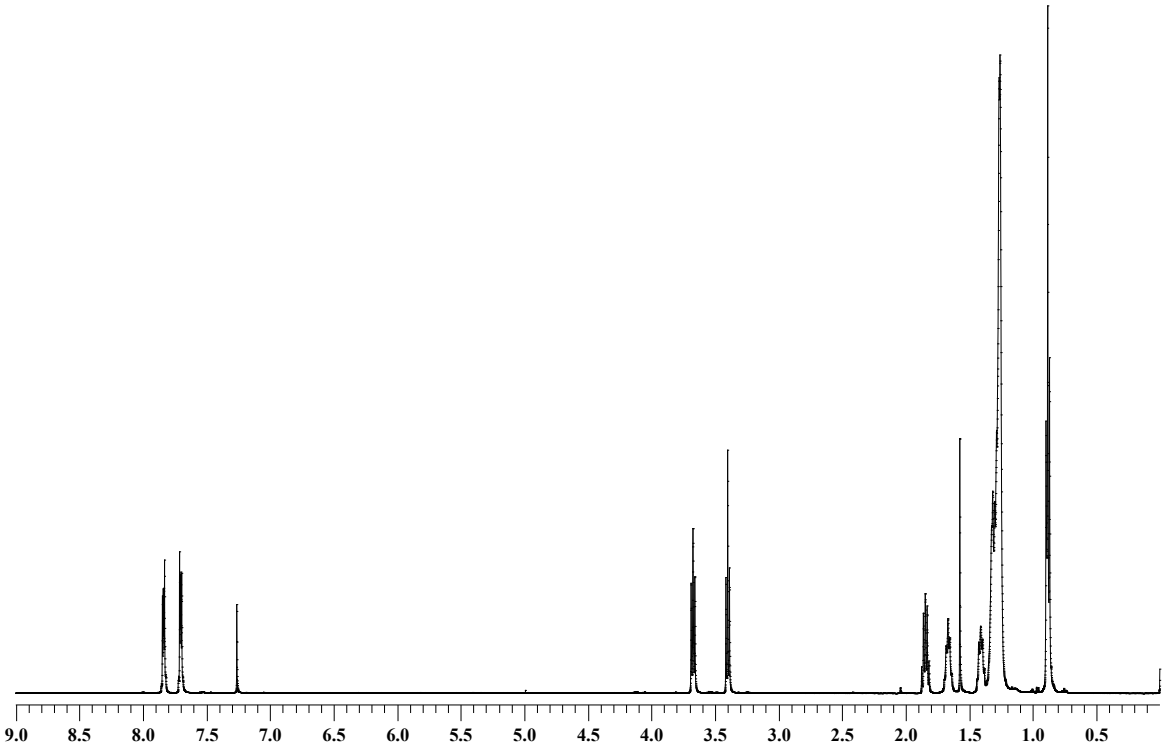

Fig. 70. 1H- NMR spectrum of N-(12-bromododecyl)pthalimide

VI. 26 Synthesis of 2-hydroxy-3-oxy-dodecyl-pthalimido-benzaldehyde

1 g (7,24 mmol) of 2-3-di-hydroxy-benzaldheyde were diluted in 10 mL DMSO in a 100 mL 3 naked flask; to this were added 800 mg (33,3 mmol) of sodium hydride 60% previously washed in pentane.
After this added was noted a chromatic change of the solution that soonely change from yellow to dark brown the reaction were left stirring for a hour.The reaction proceed at room temperature under stirring for a hour at room temperature.
After this time, to the reaction mixture were added dropwise 3,2 g of 12-bromododecyl pthalimide previously dissolved in 20 mL of DMSO under stirring and at room temperature.
The reaction were monitored by TLC (eluent chloroform) and were noticed the formation of two spots corresponding to the mono-alkilated and the di-alkilated aldehyde, the reaction was stopped after 7 hours.
At the end of the reaction the reaction mixture were poured into 100 mL of cold water and the crude product extracted 5 times with chloroform.
The organic layer were dried with dry magnesium sulphate, filtered and the solvent removed under reduced pressure.
The product were purified by column chromatography (SiO_2 / Chlorophorm) with 40% yield. The product were presented as a pale yellow solid.
^{1}H-NMR (500 MHz,$CDCl_3$,δ ppm) 10.98 (s, 1H, OH), 9.92 (s, 1H, ArC**H**O), 7.83 (d di d, 2H, J=2.5 Hz, ArPhtH), 7.70 (d di d, 2H, J=2.5 Hz, ArPhtH), 7.17 (d, 1H, J=1, ArH), 7.11 (d, 1H, J=1, ArH), 6.93 (t, 1H, J=7.5, ArH), 4.04 (t, 3H, J= 7,PhtN$\boldsymbol{CH_2}(CH_2)_{11}$Ar), 3.68 (t, 2H,J=7,Pht$(CH_2)_{11}\boldsymbol{CH_2}$-Ar), 1.28 (m, 20H, Pht-$CH_2(\boldsymbol{CH_2})_{10}CH_2$Ar). ESI-MS m/z 438 $[M+H]^+$
^{13}C-NMR (125 MHz, $CDCl_3$) 196.4, 188.4, 151.9, 147.7, 133.8, 132.2, 130.8, 128.8, 124.5, 123.1, 120.94, 119.54, 119.47.

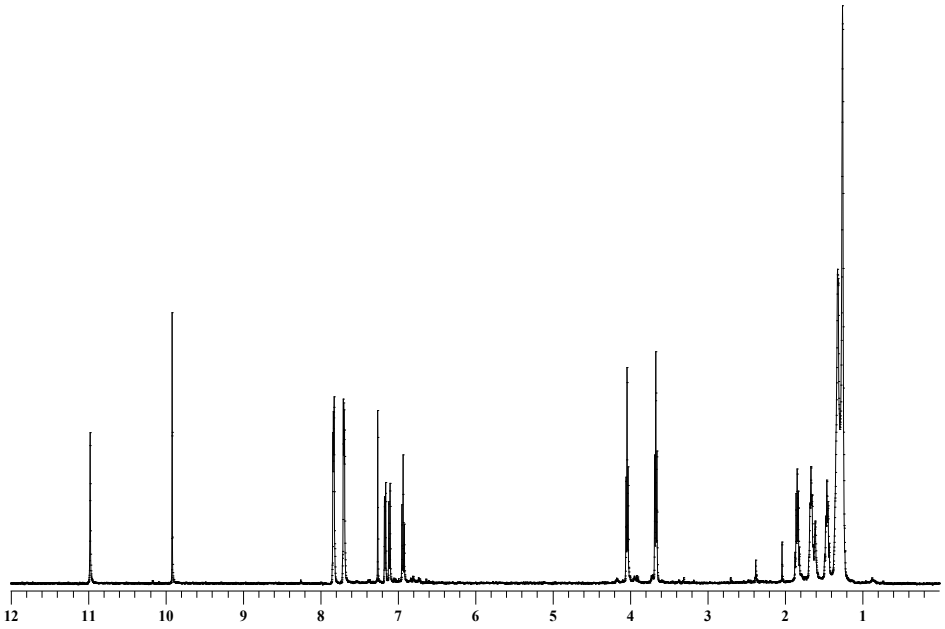

Fig. 71. ^{1}H-NMR spectrum of 2-hydroxy-3-oxy-dodecylphtalimido-benzaldheyde

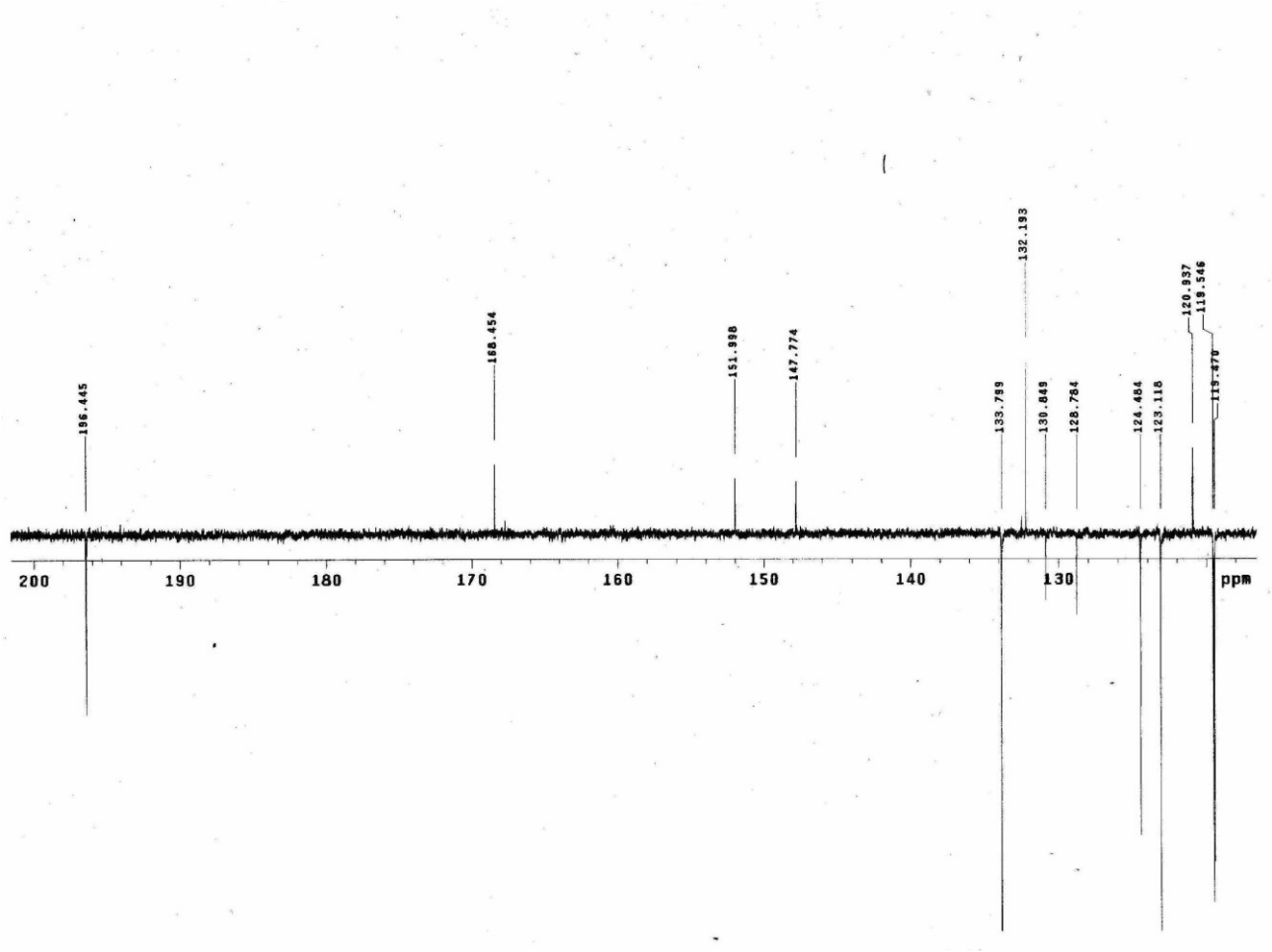

Fig. 72. ^{13}C-APT spectrum of 2--hydroxy-3-oxy-dodecylphtalimido-benzaldheyde

VI. 27 Synthesis of the ligand

To 200 mg (0,44 mmol) 2-hydroxy-3-oxo-dodecyl-pthalimido-benzaldehyde was dissolved in the minimum amount of dichloromethane and 20 mL of ethanol absolute to this were added 47 mg (0,22 mmol) of 1R,2R diphenylethylendiamine previously diluted in 5 mL of absolute ethanol.
The reaction proceed until the disappearing of the reagent, the reaction was monitored by TLC. Quantitative yield.
^{1}H-NMR (500 MHz,$CDCl_3$,δ ppm) 13.66 (s, 2H, OH), 8.36 (s, 2H, ArC**H**N), 7.84 (dd, 4H, J= 8.5, ArPht**H**), 7.71 (dd, 4H, J=8.5, ArPht**H**), 7.16 (m, 10H, ArH diphenylic bridge), 6.88 (d, 2H,J=7.5, ArH), 6.78 (d, 2H, J=7, ArH), 6.71 (t, 2H, J= 8, ArH), 4.68 (s, 2H, CH diphenylic bridge) 4.00 (t, 4H, J= 7, PhtN***CH₂***$(CH_2)_{11}$Ar), 3.69 (t, 4H, J= 7.5, Pht$(CH_2)_{11}$***CH₂***-Ar), 1.28 (m, 20H, Pht-CH_2(CH_2)$_{10}$$CH_2$Ar). ESI-MS m/z 1080 $[M+H]^+$
^{13}C-NMR (125 MHz, $CDCl_3$, δ ppm): 166.2, 151.3, 147.4, 139.3, 133.8, 133.7, 132.1, 128.2, 127.7, 127.6, 123.4, 123, 118.6, 115.7, 80.43, 69.2, 38, 29.7, 29.5, 29.4, 29.3, 29.2, 28.6, 28.8, 26.

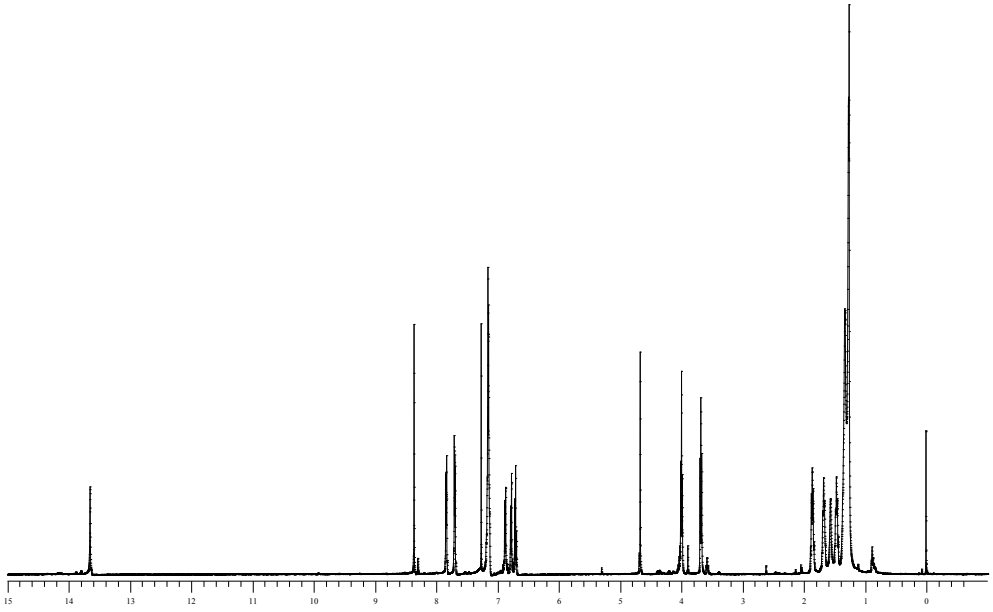

Fig. 73. ^{1}H-NMR spectrum of the ligand-pht

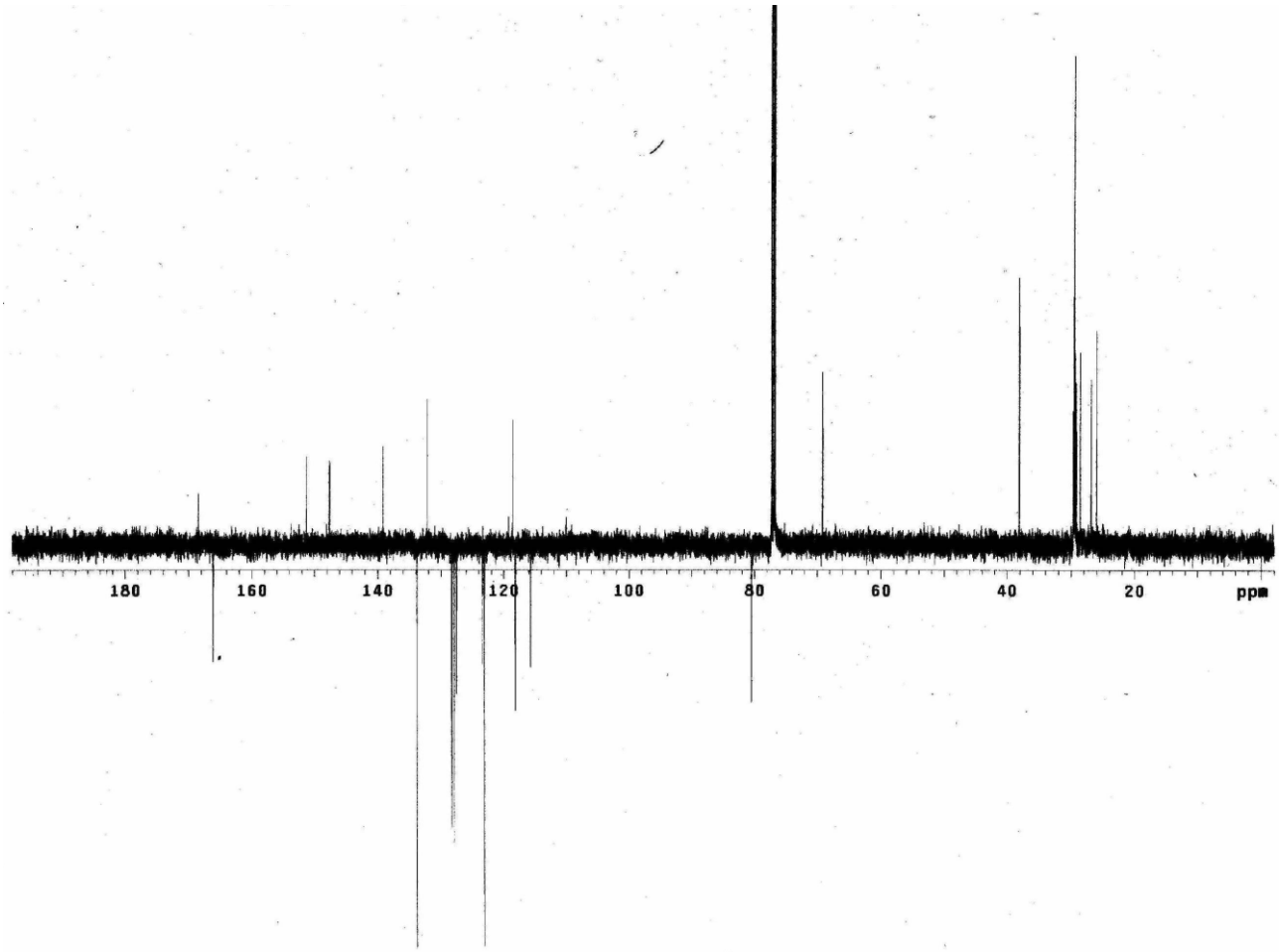

Fig. 74. ^{13}C-APT spectrum of the ligand –pht

VI.28 Ligand deprotection

50 mg (0,046 mmol) of ligand were diluted in 10 mL of absolute ethanol and poured in a 50 mL flask.
To this solution were added 111 μL (2,3 mmol d= 1.032 g/mL) of hydrazine monohydrate and the reaction left to reflux for 6,5 hours. During the reaction were noticed a chromatic change from intense yellow to colorless.
At the end of the reaction the solvent was removed under reduced pressure and the residue replaced with chloroform where the phtalate residue precipitate, then the precipitate were filtered off by using a Millipore filter. Hydrazine monohydrate unreacted was removed under vacuum. (b.p 128° C).
^{1}H-NMR (500 MHz,$CDCl_3$,δ ppm) 11.07 (s br., 2H, OH), 7.87 (s, 2H, ArCHN), 7.30÷7.26 (m, 10H, ArH, diphenylic bridge), 6.85 (dd, 2H, J= 1.5, ArH), 6.78 (t, 2H, J= 8, ArH), 6.73 (dd, 2H, J=1.5, ArH), 5.45 (s br., 4H, NH_2), 4.10 (s, 2H, CH diphenylic bridge), 4.03 (t, 4H, J=7, PhtN $(CH_2)_{11}$ CH_2NH_2), 2.68 (t, 4H, J=7.5, PhtN CH_2 $(CH_2)_{11}$ NH_2), 1.28 (m, 20H, Pht-$CH_2(CH_2)_{10}CH_2$Ar).
ESI-MS a m/z 784,4 $[M+H]^+$

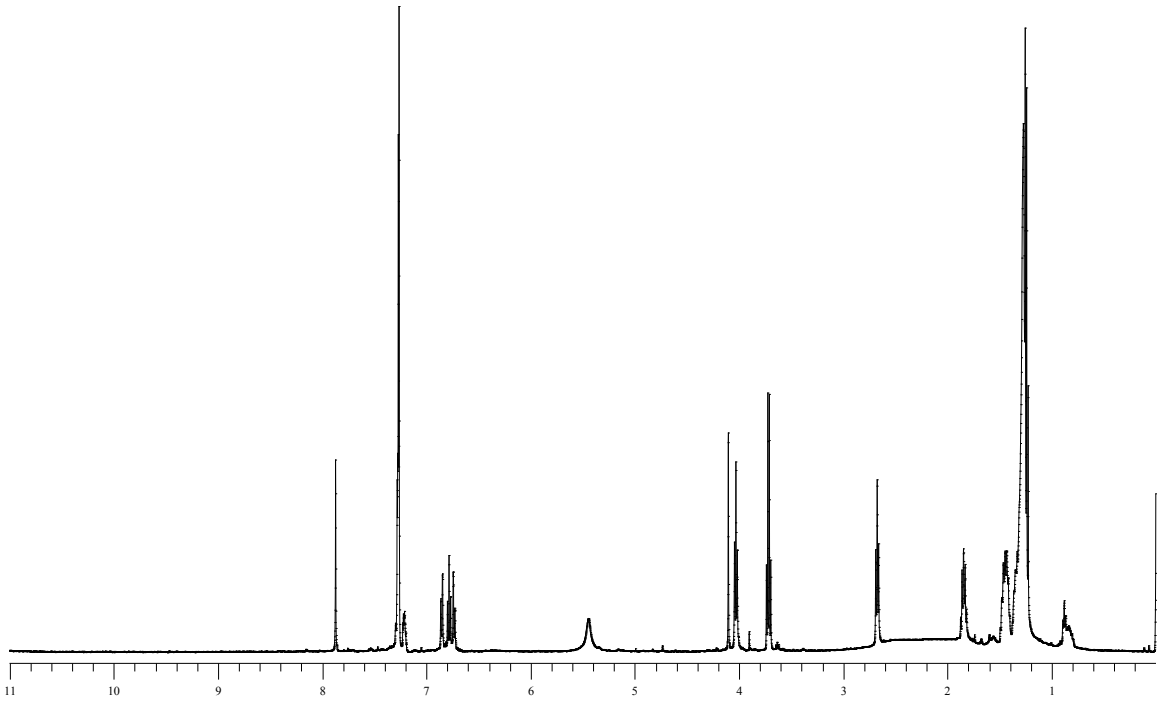

Fig. 75. ^{1}H-NMR spectrum of the deprotected ligand

VI. 29 Synthesis of the Mn(III) salen complexes

20 mg (0,0186 mmol) of ligand were diluted in the minimum amount of dichloromethane and 20 mL of absolute ethanol under stirring, to this solution were added 5 mg (0,0186) of manganese(III) acetate and the reaction proceded overnight. The reaction was monitored by TLC until the complete disappearing of the reagent.
ESI-MS m/z 1132 $[M+Mn]^+$

VI. 30 Synthesis of 3-tert-butyl-salycil-aldehyde

In a 3 naked 1L flask were poured 2,2 mL of 2-tert-butyl-phenol (14 mmol) and 5 mL of di-chloromethylmethyl-ether (55 mmol), 56 ml of tin tetrachloride with 600 mL of chlorophorm as solvent.
The solution was left for 1 hour on ice bath and the proceding of the reaction was monitored by TLC and the reaction stopped at the disappearing of the starting reagent. At the end of the reaction the solvent was removed under reduced pressure and the crude product (900 mg) was purified by column chromatography (SiO2,exhane/ ethyl acetate 9:1) to give pure product with 35% yield.
The product has been fully charachterized by ^{1}H-NMR, and ESI/MS.
^{1}H- NMR, (500MHz, $CDCl_3$, **δ ppm**): 11.7 ppm (s, 1H), 9.9 ppm (s, 1H); 7.5 ppm (dd, 1H, J=1.5), 7.4 ppm (dd, 1H, J= 1.5); 1,4 ppm (s, 9H). ESI/MS: $[M+H]^+$ = 178,2.

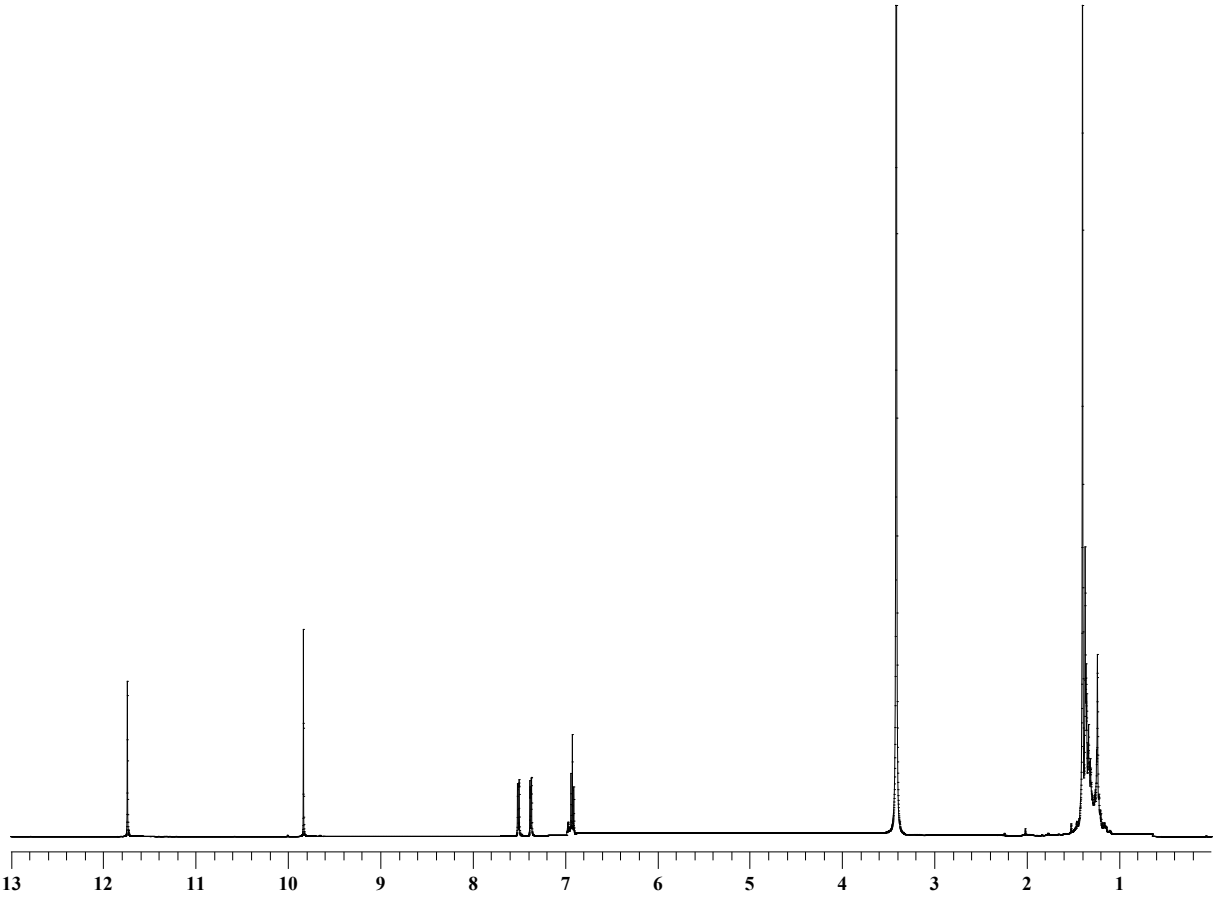

Fig. 76. ^{1}H-NMR spectrum of 3-tert-butyl-salycil-aldehyde

VI. 31 Synthesis of 3-tert-butyl-5-chloromethyl-salicyl-aldehyde

500 mg (2,8 mmol) of the aldehyde previously synthetized reacted with 170 mg (5,9 mmol) of p-formaldehyde , with 95 mg (0,28 mmol) of TBABr , and 40 mL of chloridric acid concentrated as solvent.
The solution was left stirring at room temperature for 3 days.
At the end of the reaction the product was exctracted from the acidic solution with di-ethyl-ether (3 times). The organic layers were washed with a 30% solution of sodium carbonate, until neutrality of the solution monitoring the pH with litmus paper; the solution were dried with magnesium sulphate. The resulting pale yiellow solution was filtered and the solvent removed by reduced pressure. The product was monitored by TLC (eluent exhane/ethyl acetate 9:1).
It has been obtained 600 mg 94% yield of 3-di-tert-butyl-5-chloromethyl-salicyl-aldehyde. The product was charachterized by ^{1}H-NMR spectroscopy and ESI/MS.
^{1}H-NMR (500 MHz, $CDCl_3$, δ ppm): 11.8 ppm (s, 1H), 9.9 ppm (s, 1H), 7.5 ppm (dd, 1H, J=2), 7.4 ppm (dd, 1H, J=2), 4.5 ppm (s, 2H), 1.5 ppm (s, 9H).
ESI/MS: $[M+H]^+$ = 226,1.

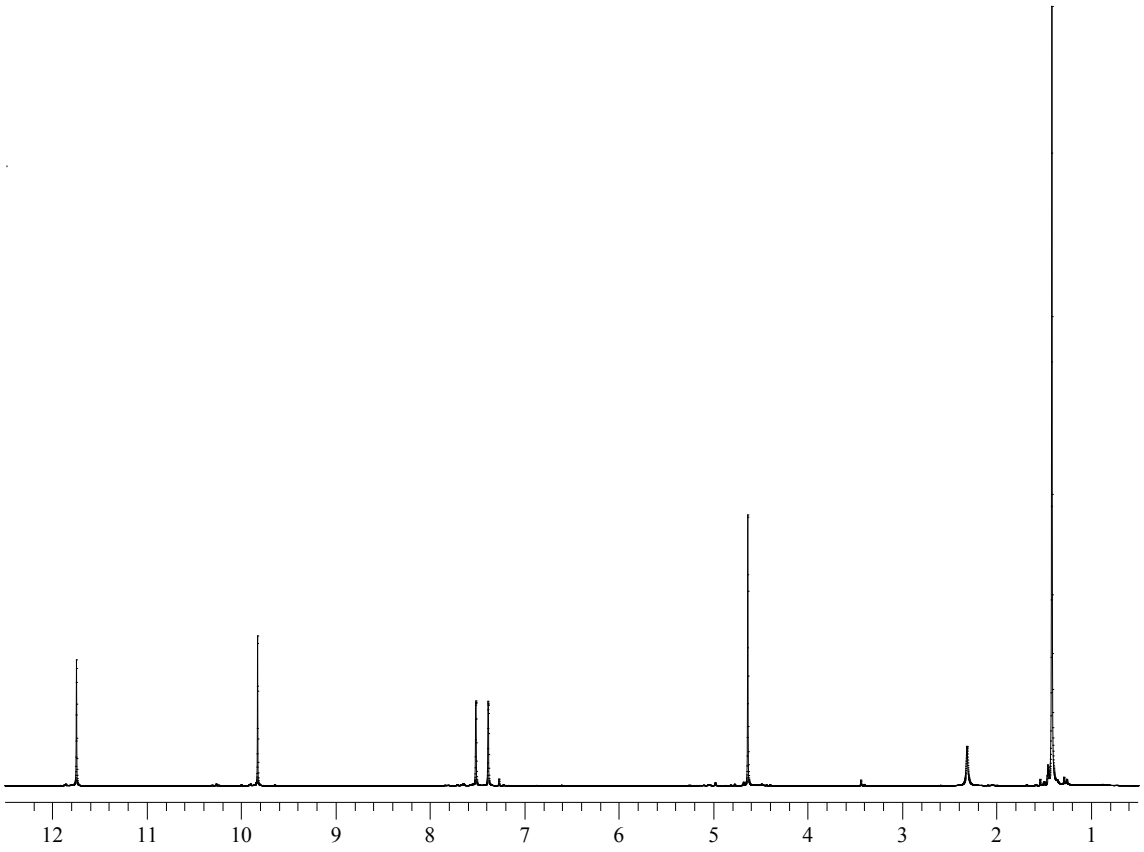

Fig. 77. ^{1}H-NMR of 3-tert-butyl-5-chloromethyl-salicyl-aldehyde

VI. 32 Synthesis of exhanol-pthalimide

In a microwave vessel were poured 1 g (6,9 mmol) of pthalic anydride and 792 mg (6,8 mmol) 6-amino-1-exhanol.
The reaction was conducted in a microwave apparatus in dry conditions :
power 80 Watt;
temperature 160°C;
time: 5 minutes.
It was obtained 1.58 g of pure product,94% yield as a dark brown solid has been charachterized by ^{1}H-NMR and ESI/MS.
^{1}H-NMR (500 MHz, $CDCl_3$,**δ ppm**): 7.9 ppm (d, 2H, J=9); 7.8 ppm (d, 2H, J=9); 3.70 ppm (t, 2H, J=7), 3.64 ppm (t, 2H, J= 7),1.7 ppm (m, 2H),1.6 ppm (m, 2H), 1.5 ppm (m, 4H), 1.4 ppm (m, 4H); ESI/ MS: $[M+H]^+$ = 437,2.

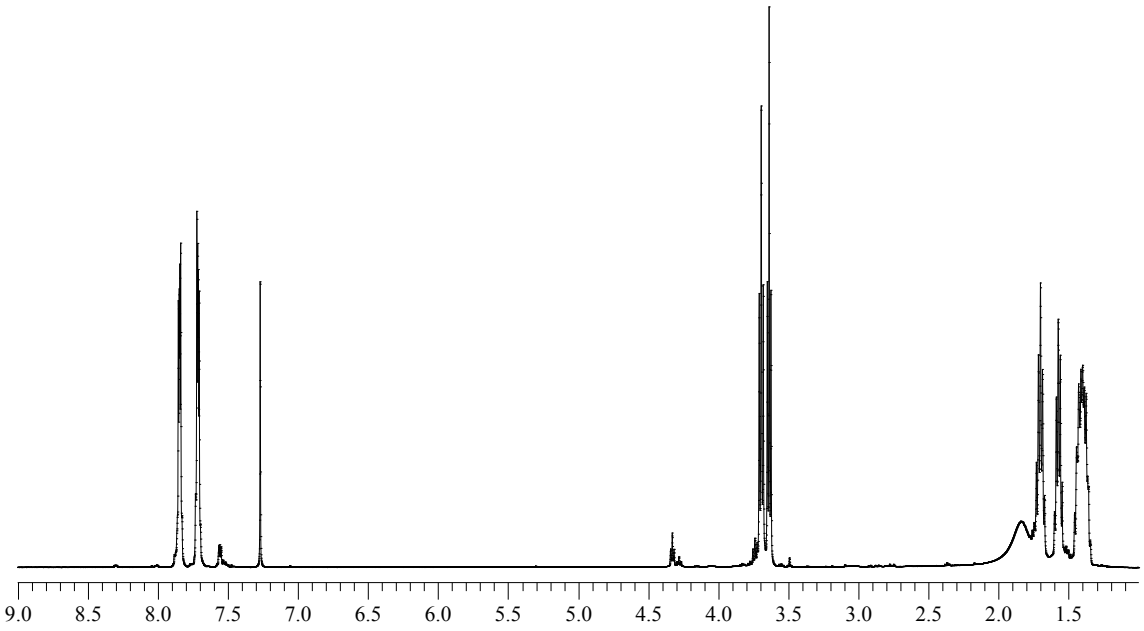

Fig. 78. ^{1}H-NMR exhanol-pthalimide

VI. 33 Synthesis of 3-tert-butyl-methoxy-exhyl-pthalimido-salicyl-aldehyde

In a microwaves Vessel were poured: 200 mg (0,9 mmol) of 3-tert-butyl-5-chloromethyl-salicyl aldehyde, 220 mg (0,9 mmol) of exhanol-pthalimide, 54 mg (0,9 mmol) of potassium hydroxide , 286 mg (2,1 mmol) of potassium carbonate, 30 mg of TBABr (0.09 mmol), under stirring.
The microwave conditions are:
Temperature: 127°C
Power: 30-80 Watt
Time: 5 minutes.
At the end of the reaction the crude product was extracted with water and dichloromethane ; the organic layers were collected and dried with magnesium sulphate, filtered and the solvent was removed under reduced pressure. The crude of the reaction was purified by column chromatography (SiO_2 exhane/ ethyl acetate 9:1). Were collected 200 mg (51% yield) of 3-tert-butyl–5-methoxyexhyl-pthalimido-salicyl-aldehyde.
The synthesized compound has been fully charachterized by ^{1}H-NMR spectroscopy.
^{1}H-NMR (500 MHz, $CDCl_3$) : δ 11,8 ppm (s, 1H); 9,9 ppm (s, 1H); 7,5 ppm (d, 1H); 7,4 ppm (d, 1H); 4,5 ppm (s, 2H); 1,4 ppm (s, 9H); 1,7 ppm (t, 2H); 1,3 ppm (m, 4H); 3,7 ppm (t, 2H); 3,5 ppm (t, 2H); 1,62 ppm (m, 2H); 7,8 ppm (m, 1H); 7,7 ppm(m, 1H).

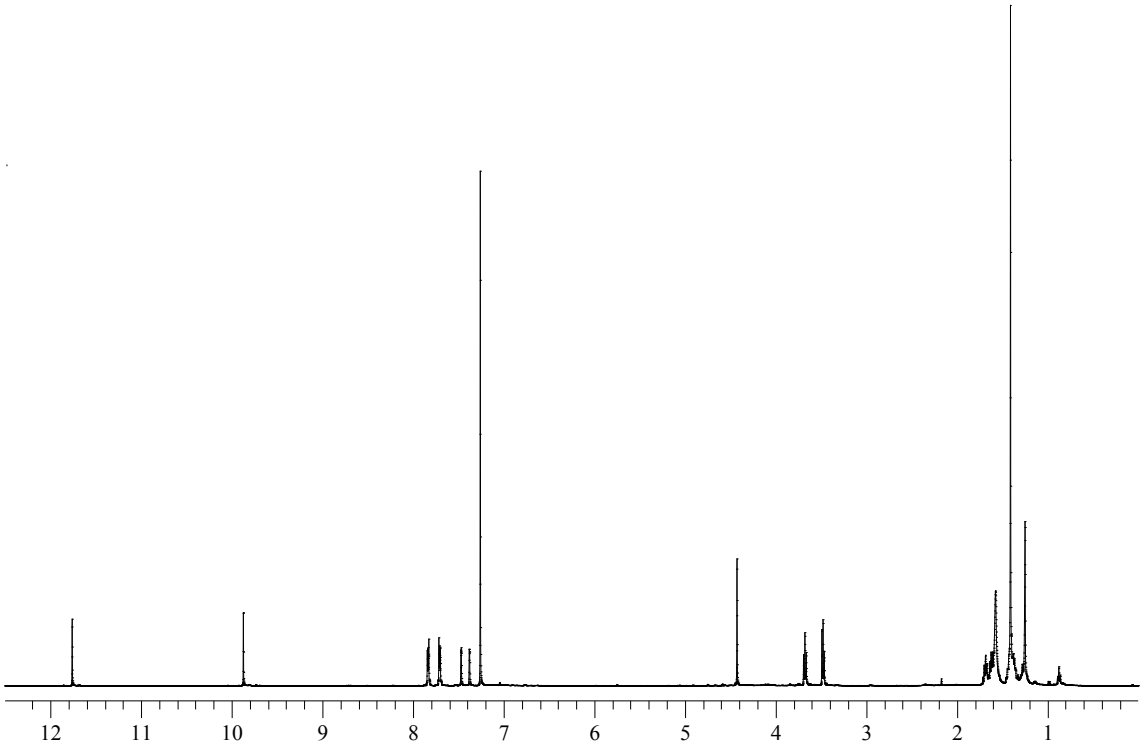

Fig. 78. ^{1}H-NMR of 3-tert-butyl-methoxy-exhyl-pthalimido-salicyl-aldehyde

VI. 35 Synthesis of 1R,2R-diphenyl-ethylen-diamine-chloridrate

In a 50 mL flask were diluted 0.5 g (2.36 mmol) of *1R,2R*-diphenylethylendiamine with 20 mL of anhydrous ethylic ether, the solution were shaken vigorously and then were added 1.18 mL (2.36 mmol) of HCl anhydrous (2M solution in Et_2O) in a time of 20 minutes. At the end of the additions the solution was stirred for 16 h at room temperature. A precipitate was formed and was collected by filtration washed with ether and dried under vacuum, giving 90% yield.
^{1}H-NMR (500 MHz, D_2O, δ ppm): 4.5 ppm (s, 2 H), 7.2-7.4 ppm (m, 10 H).
FAB(+) *m/z* 213 $[M]^+$

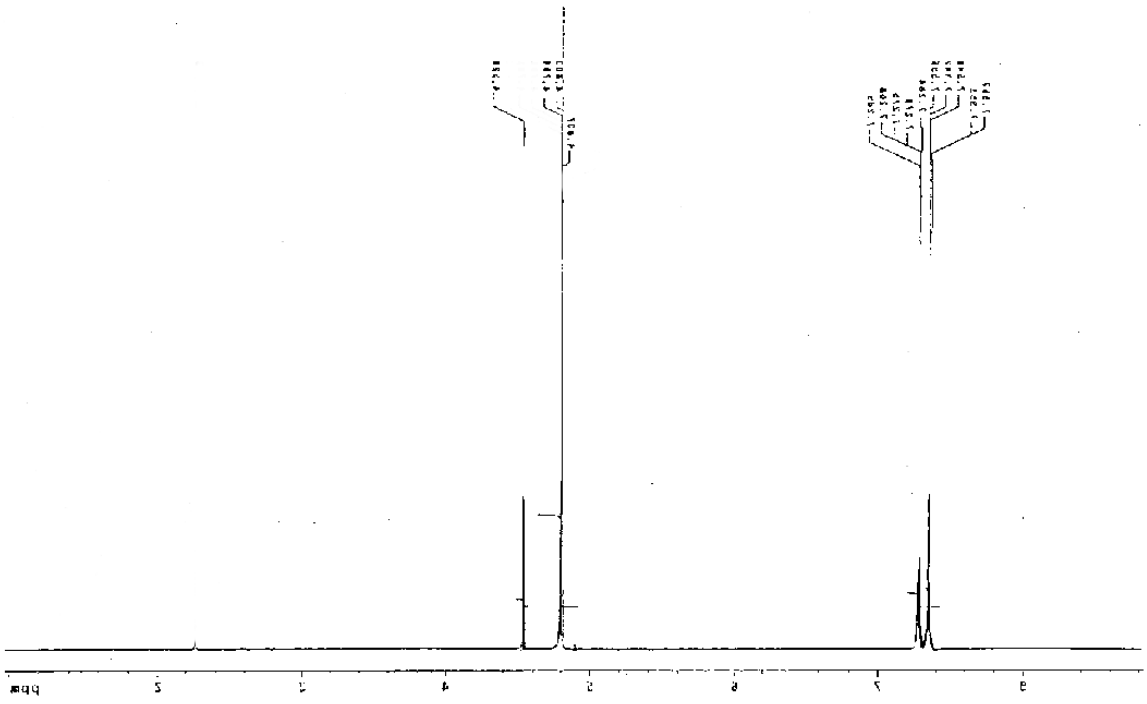

Fig. 79. ^{1}H-NMR of 1R,2R-diphenyl-ethylen-diamine-chloridrate

VI. 36 Synthesis of *1R,2R*-diphenyl-ethylen-3,5-di-tert-butyl-salicyl aldehyde-mono-imine-chloridrate

In a 100 mL flask were diluted 0.52 g (2.1 mmol) of *1R,2R*-diphenylethylendiamine chloridrate in 20 mL of a 1:1 mixture of ethanol/methanol. At the same time a solution of 3,5-di-tert-butyl-salicyl-aldehyde 0.49 g, (2.1 mmol) diluted in 20 mL of the same mixture were added dropwise and the solution left stirring for 24 h; at the end of the reaction the solvent was removed under reduced pressure and the residue washed with water (in order to remove the unreacted diamine) and with ethyl ether (to remove the unreacted aldehyde) 90% yield.
^{1}H NMR (500 MHz, DMSO-d_6) δ 1.2 ppm (s, 9 H), 1.4 ppm (s, 9 H), 4.8-5.2 ppm (m, 2 H), 7.0-7.4 ppm (m, 12 H), 8.6 ppm (bs, 3 H), 8.8 ppm (s, 1H), 13.2 ppm (s, 1 H). FAB(+) *m/z* 429 [M]$^{+}$.

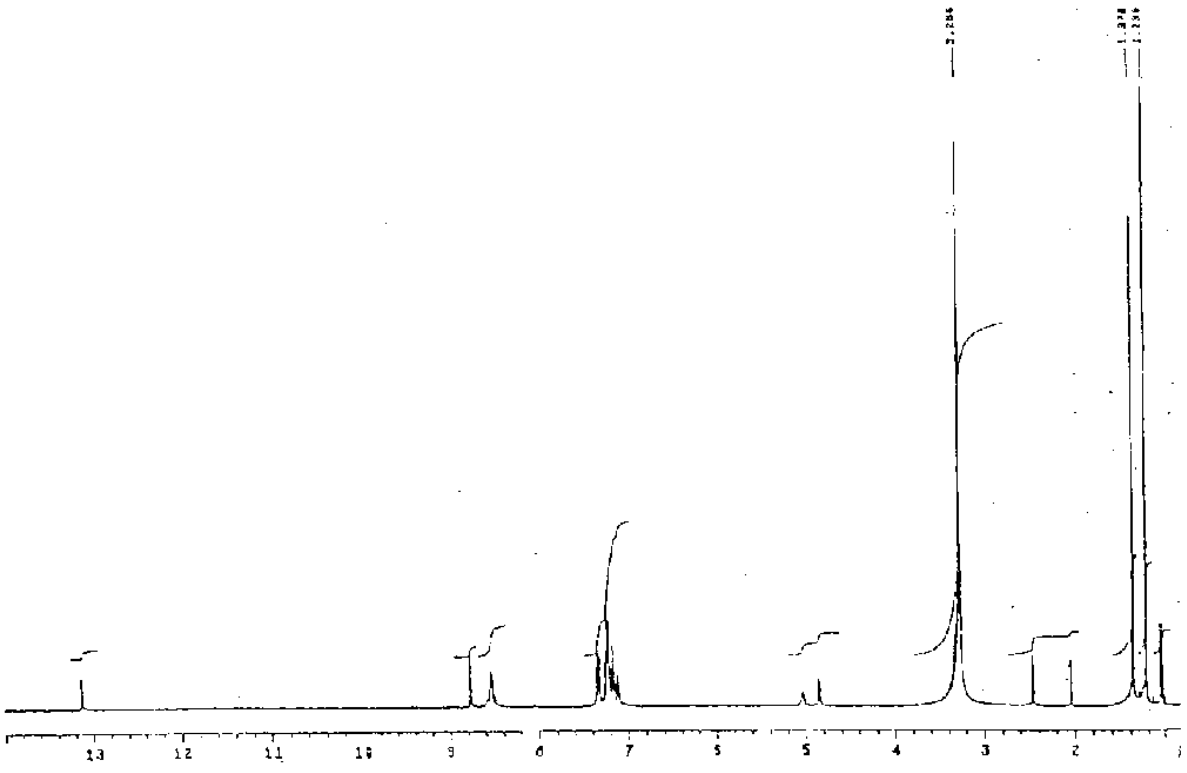

Fig. 80. ^{1}H-NMR of *1R,2R*-diphenyl-ethylen-3,5-di-tert-butyl-salicyl aldehyde-mono-imine-chloridrate

VI. 37 Synthesis of the asymmetric ligand

In a 25 mL flask were poured 200 mg (0,46 mmol) of 3-tert-butyl-5-methoxy-exhyl-pthalimido-salicyl-aldehyde, 212 mg (0,46 mmol) of chiral mono-imino-imine-chloridrate and 95 μL (d= 0,726 gr/ml) of triethylamine as base, in the minimum amount of absolute ethanol, under stirring at room temperature for 36 h.

The gradual formation of the product was monitored by TLC (eluent exhane/ ethyl acetate 9:1), at the end of the reaction the solvent was removed under reduced pressure and the crude product purified by flash chromatography (SiO_2 pH=7, M= 60.09 g/mol, particle size eluent < 0,063 mm) by using the same mixing previously used. It has been obtained 37 mg, 10% yield of ligand. The pure product was charachterized by ^{1}H–NMR , ^{13}C–NMR *e* ^{1}H-^{1}H COSY.

^{1}H-NMR (500 MHz, $CDCl_3$, δ ppm): 13,79 ppm (s, 1H), 13,54 ppm (s, 1H), 8,4 ppm (s, 2H), 7,8 ppm (q, 2H, J= 8), 7,7 ppm (q, 2H, J=8), 7,3 ppm (s, 2H), 7,2-7,1 ppm (m, 11H), 7,0 ppm (dd, J= 7.5 Hz, 2H), 4,3 ppm (s, 2H), 3,7 ppm (t, 2H, J= 7), 3,4 ppm (t, 2H, J= 7), 1,7 ppm (m, 2H), 1,6 ppm (m, 2H), 1,42 ppm (s, 9H), 1,4 ppm (s, 9H), 1,3 ppm (m, 4H), 1,2 ppm (s, 9H).

^{13}C-NMR (500 MHz, $CDCl_3$): δ 168,4; 166,8; 159,8; 157,9; 140,0; 139,6;137,2; 136,4; 133,8; 132,2; 129,6; 128,4; 128,4; 128,2; 127,4; 127,6; 127,2; 126,2; 123,1; 118,2; 117,8; 80,1; 77,6; 77,0; 76,8; 72,7; 70,1; 38,0; 35,0; 34,8; 34,1; 31,4; 29,6; 28,5; 26,9; 25,8; 22,7; 14,1.

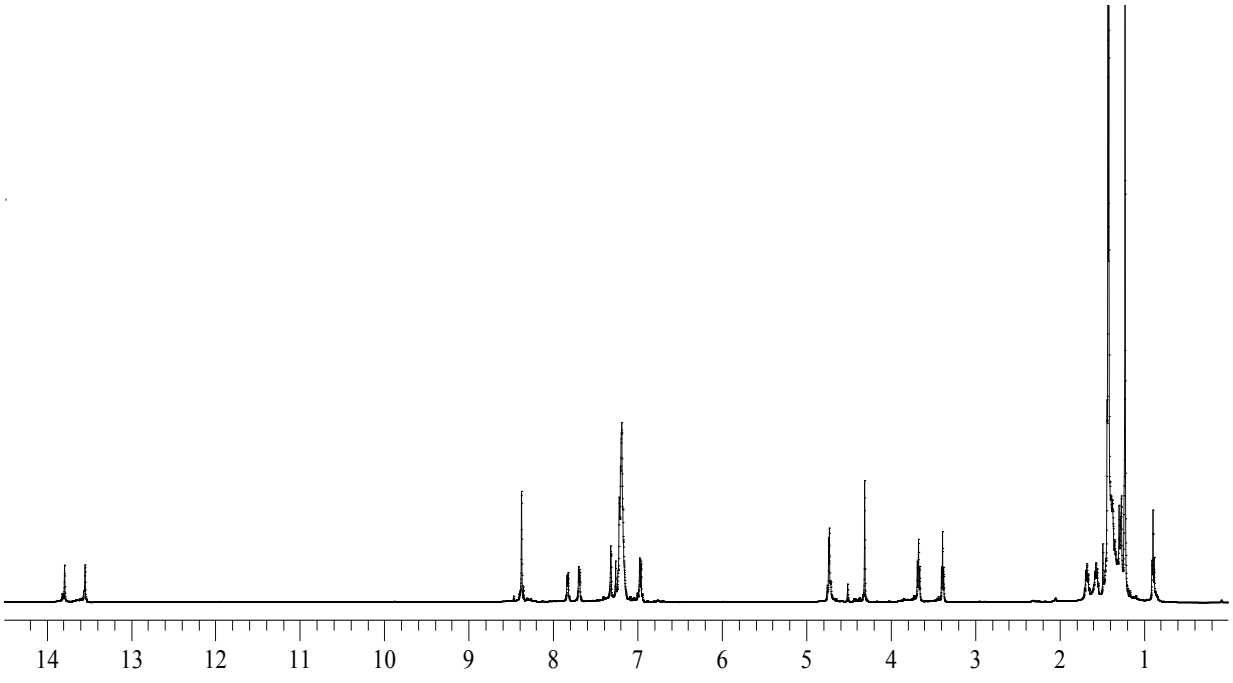

Fig. 81. ^{1}H-NMR of the asymmetric ligand

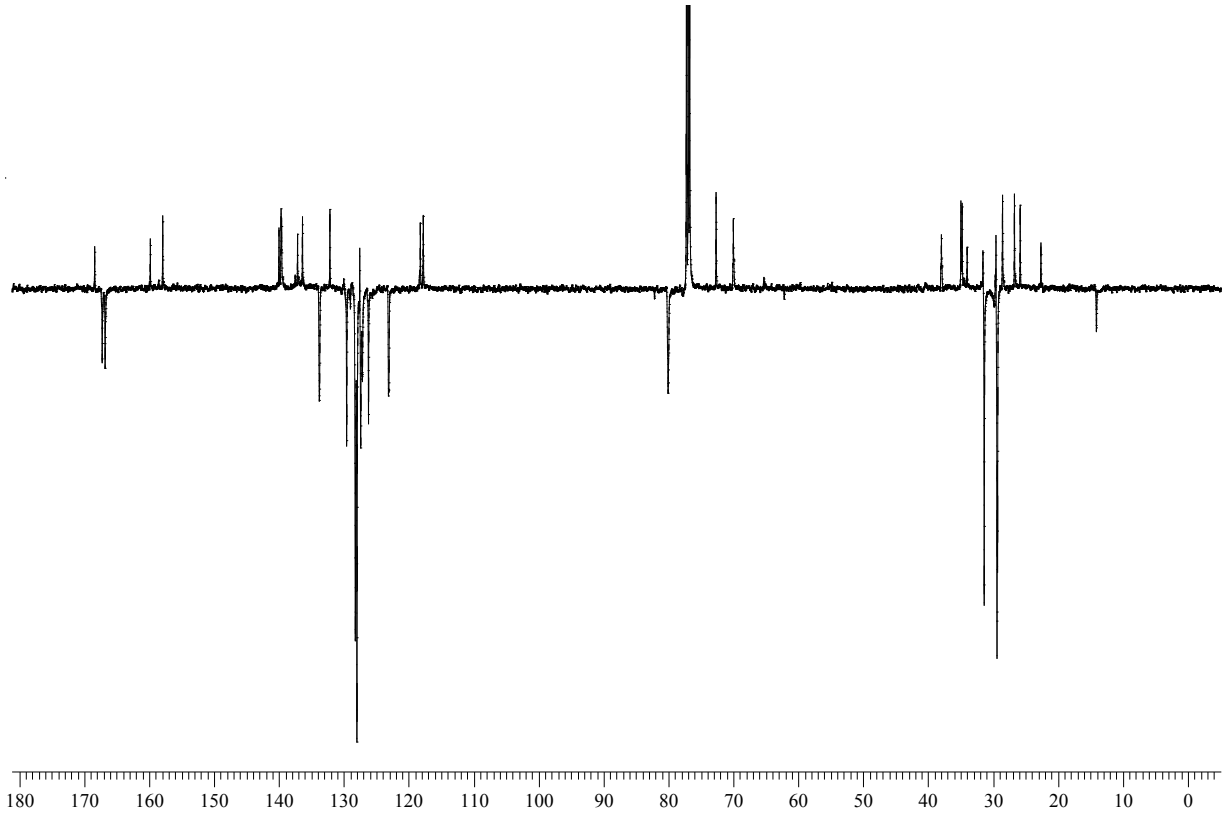

Fig. 82. ^{13}C-NMR of the asymmetric ligand

VI.38 Synthesis of the complex salen-Mn(III)

The formation of the salen-Mn(III) complex was conducted by pouring in a 25 mL flask 37 mg (0,044 mmol) of the ligand previously synthesized and 15 mg (0,13 mmol) of manganese acetate; the reaction mixture were put under stirring at room temperature for 24 h.
At the end of the reaction the solvent was removed under reduced pressure and the crude replaced with dichloromethane and filtered in order to remove the unreacted manganese acetate. The product has been charachterized by ESI/MS. Quantitative yield 42 mg (0,044 mmol) of manganese salen complex.

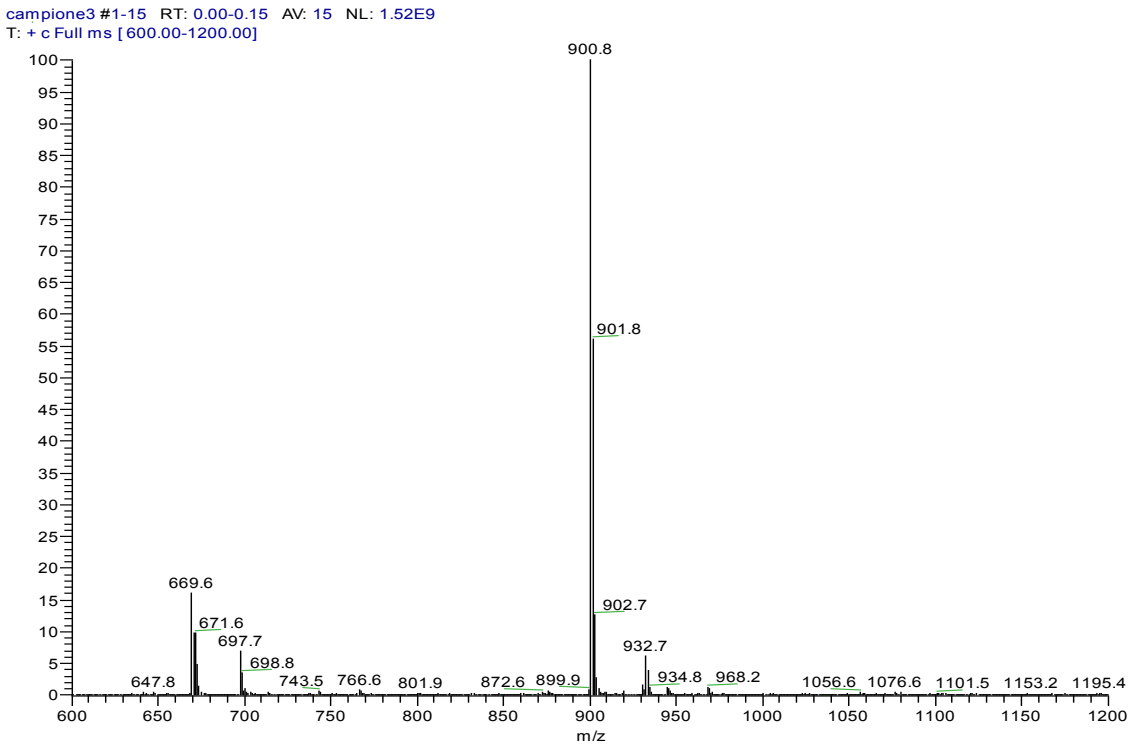

Fig. 83. ESI-MS spectrum of CAT_3

VII. REFERENCES:

[1] A. Hulanicki, S. Glab, F. Ingman, *Pure and applied chemistry,* **1991**, *63*, 1247.
[2] Fluorescent Chemosensors for Ion and Molecole Recognition, (Ed. A. W. Czarnik) *American Chemical Society,* Washington DC, **1992**
[3] M.Montalti, L. Prodi, N. Zaccheroni in: *Handbook of photochemistry and photobiology,* Ed. M. S.
[4] A. Abdel-Mottaleb, H. Nalwa, *American Institute of physic,* **2003**, *3*, 271.
[5] K. Stein, G. Schwedt, *Anal. Chim. Acta*, **1993**, *272*, 73.
[6] L. Prodi, F. Bolletta, M. Montalti, N. Zaccheroni, *Coord. Chem. Rev*. **2000**, *205*, 59.
[7] R. Pinalli, F. F. Nachtingall, F. Ugozzoli, E. Dalcanale, *Angew. Chem. Int. Ed*. **1999**, *38*, 2377.
[8] F. C. J. M. Van Veggel in: *Comprehensive Supramolecular Chemistry*, Ed. J. L. Atwood, J. E. D, D. MacNicol, F. Vogtle, D. N. Reinhoudt (Pergamon, Oxford), **1996**,*10*, 171.
[9] V. Balzani, A. Credi, F. Scandola, *Chemistry and life, science and technology*, **1996**, *78*, 1221.
[10] Hans-Jorg Schneider, *Angew. Chem. Int. Ed*, **2009**, *48*, 3924.
[11] Paul D. Beer and Philip A. Gale, *Angew. Chem. Int. Ed*, **2001**, *40*, 486.
[12] Colette McDonagh, Conor S. Burke, Brian D. MacCraith, *Chem. Rev*, **2008**, *108*, 400.
and references therein citated.
[13] A. P. De Silva, H. Q. N. Gunaratne, T. Gunnalaugsson, A. J. M. Huxley, C. P. McCoy, J. T. Rademacher, T. E. Rice, *Chem. Rev*, **1997**, *97*, 1515.
[14] R. Martinez-Manez, F. Sancenòn, *Chem. Rev*, **2003**, *103*, 4419.
[15] Sook Kyung Kim, Dong Hoon Lee, Jong-in Hong and Juyoung Yoon, *Acc. of Chem. Res*, **2009**, *42*, 23.
[16] R. Y. Tsien, *Ann. Rev. Neuroscience*, **1989**, *12*, 227.
[17] A. Gulino, G. G. Condorelli, P. Mineo, I. Fragalà, *Nanotech*, **2005**, *16*, 2170.
[18] A. Gulino, P. Mineo, E. Scamporrino, D. Vitalini, I. Fragalà, *Chem. Mater*, **2004**, *16*, 1838.
[19] S. Royo, R. Martinez Manez, F. Sancenon, A. M. Costero, M. Parra, S, Gil, *Chem. Commun*, **2007**, 4839.
[20] S. O. Obare, C. De, W. Guo, T. L. Haywood, T. A. Samuels , C. P. Adams, N. O. Masika, D. H. Murray, G. A. Anderson, K. Campbell, K. Fletcher, *Sensors,* **2010**, *10*, 7018.
[21] A. J. Russel, J. A. Berberich, G. F. Drevon and R. R. Koepsel, *Annu. Rev. Biomed. Eng*, **2003**, *5*, 4.
[22] M. Wheelis, *Pure Appl. Chem*, **2002**, *74*, 2247.
[23] B. Yu, E. Shiu and K. Levon, *Anal. Chem*, **2004**, *76*, 2689.
[24] K. Anitha, S. V. V. Mohan and S. J. Reddy, *Biosens. Bioelectron*, **2004**, *19*, 848.
[25] M. H. Hammond, K. J. Johnson, S. L. Rose- Pehrsson, J. Ziegler, H. Walker, K. Coudy, D. Gary, D. Tillett, *Sens. Actuators B*, **2006**, *116*, 135.
[26] W. E. Steiner, S. J. Klopsch, W. A. English, B. H. Clowers, H. H. Hill, *Anal. Chem*, **2005**, *77*, 4792.
[27] Karl J. Wallace, Jeroni Morey, Vincent M. Lyncha, Eric V. Anslyn, *New J. Chem*, **2005**, *29*, 1469.
[28] Karl J. Wallace, Ruth I. Fagbemi, Frantz J. Folmer- Andersen, Jeroni Morey, Vincent M. Lynth, Eric V. Anslyn, *Chem. Commun*, **2006**, *37*, 3886.
[29]A. M. Costero, S. Gil, M. Parra, P. M. E. Mancini, R. Martinez- Manez, F. Sancenon, S. Royo, *Chem. Commun*, **2008**, *43*, 6002.
[30] Daniel Knapton, Mark Burnworth, Stuart J. Rowan, Christoph Weder, *Angew. Chem. Int. Ed*, **2006**, *45*, 5825.
[31] Karl J. Wallace, Jeroni Morey, Vincent M. Lyncha and Eric V. Anslyn, *New J. Chem*, **2005**, *29*, 1469

[32] K. J. Wallace, R. I. Fagbemi, F. J. Folmer- Andersen, J. Morey, V. M. Lynch, E. V. Anslyn, *Chem. Commun*. 2006, 3886.
[33] F. Terrier, P. Rodriguez- Dafonte, E. Le Guevel, G. Moutiers, *Org. Biomol. Chem*, **2006**, *4*, 4352.
[34]Sabapathi Gokulnath, Viswanathan Prabhuraja, Jeyaraman Sankar, Tavarekere K. Chandrashekar, *Eur. J. Org. Chem*, **2007**, 191.
[35] S. A. Kuvshinova, A. V. Zav'yalov, O. I. Koifman, V. V. Aleksandriiskii, V. A. Burmistrov Russian Journal of Organic chemistry, 2004, 40, 8.
[36] Colette McDonagh, Conor S. Burke, Brian D. MacCraith, *Chem. Rev*, **2008**, *108*, 400 and references therein citated.
[37] A. I. Bush, *Curr. Opin. Chem. Biol*, **2000**, *4*, 184.
[38] E. R. Kandel, J. H. Schwartz, T. J. Jessell, *Principles of Neural Science*, 4th ed; McGraw-Hill: New York, **2000**.
[39] M. E. Go¨tz, G. Kunig, P. Riederer, M. B. H. Youdim, *Pharmacol Ther*. **1994**, *63*, 37.
[40] B. Alberts, A. Johnson, J. Lewis, M. Raff, K. Roberts, P. Walter, *Molecular Biology of the Cell*, 4th ed.; Taylor & Francis Group: New York, **2002**.
[41] Emily L. Que, Dylan W. Domaille, Christopher J. Chang, *Chem. Rev*, **2008**, *108*, 1517 and references therein citated.
[42] J. Roeper, O. Pongs, *Curr. Opin. Neurobiol*, **1996**, *6*, 338.
[43] M. J. Berridge, M. D. Bootman, P. Lipp, *Nature,* **1998**, *395*, 645.
[44] H. Bito, K. Deisseroth, R. W. Tsien, *Curr. Opin. Neurobiol*. **1997**,*7,* 419.
[45]D. E. Clapham, *Cell*, **2007**, *131*, 1047.
[46] A.Wolf Torsello, S. Fasanella, A. Cittadini, *Mol. Aspects Med,* **2003**, *24*, 11.
[47] J. Sto¨ckel, J. Safar, A. C.Wallace, F. E. Cohen, S. B Prusiner, *Biochemistry***, 1998**, *37*, 7185.
[48]J. R. Prohaska, *Physiol. ReV*. **1987**, *67*, 858.
[49] M. Kozma, P. Szerdahelyi, P. Kasa, *Acta Histochem*, **1981**, *69*, 12.
[50] S. Puig, D. J. Thiele, *Curr. Opin. Chem. Biol*, **2002**, *6*, 171.
[51] J. R. Prohaska, A. A. Gybina, *J. Nutr*, **2004**, *134*, 1003.
[52] P. A. Cobine, L. D. Ojeda, K. M. Rigby, D. R. Winge, *J. Biol. Chem,* **2004**, *279*, 14447.
[53] J. F. B. Mercer, R. M. Llanos, *J. Nutr,* **2003**, *133*, 1481.
[54] D. Strausak, J. F. B. Mercer, H. H.Dieter, W. Stremmel, G. Multhaup, *Brain Res. Bull.***,2001,** *55*, 175.
[55] D. J.Waggoner, T. B., Bartnikas, J. D. Gitlin, *Neurobiol. Dis*. **1999**,*6*, 221.
[56]D. R. Brown, H. Kozlowski, *Dalton Trans* , **2004**, 1907.
[57] C. J. Maynard, R. Cappai, I. Volitakis, R. A. Cherny, A. R. White, K. Beyreuther, C. L. Masters, A. I. Bush, Q. X. Li, *J. Biol. Chem***.2002**, *277*, 44670.
[58] A. R.White, R. Reyes, J. F. B. Mercer, J. Camakaris, H. Zheng, A. I. Bush, G. Multhaup, K. Beyreuther, C. L. Masters, R. Cappai, *Brain Res.* **1999**, *842*, 439.
[59] T. Okamoto, S. Takeda, Y. Murayama, E. Ogata, I. Nishimoto, *J. Biol. Chem*. **1995**, *270*, 4205.
[60] R. A. Cherny, J. T. Legg, C. A. McLean, D. P. Fairlie, X. D. Huang, C. S. Atwood, K. Beyreuther, R. E. Tanzi, C. L. Masters, A. I. Bush, *J. Biol. Chem.* **1999**, *274*, 23223.
[61] G. L. Millhauser, *Acc. Chem. Res,* **2004**, *37*, 79
[62] G. Yamin, C. B. Glaser, V. N. Uversky, A. L. Fink, *J. Biol. Chem***, 2003**, *278*, 27630.
[63] Y. S. Kim, D. Lee, E. K. Lee, J. Y. Sung, K. C. Chung, J. Kim, S. R. Paik, *Brain Res*, **2001**, *908*, 93.
[64] J. S. Valentine, P. A. Doucette, S. Z. Potter, *Annu. ReV. Biochem*, **2005**, *74*, 563.
[65] J.Wang, H. Slunt, V. Gonzales, D. Fromholt, M. Coonfield, N. G. Copeland, N. A. Jenkins, D. R. Borchelt, *Hum. Mol. Genet*, **2003**, *12*, 2753.
[66]S. Zanarini, E. Rampazzo, S. Bonacchi, R. Juris, M. Marcaccio, M. Montalti, F. Paolucci, L. Prodi, *J. Am. Chem. Soc,***2009**, *131*, 14208.

[67] J. Huang, Y. Xu, X. Qian, *Chem. Rev,* **2008**, *108*, 1517 and references therein citated
[68] R. Noyori, *Angew. Chem. Int. Ed*, **2002**, *41*, 2008.
[69] K. B. Sharpless, *Angew. Chem., Int. Ed,* **2002**, *41*, 2024.
[70] E. N. Jacobsen, W. Zhang, A. R. Muci, J. R. Ecker, L. Deng, *J. Am. Chem. Soc,* **1991**, *113*, 7063.
[71] Sharpless, K. B. Tetrahedron **1994**, 50, 4235.
[72] E. N. Jacobsen, W. Zhang, A. R. Muci, J. R. Ecker, L. Deng, *J. Am. Chem. Soc,* **1991**, *113*, 7063.
[b] E. N. Jacobsen, W. Zhang, M. L. Guler, *J. Am. Chem. Soc,***1991**,*113*, 6703.[c] W. Zhang, E. N. Jacobsen, *J. Org. Chem,* **1991**, *56*, 2296, [d] W. Zhang, J. L. Loebach, S. R.Wilson, E. N. J. Jacobsen, *Am.Chem. Soc,* **1990**, *112*, 2801, [e] R. Irie, K. Noda, Y. Ito, N. Matsumoto, T. Katsuki, *Tetrahedron Asymmetry*,**1991**, *2*, 481.
[73] Cozzi, P. G. Chem. Soc. ReV. **2004**, 33, 410, b. Katsuki, T. Chem. Soc. ReV. **2004**, 33, 437, [c.] Darensbourg, D. J.; Mackiewicz, R. M.; Phelps, A. L.; Billodeaux, D. R. Acc. Chem. Res. 2004, 37, 836. [d]. Leadbeater, N. E.; Marco, M. Chem. ReV. **2002**, 102, 3217, [e.] Bandini, M.; Cozzi, P. G.; Umani-Ronchi, A. Pure Appl. Chem. **2001**,73, 325,[f.] Jacobsen, E. N. Acc. Chem. Res. **2000**, 33, 421
[74] J. A. Gladysz, *Chem. ReV,* **2002**, *102*, 3215.
[75] J. F. Larrow, E. N. Jacobsen, *Top. Organomet. Chem,* **2004**, *6*, 123.
[76] A. Corma, H. Garcia, *Chem. ReV,* **2002**, *102*, 3837.
[77] P. Pfeiffer, E. Breith, E. Lubbe, T. Tsumaki, J. Liebigs, *Ann.Chem*, **1933**, *503*, 84.
[78] R. Irie, T. Hashihayata, T. Katsuki, M. Akita, Y. Moro-oka, *Chem.Lett,* **1998**, 1041.
[79] K. B. Hansen, J. L. Leighton, E. N. Jacobsen, *J. Am. Chem. Soc*, **1996**, *118,* 10924.
[80] J. M. Hawkins, T. J. N. Watson, *Angew. Chem. Int. Ed,* **2004**, *43*,3224.
[81] C. Baleiza, H. Garcia, *Chem. Rev*, **2006**, *106*, 3987 and references therein citated.
[82] C. K. Shin, S. J. Kim, G. J. Kim, *Tetrahedron Lett,* **2004**, *45*, 7429, [b] S. S. Thakur, W. J. Li, S. J. Kim, G. J. Kim, *Tetrahedron Lett*, **2005**, *46*, 2263,[c.] S. S. Thakur, W. J. Li C. K. Shin, G. J. Kim, *Catal. Lett,* **2005**,*104*, 151.
[83] P. McMorn, G. Hutchings, *J. Chem. Soc. ReV,* **2004**, *33*, 108, [b.] D. J. Darensbourg, J. C. *J* Yarbrough, *Am. Chem. Soc,* **2002**, *124*,6335.[c] M. Alvaro, C. Baleizao, D. Das, E. Carbonell, H. Garcia, *J. Catal*, **2004**, *228*, 254.
[84] C. Baleiza, H. Garcia, *Chem. Rev,* **2006,** *106*, 3987.
[85] F. Lupo, S. Gentile, F.P. Ballistreri, G. A. Tomaselli, M. E. Fragalà, and A. Gulino, *Analyst*, **2010**, *135*, 2273.
[86] Li Zeng, E. W. Miller, A. Pralle, E. Y. Isacoff, C. J. Chang*, J. Am. Chem. Soc*., **2006**, *128*, 10.
[87] N. K. Huang, Y. Chern, J. M. Fang, C. I. Lin, W. P. Chen, Y. L. Lin, *J.Nat.Product,* **2007**, *70*, 571.
[88] K. J. Wallace, J. Morey, V. M. Lyncha, Eric V. Anslyn, *New J. Chem.,* **2005**, *29*, 1469.
[89] S. A. Kuvshinova, A.V. Zav'ylaov, O.I. Koifman, V. V. Aleksandriiskii and V. A. Burmistrov, *Russian Journal of organic chemistry*, **2004**, *40*, 1113.
[90] R. Siewertsen, H. Neumann, B. Buchheim-Stehn, R. Herges, C. Nather, F. Renth, F. Temps, *J. Am. Chem. Soc.*, **2009**, *131*, 15595.
[91] S. D. Ross, M. Finkelstein, R. C. Petersen, *J. Am. Chem. Soc*., **1958**, *80*, 4327.
[92] A. T. Peters, Y. S. Behesti, *J. of the Society of Dyers and Colourists,* **1989**, *105* , 29.
[93] Z. Xu et al, *Tetrahedron*, **2006**, *62*, 10117.
[94] Z. Xu, X. Qian, J. Cui, R. Zhang, *Tetrahedron,* **2006**, *62*, 10117.
[95] S. Onclin, B. J. Ravoo, D. N Reinhoudt, *Agew. Chem. Int. Ed.*, **2005**, *44*, 6268.
[96] S. Zhang, F. Lue, L. Gao, L. Ding, and Y. Fang, *Langmuir*, **2006**, *22*, 7437.
[97] A. Gulino, G. P. Mineo, S. Bazzano, D. Vitalini and I. Fragalà, *Chem. Mat.*, **2005**, *17*, 4043.
[98] S. Royo, R. Martinez-Manez, F. Sancenon, A. M. Costero, M. Parrab and S. Gilb, *Chem. Commun.* **2007**, 4839.
[99] A. A. Andrade, S. B. Yamaki, L. Misoguti, S. C. Zilio, T. D. Z. Atvars, O. N. Oliviera Jr, C. R. Mendonca, *Optical Materials*, **2004**, *27*, 441.

[100] S. Gokulnath, V. Prabhuraja, J. Sankar, and T. K. Chandrashekar, *Eur. J. Org. Chem.* **2007**, 191.
[101] H. Heinz, R. A. Vaia, H. Koerner, and B. L. Farmer, *Chem. Mater.* **2008**, *20*, 6444.
[102] G.G. Birch, M. L. Wolfrom, R. S. Tyson , *Adv. Carbohydr. Chem. Biochem*. **1963**, *18*, 201.
[103] A. Elbein, Y. Pan, I. Pastuszak, D. Carroll *Glycobiology* **2003**, *13*, 17R.
[104] R. Liu, H. Barkhordarian, S. Emadi, C. B. Park, M. R. Sierks, *Neurobiol. Dis*. **2005,** *20*, 74.
[105] S. Hannessian, P. Lavallèe *Carbohydrate Research* **1973**, *28,* 303-311.
[106] B. Di Blasio, S. Galdiero, M. Saviano, C. Pedone, E. Benedetti, E. Rizzarelli, S. Pedotti, G. Vecchio, W. Gibbons, *Carbohydrate Research,* **1996**, 282, 41.
[107] Z. Xu, X. Qian, J. Cui, R. Zhang, *Tetrahedron*, **2006**, *62*, 10117.
[108] M.J. Pfammatter,V. Siljegovic. *Helvetica Chimica Acta,* **2001**, *84*, 678.
[109]O. Garcia, E. Nicolàs, F. Albericio, *Tetrahedron Letters*, **2003**, *44*, 4961.
[110] L. L. Lou, K. Yu, F. Ding, X. Peng, M. Dong, C. Zhang, S. Liu, *Journal of catalysis***, 2007**, *249*, 102.
[111] T. Vidal, A. Petit, A. Loupy, R. N. Gedye, *Tetrahedron*, **2000,** 56, 5473.

[112] Y. Peng, G. Sang, *Green chemistry,* **2002***, 4*, 349.
[113] M. E. Amato, F. P. Ballistreri, A. Pappalardo, G.A. Tomaselli, R. M. Toscano, D. J. Williams *Eur. J.Org. Chem.,* **2005**, 3562.